THE IMPROVEMENT OF DROUGHT TOLERANCE IN RICE

Umar Mohammed, MSc.

Thesis submitted to the University Of Nottingham for the degree of

Doctor of Philosophy

August 2017

Abstract

The unpredictability of spatio-temporal drought patterns in the field and complexity of the physiological stress response mechanism involved have made it difficult to identify the essential traits for improved productivity under drought stress without compensating yield performance. (Serraj et al., 2011). Drought (severe water limitation) limits rice productivity, particularly in upland and rainfed systems which are prone to frequent drought and other abiotic stresses. Vulnerability in such areas is likely to worsen in the future. It is therefore critical to develop genetic improvement strategies to focus on improving productivity in such regions. The development of improved root system architecture, shoot morphology and whole plant physiological processes in order to generate drought tolerant rice cultivars

It is in this context that this thesis used a multidisciplinary approach to improving drought tolerance in rice. One of the major phases was to study a diversity panel of African rice lines (*Oryza sativa* L) selected for being particularly well adapted to upland (aerobic) cultivation and was compared to a set of typical lowland (Asian in origin) cultivars. Plants were grown in plastic columns in expanded clay and exposed to temporary drought at key growth stages. In particular, the characterisation of these African accessions has improved our understanding of the interaction between photosynthetic response and how their roots interact with their environment and also in response to the above ground physiology. For example, a high leaf gas exchange CO_2 assimilation, stomatal conductance and transpiration identified in two upland genotypes, N8 and N7 with high leaf water use efficiency as a result of a low stomatal conductance and high photosynthesis. The N8 also showed well-developed root system with significantly higher root depth and length, while the N7 has relatively higher central metaxylem area and higher stomatal density. A strong correlation was observed between root morphological properties (e.g. root average diameter, root length and root central metaxylem area) was observed, providing real evidence that optimal root morphology is needed to support high photosynthesis through increased

water access and possibly higher hydraulic conductance across diverse genotypes.

Another reverse genetic approach used transformation of key genes in stomatal patterning. The overexpression of the rice homolog *EPIDERMAL PATTERNING FACTOR* (EPF) resulted in the alteration of stomatal density and size. *OsEPF2* exhibited reduced stomatal density, and *OsEPFL9* showed increased stomatal density. As a result of reduces numbers of stomata, the *EPF2OE* showed significantly improved intrinsic water use efficiency and drought tolerance through reduced stomatal conductance and transpiration whilst maintaining a high relative rate of photosynthesis. The *OsEPF2* unlike in Arabidopsis (Franks et al., 2015) has shown significantly low stomatal conductance without loss in carbon gain. Unexpectedly the *OsEPF2* lines also showed enhancement of lysigenous aerenchyma when growing in both stagnant and aerated hydroponic media, in comparison to the WT. This has a vast implication in the improvement of respiratory losses potentially in non flooded and flooded conditions.

The creation of transgenic lines with the *Ethylene Responsive Factor* (*ERF*) group VII motif signature in the GUS N-terminus has been used to show the activity of the *ERF*VII under drought conditions. The result revealed GUS expression under abiotic stresses; notably hypoxia, submergence and drought. Therefore, the motif of the ERFVII could be used as a sensor for drought in rice and can also be used in the understanding of the role of protein modification in genes related to submergence and drought tolerance such as the *SUBMERGENCE 1* (SUB1A)through the principles of N-end Rule Pathway.

In conclusion, this thesis has demonstrated that multiple approaches can be used toward the improvement of water use efficiency and drought responses in rice crops. A reduction in stomatal density can improve water use efficiency in water limited conditions and should be considered in upland or other similar agroecosystems where yield is determined by low rainfall and soil water conservation is critical. This may also be applicable to irrigated rice but there is a possibility of a limitation to the maximum rate of photosynthesis by stomatal conductance. The use of existing natural genetic variation in African genotypes has been shown to be another promising route, especially because drought tolerance is a complex multi-gene trait. It is concluded that both the

single gene approach and breeding using existing tolerant lines should be explored as routes to maintaining food security in coming decades. It has also demonstrated clearly that coordination of above and below ground processes is required.

Acknowledgments

First and foremost, my utmost gratitude to my two supervisors, Dr Erik Murchie and Dr Ranjan Swarup for all the advice, supports and encouragements, without which this project would not have been materialized.

I wish to thank Prof. Malcolm Bennet and Prof Michael Holdsworth for their guidance and various helpful intellectual discussions. I must also express my appreciation to all my collaborators, Prof. Julie Gray, Prof, Yusaku Uga and Dr Guillermina Mendiondo for their immense support and guidance. Equally, I offer special thanks to Dr Jitender Giri, Dr Jose Fernandez, Dr Behzad Talle, Dr Ken Davis and Dr Jonathan Atkinson, who were instrumental to my PhD, particularly within the early days. I must thank my colleagues from Murchie's lab and Plant Science Lab A29/20 members for the support they offered throughout the time of my PhD.

I gratefully want to thank my father, Mohammed Abubakar and father in law Prof. Munzali Jibril for funding my PhD. I must also thank Bayero University Kano for funding part of my living expenses during the PhD. My deepest regards and blessing to my family and friends for the love, support and crying shoulder throughout this journey.

Last but not the least, I would like to thank my wife, Dr Halima M. Jibril and my little daughter, Adeelah (Aisha) for the unwavering emotional support and encouragement throughout this journey.

Finally, I dedicate all my work to my father, Mohammed Abubakar and my mother Aishatu Abubakar who always wanted me to do a PhD.

Table of Contents

List of Figures

List of Tables

CHAPTER ONE: INTRODUCTION AND LITERATURE REVIEW

1.1 RICE AND ITS IMPORTANCE

Rice is widely known as an important crop that feeds more than half of the world population. It is considered a staple food in Asia and Africa where it provides 40% -70% of the total food calories consumed and a substantial amount of protein intake.

Rice is a semi-aquatic crop from the grass family that has approximately 22 species of *Oryza,* of which 20 are wild and two are cultivated for consumption (Muthayya et al., 2014). Two species of rice, *Oryza sativa* and *Oryza glaberimma,* are the known cultivated rice plants considered cereals for human nutrition. The former is grown worldwide including Asia, North and South America, Europe, Middle East, and Africa; the latter is confined to only Africa, and is thought to have been domesticated from its wild ancestor, *Oryza barthii* (Maclean and Dawe, 2002). Rice is the only crop consumed by almost every human in the world and it is cultivated in every continent except Antarctica.

There are thousands of rice cultivars grown in many countries around the world and are characterized based on their cultivated ecology; the long grained *indica* are grown in tropical and subtropical Asia. The short-grained japonica is often grown in temperate regions of Japan and Northern China. Japonicas are short with round seeds, and are glutinous when cooked. The medium grained *japonica* is grown in the Philippines, Indonesia and part of Madagascar (Khush, 1997, Muthayya et al., 2014, Hoshikawa, 1989).

Rice is cultivated as an annual crop, although in tropics it can also survive as a perennial crop so that after harvest, new tillers emerge from the nodes in a process called ratooning (Vergara et al., 1988). Rice generally has a main stem and several tillers, where each tiller can bear a terminal flowering panicle that produces seeds. The height of a mature rice plant ranges from 40cm to more than 500cm in some floating types (Maclean et al., 2013). The rice growing cycle is divided into two morphological phases: the vegetative stage, including germination, seedling and tillering; and

reproductive stages including booting or panicle initiation and flowering. The rice kernel, commonly called the seed, consist of hull and caryopsis (brown rice). The seed is essentially composed of the embryo and the endosperm with several thin layers of tissues around them. The rice seed germinates as soon as the dormancy is broken (Figure 1.1 A). With adequate water and a temperature (ranging from 10^{o}C to 40^{o}C) the coleoptile and or radicle will emerge from the ruptured seed husk (see Figure 1.1 B) in both aerated and hypoxic conditions (Adachi et al., 2015). The only differences in the germination under hypoxia is that the coleoptile emerges first before the seminal root and vice versa under aerated environments (Moldenhauer and Gibbons, 2003, Maclean et al., 2013). Their stems are made up of nodes and internodes with varying lengths, depending on the variety and growing condition. The nodes bear leaves which grows asymmetrically along the stem.

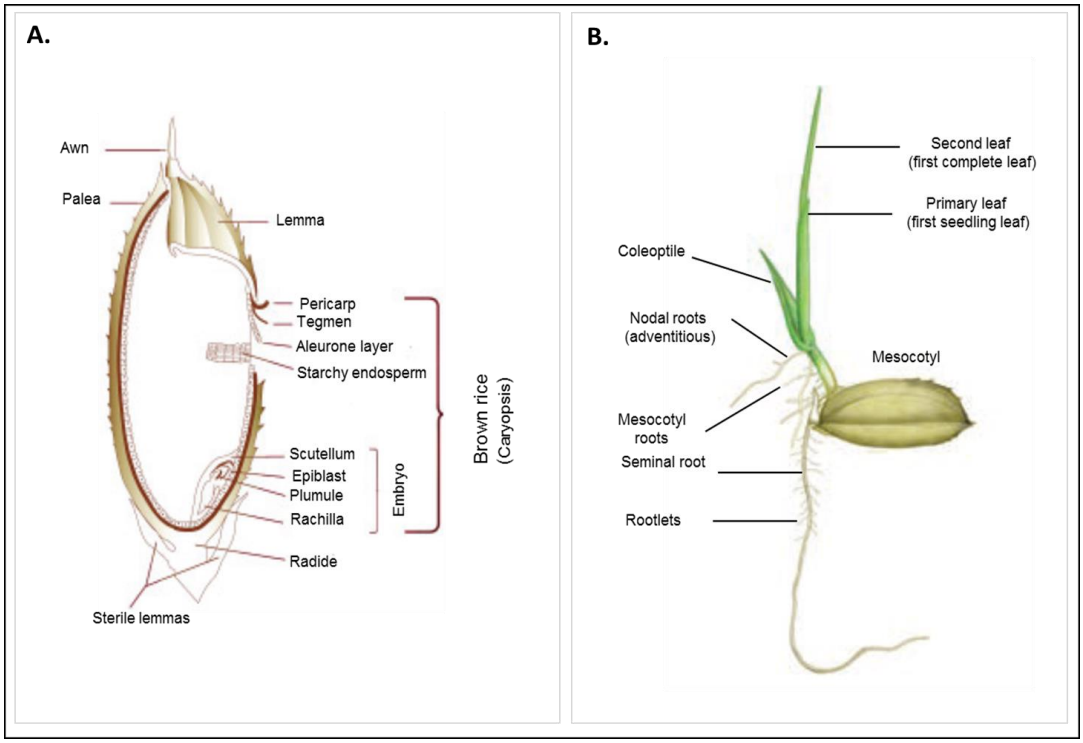

Figure 1.1. **A**. Cross section of the rice grain. **B**. Part of young seedling germinated in the dark. Image taken from Maclean et al. (2013).

Rice is grown worldwide on 154 million ha representing about 11% of the worlds cultivated land (Chandra, 2010), with global production of 495.6 million tonnes in 2014 -2015 (Muthayya et al., 2014). Rice grows under

various water regimes: irrigated, rainfed lowland, upland and flood-prone ecosystem with estimated proportion of 53%, 26%, 13% and 8% of the total land area of rice production worldwide respectively (Khush, 1997). The irrigated lowland rice grows in bunded fields, is harvested 2 -3 times in a year, and accounts for three-quarters of the total world rice production. The rainfed lowland is grown in bunded field flooded with rain water that is often unpredictable. This is very common among areas of South Asia and many parts of Africa where the poverty level is high, and it accounts for the 17 - 20%, while flood-prone system accounts for 6% of the total global rice production. Upland rice is produced in aerobic soil conditions and it produces least among the three, with only 4% of the world total rice production (Fukai et al., 1997, Muthayya et al., 2014).

The global population is predicted to reach 9 billion by the year 2050. This suggests the need for increasing pressure to improve and increase yield per hectare, particularly in less developed countries that are threatened by food insecurity and climatic calamities. This, therefore, means that 40% more rice needs to be produced (to around 1 billion tonnes by 2050) with less land and water; and with reduced agrochemicals application (Datta, 2004). Studies have also shown that the current pace of global rice production is not sufficient to meet 2050 demand. At around the current pace of production, only 705 million tonnes will be achieved with a shortfall of 295 million of the projected demand in 2050 (Ray et al., 2013). Also, yield may not be increasing in several top crop producing nations around the world due to the increase in the population, affluence and urbanization pressure.

1.1.1 Rice production in Africa

The total global land area covered by rice production is 156 million hectares with 7.62 million hectares in Africa. Nigeria, for instance, has a potential of the land area for rice production between 4.6 million and 4.9 million ha but only 1.7 million ha is being utilised (Namazzi et al. 2010; Imolehin and Wada, 2000). Nigeria, together with many other African countries, has ecologies that are suitable for different rice varieties and that can be strapped to boost rice production to meet domestic demand and even to produce a surplus for export.

West African Rice Development Association (WARDA), International Institute for Tropical Agriculture (IITA), National Cereals Research Institute (NCRI), ministries of Agriculture and many non-governmental organisations focus on the improvement of the adaptation measures in rice agriculture in Africa paddy rice production tremendously increase in area planted to 666,000 ha, output to 1.09 million tonnes and productivity to 2.07 tonnes/ha over the last two decades. Since 1980, Nigeria has become the largest rice producing country in West Africa and third largest in Africa, after Egypt and Madagascar (Imolehin and Wada, 2000). However, rice production in Africa faces various challenges from biotic and abiotic stresses to poor policies and low capital investment. Thus the production has not been able to match the growing demand instead, which the import rate increases rapidly at a rate of 8.4% per annum since 1997. Imports fill the gap between regional supply and the demand in Africa. African imports three-quarter of the total quantity of the traded rice on the global market (Nwanze et al., 2006). Africa consumes a total of 11.6 million tonnes of rice per annum of which 34% is imported (FAO, 1996).

The inability of the African nations to be self-sufficiency in rice productions require urgent attention to address the trend of over-reliance on imports and to meet its increasing demand (Oteng and Sant'Anna, 1999).

1.2 DROUGHT STRESS

1.2.1 Concepts of drought

Drought implies the inadequacy of water, including soil moisture storage, for crop plants during the growth cycle that restricts the expression of full genetic yield potential (Biswas et al., 2002).

Two physiologically relevant factors associated with drought effects are the water content and the water potential of plant tissues. These factors directly depend on the fluxes of gas and water in and out of the plants within the soil-plant-atmosphere continuum (SPAC) (Zhu, 2002). The SPAC creates a gradient of water vapour pressure between leaf to air and soil water content, and the potential to show the drought condition on the plant

(Jones, 2007). With any slight changes in the water potential, a great response in the physiological processes are induced.

Plants use three different defence mechanisms to resist drought stress during their growing cycle. Namely; drought escape (flowering to complete life cycle before drought), drought tolerance (this divides into dehydration avoidance and dehydration tolerance) and drought avoidance (maintenance of tissue water potential)(Levitt, 1972). These changes may occur either by the responses that are caused by a change in water status in the plant tissue, or by plant hormones that signal changes in water status in the plant tissue. As such, it may be very difficult to identify a single or specific response pattern that is highly correlated with yield under all drought conditions. Different crops respond differently to drought at different developmental stages (Cattivelli et al., 2008, Wani et al., 2010), see table 1.1.

Plant traits	Effects relevant for yield	Modulation under stress
Stomatal conductance/leaf temperature	More/less rapid water consumption. Leaf temperature reflects the evaporation and hence is a function of stomatal conductance	Stomatal resistance increases under stress
Photosynthetic capacity	Modulation of concentration of Calvin cycle enzymes and elements of the light reactions	Reduction under stress
Timing of phenological phases	Early/late flowering. Maturity and growth duration, synchrony of silk emergence and anthesis, reduced grain number	Wheat and barley advanced flowering, rice delayed, maize asynchrony
Starch availability during ovary/embryo development	A reduced starch availability leads to abortion, reduced grain number	Inhibition of photosynthetic activity reduces starch availability
Partitioning and stem reserve utilization	Lower/higher remobilization of reserves from stems for grain-filling, effecting kernel weight	Compensation of reduced current leaf photosynthesis by increased remobilization
Stay green	Delayed senescence	
Single plant leaf area	Plant size and related productivity	Reduced under stress (wilting, senescence, abscission)
Rooting depth	Higher/lower tapping of soil water resources	Reduced total mass but increased root/shoot ratio, growth into wet soil layers, regrowth on stress release
Cuticular resistance and surface roughness	Higher or lower water loss, modification of boundary layer and reflectance	
Photosynthetic pathway	C_3/C_4/CAM, higher WUE and greater heat tolerance of C_4 and CAM	
Osmotic adjustment	Accumulation of solutes: ions, sugars, poly-sugars, amino acids, glycinebetaine	Slow response to water potential
Membrane composition	Increased membrane stability and changes in aquaporine function	Regulation in response to water potential changes
Antioxidative defence	Protection against active oxygen species	Acclimation of defence systems
Accumulation of stress-related proteins	Involved in the protection of cellular structure and protein activities	Accumulated under stress

Table 1.1: Physiological traits associated with response to drought stress amended from Cattiveli et al (2008)

Water-deficit may occur early in the growing season or at any growth stage from flowering to grain filling and restricts the expression of full genetic yield potential (Biswas et al., 2002). Drought suppresses leaf expansion and tillering, while reducing photosynthetic rate due to lowered leaf conductance and enhanced leaf senescence (Ji et al., 2012). Generally, drought is considered a serious limitation to the sustainability of rice yields under rain fed conditions (Wu and Cheng, 2014). This is especially the case in marginal areas characterized by erratic and unpredictable rainfall, the occurrence of high temperatures, high levels of solar radiation, and poor soil characteristics (Serraj et al., 2011). Due to uneven distribution of rainfall, a water stress can cause a serious economic damage on rice yield as a result of its shallow rooting system. Among cereal crops, rice is the most susceptible to damage from water deficit (Tsuda et al., 1994). Unfortunately, the predominantly rice growing areas in Asia and Africa are often threatened by abiotic stress, notably extreme drought.

1.2.2 Economic Impact of drought to rice production

The economic impact of drought stress on global rice production scale averages to 18 (14% of the total production) metric tonnes annually. Drought stress has a tremendous impact on rice production with annual losses reported to cost around the US $580, $880 and $3,600 million annually in the Eastern India, China and the globe (O'Toole, 2004). Evidently, millions of rice farmers are mostly affected due to the recurrent drought shock that affects the drought-prone environments around Asia, African and South America. Drought mostly affects poor farmers disproportionately and thus, the impact on poverty is very direct. Drought imposes severe economic consequences on society, and the burden has been historically associated with food shortages in varying intensities as seen in different part of Africa and Asia (Wassmann et al., 2009). Loss of yield to poor farmers means reducing the number of feed consumptions, withdrawing children from schools and migration to cities for other employments (Bernier et al., 2008). Around 20% of the total rice area (23 million ha) of rainfed are estimated to be drought-prone. Similarly, the traditional irrigation system that accounts for almost 75% of the total rice

production also faces an increasing problem of water scarcity, resulting from rising demand for water.

1.3 PROMISING APPROACHES TO THE IMPROVEMENT OF DROUGHT TOLERANCE

So far, various efforts have been made to explain the mechanisms of drought tolerance and resistance in rice with attention to the type, location and the number of genes associated with drought response signalling, but only a little progress is recorded. This may be because drought tolerance/resistance is a complex trait and it is controlled by many genes having different effects; morphology (leaf area adjustment, leaf rolling, wax secretion, development of efficient root system, reduced tillering), physiology (reduced transpiration, stomatal closure, high water use efficiency, oxidative stress, osmoregulation, antioxides) (Farooq et al., 2009), and biochemical (regulation of Rubisco activity, accumulation of proline, polyamine, trehalose and production of abscisic acid) on different timing and severity (Bernier et al., 2008). Many studies have reported great insights in the understanding of the physiological and molecular responses of plants to drought stress, but the dramatic yield reduction under stress compared to optimal conditions still remains a gap to fill (Ji et al., 2012).

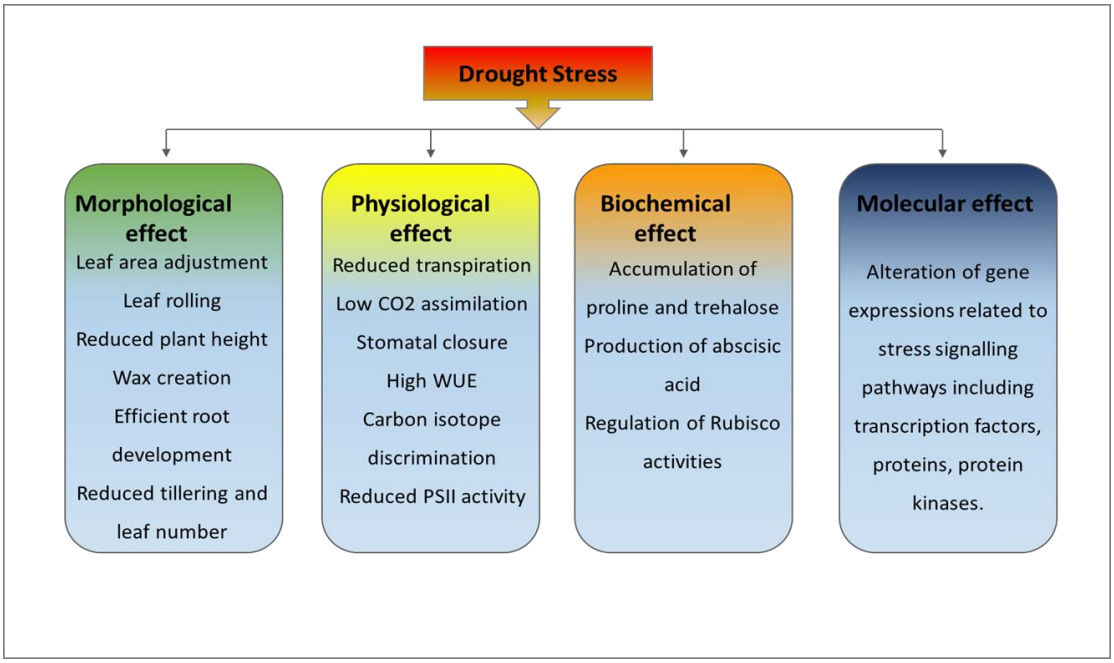

Figure 1.2. The various responses to drought in rice grouped in four; morphological, physiological, biochemical and molecular. Source: created by authors.

1.3.1 EFFECTS OF DROUGHT ON PHYSIOLOGY

1.3.1.1 Photosynthesis

Photosynthesis is a complex process of plants in the conversion of light energy into chemical energy through the fixation of CO_2 into sugar. The process of photosynthesis involves the production of biochemical energy adenosine triphosphate (ATP) from the adenosine di phosphate (ADP) and inorganic phosphate (Pi) through the energy from light to excite electrons that passed along an electron transport chain. The photosynthesis in the chloroplast of the leaf first starts when light in the form of photon is first absorbed by the chlorophyll which is surrounding the photosystem II (PSII) complex in the thylakoid membrane. This creates a resonance energy that is transferred through neighbouring chlorophyll molecules. The energy then reaches the reaction centre around the PSII, an electron is then released, which can be transferred when excited. At this point, the light energy absorbed by the chlorophyll can be derived to either photosynthesis (photochemistry), be re-emitted or dissipated as heat, or re-emitted as light (fluorescence) (Murchie and Lawson, 2013) (Figure 1.3).

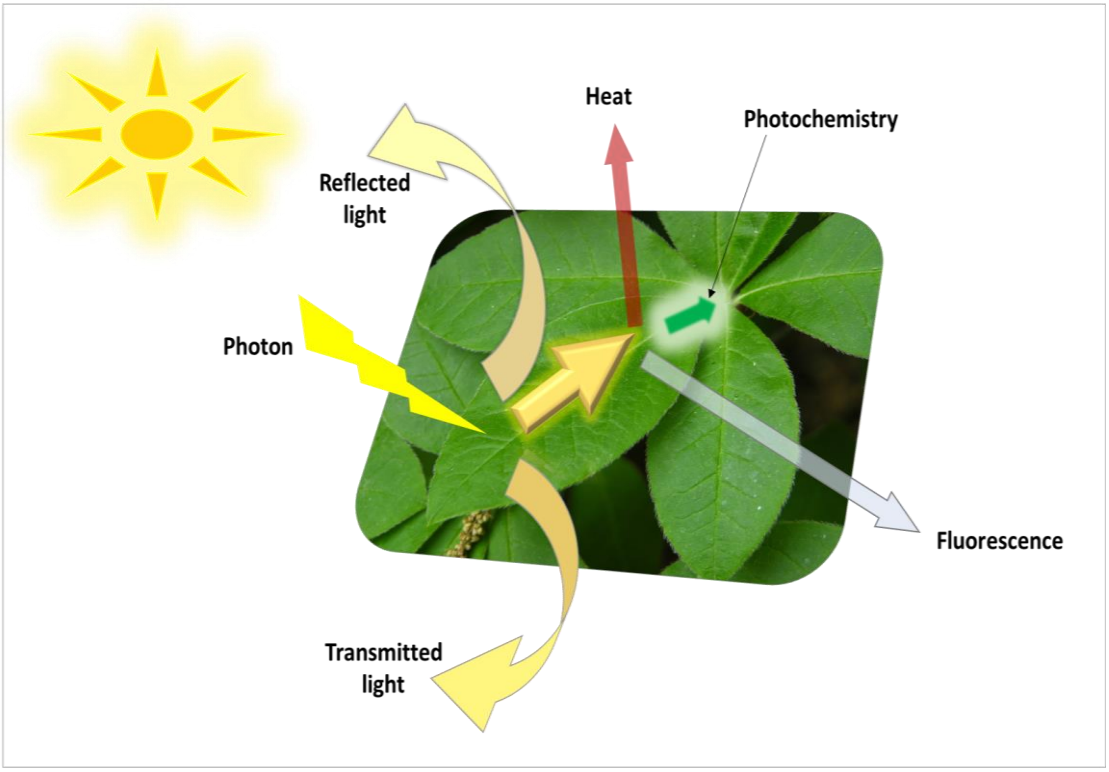

Figure 1.3. Incident light on leaf and the fate of the complementary pathways. Light energy absorbed by the chlorophyll, a portion goes to photochemistry, while the two other portions are lost by heat and fluorescence. Source: created by authors.

The three processes compete with each other. In the photosynthesis pathway, the excited electrons are transferred by a mobile carrier to the PSI complex. The electrons are re-energised in the PSI and then transferred to Ferredoxin-NADP-reductase where Nicotinamide adenine dinucleotide phosphate (NADPH) is made by adding an H^+ to $NADP^+$. The gradient created in the electron transport chain is utilized by ATP synthase, where ATP is made for Calvin-Benson cycle utilization (Murchie et al., 2015).

1.3.1.2 Effect of drought on photosynthesis in rice

Drought stress has profound effects on rice physiology. Drought causes the reduction of photosynthetic activity as a result of several coordinated events, such as stomatal closure with a consecutive reduction in transpiration and the reduced activity of photosynthetic enzymes (Tezara et al., 1999, Valliyodan and Nguyen, 2006, Li et al., 2011). Two physiologically relevant factors associated with drought effects are the

water content and the water potential of plant tissues. These factors directly depend on the fluxes of gas and water in and out of the plants within the SPAC. The two major components that limit photosynthesis under drought condition are the diffusivity (stomatal or mesophyll conductance) and biochemical impairments (Rubisco activity). The stomatal conductance is essential for CO_2 diffusion into the leaf and is regulated by the opening and closure of stomata. Changes in the stomatal conductance and Rubisco activity can alter the photosynthetic efficiency. Thus, the ability to maintain the mesophyll conductance during drought stress determines the tolerance of the crop under drought (Lauteri et al., 2014). Previous studies have shown that drought stress significantly affects leaf net CO_2 assimilation rate (A), transpiration rate (E) and stomatal conductance (g_s) largely by the synthesis of ABA (Serraj et al., 1999, Lawlor and Cornic, 2002, Li et al., 2011). Other factor affected includes the water use efficiency, intercellular CO_2 (C_i), activity of the PSII, and relative water content (RWC).

A decrease in the leaf cell turgor and the increase in the vapour pressure deficit (VPD), causes a rapid closure of stomata in response to drought. Stomatal limitation, therefore, is the key cause of the decrease in the photosynthesis that occurs under water stress (Lawlor, 2002). Drought decreases internal CO_2 concentration (C_i) and inhibits the ribulose-1, 5-bisphosphate carboxylase/oxygenase enzyme activity and ATP synthesis and leads to decrease of net photosynthetic rate (Hu et al., 2010). Drought severely impairs the PSII activity and to some extent, leads to the photoinactivation of the PSII reaction centre. This is due to the induced degradation of the D1 protein within the PSII complex. Thus, a new D1 protein will need to be produced into the PSII complex for the reaction centre to function again as highlighted by (Aro et al., 2004)

Changes in pigment content (carotenoid and chlorophyll) are another response of plants to drought. Carotenoids help plants to resist drought stress by forming a major part of plant antioxidant protection system (Xiao et al., 2008). *Chlorophyll a* and *b*, on the other hand, plays role in light harvesting (Farooq et al., 2009) and photoprotection. Drought stress inhibits the synthesis of chlorophyll and decreases the content of both *chlorophyll a* and *b* binding proteins leading to the lower content of light

harvesting pigment proteins and photosystem II (Rahbarian et al., 2011). Other effects include an increase in the formation of reactive oxygen species (ROS). This results in lipid peroxidation, protein denaturation and nucleic acid damage (Ji et al., 2012). Photosystem efficiency (Fv/Fm), electron transport rate (ETR) and the effective quantum yield of PSII photochemistry (PhiPSII) are all shown to be affected by drought (Pieters and El Souki, 2005, Jiang et al., 2006, Rahbarian et al., 2011, Yang et al., 2014). However, the level of drought stress determines the integrity of the Fv/Fm change by drought. Mild drought that is largely limited by stomatal closure, may not result in a substantial decline in the *Fv/Fm* (Murchie and Lawson, 2013).

1.3.1.3 Metabolic process of photosynthesis in rice

Rice is classified as a C_3 plant based on its carbon fixation within the Calvin - Benson cycle. Their first product of the Calvin cycle is the 3- carbon molecules of the 3-phosphoglyceric acid (3-PGA) produced through the catalysis of the CO_2 molecules by an enzyme ribulose 1,5-bisphosphate carboxylase/oxygenase (Rubisco). The same enzyme catalyzes the oxidation of ribulose 1,5-bisphosphate (RuBP) in an inefficient process called photorespiration that can incur a loss of fixed carbon by more than 25% (Sage, 2004).

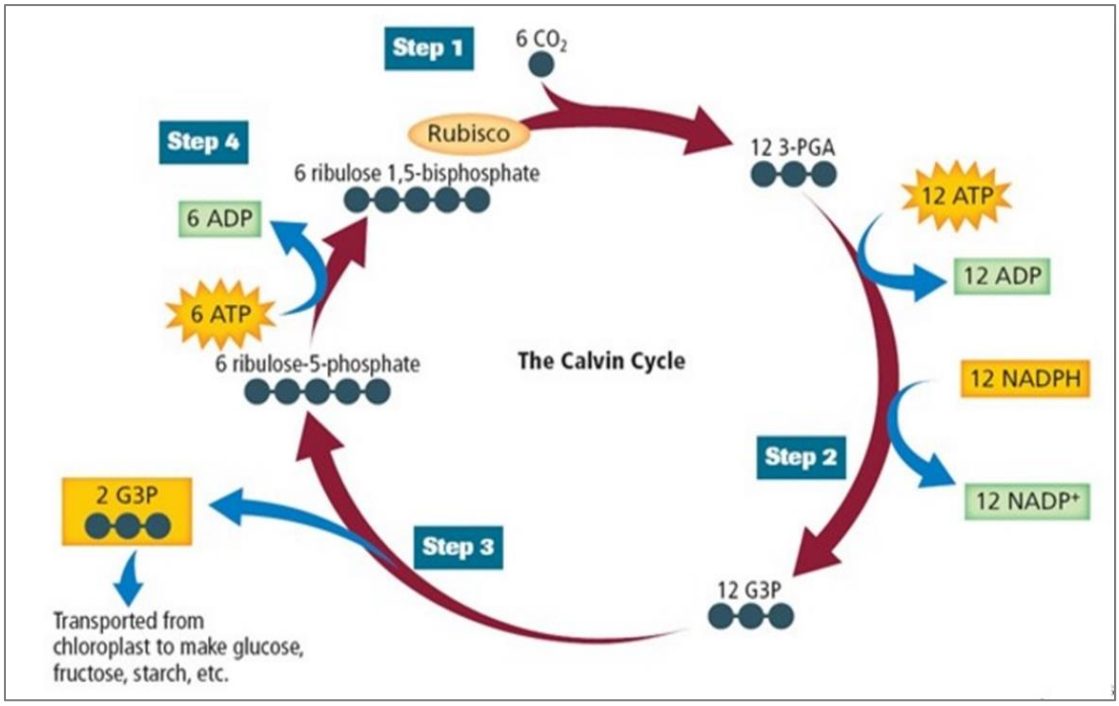

Figure 1.4. The light independent reaction of photosynthesis from the Calvin-Benson cycle of C3 plants. Source: taken from photosynthesis–calvin cycle: https://www.slideshare.net/MrTullis/82-photosynthesis-2014.

The effect of drought stress on the activity of Rubisco varies with plant species, the level of drought (ranging from high reduction to very little to no changes in the activity) as well as an increase in the growing temperature (Hu et al., 2010, Karki et al., 2013). Photosynthesis is essentially determined by the amount of CO_2 demand and supply by the chloroplast. However, the major limiting factor affecting the rate of photosynthesis is the rate of CO_2 diffusion from the atmosphere to the site of carboxylation, which is largely limited by the stomatal opening. However, photosynthetic enzyme activity (Rubisco), limited capacity in the formation of RuBP due to the low triose-phosphate formation, as well as the decrease photochemical efficiency of photosystem II (PSII) have all been linked to photosynthesis limitation (Centritto et al., 2009, Takai et al., 2013). There has been a long standing argument as to whether drought stress primarily limits photosynthesis by diffusive resistance through the stomatal closure or photosynthetic biochemistry impairment. Flexas et al. (2004), therefore, suggested that drought and salinity stress predominantly affects CO_2 diffusion with decreased stomatal and mesophyll

conductance. They added that the biochemical capacity to assimilate CO_2 may not be affected except during severe stress.

Mild drought results to the decrease in the leaf diffusive conductance of CO_2 (g_{CO2}) owing to reduced intercellular CO_2 concentration relative to the ambient concentration (C_a) see equation 1.1.

Equation 1.1:

$$C_i = C_a - \frac{A}{gCO_2}$$

Where:

A = CO_2 assimilation rate

C_i = intercellular CO_2

C_a = ambient CO_2

$g_{CO2} = g_{H2O}/1.6$

g_{CO2} = leaf diffusive conductance of CO_2

g_{H2O} = leaf diffusive conductance of H_2O

1.6 = the diffusivity ratio of H_2O and CO_2 in air

(Tezara et al., 1999)

This means that as the g_{CO2} decreases with stress, the photosynthesis also decreases because of the low *Ci*.

Tezara et al. (1999) tested this hypothesis (equation 1.1) through the relationship between *A* and C_i by using higher ambient concentration to overcome the limiting g_{CO2}, and also to determine the effect of stress on electron transport by measuring O_2 evolution and NADPH. They discovered that both the rate of maximum carbon assimilation (A_{max}) and the carboxylation efficiency (*CE*) decreases with increases in stress. The C_i, therefore, decreases with mild drought but increase with further drought increase. They concluded that water stress does not primarily limit photosynthesis by reducing CO_2 diffusion or inhibiting O_2 production and electron transport, but by the inhibition of the Calvin cycle. On the

contrary, Cornic and Fresneau (2002) shows that stomatal closure plays the main role in the inhibition of photosynthesis during mild drought. Their argument was that, in the light limited condition in C_3 plants, oxygenation of RuBP entirely replace carboxylation of RuBP when the stomata shut.

A response of A to C_a cannot properly interpret a convincing information due to boundary layer interferences. Therefore, it is worth mentioning that the two major resistance steps that occur in the uptake of CO_2 for photosynthesis are at the stomata and at the surface of the mesophyll cell layer. Boundary layer conductance may play an important role in some species. Stomatal and mesophyll conductance (g_m, the rate of CO_2 diffusion from the intercellular spaces to the chloroplast stroma) to CO_2 usually decreases in similar way in response to environmental stresses (Lauteri et al., 2014). Soil drying triggers signalling factors that affect stomatal regulation and was found to be an adaptation strategy to avoid dehydration of plant tissue under water deficit (Centritto et al., 2009).

A/Ci response gives a simple empirical analysis of quantifying the limitation impose by stomata on A. The interpretation of the model depends on the Rubisco activity through the calculation of *in vivo* maximum rates of Rubisco carboxylation (V_{cmax}), maximum rate of electron transport driving regeneration of RuBP (J_{max}) and triose-phosphate utilization (V_{TPU}). See Figure 1.5.

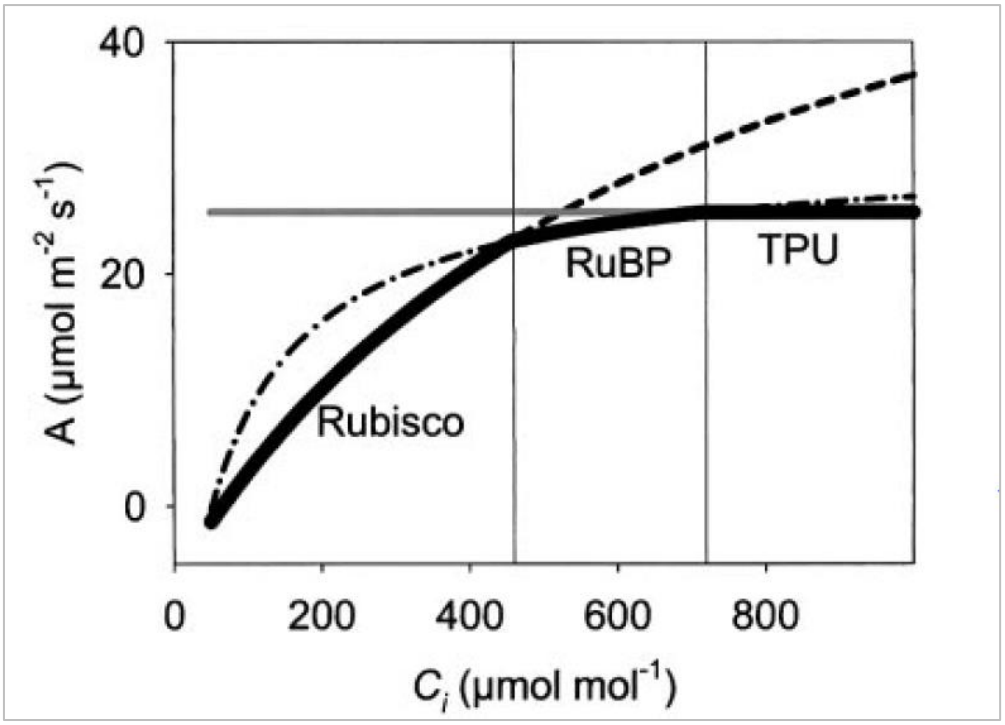

Figure 1.5. Shows the response of *A* in different phases (Rubisco, RuBP or TPU) each with its limiting point indicated. The black solid line is the actual photosynthesis rate at a given *Ci* is the minimum of these three potential limitations. From the graph: V_{cmax} = 70µmolm^{-2}s^{-1}, J_{max} =130 µmolm^{-2}s^{-1} , V_{TPU} = 9.1 µmolm^{-2}s^{-1} and Rd= 2 µmolm^{-2}s^{-1} . Image taken from Long and Bernacchi (2003).

These three parameters are explained in three phases to represent the major limitations imposed on *A* in the light stage. According to Farquhar et al. (1980), as *Ci* increases from its minimum concentration, the change in the *A/Ci* is high and determined by Rubisco activity. This is called the Rubisco-limited state of photosynthesis and it normally occurs when the CO_2 concentration is low. Sharkey et al. (2007) added that the limitation by Rubisco is mostly associated with low *Ci* concentration than the maximum rate of Rubisco (V_{cmax}). With further increase in the *Ci*, there is a change in curvature with a lower response that approaches to zero where RuBP regeneration is limiting. In this state, the RuBP regeneration limited photosynthesis increases as the *Ci* increases (Figure 1.5). In this stage, the increase of the *Ci* causes more RuPB to be carboxylated instead of oxygenation. In some instances with further increase in the *Ci*, the RuBP reaches a plateau or approaches zero with an increase in *Ci* if the TPU is limiting (Long and Bernacchi, 2003). By using the Farquhar C3 model of photosynthesis amended by Von Caemmerer, (2000), the key biochemical

kinetics that determines photosynthetic rate V_{cmax}, J_{max} and V_{TPU} can be obtained *in vivo* by fitting in the parameters into the A/Ci model curve.

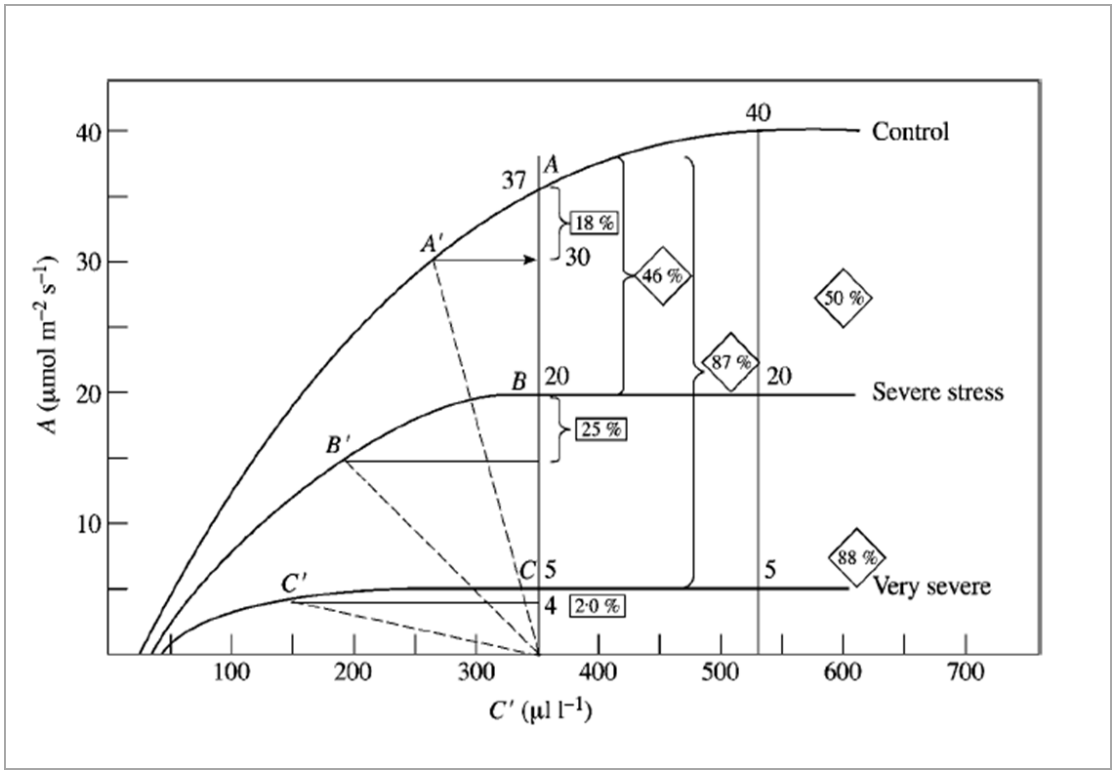

Figure 1.6. A descriptive analysis of limitation of A imposed by stomata (L_s) applied on well-watered, severe drought and very severe drought. Image taken from Lawlor (2002).

The relationship between *A* and C_i has been used extensively to assess stress in plants. The relationship is used to estimate relative influence of stomatal and non-stomatal components of photosynthesis (Hu et al., 2010). Leaf conductance usually decreases with different factors that decrease photosynthesis. This, however, does not always means stomata are more limiting to photosynthesis. Long and Bernacchi (2003) reviewed the graphical work of Farquhar and Sharkey (1982) with several methods used to quantify the limitation that the stomatal and boundary layer conductance imposes on leaf photosynthesis. Figure 1.6, illustrates how stomatal limitation (L_s) is estimated. If a leaf has a CO_2 assimilation rate *A′* and the stomatal and layer boundary conductance at the ambient CO_2 concentration (~350μmol^{-1} in Figure 1.6), it can, be predicted that, the hypothetical (A, B or C) that would be obtained if the mesophyll allows free

diffusion of CO_2 (making $g_s=g_m=\infty$) then the $C_i=C_a$. Therefore the limitation imposed is given as

Equation 1.2

$$L_s = \frac{(A - A')}{A} \times 100$$

It is worth mentioning that at a very severe drought stress, the Ls is unreliable and thus, the limitation is shifted to biochemical rather than stomatal. In Figure 1.7.

1.3.2 MOLECULAR MECHANISMS OF DROUGHT RESPONSES

Plants respond to environmental stress by first sensing and then signalling the stress internally leading to the activation of stress-related genes and the synthesis of different functional proteins. This results in changes in various physiological and metabolic responses (Hu et al., 2006, Zhou et al., 2009) such as stomatal conductance, membrane stability, ABA synthesis etc.

Phytohormones play a key role in the regulation of the expression of stress related genes as effective regulatory pathways for plants to respond to adverse stress. The plant induces ABA synthesis in the roots in response to decreased soil water potential which activates the ABA signalling pathway to regulate expression of stress-responsive genes to enable them to acclimate to the new environment (Du et al., 2010, Zhang et al., 2010a, Shinozaki and Yamaguchi-Shinozaki, 2007). Likewise, the inhibition of ABA synthesis greatly decreases plant's ability to acclimate to the drought condition (Liu et al., 2016). Regulating the expression of stress related genes is one of the most promising regulatory pathways for the plant to adapt to a change in environment. Many genes that are triggered by drought stress have been identified together with the transcriptional

activities of many stress responsive genes. These are well studied but the signalling pathways for most of these genes remain unknown (Seki et al., 2003, Zhou et al., 2009). The genes involved in drought stress are divided into two types; the first is the functional proteins involved in cell protection during drought stress. This includes proteins involved in osmotic regulation, degradation, repair, detoxification and structural adaptation. The second are the proteins involved in the regulation of expression of genes related to drought responses such as protein kinases (protein kinases is a kinase enzyme that modifies other protein by adding phosphate groups (phosphorylation) to result in the a functional change in the target protein) and transcription factors (Shinozaki and Yamaguchi-Shinozaki, 2007, Valliyodan and Nguyen, 2006). See figure 1.7.

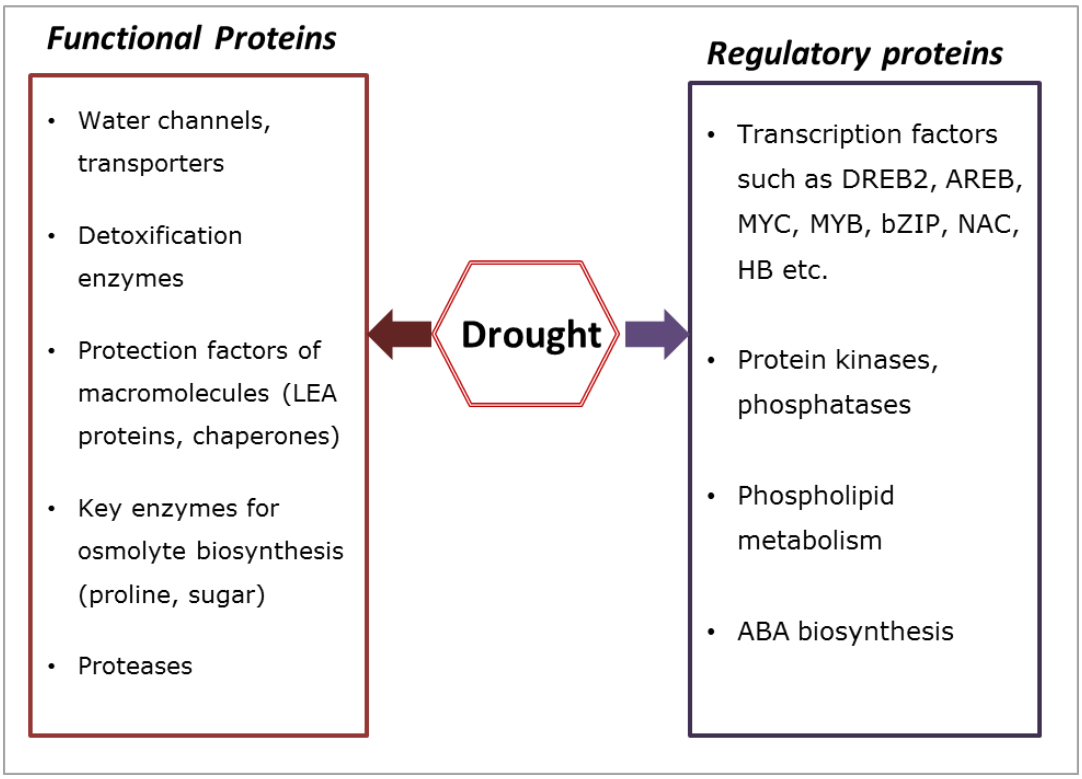

Fig 1.7 Drought stress-inducible gene are classified into two; functional protein and regulatory proteins. Source: Image created by author.

Transcription factors (*TF*) can be considered to be more promising for the enhancement of stress tolerance. Most of the TFs can regulate a wide range of target genes whose product may confer stress tolerant properties. This may be because many abiotic stress inducible genes contain two cis-acting

elements in their promoter region which interact with the TFs to regulate the stress-responsive genes. Examples of these cis-elements include dehydration-responsive element (*DRE*) and ABA – responsive element (*ABRE*), *NAC* (derived from three proteins; No Apical Meristem, ATAF1-2 and Cup-shaped Cotyledon) recognition sequence (*NACRS*) *ZFHD* recognition sequence (*ZFHDRS*) and MYCRS/MYBRS (Narusaka et al., 2003, Redillas et al., 2012). Hence, TFs have a superior advantage in engineering multi-gene drought tolerance over manipulation of individual proteins with specific protective function. These TFs regulate their target gene expression through binding to the related cis-element in the promoters of the stress-related genes. Over expression of TFs such as *bZIP, NAC, MYB, MYC,* zinc-finger, *WRKY* and *ERF* may prove to be a powerful approach to modify plant tolerance to abiotic stress (Quan et al., 2010). Recently, the overexpression of an ethylene responsive factor (*ERF*) transcription factor *TSRF1, TaSTRG, JERF* and *NAC1* resulted in drought/salt tolerance in rice (Quan et al., 2010, Zhou et al., 2009, Zhang et al., 2010a, Hu et al., 2006).

1.3.2.2 Genes and metabolites conferring drought tolerance

Several approaches have been developed to combat drought stress. One key approach is to over express a key TF to regulate the expression of stress related genes. Other approaches include the production of specific metabolic or physiological processes within the plant to escape or avoid drought (Yang et al., 2004, Swarup et al., 2005, Uga et al., 2013) (Doheny-Adams et al., 2012, Franks et al., 2015).

Chen et al. (2008) overexpressed the TF *OsDREB2A* which specifically interacts with C-repeat/DRE (A/GCCGAC) and is involved in ABA-independent gene expression in response to water stress and salinity. The results showed a significant improvement in the transgenic rice tolerance to water deficit. Similarly, another *ERF* transcription factor of the ERF class – *JERF1* that triggers and increases the biosynthesis of ABA in rice, has been shown to improve drought tolerance in rice (Zhang et al., 2010b). *Beta Carotene Hydroxylase* (BCH), has been shown to confers drought resistance in rice through the increase in the xanthophyll's cycle and ABA

synthesis (Du et al., 2010). Table 1.3 lists a number of genes that have been reported to improve drought tolerance.

Transgene	Notes	Source organism	Transformation method	Trait improved	Reference
SNAC 1		*Oryza sativa L.*	*Agrobacterium*	SNAC1 encodes a NAC TFs and is induced predominantly in guard cells under dehydration. They significantly enhanced drought tolerance	(Hu et al., 2006)
Os LEA-3-1		*Oryza sativa L.*	*Agrobacterium*	Transgenic plants shows increased yield under drought condition	(Xiao et al., 2007)
OsDREB2A	Rice gene with stress-inducible promoter (4ABRC)	*Oryza sativa L.*	*Agrobacterium*	Over expression of OsDREB2A significantly enhanced drought and salt tolerance of transgenic rice	(Cui et al., 2011)
OsDREB2A	Rice gene with stress-inducible promoter rd29A	*Oryza sativa L.*	*Agrobacterium*	Over expression of OsDREB2A significantly enhanced drought and salt tolerance of transgenic rice	(Mallikarjuna et al., 2011)
OsSDIR1		*Oryza sativa L.*	*Agrobacterium*	Over expression of OsSDIR1 gene significantly enhanced drought and salt tolerance	(Gao et al., 2011)
DSM2	It is a Beta carotene hydroxylase gene	*Oryza sativa L.*	*Agrobacterium*	DSM2 improves the biosynthesis of zeaxanthin. Over expression of DSM2 Significantly Improves Drought Resistance	(Du et al., 2010)

Table 1.2 List of transgenic lines produced in rice with enhanced drought tolerance. Table created by author.

The second target involves the development of specific metabolites, tissues or physiological processes that directly or indirectly improve drought tolerance. Such as roots (Yang et al., 2004, Swarup et al., 2005, Uga et al., 2013) and stomatal development (Doheny-Adams et al., 2012, Franks et al., 2015).

1.3.3 MORPHOLOGICAL CHANGES CAUSED BY DROUGHT STRESS

Plants show sign of stress in limited water condition either, when the water supply in the roots is limited or when transpiration rate by the plant is so high relative to the amount accumulated by the roots. When plants are beginning to experience stress, they respond through slow adjustment in

growth and development. A complex consequences of drought through reduced growth and development could be as a result of poor root development and poor leaf surface characteristics (such as shape, orientation, and composition of cuticular wax, leaf pubescence and leaf colour) that affects the amount of radiation received on leaf canopy and inhibition of stem reserves (Murchie et al., 1999, Blum, 2000, Burgess et al., 2017). Many other morphological changes have been reported in rice under drought stress. Drought induces adjustments/reduction in growth and development of rice (Fukai et al., 1999, Moldenhauer and Gibbons, 2003, Maclean et al., 2013). As drought progress, plant losses its turgor pressure, the cell becomes impaired, the cell enlargement and division are inhibited (Taiz and Zeiger, 2002, Jaleel et al., 2009). Plant height and the number of tillers reduce, and an overall reduction in biomass (including both roots and shoots) (Henry et al., 2012, Yang et al., 2012) and yield occurs (Moldenhauer and Gibbons, 2003, Ji et al., 2012).

1.3.3.1 Importance of the leaf in drought response

Leaf area increase contributes to canopy development. Canopy light interception is a function of the rates of leaf formation, expansion and abscission, density and arrangement in plants (Lopez et al., 1997, Hsiao and Xu, 2000). However, leaf area development is more sensitive to drought than leaf abscission. Depending on the severity of the drought, mild stress reduces leaf expansion to a greater extent than leaf formation with little damage by leaf senescence. Severe stress, on the other hand, reduces leaf area greatly with accelerated leaf senescence (Lopez et al., 1997).

The youngest fully most expanded leaf on the top of rice plant is termed 'flag leaf'. Top three leaves especially the flag leaf are considered the most important leaf in many cereal plants during flowering. It contributes most photoassimilate (relative to other individual leaves) to grain yield, greater carbohydrates translocation to the spikelet and large leaf area index (LAI) during grain filling stage (Al-Tahir, 2014). During drought, the uncompromised function of flag leaf is required to maintain synthesis and transport of photoassimilates. Various traits of the flag leaf have been proposed for the selection of drought tolerant varieties in rice, and studies

have shown a positive correlation between those flag leaf traits and yield under drought stress (Biswal and Kohli, 2013).

Leaf rolling is one the most common acclimation response in rice to drought caused by the closure of stomata, which is induced by altered osmotic pressure between internal and external tissues at varying level of dehydration (Price et al., 1997). This phenomenon is an adaptive response to helps plant maintain its internal water status (Jnandabhiram and Sailen Prasad, 2012). Under severe drought, the leaf rolling leads to reduced light interception in order to avoid water loss and radiation damage. (Murchie et al., 2002, Jnandabhiram and Sailen Prasad, 2012)

1.3.3.2 Role of stomata in response to drought stress

Stomata are microscopic pores on the surface of a leaf that are formed by a pair of specialized epidermal cells (called the guard cells), which are surrounded by subsidiary cells. This group of cells forms the stomatal complex (see Figure 1.8).

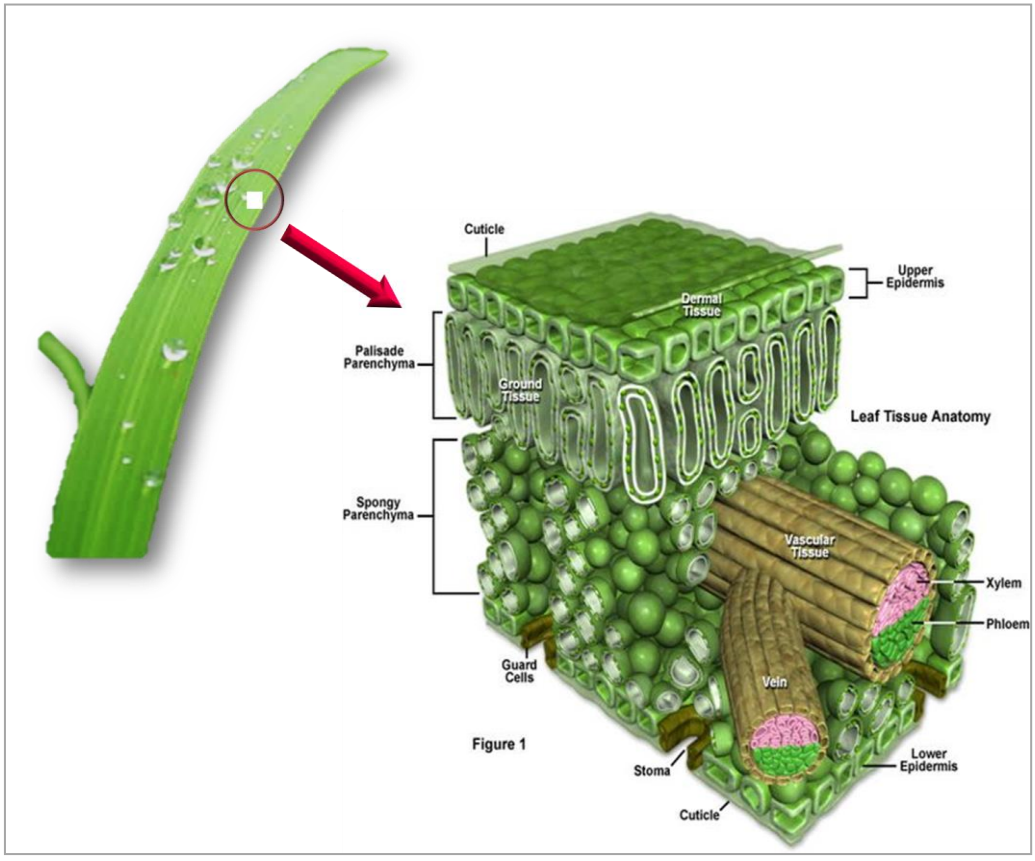

Figure 1.8. Schematic illustration of the leaf epidermal layer. Source: Image taken from Pinterest. https://www.pinterest.co.uk/trishasadiq/plants

The presence of the waxy impermeable layer on the epidermal surface makes the two guard cells surrounding the stoma act as a gateway that controls gas exchange (for photosynthesis) between the plant and the surrounding atmosphere (Sirichandra et al., 2009). Environmental factors such as drought, light intensity, CO_2 concentration, air humidity, salt stress, heat stress plant density or canopy density, as well as hormones have all been shown to affect the stomatal opening and closure (Hetherington and Woodward, 2003, Shimazaki et al., 2007, Galmés et al., 2007). A plant hormone called abscisic acid (ABA) is considered the major player in the regulation of stomatal movements whose function depends on the biological appropriate level of the active ABA within the cell. It plays a major role in the control of plant development and in the responses to various abiotic stresses (Leckie et al., 1998). ABA has been the focus of many research groups since the early 90s, especially in the control of transpiration against drought condition (Zhang et al., 2006, Zheng et al., 2009).

1.3.3.3 Stomatal movement

The opening and closure of stomata are regulated by the osmotic pressure that requires increase or decrease in the turgor of the guard cells. The changes in the turgor of the guard cells were attributed to dynamics in the proportion of intercellular concentration starch and malate (Taiz and Zeiger, 2002). The mechanism of guard cells interacting with the environment starts from sensing biotic and abiotic stimuli and signals coming from both the roots and the atmosphere. The cells then respond with appropriate changes in the turgor (Araújo et al., 2011). Through this mechanism, the guard cells control the stomatal opening in response to the environmental condition to preserve or control CO_2 and water flux. The response of the plant to water shortage is the utilisation of CO_2 gain through the stomata while minimising water loss (Price et al., 2002b).

1.3.3.4 Regulations of stomatal opening and closing

The opening of stomatal involves the activation of H^+ ATPases in the plasma membrane of guard cells. The activated H^+ ATPases induces K^+ uptake. The

influx of the ions (K^+, Cl^-, NO_3^-) and production of malate from osmotically inactive starch lead to an increase in tugor of the guard cells which then induces the opening of the stomata (Kim et al., 2010).There are several mechanisms and signalling pathways associated with the closure of stomata and are broadly divided into passive and active. The former (passive), occurs when the balance between the water losses by transpiration outweighs the water movement into the cells. The water content of the cells reduced to the point where to osmotic pressure drops, the cell loses turgor and pressure. At this point, the guard cells are unable to maintain firmness and shape; the stomatal pore becomes smaller (Luan, 2002). The latter (active) therefore, occurs through ion and water transport through protein channel across the plasma and vacuole membrane. The guard cells sense an increased level of ABA, the water level and the turgor are reduced by the efflux of (anions and potassium, K^+) ions by the conversion of malate into starch, causing the stomatal closure. The ABA triggers the increase and sensitivity of cytosolic (Ca^{2+}) which activates two anion channels (Kim et al., 2010).

The opening and closure of stomata in the physiological point of view is driven by a number of external environmental and internal signalling cues among various different species. Stomata open in response to light, low CO_2 concentration, high humidity, high temperature, and low vapour pressure deficit (VPD). Stomatal closure is driven by the opposite factors that enhance the stomatal opening (Lawson and Blatt, 2014). Stomata must respond optimally to a hierarchy of environmental signals in order to meet the stomatal conductance (*gs*) with the demands of CO_2 assimilation (*A*). However, stomata may respond differently in naturally fluctuating environmental conditions where photosynthetic responses do not synchronise with the stomatal responses. Thus, uncoupling of the synchronisation between the *gs* and *A* results, temporal (patch stomatal behaviour) and spatial variation in gas exchange. Such disconnect between the *gs* and the *A* can result in the period when the A is limited due to low CO_2 uptake caused by low gs (Lawson et al., 2012). This process is called the stomatal limitation.

1.3.3.5 Variability of stomata among species and its response to environmental variables

Stomatal aperture responds negatively with an increase in the ambient CO_2 concentration and vice versa. In a temporary or short-term exposure to CO_2 concentration, the response can be reversible and is considered among several feedback mechanisms regulating leaf gas exchange. Conversely, long-term elevated ambient CO_2 exposure, results in permanent downregulation of stomatal conductance. In this situation, the mature leaf senses the ambient CO_2 concentration and then transmit the signal to the epidermis for the regulation of the stomatal density in the developing leaves (Doheny-Adams et al., 2012).

More recently, another stomatal response to change in ambient CO_2 concentration was suggested apart from the aperture, and the density earlier mentioned; the stomatal size. Franks and Beerling (2009) have shown that the stomatal density and size can be altered by changes in the ambient CO_2 concentration. Leaves in the (current) period of low atmospheric CO_2 concentration in the prehistoric time are characterized by a high density of small-sized stomata, whereas those in the period with high atmospheric CO_2 concentration had a low density of large-sized stomata. In their work on fossil leaves based on fossil history of stomata under impoverished atmospheric CO_2 of the Permo-Carboniferous and Cenozoic glaciations, they discovered that high density of small-sized stomata could only be attained at low atmospheric CO_2 concentration. The pattern was reversed in elevated atmospheric CO_2 concentration. Similar results have been shown by Beerling and Chaloner (1992), Vanderburgh et al. (1993) Woodward and Kelly (1995), Tricker et al. (2005) (Doheny-Adams et al., 2012). It was concluded that regarding gas exchange, the small-sized stomata are expected to have shorter closing and opening response time. Therefore have greater control of water loss (Franks et al., 2009).

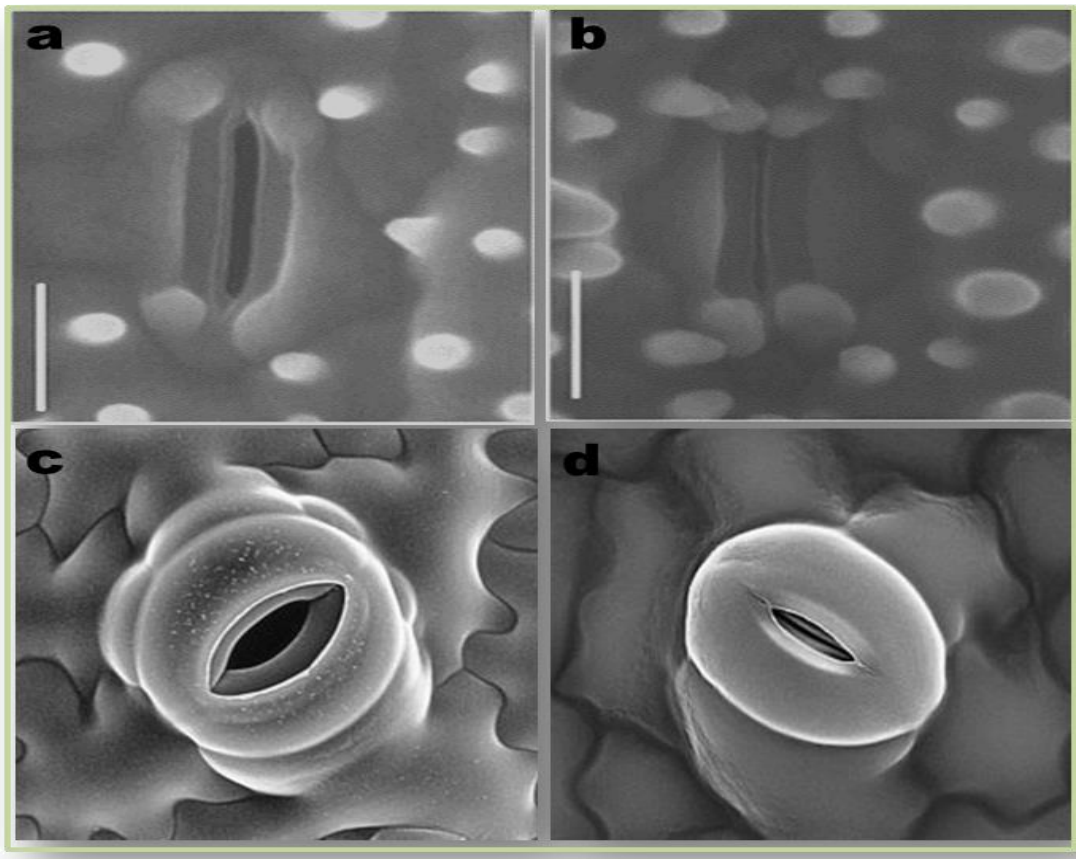

Figure 1.9. Two different types of stomata. Image **a** and **b** are opened and closed monocot stomata (rice). They have dumbbell shape with bulbous ends and has its pore as a long slit, **c** and **d** are opened and closed dicot stomata (Arabidopsis). They have a kidney-shaped with an elliptical contour with a pore in the centre. *Photograph credit: amended from Jeremy Burgess Science photo library*

Stomatal movement, size, density and other epidermal features may affect gas exchange quite remarkably in relationship to major environmental factors such as drought.

1.4 ROOT SYSTEM ARCHITECTURE (RSA)

Root systems are central to the acquisition of water and nutrients by plants. Root system architecture (RSA) determines the distribution of root surface area within the soil profile and so the plant's capacity to capture nutrients and water. These traits, therefore, have a direct bearing on crop productivity, particularly under conditions of low resource availability.

1.4.1 ROOT STRUCTURE FOR RICE

Rice, unlike *Arabidopsis*, has a fibrous root system like many other cereals such as maize. Rice roots are classified into five different types; radical (the first seminal roots, formed from the coleoptilar phytomer), embryonic crown roots (emerges from the coleoptilar node during the emergence of the first and second leaf), post-embryonic crown roots (also called nodal roots, emerges from the nodes at the base of the main stem and tillers), large lateral roots (arise from all roots types except small lateral roots and they grow downward in response to gravity) and small lateral roots (most numerous of all rice lateral roots and grows laterally in the soil) (Rebouillat et al., 2009)

When the seed germinates, the coleorhiza first emerges for a short period followed by the radicle roots which emerge from an embryo after breaking the covering. Two to three days after germination, the primary root is then joined by five embryonic crown roots which emerge from the coleoptilar node during the emergence of the first and second leaf. They grow rapidly until their length reaches 12cm. As the plant develops further, the nodal roots (also called the adventitious post-embryonic crown roots) arise from the nodes at the base of the main stem and tillers. This secondary root structure elongates deep into the soil thereby making the framework of the whole roots architecture (Rebouillat et al., 2009, Gowda et al., 2011a). When the nodal roots reach a certain size, the branching process starts by the growth of lateral roots from the root pericycle and epidermis. These comprise a greater proportion of the entire root system and are responsible for the greatest uptake of water and nutrients. They show indeterminate growth bearing small lateral roots that elongate laterally and large lateral roots which elongate downward thus responds to gravity (Rebouillat et al., 2009).

The mesocotyl roots are those that grow from the axis between the node of the coleoptile and the base of the radicle. They grow only when the seeds are sown deep or when the seeds are treated with chemicals.

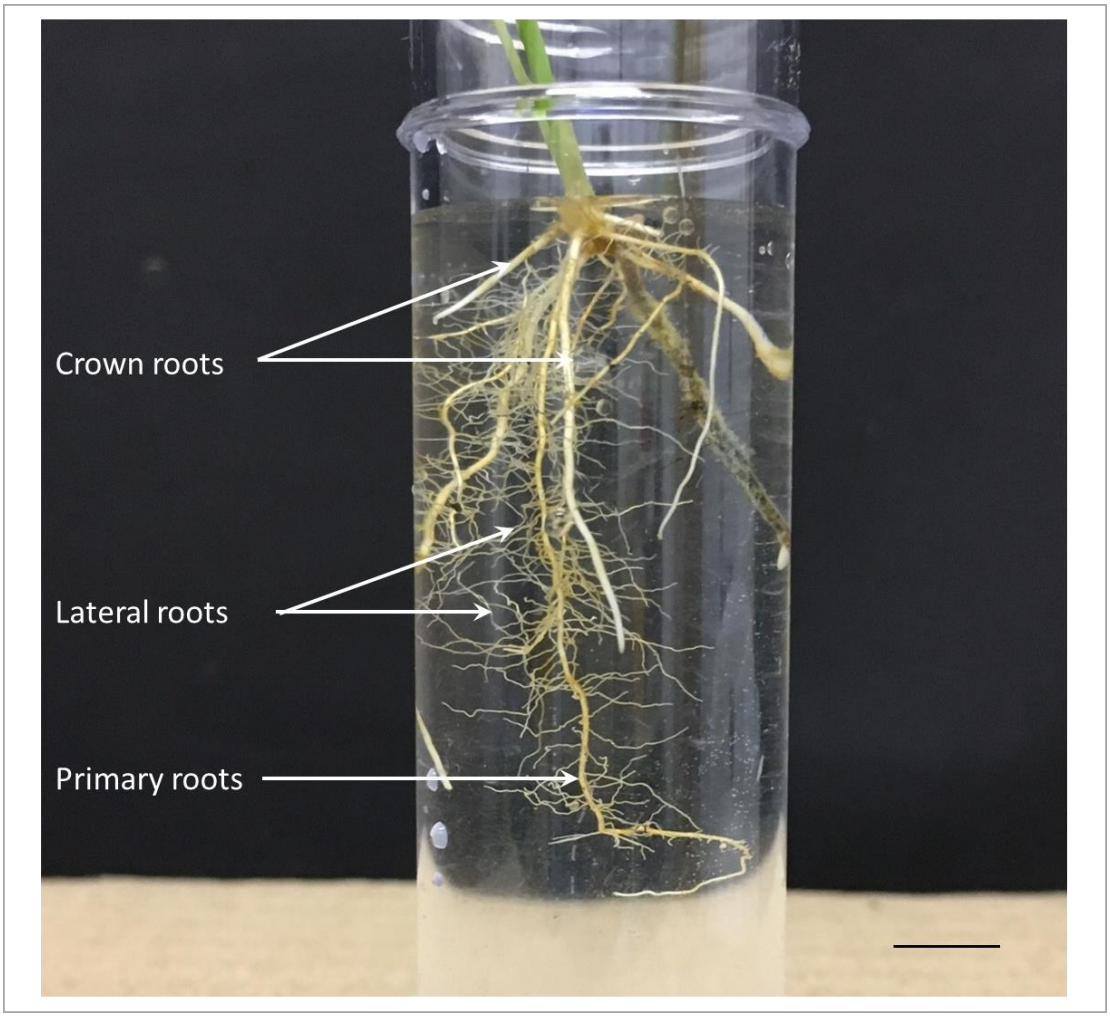

Fig 1.20. Labelled roots of 17-day old Nipponbare rice seedling. Scale bar is 1 cm. Source: authors photograph.

1.4.2 EFFECTS OF DROUGHT ON ROOTS

As mentioned earlier, roots are very critical for plant survival and an increase of yield under water stress. The structure and development of rice roots architecture strongly determine crop performance during water stress (Rebouillat et al., 2009). In a situation of mild water stress, plants maintain root growth by osmotic adjustment but the shoot growth is slowed. This is because there is an adjustment in the osmotic gradient that permits loosening ability of the cell wall, hence roots continue growing under low water potential. Conversely, the mechanism is not present in the leaf which consequently slows down or inhibits the growth of leaves (Hsiao and Xu, 2000).

Drought recovery is mentioned in some literature (Taiz and Zeiger, 2002). However, many of these mechanisms are associated with the shoots but roots are more closely associated with drought avoidance than any other mechanism. Cultivars with deep, coarse roots with high ability of branching and penetration along with elasticity in leaf rolling and early stomatal closure are best-described traits of drought avoidance (Samson et al., 2002). Roots with larger diameter have greater penetration ability, branching, large xylem vessel radii and lower axial resistance for water flux. This type of root may improve water acquisition in deep soil water level. However, root traits with small fine root diameters, long root length with considerable length density, at a soil depth of available water is associated with maintenance of plant productivity under water stress (Comas et al., 2013). In drought-prone environment, small xylem diameter in specific seminal roots saves soil water present in the deep soil profile for plant use during crop maturity. See figure 1.3.

Root Traits/Phenes	**Description**
Rooting depth	
Primary root length	Deeper roots provide plants with better access to stored water in the deeper layers of the soil substratum.
Root tip diameter	Root tips with large diameters have improved root penetration of hard, drying soils.
Gravitropism	Steeper root angles and more robust seedling gravitropic responses (which translates to deeper root systems) results in plants that are more tolerant to drought.
Root hairs	
Root hairs	Root hairs protect the water status of young root tissue.
	Root hairs improve root penetration of hard, drying soil.
Rhizosheaths	These protect the water status of young root tissues.
Root Branching	
Length and number of lateral roots (LRs)	Lateral roots are considered the most active portion of the root system for water uptake and represent the majority of the length and surface area of root systems in various types of plants.
Anatomical root traits	
Root cortical aerenchyma	Root cortical aerenchyma are induced by drought and nitrogen, phosphate or potassium limitation in maize. Their formation reduces respiration, nutrient content of root tissues and the metabolic cost of soil exploration.
Cortical cell file number and cell size	Reduced root cortical cell file number and large root cortical cell size improve maize drought tolerance.
Cell wall modification	Suberization/lignification affect radial water conductance, and may be important in reducing water loss from mature roots into dry soil.

Table 1.3. The relationship between root architectural traits and drought condition amended from Paez-Garcia et al. (2015).

Environmental factors and water management have shown to have a strong effect on rice root mass and root length density. Fang and colleagues (2013) found that rice root size is highly dependent on the available growing space, root penetration resistance (by any physio-chemical impediment) and the type of the competitor plants growing around. Due to environmental factors in different rice ecosystem, Upland rice develops longer root system compared to the lowland rice (Samson et al., 2002). The upland condition with well-drained soil allows water movement in the soil due to better aeration and that favours rice root elongation. Conversely, the anaerobic field condition of the lowland limits air diffusion which may consequently impede root elongation and a formation of root hairs (Fukai and Cooper, 1995, Kato et al., 2006). Deep rooting is considered a target trait for drought tolerance in rice breeding programme (Uga et al., 2013). Apart from the thick, coarse rooting nature of mostly drought tolerant upland rice cultivar, greater lateral roots growth has also been discovered to increase water uptake and yield in drought conditions (Henry et al., 2012).

1.4.3 RESPONSES OF RICE ROOTS UNDER DIFFERENT ECOSYSTEM

Upland rice is typically characterized by deep coarse root system with thick and tall stems and fewer tillers. In upland field during water stress, most of the water used by the plants is either the rain or the groundwater retained in the soil after rain. Advantages associated with coarse and deep root system depends on the duration of the drought period, availability and depth of the ground water and the rate of water uptake (Yoshida and Hasegawa, 1982, Kato et al., 2006, Kato et al., 2007). Various studies have been carried out on the upland root traits to combat drought stress in rice. Puckridge and O'Toole (1980) in their studies discovered that an upland rice cultivar; Kinandang Patong (KP) has a deep root and was able to extract water from a depth of about 40-70cm deep than a shallow lowland cultivars IR36 and IR20. Similar results were reported by Kondo et al. (2000), Kato et al. (2007) and Samejima and Tsunematsu (2016). On the contrary, other trends of studies have reported different responses of root growth to drought among upland rice cultivars which show growth

inhibition and promotion. Ghildyal and Tomar (1982) argued that roots are generally more likely to grow in the flooded field but not determined by varietal differences. Similarly, Cairns et al. (2004) and Kondo et al. (2000) demonstrated that the deep root development is affected by the soil condition.

Recently, Uga et al. (2011) improved the root system of a shallow rooted lowland cultivar IR64 to deep root system, through a cross with an upland Kinandang Patong (KP) cultivar. They discovered that the IR64 with the KP allele had significantly increased root dry weight in deep soil layer (25 -50 cm) than that of the IR64. Uga et al. (2013) later identified the locus responsible for deep root in KP and demonstrated that when this *DEEPER ROOT (DRO1)* gene was introduced in shallow rooted cultivars resulted in improved yield under drought condition.

Lowland rice cultivars are short and typified by with many tillers and a shallow rooting system. Drought tolerance mechanisms differ among the ecotype. The mechanisms exhibited by the uplands system may not be suitable for the lowland condition. This could be due to various factors such as, the anaerobic condition, hardpans (physical barriers), soil acidity/alkalinity/ salinity (chemical barriers), drought in soil with poor holding capacity and poor adaptation developed by the roots to anaerobic condition, then to sudden drought and aerobic condition. These could limit the effectiveness and function of a root to go into the deeper layer to extract water during water stress. Essentially, due to the unique soil water transition among the lowland condition from flooded and anaerobic to drought and the aerobic condition has significant consequences to root growth (Wade et al., 1999). Various results from a lowland experiments reported that large proportion of roots (about 69-94%) are located within the 10cm of the top soil layer, and very few go below 30cm .

1.4.4: EFFECT OF TEMPERATURE ON ROOT DEVELOPMENT UNDER WATER DEFICIT

Roots are extremely sensitive to high temperature and water deficit. High temperatures affect both root development and penetration. Batts et al. (1998) suggested that root growth diminished under high temperature due to the reduction in the amount of carbon channelled partitioned below

ground. They also observed a huge reduction in the number, length and diameter of roots at high temperatures, particularly during the reproductive stage. Drought, however, depending on the severity, promotes primary root development due to an increase in the carbon assimilates channelled to the roots but lateral roots are repressed (Rebouillat et al., 2009, Smith and De Smet, 2012). Through a canopy temperature study observed that cool temperatures promote deeper rooting allowing the extraction of more water when compared with high temperature. Heat leads to the concentration of roots at the surface layer of the soil where water was more available from surface irrigation.

1.4.5 ROOT SCREENING FOR DROUGHT TOLERANCE

Genetic differences in water uptake in drought stressed rice is thought to be due in part to root architecture and root function (Henry et al., 2012). There are various screening methods used to identify important root traits that are linked with drought tolerance in rice. Many studies restricted their analysis to a set of morphological parameters in which trait can be functionally characterized. Root length and dry masses are the common direct root evaluation parameters that are used to predict yield, nutrients assimilation and stress tolerance in rice (Fageria and Moreira, 2011, Shashidhar et al., 2012). Root pulling resistance is also an interesting drought tolerant trait that is highly correlated with length, thickness and branching of the root. Summarized in Table 1.2.

Root traits	Functional Characteristics
Maximum root depth	Potential for absorption of soil moisture and nutrients in deeper soil layer
Root to shoot ratio	Assimilates are allocated between the different components
Root volume	The ability to permeate a large volume of soil
Root number	Physical strength, potential for root system architecture
Root diameter	Potential for penetration ability, branching, hydraulic conductivity
Deep root to shoot ratio	Vertical root growth, potential for absorption of soil moisture and nutrient in deeper soil layers
Root length/weight density	Rate at which water and nutrient are assimilated
Root branching	Power of soil exploration (the major contribution to total root length)
Total root length/surface area	Total root system size: the size of contact with soil (major determinant for water and nutrient uptake as an entire root system)
Specific root length	Degree of branching, density of root materials, porosity due to aerenchyma development
Hardpan penetration ability	Ability to penetrate subsurface hardpans

Table 1.4. The morphological root traits and their functional characteristics used in root phenotyping amended from Gowda et al 2011.

Other modern techniques used in the study of root architecture includes the two dimensional (2D) quantification approaches (Pierret et al., 2003, Adu et al., 2014) and three dimensional (3D) quantification systems such as the minirhizotrons, X-ray computed tomography (CT) (Mairhofer et al., 2013), digital cameras, ground-penetrating radar, 3D laser scanning etc.

1.5 RICE TRANSFORMATION

About two decades ago, the first successful rice transformation using *Agrobacterium tumefaciens* was reported by Chan et al. (1993). They obtained few transgenic rice plants by inoculating the immature embryo with Agrobacterium. Progeny from only one plant was ascertained to have inherited the transfer DNA through southern blot hybridization. A year later, Hiei et al. (1994) reported an *Agrobacterium* mediated transformation with higher efficiency in the production of transgenic rice plants with fertile and heritable traits. He developed an efficient

transformation protocol which was adopted and improved for the production of genetically stable transgenic rice genotypes (*indica* and *japonica*) within a short period of time (Toki, 1997) and with higher regeneration efficiency (Toki, 1997, Chen et al., 2004, Saika and Toki, 2010). The amendments centred around using different explants (Arockiasamy and Ignacimuthu, 2007, Saika and Toki, 2010) or composition of culture medium, different gelling agent (Sahoo et al., 2011) and different *Agrobacterium* strains to improve transformation efficiency. Yet, the protocol suffers one setback or the other.

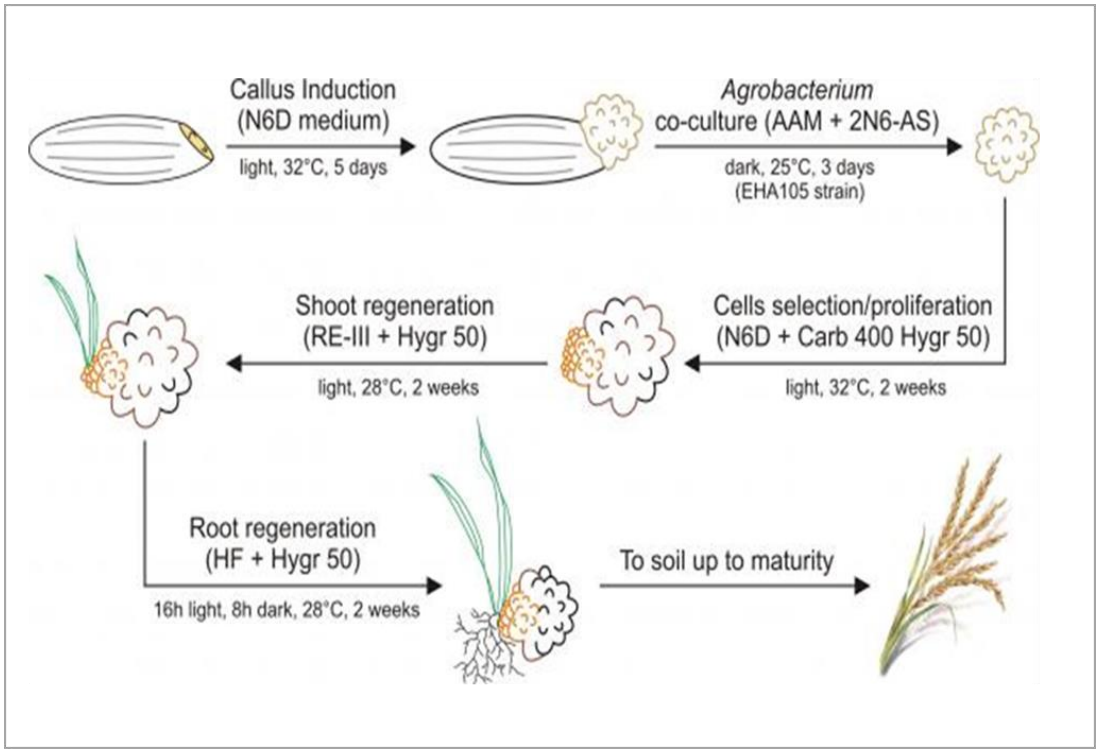

Fig 1.7. Schematic illustration of the *Agrobacterium* mediate rice transformation method. Image taken from Toki et al. (2006)

One of the challenges in rice transformation is that the response of seeds to callus formation is very much dependent on the genotype. The theory, however, is that any seed capable of germinating can be used (Hiei and Komari, 2008). For certain *japonica* cultivars such as Nipponbare, the preparation is straight forward and reproducible (Hervé and Kayano, 2006, Toki et al., 2006, Jian-Jun et al., 2009, Wagiran et al., 2010). Conversely, many *indica* varieties (e.g. IR64) are calcitrant to callus induction and slightly difficult for transformation (Sahoo et al., 2011). Frequently, the

culture medium for one genotype may not work for another. Similarly, a technique developed in one laboratory may not work in another laboratory.

AIMS AND OBJECTIVES

- To determine the variation in photosynthesis, water loss and root structure of a diversity panel of African rice genotypes
- To establish a suitable and efficient *Agrobacterium*-mediated rice transformation protocol applicable to the selected genotypes.
- To create transgenic lines by manipulation of leaf stomatal density using the *EPIDERMAL PATTERNING FACTOR (EPF)* genes overexpression.
- To investigate the effect of the stomatal number on the rate of transpiration to manipulate water use efficiency and improve drought tolerance.
- To create transgenic lines bearing the motif of ERFVII signature as a sensor to of N-end rule pathway
- To investigate the role of N-end rule pathway as a sensor of drought stress in rice.

CHAPTER TWO: MATERIALS AND METHODS

2.1 PLANT MATERIAL

The plant material used for this study was rice (both *Oryza sativa* and O. *glaberimma*) species. For the chapter 3 experiment, the genotypes used are the combination of different African rice genotypes. They include NERICA 2, NERICA 6, NERICA 7, NERICA 8, NERICA L41, WAB56-104, WAB759-55-22-HB, WAB 181-18, Faro 52 and CG14 (*O. glaberimma*); Moroberekan, Kaybonnet, IR64 and IR4630-22-2-5-1-3 (Magic Line 4) are used for the check. The seeds used were obtained from Consultative Group on International Agricultural Research (CGIAR), Benin Republic; National Cereal Research Institute (NCRI), Nigeria; and the University of Nottingham.The experiments of chapters 4 to 6 were performed with transgenic rice from *Oryza sativa* L. japonica Nipponbare background created for the study. The rice material used for chapter 7 where the transgenic *O. sativa* L. Japonica of Kaybonnet and Nipponbare background also created for the study. More detail on the plant material is given in each chapter.

2.2 GROWTH CONDITIONS

Some of the experiments took place in a south-facing glasshouse at Sutton Bonington campus, University of Nottingham (52°49'59"N, 1°14'50"W). Supplementary sodium lamp (Son T-Agro, Phillips) was supplied at a position of approximately 3m above ground level and was regulated via a light sensor external to the glasshouse such that it was activated only when external irradiance fell below approximately 200μmol m^{-2} s^{-1} and inactivated when this was exceeded. A time delay of approximately 15 minutes was used before switching back on. In this way, periods of low light were supplemented and excessive combinations of sunlight and artificial lighting avoided. Photoperiod in the glasshouse was regulated to 12 hours using automated black out blinds (07:00-19:00). The temperature in the glasshouse was regulated to 28°C ± 3°C

by automated venting and two gas-fired boilers. Humidity in the glasshouse was not regulated and varied between 60 and 70%. For other experiments, plant growth took the plant in a growth room at the old workshop, South Laboratory Annexe, Sutton Bonington Campus, University of Nottingham. The growth room was supplemented with 400W metal halide lamps (Siemens, UK; bulbs Osram, Germany) and were positioned with adjustable lamp holder. The temperatures during the light and dark period were set to 28°C and 26°C, respectively. The Photoperiod was set to 12/12 hours.

2.2.1 Polyvinyl chloride (PVC) column construction

The Polyvinyl chloride (PVC) columns were constructed from commercially available piping with 15-cm diameter and cut to be 100 cm long. Each tube was cut lengthwise forming two identical parts which were then sealed back together with parcel tape to re-form the pipe (column) within which was filled with growing medium. This allowed the column to be dismantled for easy access to roots at the end of the experiment. A 2-mm sized mesh was attached at the bottom of each column to allow free flow of water but retain the growing medium. The columns were stacked together into groups of 24, held together by a metal scaffold (Figure 2.1).

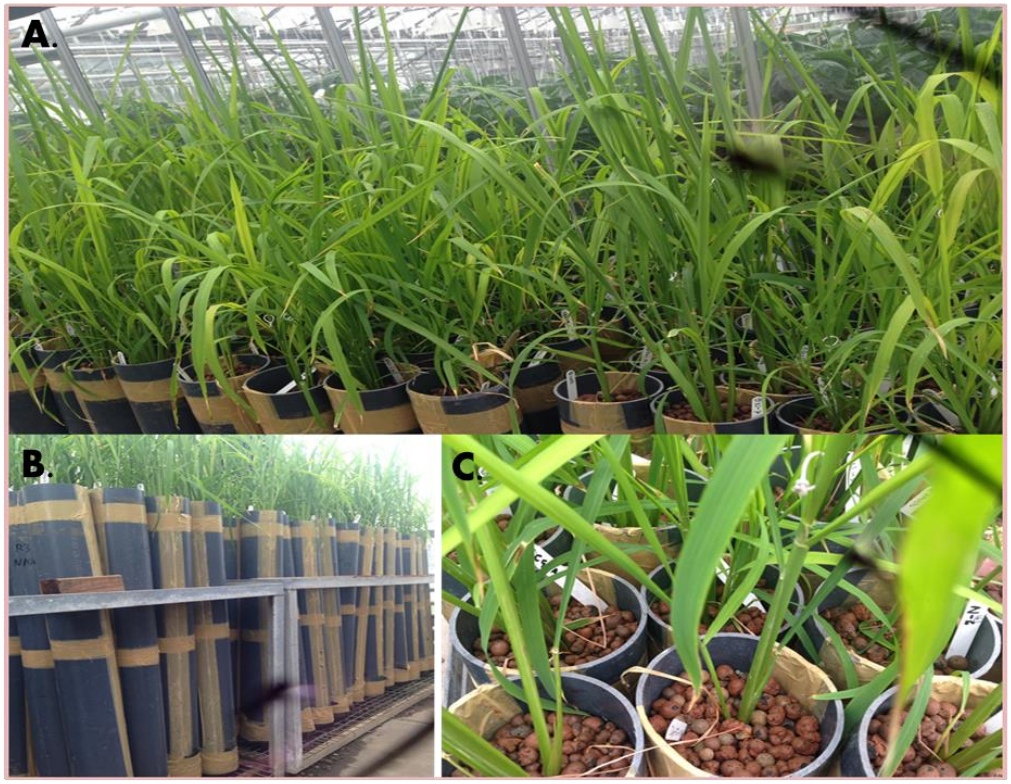

Figure 2.1 The PVC columns containing expanded clays as growing media stacked together by a metal scaffold.

2.2.2 Growth media

Three growth media were used in this study.

- Expanded clay pebbles (hydroleca): Hydroleca pebbles are a light-weight clay aggregate made from special clay minerals and can absorb up to 40% of their own weight in water but have limited water and nutrient retention. The size used was the 8-10-mm diameter and were used in the column experiment (see Figure 2.1 C).
- Compost: Rice growth compost with a combination of growth compost of 1:1 (w:w) ratio of John Inns No1 (John Inness, Norwich UK): Levington M3 (JFC Monro, Devon, UK) was used in all pots experiments. The size of pots used ranged from 1- 5 L depending on the age and the type of the experiment and 6 – 10 pots placed on a tray (depending on the experiment).
- Hydroponic media: The hydroponic media solution protocol was adapted from Makino et al. (1985), modified by Murchie et al. (2005). The table

2.1 showed the composition of the nutrients compounds formed and the concentrations used from the stock to form the 3 separation solutions. The hydroponic solution was formed in 20L tubs and the pH was adjusted to 5.5 with Hydrochloric acid (HCl). The stock solutions prepared were stored in the fridge until needed. All but one (Fe-EDTA) of the chemical compounds in table 2.1 were supplied by Fisher Scientific, UK. The Fe-EDTA was supplied by Sigma-Aldrich, UK.

Element Required	Compound Used	[Stock Solotion] Mol	Concentrated Nutrient Solution (ml Stock solution per l)	ml concentrated nutrient solution per 20l hydroponic container
N	NH_4NO_3	4.28536	80	
P	$NaH_2PO_4.2H_2O$	0.85571	166	
K	K_2SO_4	0.38377	312	
Mg, S	$MgSO_4$	1.20497	160	
Mn	$MnCl_2.4H_2O$	0.05457	40	75
Mo, N	$(NH_4)6Mo_7O_{24}.4H_2O$	0.00045	54	
B	H_3BO_3	0.55636	16	
Cu, S	$CuSO_4.5H_2O$	0.00192	40	
Zn	$ZnSO_4.7H_2O$	0.00900	20	
Ca	$CaCl_2.6H_2O$	1.50000		8
Fe	Fe-EDTA	0.17488		8

Table 2.1. The ingredients of the hydroponic solution

2.2.3 Seed Germination

2.2.3.1 Module tray germination

Seeds were directly germinated in a module tray containing rice growth compost of a mixture of 1:1 (w:w) ratio of John Inns No1 (John Inness, Norwich UK): Levington M3 (JFC Monro, Devon, UK) for 8 - 12 days in the glasshouse. The uniformly sized seedlings were selected for transplants

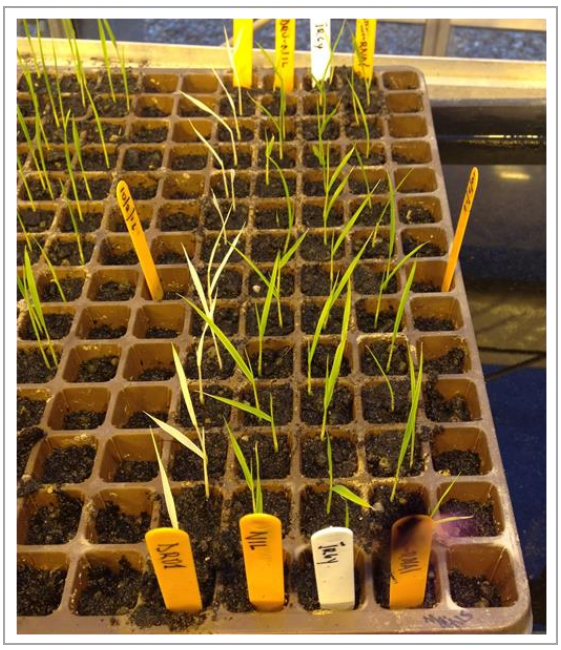

Figure 2.2. Seeds germinating in module tray

2.2.3.2 Petri dish germination

Seeds were thoroughly washed with distilled water and were germinated in the 9cm diameter Petri dishes on a damp filter paper (Whatman) for 3 to 5 days in the growth room. The Petri dishes were sealed with paraffin film or surgical tape to prevent seed contamination and loss of water. This type of germination was used for the hydroponic system. By the emergence of the second leaf, the seedling was temporarily transferred into the hydronic media on a polystyrene for 10-12 days until the shoots they are about 6-7cm height. At the 6-7cm height, the seedling was then

transferred onto a drilled light weighting PVC foam support with 2cm diameter holes. The seedlings were supported in the holes with a foam.

2.3 WATER STRESS AND TREATMENT

The plants the in experiments of chapters 3, 5 and 7 were subjected to drought stress by withholding irrigation for a certain period of time, depending on the plant age and the purpose of the experiment, to achieve moderate or severe drought stress. More details are provided in the individual chapters.

2.4 MEASUREMENTS

2.4.1 Growth development assessment

One week after transplanting, the numbers of leaves and tillers were monitored every day to assess the genetic variability in growth development in both well-watered and in drought stress. The number of leaf assessment began a week after transplant from the module tray or from the Petri dish when the primary and the secondary leaf were fully established. Light wire rings were placed on new emerging leaf every other day for easy identification of the main tiller and the number of leaves developed from the last count. The number of tillers were counted every day, at the same time as a leaf number assessment was taken. Usually, rice plants have a main tiller and then primary and secondary tillers which are considered physiogically similar to the primary, but that is strongly dependent on the genotype. Tillers were counted every other day by counting all the developed tillers excluding the main stalk. The tiller number count ran through the drought stress period in order to assess the genetic differences between the lines/ecotype to drought tolerance.

2.4.2 Soil water status and Relative Water Content (RWC)

This level of available water in the compost was measured using the theta-probe from Delta T (Cambridge, UK) with three pin sensors. Immediately after the onset of drought stress, the theta-probe was inserted to the soil compost within a minimum of three different positions

within the pot. The theta probe was pre-calibrated for compost and so data was collected in m^3/m^3 mineral water content, which served as a proxy for the available water content in the soil compost.

The relative water content method of Weatherly (1950), modified by Weatherly and Barrs (1962), was partially destructive because it involves the collection of leaf tissue. A 0.5cm diameter Leaf disk or $1cm^2$, depending on the age of the leaf leaf material was collected at a different point of drought stress to assess the amount of water present in the leaf. The collected leaf tissue was immediately weighed on a sensitive weigh balance and recorded as the fresh weight (FW). The weighed leaf tissues were then immersed in water in a well-labelled falcon tube for 4-6 hours. The weight was re-taken and the were recorded as turgid or saturated weight (TW). Finally, the tissues were then oven dried at 80°C overnight to record the dry weight (DW).

The RWC was calculated as:

$$RWC = \left(\frac{(Fresh\ weight - Dry\ weight)}{(Turgid\ weight - Dry\ weight)} \right) X\ 100 \qquad [1]$$

2.4.3 Leaf Gas Exchange measurements and Chlorophyll fluorescence

2.4.3.1 Infrared Gas Analyser (IRGA) overview

The most commonly used single-point measurements generated by the IRGAs are CO_2 assimilation (*A*), stomatal conductance to water vapour (*gs*), transpiration rate (*E*), leaf internal CO_2 concentration (C_i), and vapour pressure deficit (VPD) (Johnson and Murchie, 2011). The leaf gas exchange measurements were carried out with an open circuit IRGA, Licor 6400XT (Lincoln, Nebraska, USA). The system works based on the differences in the CO_2 and H_2O between a reference line and the leaf cuvette (leaf sample) and with flow rate, which is used to calculate the flux in CO_2 and H_2O per unit leaf area. Any given change from the

differences of air flow rate and the leaf surface, the *A* is automatically calculated and expressed in μmol CO_2 $m^{-2}s^{-1}$ (see equation 2). similarly, the change in water level of the air stream within the cuvette is determined as the *E* and expressed in mmol H_2O $m^{-2}s^{-1}$ (see equation 3).

$$A = \frac{\text{Flow rate} \times \Delta CO_2}{\text{Leaf Area}} \quad [2]$$

$$E = \frac{\text{Flow rate} \times \Delta H_2O}{\text{Leaf Area}} \quad [3]$$

The gs was obtained from the total conductance by removing the contribution from the boundary layer conductance, which depends on the presence of stomata on one or both sides of the leaf. Whereas the internal C_i is derived from the simultaneous measurement of *A* and *gs*, using the Fick's first law of diffusion.

$$C_i = C_a - \left(\frac{A}{gs}\right) \quad [4]$$

Where C_a is the ambient CO_2 concentration.

The Chlorophyll fluorescence measurements were made with the fluorescence chamber head (Licor-6400XT leaf chamber fluorometer) integrated into the Licor. The fluorescence chamber is composed of three different light sources; modulated red and blue actinic, saturating flash lights, and infrared light to excite PSI. the light source (light emitting diode, LED) generates a pulse light that induces a pulse fluorescence on the leaf sample that is electronically identified and amplified.

2.4.3.2 Instantaneous gas exchange measurement (P_{max})

Measurements were made on a fully expanded flag leaf utilising a method for measuring the leaf area by recording leaf width, calculating the leaf area taking into account the circular shape of the cuvette window and entering this value of leaf area into the device software prior to measurement so that relevant area-based parameters could be calculated in real time. The photosynthetically active radiation (PAR) was supplied at 2000 μmol m^{-2} s^{-1} (glasshouse experiment) and 1500 μmol m^{-2} s^{-1} (growth room experiment) of saturated red LED light with an additional 10% blue LED to induce maximal stomatal opening. The reference CO_2 concentration (C_a) was set to 400 μmol mol^{-1} in the cuvette and the relative humidity of the incoming air was controlled in the cuvette in all the experiment, ranging between 10 – 65% depending on the type of experiment. The cuvette block temperature was maintained at 30°C in the glasshouse experiment and 28°C in the growth room experiments. The flow rate of gas was also set to 500μmol s^{-1} and the cuvette fan was made to work at maximum speed (FAST). Vapour pressure deficit (VPD) was not controlled but was measured. Each leaf was exposed to the constant CO_2 and PAR for a maximum of three minutes and a minimum of 2 minutes to allow the rate of photosynthesis to stabilize. At the end of every measurement, the reference and the analysis flux were matched before next measurement.

2.4.3.3 Intrinsic and instantaneous leaf water use efficiency (WUE)

Instantaneous measurements of the net *A, E* and *gs* obtained from the instantaneous gas exchange measurements allowed determination of both the intrinsic and instantaneous water use efficiency at leaf level from the ratio between A/gs (equation 6) and A/E (equation 5) respectively.

$$WUE_{instantanous} = \left(\frac{A}{E}\right) \quad [5]$$

$$WUE_{intrinsic} = \left(\frac{A}{gs}\right) \quad [6]$$

2.4.3.4 Photosynthetic intercellular CO_2 response curve (AC_i curve)

The response of *A* to external CO_2 concentrations was assessed on the fully expanded flag leaf. The leaves were placed in the cuvette of the IRGA. Leaf temperature was controlled at 30°C and 28°C (depending on the experiment). The light photon flux was set to 1000µmol m^{-2} s^{-1}, reference CO_2 to 400 µmol mol^{-1} until *A* reached the steady state. The light was increased to 2000 and 1500 µmol m^{-2} s^{-1}, depending on the experiment. When *A* reached a stable state at the new light level, the CO_2 concentration was then set in stepwise sequence starting from 400, 300, 200, 100, 400, 400, 600, 800, 1000, 1200, 1500 then 400 µmol mol^{-1}. Each step was allowed for 3 minutes for *A* to stablise before the measurement was automatically recorded. The potential Rubisco carboxylation rate (V_{cmax}) and maximum rate of electron transport (J_{max}) were derived from the *A vs Ci* response curve using the curve fitting model by Farquhar *et al* (1980) modified by Long and Bernacchi (2003) corrected with 25°C temperature.

The changes in *A* to CO_2 concentrations around the leaf (*ACi* curves) are used to determine the photosynthetic limitations (Long and Bernacchi, 2003, Sharkey et al., 2007). The curve is divided into three phases (as described in chapter one); at low Ci concentrations, response is linear and it refers to maximum Rubisco activity. The second phase is the maximum electron transport rate (RuBP-regeneration) and the last phase is constant or decline of A with increase in Ci, and is being limited by the utilization of triose-phosphate (*TPU*)

Stomatal limitation (L_s) at the current ambient CO_2 concentration is 400 µmol mol^{-1} was derived from the *A vs Ci* response curve which is the proportion of *A* limited by gs described by Long and Bernacchi (2003).

2.4.3.5 Photosynthetic light response curve (LRC)

Measurements were made on fully expanded flag leaf with its area recorded in the machine. Leaves were placed in the Licor XT-6400 cuvette and were allowed to adapt to the incident PAR of 2000 and 1500 µmol m^{-2} s^{-1}, depending on the experiment with reference CO_2 concentration of 400 µmol mol^{-1} and block temperature controlled to 30 and 28°C. After the stability was maintained automatically, the photon flux was set in a step wise manner, starting from low to high; 0, 50, 100, 200, 300, 450, 600, 800, 1000, 1200, 1500, 2000*µmol m^{-2} s^{-1}. At each light level, once a steady state was achieved, the gas exchange and chlorophyll fluorescence rates were recorded.

The light response to *A* curve was achieved as described by a four-parameter non-rectangular hyperbola, according to Marshall and Biscoe (1980)

$$A = \frac{\phi_{max} I + A_{sat} - \sqrt{[(\phi_{max} I + A_{sat})^2 - 4\theta\phi_{max} I A_{sat}]}}{2\theta} - R_d \qquad [7]$$

Where A is the CO2 assimilation rate, ϕ_{max} is the apparent maximum quantum yield, I is the photon flux, A_{sat} is the A at saturating I, θ is the curve convexity and R_d is the mitochondrial respiration in the light. The Light compensation point (LCP) was determined as the I where A=0 as predicted from the fitted curve.

2.4.4 Canopy temperature

The canopy temperature was examined through thermography. The canopy temperature was remotely measured using infrared Camera FLIR C2 (Flir systems USA) in the glasshouse. The position was approximately 1m away from the plant material and 0.5m above the leaves. Infrared images of the plants were taken from different angles behind a black

curtain (as a screen) in the glasshouse. Around 60 -70 infrared images of all plants were taken in all experiments each time, depending on the experiment. The photograph always started in early hours of the morning (3-4 hours from the beginning of the daylight). The infrared images were taken in the comparison between treatments and genotypes. The camera was very sensitive and had a very good thermal accuracy (~0.08^{o}C and accuracy of ±2 ^{o}C). To minimize error with the variability of temperature in the glasshouse over time, the air temperature was collected automatically from the Tinytag ULTRA 2 (TGU-4500) located just above the plants in a disposable paper cup. The Tinytag was programmed to record air temperature and relative humidity every ten minutes.

2.4.5 Stomatal analysis: leaf impression, stomatal cell count and Light microscopy

Dentistry resin Coltene President Plus Jet (Colten Whaledent, Switzerland) was applied to both leaf surfaces on a fully expanded leaf at the widest point. A nail vanishes peels were taken from the set resin with the leaf impression to give a replica of the leaf impression. The painted portion was covered with a transparent parcel tape of about an inch and then carefully peeled and then placed over a clear microscope slide Stomatal cell counts were taken in four different positions (midrib and leaf margin) per single impression examined under Light Microscope (Leica, Wetzlar Germany) at 20X magnification. The total number of stomata counted within the area of the field of view was calculated per square millimetre (mm^{-2}). Five to six plants per line and four areas per leaf were examined.

2.4.5.1 Stomatal size

The stomatal size was calculated from the stomatal impression obtained in section 2.4.5 but examined under X40 magnification. The image of each view point was taken with scale bar on each image. The images collected were then uploaded to ImageJ (IMAGEJ software version 1.49). The scale was set from the available scale bar on each image, then the width and the length of each stoma was taken and multiplied to give the area of stomata.

2.4.6 Total leaf Area

The total leaf area was measured using the Licor (LI-3100C Area Meter). The measurement was taken straight ahead after harvest. The leaves were separated from the stalk and measured individually using the manufacturer's user guide. The total area of the stalks was also collected.

2.5 ROOT EXTRACTION AND ANALYSIS

2.5.1 Root extraction

Roots were harvested at the end of an experiment, either the column or the hydroponic. For column experiment, a column was laid on a bench with mesh wire top. Underneath the table, a large polyene mat >2 m^2 was spread, and a large dustbin was placed on top of the polyethene bag to ease the collection of the hydroleca. The parcel tape holding the column together was cut open. The maximum root depth was recorded. The roots were sectioned at different depths to provide a range of different diameter, branching and shapes of the root. The first top 10cm, 15cm then followed by the remaining depth were collected. Each section was carefully cut, separated from the hydroleca and placed in a big tray containing water for washing. The procedure was conducted cautiously to prevent supplementary root damage and losses. After washing, each root section was stored and freeze in a plastic tube, labelled and contained water (with 30% ethanol in some experiments) until use.
For hydroponically grown plants, the roots were harvested and stored directly in large plastic containers without sectioning and frozen until use.

2.5.2 Root analysis: WinRHIZO

The roots harvested in section 2.5.1 were thawed gently and rinsed multiple times with running water. The roots were carefully spread in a thin layer of water (4 – 5 mm) on a transparent tray (30 X 40cm) and scanned. The commercial software package WinRHIZO v6.1 uses a skeletonisation method for measuring the root parameters. The program operates with 256 levels of grayscale images in TIFF file format,

which were converted into binary and skeleton images. The threshold binary images were used by the system to evaluate the root diameter, and the root length was measured by the skeleton images (Himmelbauer, 2004). Measurements involved: total root length, average root diameter, surface area, root volume, root length and area measurements as a function of different root diameter classes.

2.5.3 Root Anatomy: Sectioning and Confocal microscopy

Rice plants growing in hydroponic medium (section 2.2.2) identified for root sectioning (age determined with the type experiment) were cautiously collected in Falcon tubes containing water. The roots collected and embedded in agarose block (5% v/v in water) and position for sections was carefully marked and recorded. Transverse root sections (150 -180 μm) were obtained using an HM 650 V vibratome (Microm), and sections were stained with calcofluor (Sigma-Aldrich, Co. Ltd) for 2-3mins and then observed directly under the confocal laser scanning microscope (Nikon Instruments).

2.5.3.1 Analysis of Root analysis: RootScan2 and Phiv-RootCell

The roots sections examined under the microscope were analysed for root anatomical parameter as described by Lartaud et al. (2014) (Phiv plugin with the ImageJ software) or aerenchyma (Rootscan2) using the user manual guide.

2.6 TRANSFORMATION OF MATURED RICE SEED

Media Name	Media type	Chemical compounds	pH	Temperature
YEP	Broth	10g/L Yeast extract, 10g/L bacto-peptone and 5g/L NaCl	7.0	
IM	Infection medium	4.2g/L of MS basal salt, 68g/L of sucrose 36g/L of glucose 3.0g/L of KCl 4.0g/L of $MgCl_2$ 150μM of Acetosyringone	5.8	
WS	Washing solution	Sterilized distilled water (SDW) and 200mg of Timentin		
N6D	Callus induction	3.98g/L of N6 basal salt, 1ml/L of 100X MS vitamins (sigma), 30g/L of sucrose, 2.8g/L of proline, 0.3g/L of casamino, 4.0g of Phytagel and 2mg/L of 2,4-D.	5.8	32°C
N6D-AS	Co-culture medium	N6D + 10g/L of glucose and 100mM of Acetosyringone.	5.2	25°C
N6D-SM	Selection Medium	N6D + 50mg/L of Hygromycin and 160mg/L of Timentin,	5.8	32°C
REG I	Dehydration medium	N6D+ 50mg/L of Hygromycin 160mg/L of Timentin and 6.0g/L of Phytagel (No 2,4-D), 2mg of Kinetin	5.8	28°C
REG II	Regeneration medium	4.2g of MS basal salt, 0.5g of Proline, 30mg/L of Hygromycin, 90mg/L of Timentin, 1mg/ml of 6-Benzylaminopurine (BAP), Naphthalene acetic acid (NAA), 0.5g of Glutamine, and 2.0 mg of Kinetin	5.8	28°C
ROM	Rooting medium	4.2g/L MS basal salt, 10ml/L of 10X N6 Vitamins, 20g/L of sucrose, 4.0g of phytagel	5.8	28°C

Table 2.2 Media names and composition for *Agrobacterium* mediated rice transformation.

2.6.1 Seeds sterilisation

The seeds; *Oryza sativa L. japonica* cvs. *Nipponbare* and *Kaybonnet Oryza sativa* rice lines were obtained from Erik Murchie's seeds storage, Sutton Bonington campus, University Of Nottingham, UK.
The seeds were first manually de-husked and surface sterilised with 70% ethanol for 1 minute. The seeds were soaked in 50% sodium hypochlorite (bleach) with two drops of 0.1% Triton and placed on a rotary shaker at 45 rpm for 15-20 minutes. After 20 minutes, the seeds were then rinsed multiple times (7 to 9 times) with sterile distilled water (SDW) and were allowed to dry on a sterile filter paper or petri dish.

2.6.2 Callus induction (10 - 12 days)

For callus induction*, the* **N6D** medium was used. A minimum of 80 seeds were used for each DNA transfer. 16 seeds were then placed on the 9cm petri dish containing appropriate induction medium with their scutellum facing upward. The dishes were sealed with surgical tape and incubated under continuous light at 32^{o}C for 10 days. Throughout the incubation period, the embryogenic seeds would begin to germinate into a dry and compact callus form with yellowish colour emerging from the scutellum. On the 10th day, the proliferating roots and shoots were excised and then subcultured to a fresh induction medium. The larger calluses were excised to about 3 mm in diameter. Calluses were ready for infection 2 days after the excision.

2.6.3 Co-cultivation of rice callus tissue with Agrobacterium (2 days)

The *Agrobacterium* was collected from the glycerol stock and inoculated in YEP broth (Table 2.2) medium containing suitable antibiotics. It was then incubated at 28^{o}C, 200 rpm in the dark for overnight. The secondary culture was prepared by a subculture of approximately 10-20% of the *Agrobacterium* culture into a fresh YEP broth containing suitable antibiotic and incubated for 14 hours under the same condition

maintaining the cell density of $O.D_{600}$ ~0.5. The cells were harvested in sterile SS34 tubes at 4000 rpm for 15 minutes at 4°C.

The bacterial pellets were re-suspended in infection media (IM) and adjusted to $O.D_{600}$<0.3. The bacterial suspension was transferred to a sterilised beaker and then allowed at room temperature for about 1-2 hours. The rice callus tissues were then immersed in the bacterial suspension and then placed on a shaker at 125 rpm for 15 mins. The callus tissues were gently blotted dry on six pieces of sterilised filter papers.

The single sterilised paper was placed on the freshly prepared N6D-AS medium in the 10 cm petri dish. About 20 callus tissues were then placed on the filter paper portion of the coculture medium. The dishes were then sealed and incubated in the darkness for only two days at 25°C.

2.6.4 Selection of antibiotic resistance calluses.

The co-cultivated callus tissues were transferred on to a selective medium containing suitable antibiotics (50mg/L Hygromycin, 160mg/L Timentin) and incubated at 32°C under continuous light. The plates were checked regularly for bacterial growth. After the first week, the calluses were subcultured to a fresh medium to avoid accumulation of the polyphenolic compounds from the dying callus tissue which turns the medium into yellowish brown colour. The whitish-creamy coloured proliferating calluses (transgenic calluses) emerging from the callus tissue were sub-cultured in a fresh medium for another one or two weeks, depending how good the callus was.

2.6.5 Regeneration

2.6.5.1 Dehydration of antibiotic-resistant callus tissue (REG I)

The embryogenic antibiotic-resistant callus that emerged during the selection, were transferred to a freshly prepared embryogenic induction medium/dehydration medium (REG1) containing plant hormones, antibiotics (Hygromycin, 30mg/L, Timentin 160mg/L)) and high gelling agent (6.0g/L of Phytagel). The plates were then sealed and incubated at 28 °C in darkness for 6 - 7days.

2.6.5.2 Regeneration of plantlets (REGII)

Very few calluses made it to this stage. After 10 days in the embryogenic induction media, the healthy whitish-creamy embryogenic calluses were transferred to the plantlet regeneration medium (REGII) and incubated for 3 weeks at 28 ^{o}C under continuous light. The embryogenic callus tissues were sub-cultured 2-3 times before the emergence of green shoots. The calluses with greenish appearance were sub-cultured separately from the remaining callus and maintained until approximately 2-3 cm height plantlet were obtained. Any green shoot regenerated from the same calluses tissue first shoot regeneration is likely to be clonal with the same transgene position with the genome.

2.6.5.3 Regeneration of Roots (ROM)

The plantlets at approximately 2 – 3 cm height were transferred to a 10 cm deep glass Greiner jar containing a rooting medium and incubated under continuous light at 28^{o}C. The shoots developed roots within two weeks. At 3 weeks on the rooting medium, the shoots reached to about 8 – 10 cm and ready for hardening.

2.7 RATOONING

This is the process of cutting the three-quarter (¾) of the plant, leaving the shoots to regenerate new stalks and tillers. This was done to promote the formation of more seeds (thus making rice to produce seeds more than once). With the addition of nutrients the plant re-sprouted and re-flowered.

2.8 MOLECULAR METHODS

2.8.1 The Polymerase Chain Reaction (PCR)

The PCR was carried out using the GeneAMP thermocycler (Applied Biosystem, Reading UK). The composition of the 20 µl reaction mix of PCR was made up of the: 1 µl of DNA template, 2 µl of 10X PCR buffer, 1.2 µl of $MgCl_2$ (25mM), 0.4 µl of dNTPs, 1 µl of forward primer, 1 µl of

reverse primer, 0.2 µl of *Taq* polymerase (5U/µl) and 13.2 µl of SDW. The PCR was programmed in the following temperatures: denaturation at 94°C for 2 mins, 94°C for 30 seconds, annealing 55-62°C (depending on the primer) for 30 seconds, extension at 72°C for 1 minute and a final extension at 72°C for 10mins after 35 cycles.

2.8.2 Escherichia coli Transformation

The *E.coli* competent cells (DH5α) were partially thawed on ice. The cells were then added to the digestion and left on ice for 20 mins. This was followed by heat shock at 42°C on heat block for 90 seconds. This created a sudden shock to the bacteria that made their cell membrane weak and permeable to the insert to penetrate. The mixture was then quickly transferred back to the ice for 2 mins. 500uL of LB was added to the cells and then incubated horizontally in shaking incubator for 1hr at 37°C. After an hour the cells were spread on LB agar containing suitable antibiotic and then incubated at 37°C in the dark overnight. The colonies formed overnight were then verified by PCR

2.8.3 Plasmid extraction

Plasmid DNA was extracted from the gel using the Sigma (plasmid extraction kit) as per manufacturer's guide.

2.8.4 Restriction digestion

Plasmid DNA and PCR products were all digested using appropriate restriction enzymes from NEB (NEB, Hitchin, UK) and Promega (depending on the purpose). The restriction was carried out using the manufacturer's protocol (1 µg of DNA template, restriction buffer, restriction enzyme(s) and water then followed by 1-3 hours incubation at 37°C).

2.8.5 Cloning

2.8.5.1 Cloning of DNA using the Invitrogen's Gateway technology

DNA plasmid was PCR amplified using a similar method in section 2.6.1 but with 0.2 µl of PFX proofreading DNA polymerase (Phusion, 5U/ µl)

and 2 µl of 10 X GC enhancer for 35 cycles. This created amplicons with stick end. Hence, lacks the 'A' overhang. After the PCR, a sample was collected from the total PCR solution and added 10X PCR buffer, *dATP* (10mM) and *Taq* polymerase to it and ran an extension at 72oC for 15 mins. The concentration of the DNA was then estimated by on the 1% agarose gel. The PCR generated inserts were cloned into a new Entry vector by adding 2 µl of the PCR insert to 0.5 µl salt solution and 0.5 µl pCR-8/gw/TOPO vector and incubate for 1 hour at room temperature. The incubated mix was then transformed into DH5α competent cells (see section 2.62). Once positive colonies were confirmed by PCR, a colony was then inoculated in 5ml of LB broth with the selective antibiotic and incubated at 37^{o}C for overnight. The plasmids were extracted from the overnight culture and as described in section 2.6.5.1 the extracted plasmids were analysed by restriction digestion and for DNA sequence confirmation.

2.8.5.2 LR reaction

The Invitrogen LR Gateway cloning technology kit (Invitrogen, Paisley, UK) was used in the site-specific recombination where the entry clone was recombined with the destination vector (pBRACT 214) as per the manufacturer's instructions. The presence of the *attL* (1&2) recombinant sites of the entry vector were compatible with the *attR*(1&2) recombination sites of the destination vector. The reaction was performed using, 1 µl of the generated entry vector (section 2.6.4), 1 µl of destination vector and 0.5 µl LR clonase. The reaction was then left at room temperature overnight. The following day, 0.5 µl of proteinase K was added to stop the reaction. This was followed by *E.coli* transformation.

2.8.6 Agrobacterium Transformation.

The electrocompetent *Ag*L1 *Agrobacterium* strain was used for the electroporation. The cells were thawed on ice and 1ul of plasmid DNA (LR recombination) was added to the cells. This was left on ice for a minute. The cells were then transferred into the bottom of the electroporation cuvette. An electric pulse was given to the cells for less

than three seconds using the micropulser machine. 1mL of Luria broth (L.B) was added to the cuvette and mix then transferred back to 1.5mL Eppendorf tube which was then incubated in a 28^{o}C shaker for 2 h. After 2 h, the cells were spread on YEP agar plate containing selective antibiotics and then incubated in the 28^{o}C dark for 2 days. The colonies were analysed using PCR and the positive colonies were stocked in glycerol and LB (50:50, v:v) at -80^{o}C until use.

2.9 B GLUCURONIDASE (GUS) STAINING ASSAY

The GUS gene present in the construct was used to report the activity of the N-end rule pathway. The enzymatic reaction of β-Glucuronidase and the X-Gluc formed a blue colouration at the region of the plant tissue where the gene promoter became active. A Leaf and callus tissue were incubated in the Gus staining solution containing 100mM of Phosphate buffer (Na_2PO_4), 1 mM of X-Gluc, $K_3Fe(CN)_6$, $K_4Fe(CN)_6$ and 0.5% Triton X-100. The leaf tissues were then incubated at 37^{o}C for a day or more.

2.10 GENOMIC DNA EXTRACTION

Leaf samples were collected (approximately 100mg a sample) in 1.5mL Eppendorf tube and were placed in liquid nitrogen. One metal ball was then placed in each of Eppendorf tube containing the leaf sample. The tubes were arranged and balanced on the Lysis grinder (Qiagen Mixer Mill) and then spin at a speed of 25 cycles per second for 60 seconds. To ensure the tissues have all been grinded, the tubes were swapped and then re-spun. The fine grounded powdered samples were then stored at -20^{o}C.

2.10.1 DNA extraction using sodium hydroxide (NaOH) method

The primary structure of DNA is relatively stable under alkaline solution. Hence, alkaline DNA extraction is among the fastest and simplest strategies.

- 50 µl of 0.25 M NaOH was added to the tube containing the grinded leaf sample. The mixture was homogenised by vortex to ensure all the grinded samples had been re-suspended in the NaOH.

- The mixture was then placed on 96°C heat block for 30 seconds. This helped the breakdown of the cell wall and disrupts the hydrogen bonding between DNA bases by converting double stranded DNA to single stranded DNA.
- After 30 seconds of heat, 50 µl of 0.25 M HCl was added to the mixture. This was followed by 25 µl of 0.5 M Tris pH 8.0 and 0.25% IGEPAL-G30.
- The mixture was mixed properly then heated at 96°C for 2 mins.
- After the heating, samples were then stored at -20°C as the genomic DNA samples.

2.11 RNA EXTRACTION

Leaf samples of about 100mg each were harvested with scissors into an Eppendorf tube and were immediately placed into liquid nitrogen. Using the small pestle, the sample was grinded to a fine powder. 800 µl Trizol was added to the grinded sample, mixed thoroughly by vortex and then allowed to remain at room temperature for 5 mins. 160 µl of chloroform was then added and the tube was vortexed for 5 – 10 s. The sample was then harvested at 12,000 ×g for 15 mins at 4°C. The top phase (aqueous) was carefully collected into a different Eppendorf tube without disturbing the debris. This was followed by the addition of 400 µl Isopropanol and 2 µl glycogen (optional) and then allowed at room temperature for 10 mins. The sample was then centrifuged at 12,000 ×g for 10 mins at 4°C. The supernatant was discarded and 800 µl of ethanol was added to the pellets. The sample was then vortexed to wash the pellet and centrifuged at 7,500 ×g for 5 mins at 4°C. At this stage, the RNA was clearly visible at the bottom of the tube due to the addition of glycogen. Ethanol was removed and the tube was air dried for approx. 15 mins at room temperature. 30 µl of water was added and then heated at 55 – 60°C for 10 – 15 mins. The sample was then stored at -80°c.

2.11.1 DNAse treatment

3 µg of the total RNA was used for DNase treatment. The reaction contained RNA (3ug), 2 µl of *DNAse* buffer with magnesium chloride ($MgCl_2$) and 1 µl of the *DNAse*, The sample was incubated at 37°C for 30

mins. 1 µl of EDTA was added and incubated at 65°C for 5 mins. The sample was then stored at – 20°C.

2.12 REVERSE TRANSCRIPTION /CDNA SYNTHESIS

The generation of the first strand cDNA synthesis from the RNA was made using the Invitrogen SuperScript ™ III First-Strand Synthesis SuperMix for qRT-PCR as per the manufacturer's protocol.

2.13 SEMI-QUANTITATIVE PCR (SEMI QPCR)

The semi-qPCR was carried out using cDNA and Actin or housekeeping gene with the standard PCR compositions (section 2.6.1) but with the starting volume of 50 µl and the collection of 10 µl samples at different cycles. At the end of 20, 24, 26 and 35 cycles, then ran and extension at 72°C for 10 minutes altogether.

2.14 GEL ELECTROPHORESES

Agarose was dissolved in 1x Tris-Borate-EDTA buffer at 1% w/v and heated in a microwave oven. Ethidium Bromide was added before the gel was poured into a casting tray with an appropriately sized comb and then allowed to solidify. The solid gel was then transferred to the gel electrophoreses chamber. The ladder was loaded into the well then 6x loading dye was added to the samples which were then loaded into each well of the gel. The loaded gel was then electrophoresed at 80V for 30-45 mins and then visualise on UV light transilluminator.

CHAPTER THREE: GENETIC DIVERSITY IN PHOTOSYNTHESIS, WATER LOSS AND ROOT STRUCTURE IN AFRICAN DIVERSITY PANEL

3.1 BACKGROUND

Rice cultivation in Sub-Saharan Africa is now mainly based on Asian species and land races of the African indigenous rice species that still grown in the traditional production system of upland and flooded system (Dingkuhn et al., 1998). In the late 90's, Monty Patrick Jones and his team began the development of the New Rice for African (NERICA) varieties from the interspecific hybridization between a cross from the Asian rice genotype (*Oryza sativa* L.) and the African rice genotypes (*Oryza glaberimma* Steud.) at the Western African Rice Development Association (WARDA) (Fukuta et al., 2012). This targeted the numerous constraints associated with yields loss of upland rice such as; resistance to drought, insects, weeds, diseases and low input cultural practices. The high yielding potential of Asian rice based on high spikelet number that resulted from the secondary branching of the panicles was also used.

These Asian *O. sativa* lines were WAB 56-104, then WAB 56-50 and WAB 181-18 which served as recurrent parents and belong to the sub species japonica and upland improved varieties. The other parent with a useful trait was the African rice; namely, CG 14 (*O. glaberrimma*) which has rapid leaf canopy establishment, highly weed-competitive and resistance to local biotic and abiotic stresses, and high nitrogen responsiveness (Jones et al., 1997). The main undesirable trait associated with the African rice was the low yield potential due to low spikelet number, grain shattering, and poor lodging resistance. The cross between the two genotypes effectively utilises the genes in the African rice to improve key traits in the Asian rice required for the African environment. This offers hope to millions of poor rice farmers and many others struggling in spending more of their meagre income on rice production and management.

The first generation of NERICA varieties, NERICA 1 to NERICA 11, including the WAB450 progeny, were developed from the single cross between CG14 (*O. glaberimma* Steud) and WAB 56-104 (*O. sativa* L.) (Somado et al., 2008). Among the 11 varieties from the first generation, NERICA 1 to 7 were very popular among the farmers in 2000 before the release of the second series; NERICA 12 to 18. Notably, the second series were derived from three series of crosses, using the same CG 14 (*O. glaberrima*) parent but three difference *O. sativa* parents (WAB 56-50, WAB- 56 – 104 and WAB 181 – 18). They include series of progenies WAB 880 and WAB 881. (Somado et al., 2008).

In this study, four of the first generation of the upland NERICA (NERICA 2, 6, 7 and 8) were used, together with some of the recurring parents of the first and second generation. The first generation NERICA are upland varieties with interesting agronomic characteristics, one of which is their increased drought tolerance. The NERICA cultivars generally have heavy panicles, low tillering, and early heading (Fukuta et al., 2012). A lowland NERICA used in this study was the NERICA L41; a high yielding and weed-competitive variety that was originally released in Burkina Faso in 2007. The NERICA L41 was parented from IR64, which is one the most popular rice variety created during the second phase of the Green

Revolution and it belongs to *O. sativa*, sub-species *indica* with high tiller production. The other parent was TOG 5681, belonging to *O. glaberrima* (Bocco et al., 2012). FARO 52 popularly known as WITA 4 is a Nigerian late maturing lowland variety with low tolerance to submergence (Akinwale et al., 2012). It has low resistance to drought. WAB759-55-2-HB is also a drought tolerant an African variety which has the 'WAB' name; meaning a breeding line in Cote d'Ivoire. Others were the IR4630-22-2-5-1-3, one of the Multi-parent Advanced Generation Inter-Cross population (MAGIC) which was created for their potential applications for mapping quantitative trait loci (QTLs). It has good salinity tolerance, with distinctive green leaves and a high yield potential (Bandillo et al., 2013). Moroberekan, a tropical japonica cultivar of West African origin with sturdy stems and with blast and drought tolerance (Dixit et al., 2014). Finally Kaybonnet, an American rice line originated from a cross with Katy and Newbonnet. It is a japonica variety with blast resistance (Gravois et al., 1995).

Therefore, the rice selection for this study was largely due to their genetic diversity and the contrasting origin of each genotype, which are cultivated in diverse habitats. The differences in their physiological and root architectural traits are expected to be inherently linked to their environment as a strategy for drought tolerance mechanism. Thus, this will provide a good scope to explore their diversity in photosynthesis, water loss and root structure in response to drought tolerance.

3.2 AIMS AND OBJECTIVES

- To show the variability with responsiveness to drought in the African genotypes
- To identify root traits and their impact on above ground physiology
- To determine whether their drought tolerance is stomatal and or root based.

3.3 METHODS

3.3.1 Growth Condition

The experiments were carried out in the summer of 2015 and winter of 2016 in the glasshouse for the PVC experiment (**Experiment 1**) with supplementary lamp as described in Chapter 2, section 2.2. The PVC was 100cm long with 15cm diameter (full description of the column construction in Chapter 2, section 2.2.1) filled with expanded clays as the growing media.

The pot experiments were carried out in the growth chamber (**Experiment 2**). The growing conditions were described in Chapter 2, section 2.2 and the pots used were 3 litre sized filled with growth compost (see section 2.2.2 for the composition detail). The pots were assembled on trays at 8 pots per tray.

A complete randomised design (CRD) was adopted in both the experiments. The plant materials listed in table 3.1 were used for the experiments with 3-4 replicate per genotype and each experiment was repeated at least twice. The seeds were sown into module trays for 10 days before they were transferred (transplanted) into the columns containing expanded beads (Experiment 1) and to the 3L pots containing growth compost.

11 African genotypes with varying level of drought resistance.

9 Upland and 2 lowland with

Non African lowland

Name	Ecology
Nerica 2 (N2)	UPLAND
Nerica 6 (N2)	UPLAND
Nerica 7 (N7)	UPLAND
Nerica 8 (N8)	UPLAND
WAB 56- 104 (W56)	UPLAND
WAB 759-55-22-HB (W759)	UPLAND
CG 14 (O.glaberimma) (CG14)	UPLAND
WAB 181-18 (W181)	UPLAND
MOROBEREKAN (Moro)	UPLAND
NERICA L41 (NL41)	LOWLAND
FARO 52 (F52)	LOWLAND
KAYBONNET (Kayb)	LOWLAND
IR64	LOWLAND
IR4630-22-2-5-1-3 (ML4)	

Table 3.1. List of the Rice genotypes used for the study.

Experiment 1*:* Automated irrigation system was installed with the water supply partitioned into two (one with the control valve and the other not) and the water drip pipes randomly arranged with each placed into the PVC column. The irrigation was programmed to irrigate liquid nutrient feed to all the plants at every 6 hours for one minute (the volume supplied was 37mL per minutes) until 35 days after sowing (DAS). The nutrient feed had a composition of N, P, K at a ratio of 4:5:8 and other micronutrients.

Experiment 2**:** Irrigation was made manually onto the tray daily until 35 DAS and plants were supplemented with slow release fertiliser mix, Osmocote ™ (The Scotts Company LLC, Ohio, USA) after every month.

3.3.2 Drought treatment

Experiment 1: At 35 DAS, The liquid nutrient feed in the tank was emptied and replaced with water (to avoid nutrient bias). One of the irrigation supply valves was turned off to stop the 6 hours water supply

to half to the total plants (for drought treatment). While the other half received water supply as usual. The drought treated plants were irrigated once in two days manually with 74mL per column of the liquid feed together with the well-watered (control) in the first two days of the drought imposition. The subsequent feed was reduced to 37mL after two days until the end of the experiment.

Experiment 2: At 35 DAS, the water on the trays was removed and the supply was suspended completely for two weeks.

3.3.4 Gas exchange

Steady state photosynthetic measurements (P_{max}), Photosynthesis- light response curves (LRC) and Photosynthesis vs Ci (leaf internal CO_2 concentrations, ACi) curves were measured using the infra-red gas analyser (IRGA) Licor 6400XT. All leaf gas exchange measurements were taken on the plant flag leaf. The block temperature was maintained at 30°C in experiment 1 and 28°C for experiment 2. The flow rate of 500ml min^{-1} and the cuvette humidity was set to ~10% (experiment 1), 28% and 60% (experiment 2). The CO_2 concentrations used for the steady state measurements are 600 μmol mol^{-1} to check stomatal movement (experiment 1) and 400 μmol mol^{-1} (experiment 1 and 2). The photosynthetically active radiation (PAR) were set at 2000 μmol m^{-2} s^{-1} (experiment 1) and 1500 μmol m^{-2} s^{-1} (experiment 2). Description for LRC and AC_i curves in Chapter 2.

3.3.5 Statistical analysis

Analysis of variance (ANOVA, one-way and two-way) was carried out using GenStat for Windows, 17th Edition (VSN International Ltd.) and GraphPad Prism 7.01 for Windows (La Jolla, CA, USA) to investigate the differences between genotypes and the effect of drought stress on the genotype. When an effect was detected, a Tukey's HSD (Honest Significant Difference) test was used to determine the level of significance. A correlation matrix was used to investigate the relationships between different traits.

3.4 RESULTS

We hypothesized that the variation in leaf gas exchange, biomass yield and tolerance to drought among the genotypes could be due to differences in their root structure as well as (and interacting with) stomatal and leaf properties.

3.4.1 Column experiment: Experiment 1

3.4.1.1 Relative growth rate (RGR)/Growth assessment from leaf and tiller development

Growth assessment was carried out at the beginning of the experiment (before drought treatment), based on the number of leaves and tillers produced per day. Previous literature had shown that the upland varieties have many fewer tillers than lowlands varieties (Fukuta et al., 2012). Figure 3.1 shows the time course growth development from day 10 days after transplant (DAT) onward. Between 10 DAT to 27 DAT, the mean number of the tillers produced ranged from 1-4. A Two-Way ANOVA was conducted between genotype at every time point, and it revealed that at 10 DAT, the number of tillers of W759 was higher than N6 ($P<0.01$), N7 ($P<0.05$), W56 ($P<0.01$) and Moro ($P<0.05$). From 13 to 27 DAT, N6 and W56 maintained the lowest number of tillers over than W759 and CG14 ($P<0.01$). Both the two genotypes were significantly lower than W759 at $P<0.001$ from 19 to 27 DAT. W759 has higher tillers than the many of the upland genotypes. This indicates that among the upland O.sativa, W759 has relatively closer to the Asian rice characteristics interms of tiller number.

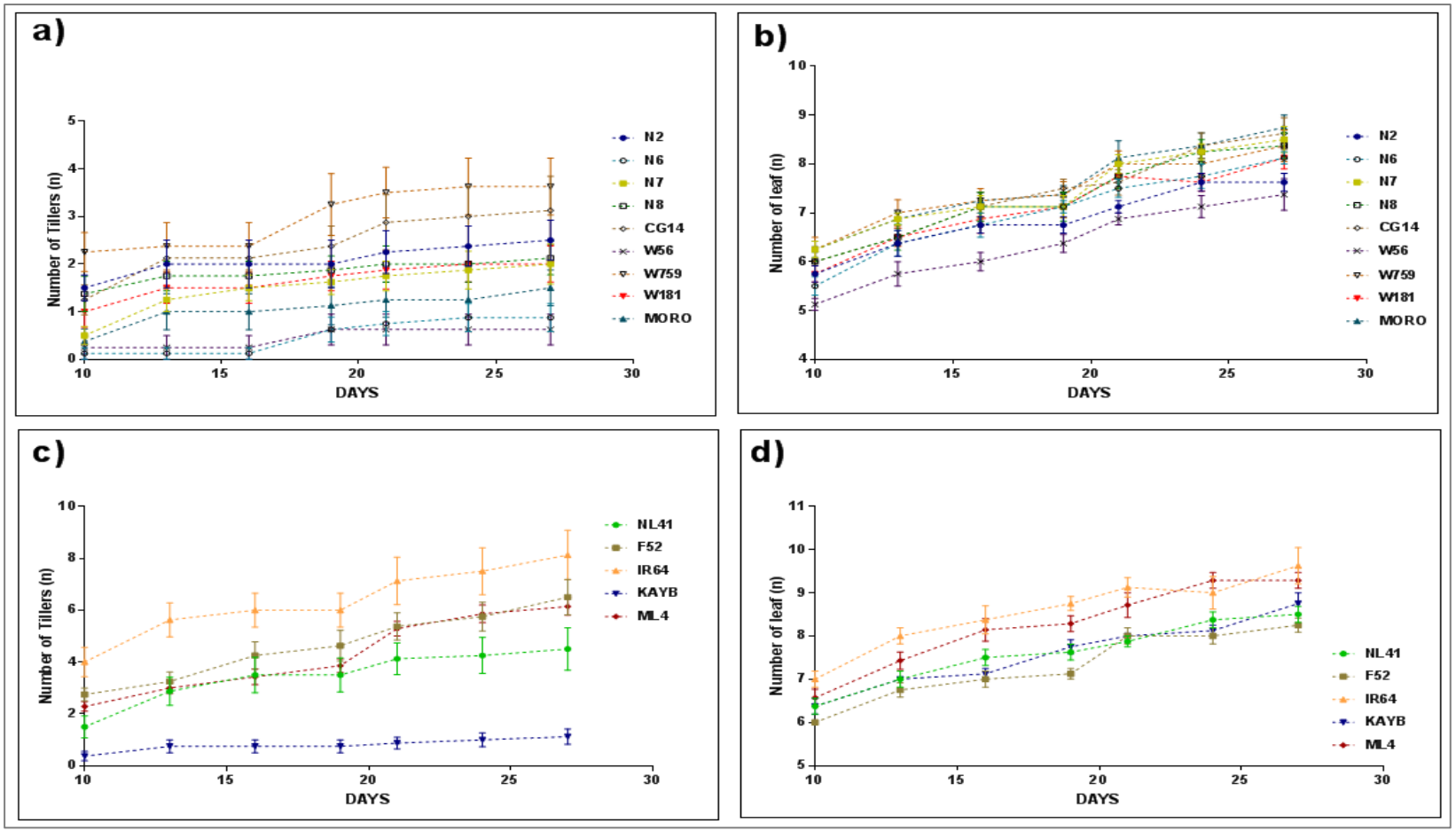

Figure 3.1. Time course assessments from leaf to tillers over 17 - DAT. Days in the graph means Days after transplant (DAT) and N in genotype names means NERICA **A**. tiller development in upland genotypes. **B**. Leaf development in upland genotypes. **C**. Tiller development in lowland genotypes. **D**. Leaf development in lowland genotypes. All point represent the mean and standard error of the mean (±SEM) and n=8.

In lowland, the situation was different. Only Kaybonnet (non-African lowland) among the lowland lines had no statistical increase in the tiller number from day 10 to 27. IR64 and F52 were significantly higher than Kayb from 16 DAS until the 27 DAS at $P<0.001$. The NL41 also had a very lower number of tillers compared to the IR64 with the level of significant differences increasing from 10 to 19 DAS at $P<0.05$ and from 21 to 27 DAS at $P<0.001$. By the 19 DAS, all the lowland genotypes had significantly higher number of tillers than Kayb. Therefore, lowland showed considerably more tillering than the uplands lines. A similar pattern was seen with regards to a number of leaves. W56 had the lowest number of leaves when compared to Moro and CG14 over the period of the 17 days assessment. From 19 DAS to 27 DAS the differences in the number of leaves of W56 and the CG14 and Moro significant ($P<0.01$). Among the lowland genotypes, IR64 had significantly higher number of leaves than F52, Kayb ($P<0.01$) throughout the 17 days assessment. From 13 DAS, the number of leaves in NL41 became significantly lower than IR64 ($P<0.01$) until at 27 DAS.

Except for W56, the NERICAs generally had fewer leaves and tillers, and drought stress did not affect leaf and tiller development (figure not shown). The lowland genotypes had a characteristic high number of tillers and leaves although the drought stress had slowed down their development (figure not shown).

3.4.1.2 Gas exchange response to moderate drought among African (upland and lowland) rice genotype

Previous work has shown that the four genotypes of the first generation of the NERICA (N2, N6, N7, and N8) had shown a superior response to drought and other abiotic stresses in the field (Somado et al., 2008, Fukuta et al., 2012). They are commonly grown in different regions of West Africa, particularly, Nigeria, Cote d'Ivoire, Benin and Burkina Faso. Some of these regions are in the northern part of Nigeria, with a characteristic high temperature and very low relative humidity (Imolehin and Wada, 2000). Air relative humidity is identified as one of the key environmental factors that mediate the changes in the stomatal

sensitivity to CO_2 (Talbott et al., 2003). This experiment mimicked such conditions during measurement to explore the photosynthetic efficiency of the African genotypes at leaf level.

Genotype	CO_2 Assimilation (A)	Stomatal Conductance (gs)	Transpiration (E)	Internal CO_2 (Ci)	Intrinsic WUE	FV'/FM'	PhiPSII
UPLAND							
NERICA 2	23.9±1.8^{c}	0.24±0.02^{abc}	7.8±0.6^{abc}	302.8±16.1^{abc}	101.0±10.1^{abc}	0.15±0.02^{a}	0.04±0.01^{abcde}
NERICA 6	19.7±3.2^{bc}	0.15±0.03^{ab}	5.6±0.9^{ab}	252.3±17.8^{ab}	133.3±11.7^{bc}	0.14±0.02^{a}	0.06±0.02^{abcde}
NERICA 7	24.0±2.1^{c}	0.34±0.13^{bc}	8.9±2.4^{bc}	299.5±46.5^{abc}	103.8±29.3^{abc}	0.17±0.03^{a}	0.05±0.02^{abcde}
NERICA 8	20.5±3.9^{bc}	0.47±0.04^{c}	12.7±0.6^{c}	399.0±11.6^{c}	42.6±6.3^{a}	0.15±0.02^{a}	0.03±0.00^{abcd}
CG-14	19.3±1.4^{bc}	0.30±0.13^{abc}	8.8±2.5^{bc}	342.4±32.7^{abc}	88.0±20.3^{abc}	0.08±0.0 ^{a}	0.03±0.01^{a}
WAB 56	13.6±3.9^{abc}	0.15±0.05^{ab}	5.6±1.6^{ab}	304.0±32.1^{abc}	101.2±19.7^{abc}	0.47±0.05^{b}	0.10±0.02^{e}
WAB 759	13.8±2.9^{abc}	0.13±0.05^{ab}	5.8±1.4^{ab}	246.3±39.7^{ab}	138.6±25.7^{bc}	0.45±0.04^{b}	0.10±0.01^{de}
WAB 181	10.2±0.1^{ab}	0.07±0.01^{ab}	2.7±0.3^{a}	397.7±39.0^{c}	140.3±10.2^{bc}	0.44±0.05^{b}	0.06±0.01^{abcde}
MORO	14.2±2.7^{abc}	0.20±0.03^{abc}	6.6±0.9^{abc}	349.6±14.8^{bc}	73.7±9.0^{ab}	0.08±0.01^{a}	0.01±00^{a}
LOWLAND							
FARO 52	15.3±1.3^{abc}	0.17±0.02^{ab}	5.4±0.5^{ab}	315.1±9.2^{abc}	96.4±6.0^{abc}	0.15±0.02^{a}	0.03±0.00^{ab}
NERICA-L41	12.43±0.8^{abc}	0.08±0.00^{ab}	3.1±0.1^{ab}	212.3±7.9^{a}	161.0±4.9^{c}	0.14±0.02^{a}	0.03±0.01^{abcde}
IR64	11.0±2.6^{ab}	0.09±0.03^{ab}	5.0±0.9^{ab}	262.6±18.6^{ab}	129.9±12.2^{bc}	0.09±0.02^{a}	0.02±0.01^{abc}
KAYBONNET	4.7±0.6^{a}	0.05±0.01^{a}	2.3±0.3^{a}	319.3±9.6^{abc}	92.7±6.1^{abc}	0.43±0.02^{b}	0.09±0.01^{bcde}
IR4630 (ML4)	10.9±1.2^{ab}	0.11±0.01^{ab}	4.3±0.2^{ab}	300.3±14.3^{abc}	104.2±9.2^{abc}	0.44±0.01^{b}	0.09±0.01^{cde}

Table 3.2. Summary of the photosynthesis. One Way Anova was used to determine the statistical differences between the genotypes.: CO_2 assimilation rate (*A*), Stomatal conductance (gs), Transpiration rate (*E*), Internal CO_2 (Ci), intrinsic Water Use Efficiency (A/gs), Quantum efficiency of PSII photochemistry (Fv'/Fm') and Quantum yield of PSII (PhiPSII). Differences in the letters indicate significant differences (vertically within a column) of a parameter between all genotypes (including upland and lowland). The ± represent the standard error. N= 3-4.

The infrared gas analyser (IRGA) was programmed to record the gas exchange measurement with reference CO_2 concentration as 600µmol mol^{-1} and a low level of cuvette relative humidity was set at 10%±3. At 5-weeks, ANOVA revealed two of the NERICAs; 2 and 7 had significantly ($P<0.05$) higher CO_2 assimilation rate (*A*) at steady state than the W181, at P=0.025 and 0.023 respectively (Table 2) under well-watered condition. Similarly, the *A* of both N2 and N7 were significantly higher than the three lowland varieties; IR64, Kayb, and the ML-4. N8 was only higher than the Kayb. Thus, the result suggests upland NERICAs had higher carbon assimilation rates under these conditions. There was a varietal difference in the responses to stomatal conductance (gs), and N8 had significantly higher gs than N6, W56, W759, W181 as well as all the 5 lowland genotype; F52, NL41, IR64, Kayb and ML4. N7 was only higher than Kayb. This effectively influences the transpiration rate (*E*) pattern with N8 showing similar responses as in gs. The computed intrinsic water use efficiency from the ratio of *A* to *gs*, revealed N8 with lowest WUE when compared to N6, W759, W181 and NL41. The NL41 had higher WUE than F52 and Kayb under well-watered condition. The maximum quantum efficiency of open PSII reaction centres (Fv'/Fm') was significantly low and comparable with N2, N6, N7, N8, CG14, Moro, F52, NL41 and IR64. Significantly higher Fv'/Fm' was observed in W56, W759, W181, Kayb and ML4. Low Fv'/Fm' can be linked to non-photochemical quenching (NPQ) which may or may not be associated with photoinhibition (Placido et al., 2013). The ϕPSII values in all genotypes were at low level <0.2, indicating a high level of saturation of electron transport (Murchie et al., 1999).

Absolute drought stress was impossible to impose in the growing condition due to the water holding capacity of the clay beads. As such, moderate drought was imposed as described in the methods. After four (4) days of water restriction, the stress led a considerable decline of *A*, gs and *E* in N7 and N8 genotypes when compared with their respective well-watered controls.

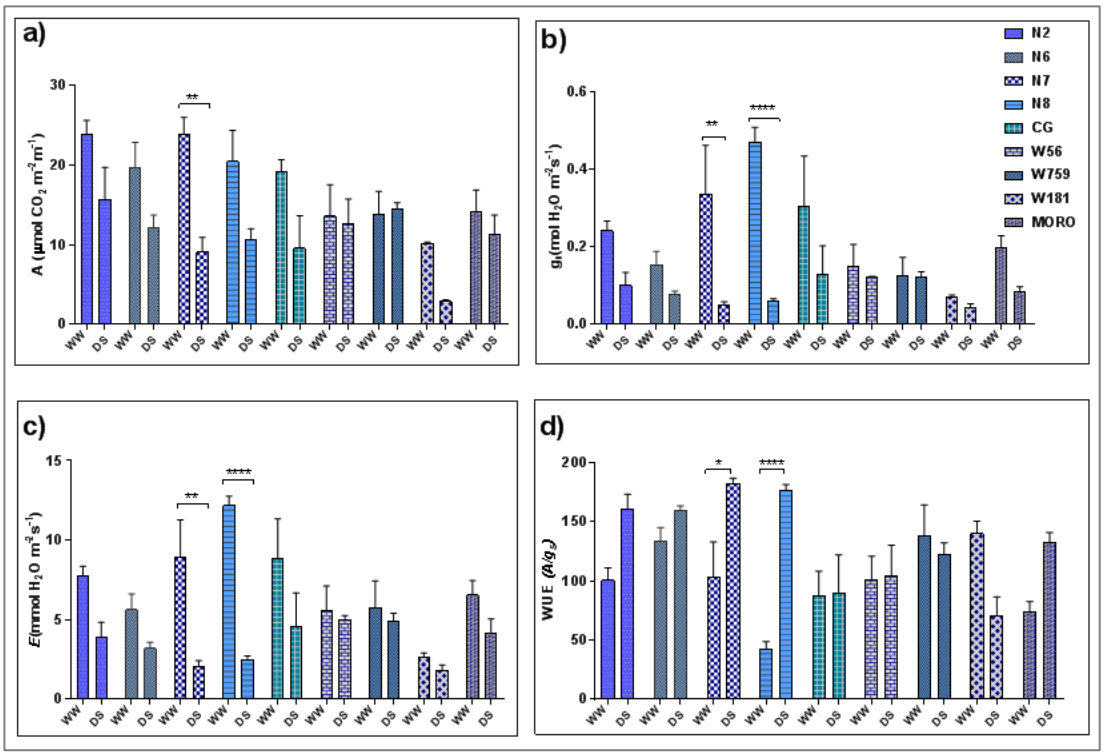

Figure 3.2 Leaf gas exchanges measurement of the upland rice to determine the relationship between moderated drought stress (DS) at day 4 and well-watered (WW) condition of each genotype. **A**. Photosynthetic rate (*A*), **B**. stomatal conductance (g_s) and **C**. transpiration (*E*). **D** the calculated intrinsic water use efficiency (*A/gs*). Statistical significance was determined using a TWO WAY ANOVA with Tukey test. The asterisks represent the significant differences between the two treatments of the same genotype. (*=P≤0.05, **= P≤0.01, ***= P≤0.001, ****= P≤0.0001). Error bars indicate the Standard Error of the Mean (±SEM).

From the ANOVA between drought (DS) and non-drought (WW) treatments, the CO_2 assimilation rate (*A*) after 4 days of moderate DS declined significantly in NERICA 7 (N7) at P=0.0132 by 61.9 . The interaction in *gs* between treatments and the genotypes was significant (P<0.01). Interestingly, the mean gs of N8 in WW conditions was significantly higher than the gs of N6 (P<0.05), W56 (P<0.01), W759 (P<0.01) and W181 (P<0.001) in WW conditions. However, the *gs* of N7 and N8 responded with a very sharp decline after 4 days of DS (Figure 3.2). The N8 reduced by 87.4% after DS (P=0.0002). While N7 significantly (P=0.0351) declined by 85.3% after water stress. The reduction of the stomatal conductance is likely due to the impact of the moderate drought stress imposed on the plants. A similar pattern was observed in their rate of transpiration which was clearly influenced by

the *gs*. Transpiration (*E*) was significantly decreased in the N8 by 79.5% and in N7 by 76.7% from their respective WW controls. Similarly, the intrinsic water use efficiency (*A/gs*) significantly improves with DS in N8 by 60% and N7 by 43% in Figure 3D.

Lowland rice generally would be expected to possess different characteristics to upland rice in terms of environmental adaptation as shown in Figure 3.3. On day 4 of the moderate water stress in Figure 3.3, F52 declined by 50.1% (P≤0.01) in *A*, 71% (P≤0.0001) decline in *gs* and 67% (P≤0.0001) in *E*. The intrinsic WUE of F52 was therefore significantly improved by 33% (P≤0.05) in Figure 3.3D.

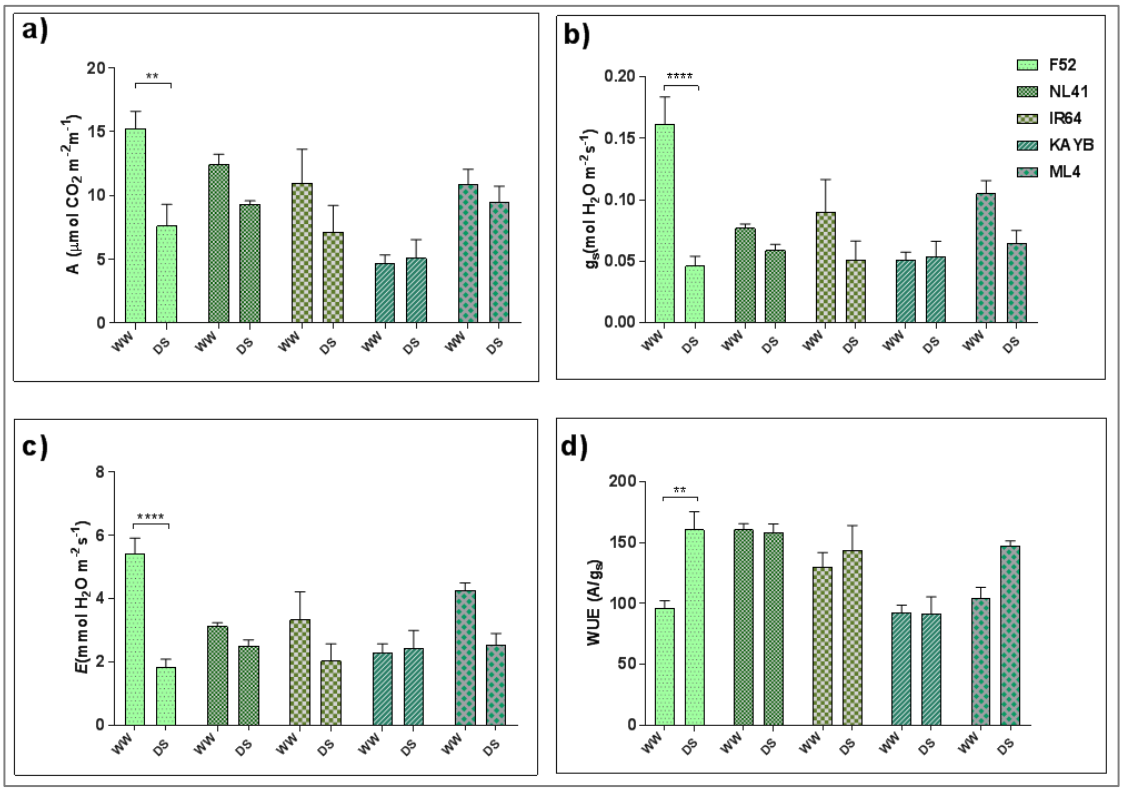

Figure 3.3. Leaf gas exchanges measurement of the lowland rice to determine the relationship between moderated drought stress (DS) at day 4 and well-watered (WW) condition of each genotype. **A**. Photosynthetic rate (*A*), **B**. stomatal conductance (g_s) and **C**. transpiration (*E*). **D** the calculated intrinsic water use efficiency (*A/gs*). Statistical significance was determined using a TWO WAY ANOVA with Tukey test. The asterisks represent the significant differences between the two treatments of the same genotype. (*=P≤0.05, **= P≤0.01, ***= P≤0.001, ****= P≤0.0001). Error bars indicate the Standard Error of the Mean (±SEM) and n=4.

Between the upland and the lowland genotypes, the upland (particularly NERICA's) has shown higher *A, gs, E* and WUE than most of the lowland varies. Even though, not all were statistically different. However, in the combination of the upland genotypes, the Asian *O.sativa* (W56, W181 and W759) genotypes were largely different from the NERICA's in terms of gas exchange.

3.4.1.3 Canopy temperature

Infra-red thermography can reveal the effect of drought on canopy temperature since a lower stomatal conductance results in a higher leaf temperature via lower transpirational cooling.

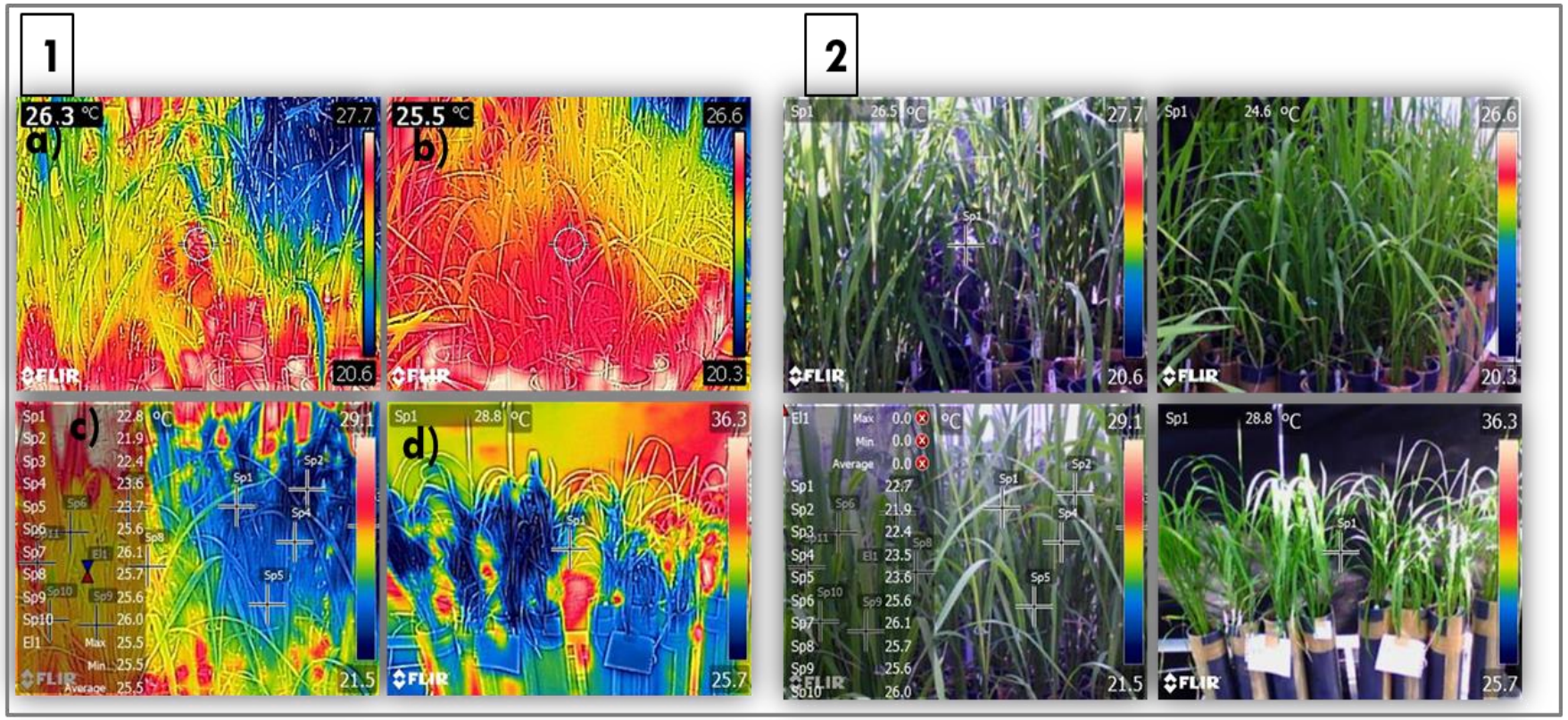

Figure 3.4. The thermography of the DS and WW treatments for demonstration only, with data in Figure 3.5.

Figure 3.4 and 3.5 shows the temperature difference, between the WW and DS plants growing side by side at day 5 of DS. Low canopy temperature during drought is a possible indicator of water status deep in the column or drought avoidance mechanism where the development of deep root length favours plant acquisition of water in deep soil layers (Jones et al., 2009).

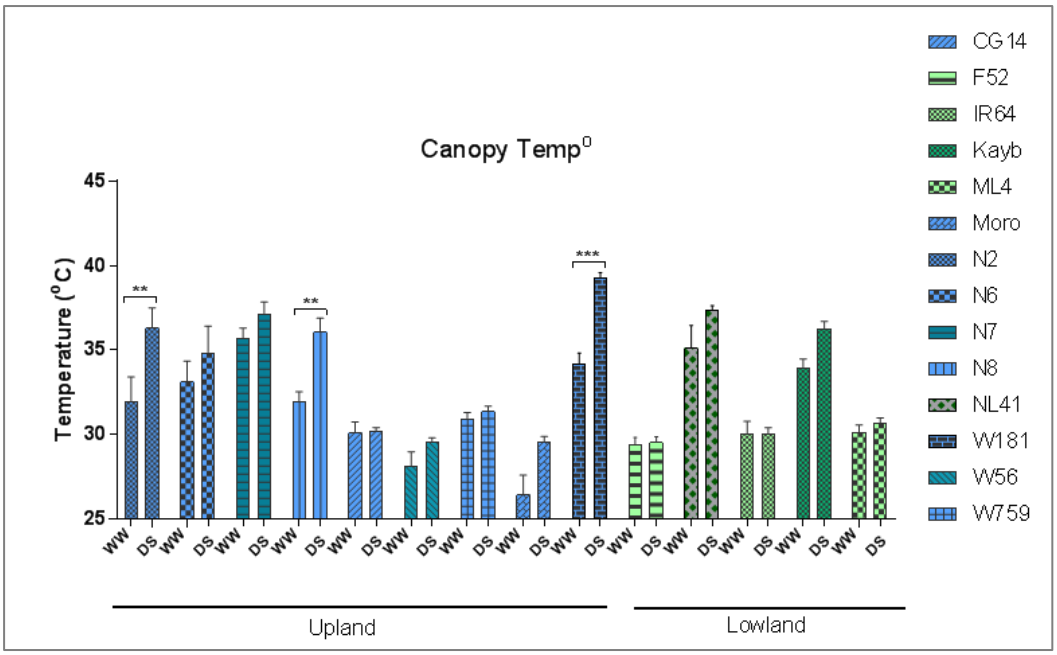

Figure 3.5. The canopy temperature collected on each genotype and treatments as seen in figure 3.4. Statistical significance was determined using a TWO WAY ANOVA with Tukey test. The asterisks represent the significant differences between the two treatments of the same genotype. (*=P≤0.05, **= P≤0.01, ***= P≤0.001). Error bars indicate the Standard Error of the Mean (±SEM)

3.4.1.4 Measurement at 400μmol CO_2mol^{-1}

A different experiment within experiment 1, with a similar setting as above but different reference CO_2 concentration was used in this study to determine the genotypic variation in gas exchange under 400μmol mol^{-1} ambient CO_2 concentration. A time course response of the upland (figure 3.6) and lowland (figure 3.7) genotype to drought stress (the well-watered data points not included in the figure).

3.4.1.4.1 Upland genotype

At day-4 of the moderate drought stress, the *A* reduced significantly in N2, N7, and N8 at (P≤0.0001) level of significance by 68.9, 67.8, and 73.3% respectively, from their well-watered controls. The *A* of N6 and W181 were also declined at (P≤0.001) level of significance by 57.7 and 68.3% respectively. The CG14 also significantly (P≤0.05) reduced by 70.2%.

The stomatal conductance (*gs*) reduced in N2 (P≤0.0001) by 92.1% and on N6 (P≤0.01) by 86.6%. The N2 showed a significantly reduced *E* at P≤0.0001 by 85.7% and N6 (P≤0.001) by 79.4% compared to their well-watered controls. Similarly, N7, N8 and W181 at the P≤0.05 level of significance have reduced considerably by 70.3%, 76.5% and 72.8% respectively. Generally, the NERICA's have high *gs* in well-watered condition but showed rapid stomatal closure with response to decrease in water and by the end had similar values to other lines.

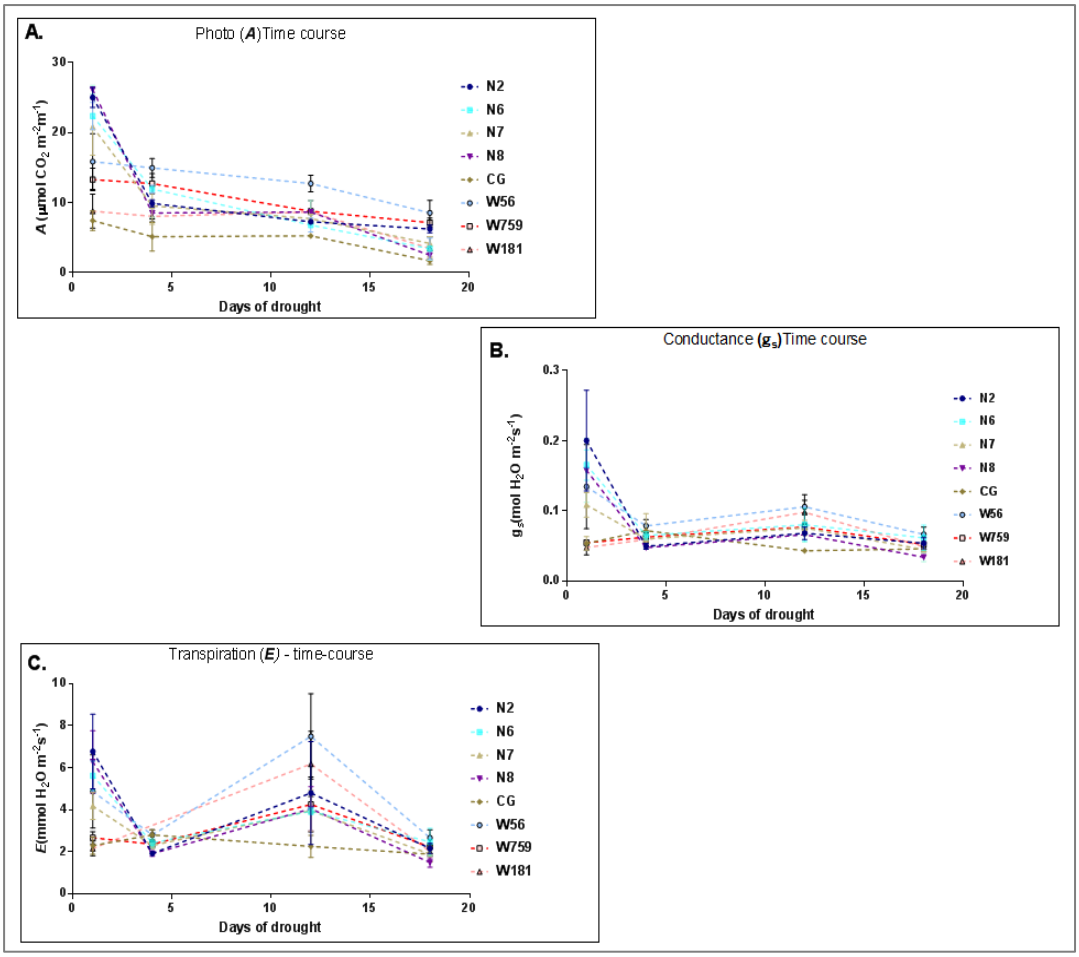

Figure 3.6. The time point effect of moderate drought stress on the mean of upland rice genotypes. **A**, Photosynthetic rate (*A*), **B**, Stomatal conductance (g_s) and **C**, Transpiration rate (*E*). Each time point is a means with SEM ± error bars. n= 3-4

Absolute drought stress was not achievable with the expanding clay beads (hydroleca). A small volume of water was added to the drought treated plants every other day (as described in the methods) to avoid rapid wilting. There was also a variation depending on when the measurements were made relative to the watering time. At the 11th day of the drought stress, the *A* of N2 and N7 were significantly (P≤0.0001) reduced by 69.4% and 66.4% respectively from their controls. W56 and W759 were significantly (P≤0.01) reduced by 44.3% and 52.1% respectively from their well-watered controls. Thus, N6, N7 and N8 had shown a significant reduction in *A* on the day 18 of the drought stress from their well-watered controls by 80% (P≤0.01), 70% (P≤0.05) and 82% (P≤0.01) respectively.

The *gs* of N2 and W56 declined significantly (P≤0.01) from the control by 85.8 and 78.7% respectively on the day 11 of drought stress. On day 18, N6 showed a significant reduction (P≤0.01) in g_s by 72.2%. Similarly, the *E* was reduced in W56 (P≤0.05) by 66.3% on day 11. On day 18, *E* of N6 has significantly (P≤0.01) reduced by 65% from the WW. Generally, all the genotypes displayed a drop in their gas exchange parameters over the period of the DS with little difference in the pattern of response between groups.

3.4.1.4.2 Lowland genotypes

The time-course of the 18 days water stress in Figure 3.7, *A* had significantly (P≤0.01) reduced in F52 on the 4th of the stress by 46% and its g_s by 65.1%. Similarly, the transpiration in the F52 was significantly reduced by 72.6% from the well-watered. No statistical differences were observed beyond the 4th day of drought stress.

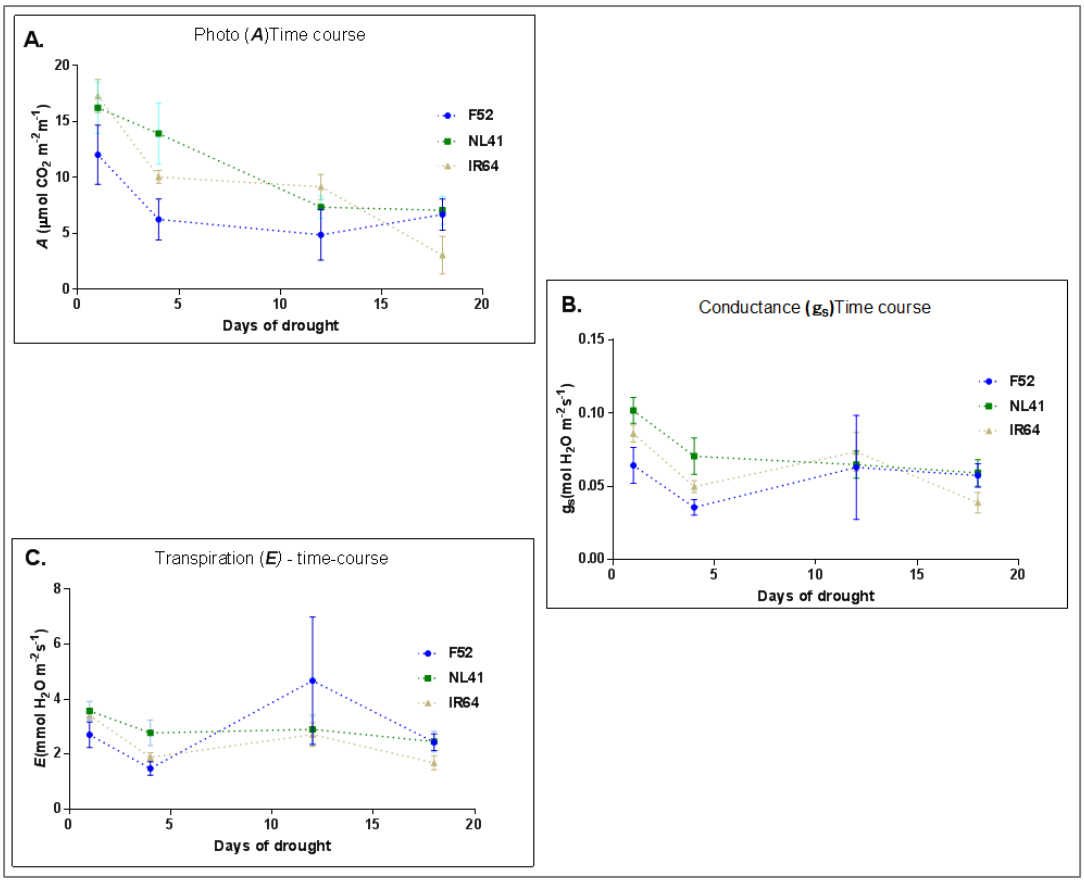

Figure 3.7. Time course effect of moderate drought stress on the mean upland rice genotypes. **A**, Photosynthetic rate (*A*), **B**, Stomatal conductance (g_s) and **C**, Transpiration rate (*E*). Each time point is a means with SEM ± error bars.

3.4.1.5 Analysis of response of CO_2 assimilation to intercellular CO_2 concentration under moderate drought stress (ACi Curve)

Changes in Photosynthesis (*A*) as a function of internal CO_2 concentration (*Ci*) were used to determine the photosynthetic biochemical potentials as well as the stomatal limitation imposed by the stomata at 7-week old.

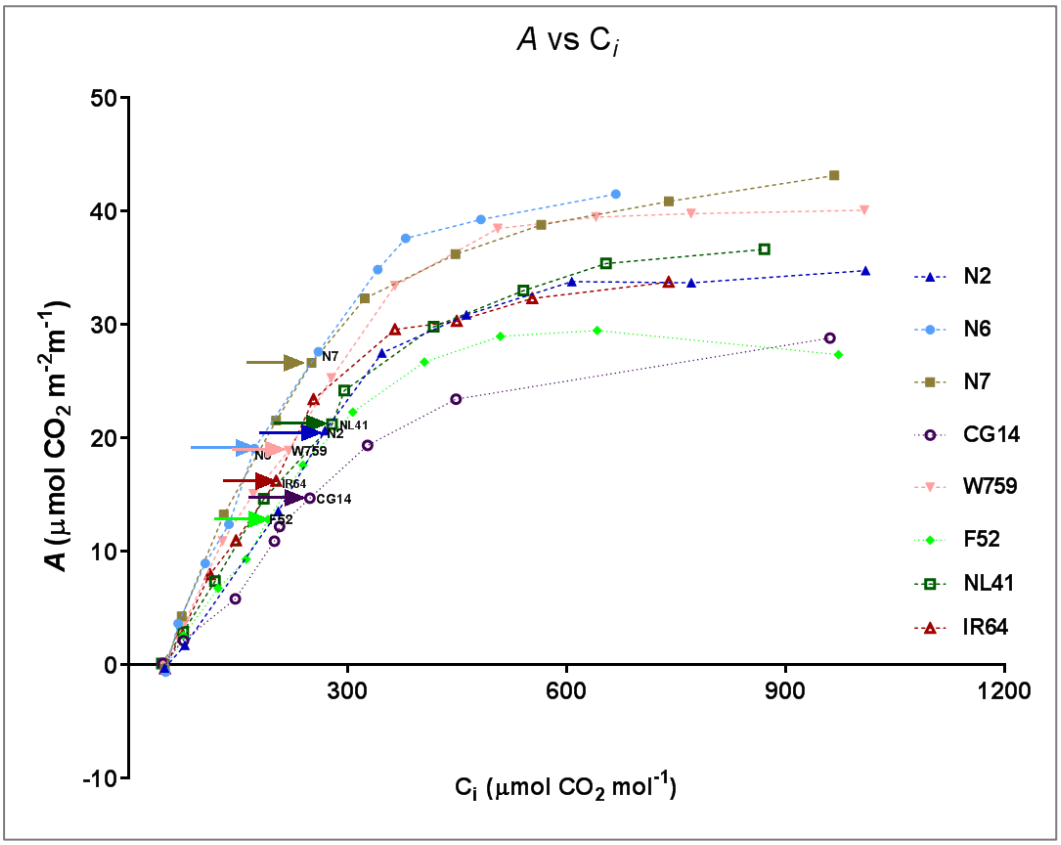

Figure 3.8. A. The net photosynthetic rate increased with increasing concentration of CO_2 (A vs C_i) in 5 upland and 3 lowland genotypes under well-watered condition. The observation was measured on fully expanded flag leaf at a PAR of 2000µmol$m^{-2}m^{-1}$, leaf temperature 28°C and RH 10±3%. The arrows indicate the operational points at 400µmol $mol^{-1}CO_2$.

Figure 3.8 shows the differences of *A* to the response to different internal CO_2 concentration in upland and lowland rice at 7 weeks after sowing. The biochemical components of CO_2 assimilation such as the maximum rate velocity of carboxylation by Rubisco (V_{cmax}) and the maximum rate of electron transport (J_{max}) were estimated by fitting the Farquhar et al (1980) using non-linear regression techniques model modified by

(Bernacchi et al., 2001). All the data were all normalised to a leaf temperature of 25°C as suggested by (Sharkey et al., 2007). The analysis of variance of the plants revealed no statistical differences in V_{cmax} and J_{max} between all the genotypes in WW condition.

3.4.1.6 Response of A to CO_2 in drought stress

A similar approach in Figure 3.8 above was used to determine the *A* vs *Ci* response among the DS genotypes and their WW control. Under DS (7 days of drought stress), the J_{max} declined significantly in N6 at P=0.0286 by 49.4% (Figure 3.9). This may suggest that the major cause of the *A* decline in N6 in drought stress could be due to Rubisco regeneration rate (electron transport). No significant difference in V_{cmax} was detected between DS and WW plants of each genotype, which perhaps indicates the major impact on photosynthesis was stomatal rather than biochemical. Despite having no differences in their slope at the region of carboxylation (V_{cmax}), the differences at operational point differs as determined by the stomatal conductance, for all the genotypes at the ambient CO_2 (400μmol^{-1}) and saturating light.

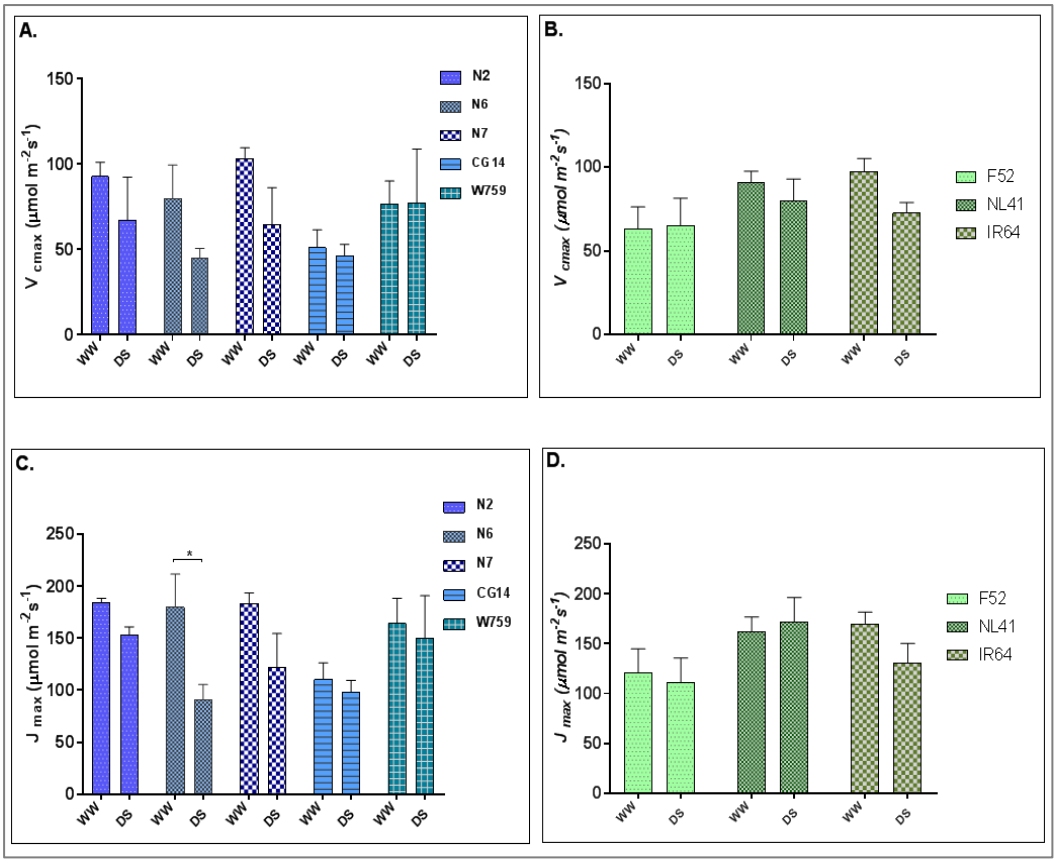

Figure 3.9. A and C the Vcmax and Jmax of the well-watered and drought upland genotypes normalized at 25°C. **B** and **D** the V_{cmax} and J_{max} of the well-watered and drought lowland genotypes normalized at 25°C respectively. All values are means with ± SEM error bars.

More so, the severity of the drought was not high as it has not impaired the photosynthetic biochemistry.

3.4.1.7 Stomatal limitations (Ls)

Changes in *A* as a function of C_i were used to determine the stomatal limitations (L_s) imposed by stomata at 7 days of drought stress using the method of Long and Bernacchi (2003).

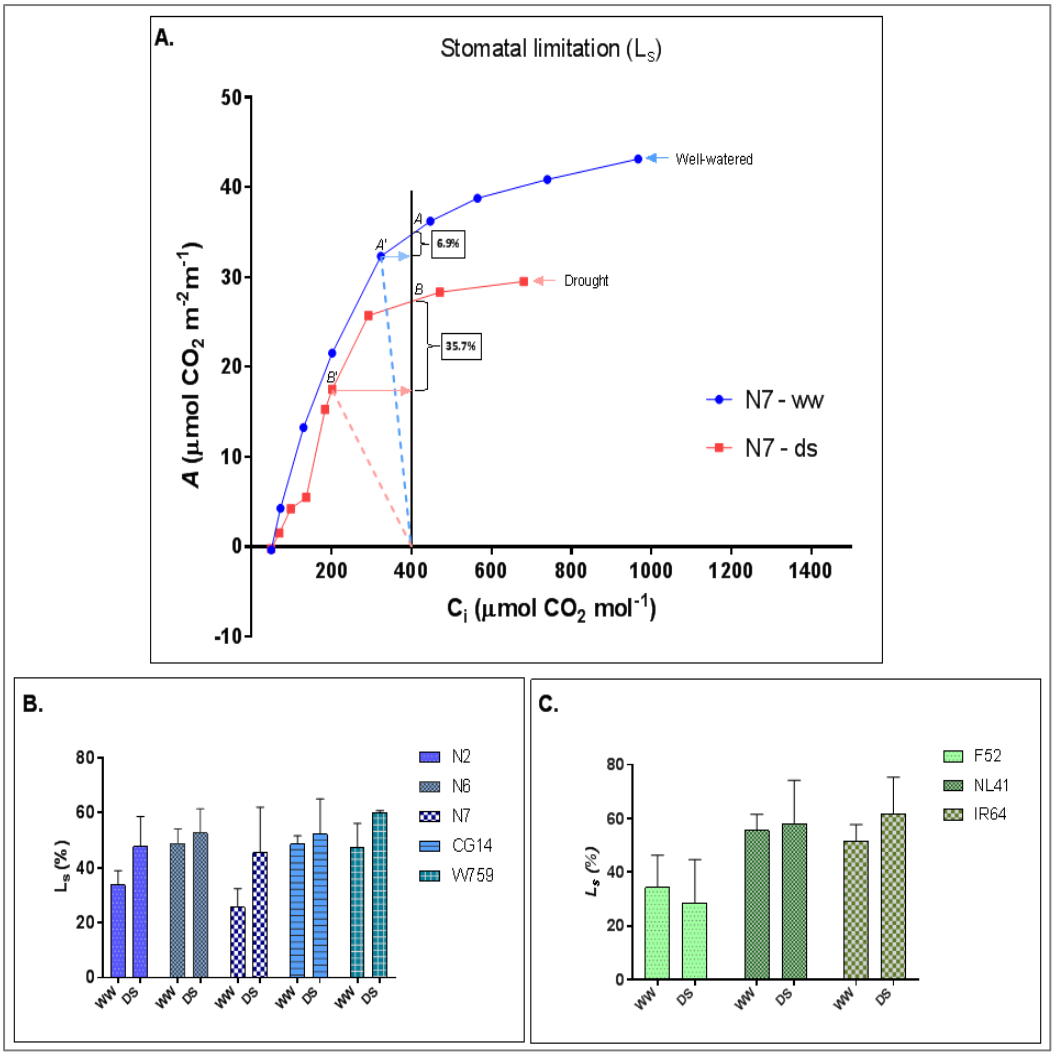

Figure 3.10. A. A simple analysis of relative limitation by stomatal (Ls) applied to well-watered and moderate drought stressed N7 leaves after 7 days of moderate drought (for demonstration). The L_s is calculated from measurements at Ca 400µmol^{-1}. For well-watered L_s= [*(A-A')/A*] × 100 = 6.9% and for stress L_s= [*(B-B')/B*] × 100 = 35.7%. **B.** Stomatal limitations imposed on upland genotypes after drought. **C.** The stomatal limitation imposed on lowland genotypes after drought All values are means with ± SEM error bars.

From the relationship between *A* and *Ci* in Figure 3.10 A, the extent of limitation on *A* imposed by stomatal and leaf boundary layer (L_s) after 7 days of moderate water stress was shown in Figure 3.10 B and C. No statistical differences were observed between genotypes in well-watered condition and as well between treatments. This may have occurred because no significant differences were observed at the site of carboxylation (V_{cmax}) at the current drought stress.

3.4.1.8 Stomatal density

The stomatal arrangement in all the tested genotypes (upland and lowland) appears in either single or double row within the viewed region of the midrib when examined at 8 weeks old in both the DS (figure not shown) and WW. Hoshikawa (1989) explained that the stomatal arrangements of rice (WT) forms in either single or double rows adjacent to the vascular bundles.

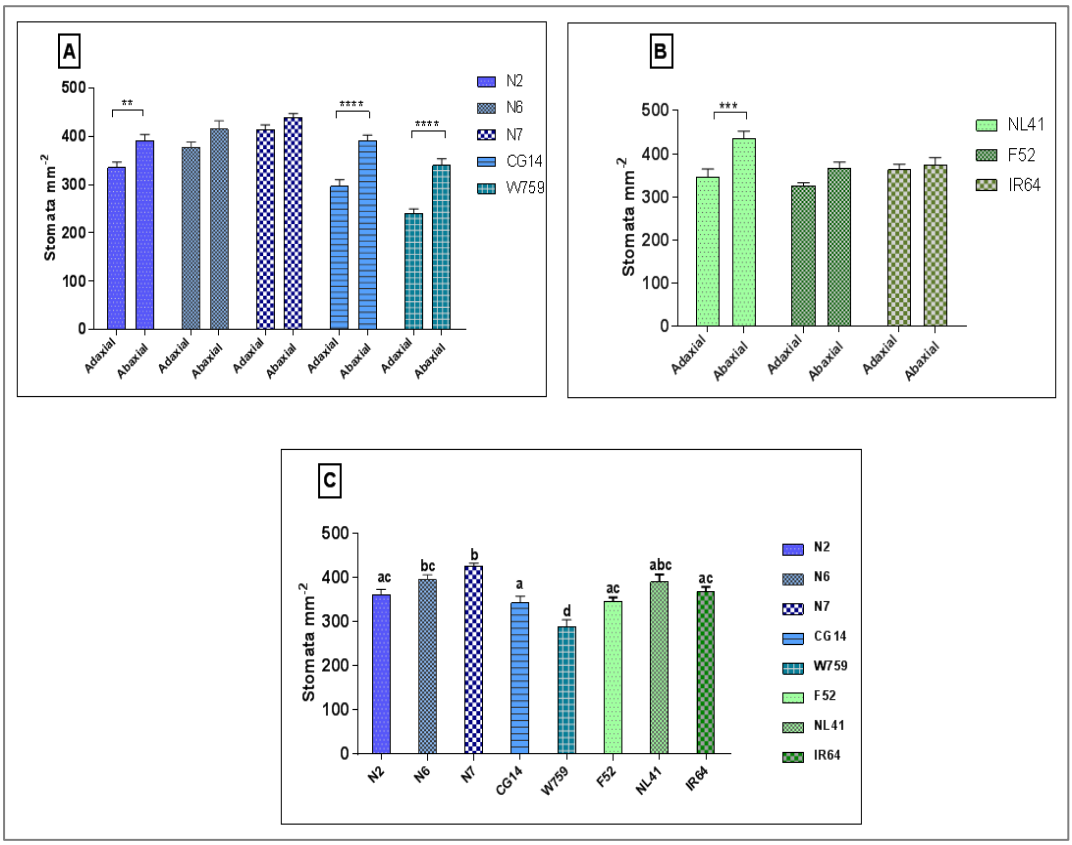

Figure 3.11. Stomatal densities on the adaxial and abaxial surfaces of flag leave across different regions of the leaf. **A**. adaxial vs abaxial surfaces of the upland rice grown in the column. **B** Adaxial vs abaxial surfaces of the lowland rice grown in the column. **C**. Total stomatal density (adaxial and abaxial) of the upland rice. All values are means with SEM error bars.

The Figure 3.11 A and B showed the abaxial (bottom) surface of a rice leaf mostly had a higher number of stomata than the adaxial (top) surface in some of the genotypes. The density on the abaxial surface of

N2 was significantly (P≤0.01) higher than its adaxial surface by 14%. Similarly, in CG14 the abaxial was significantly higher (P≤0.0001) by 23.9% and W759 (P≤0.0001) by 29.2%. The total stomatal densities (abaxial and adaxial), N7 has shown significantly higher density than CG16 by 19%, W759 by 32%, N2 by 15%, F52 by 19% and IR64 by 14%. W759 has the lowest stomatal density of all the eight (8) upland and lowland genotype examined. The stomatal density of N6 is higher than CG14 by 13%. NL41 has shown a significantly higher stomatal density than F52 by 11%. This suggested that the number of stomata does not depend on their ecosystem (upland or lowland), rather genotypic differences. The result here may suggest that the high stomatal density of N7 may have played a role in the high stomatal conductance under WW condition,

3.4.2 ROOT ANALYSIS

In the literature, a root depth has a strong link to the ecosystem with which a rice genotype belongs. The upland has longer root depth than lowland. The root growth at soil depths below 30cm may provide lowland rice with access to water reserves during the drought period. In this experiment, 1 meter PVC column was used to examine the genetic variation to depth and root development in limited water condition of African genotypes (at around 75-80 DAS). The PVC column was cut open at the beginning of the reproductive stage, the presumed stage when root development ceases. The time to flowering among the genotype in the well-watered greatly differs among the genotypes. The African diverse panel exhibited interesting phenotypic variation for root architectural traits examined in this study. The well-watered N8 revealed a significantly higher root depth than W56, F52 and IR64 (P<0.05) by 28%, 47% and 49% respectively (Figure 3.13 A). There has not been any increase observed in root depth by drought, but CG14 had significantly reduced its root depth by 56% in drought condition. The total root length computed from the commercial root software (WinRhizo) reveals among the uplands, N8 has longer root length than all the genotypes including the lowlands significantly. Similar differences were not observed in the drought treated. Drought stressed F52 was

significantly (P<0.05) shorter than the drought stressed N6 and N8 (see Figure 3.13 B).

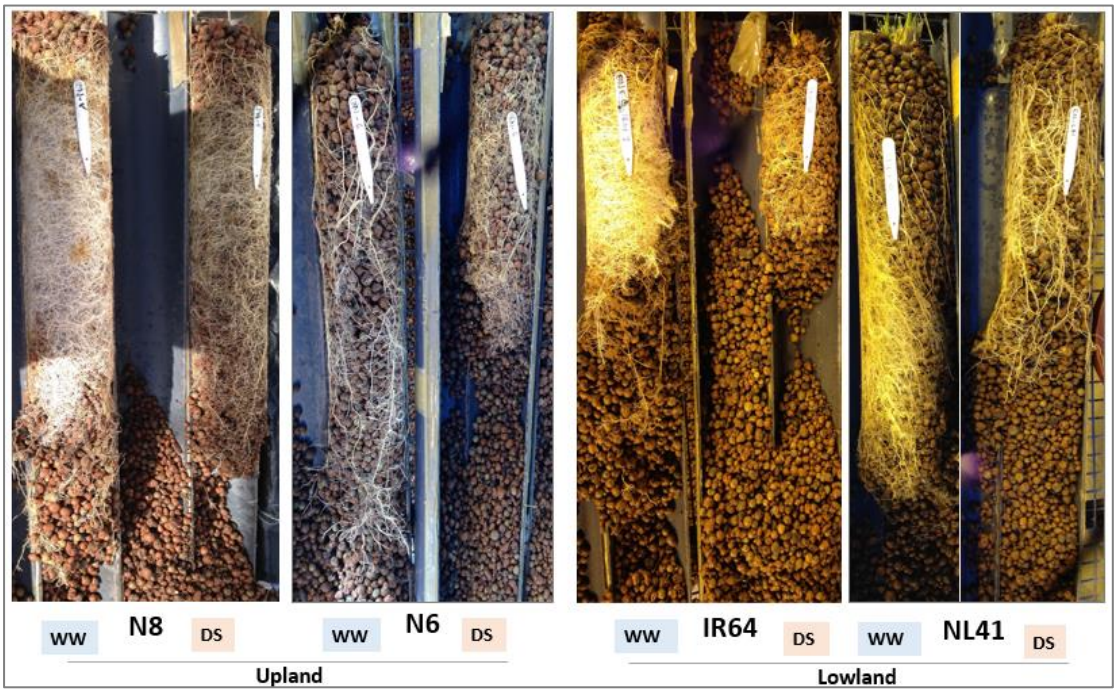

Figure 3.12. The photographic illustration of the differences in root architecture of the Uplands and lowlands following the 18 day DS versus WW. Scale: White label in the picture =10cm.

The root diameter in rice has been strongly associated with rapid water acquisition strategy under limited water stress. Rice adopt a strategy of thinning of roots in water limited stage, and it varies with position. The roots average diameter (RAD) at the top 10cm of well-watered N2 and N7 were significantly larger than N8 (P<0.05), CG14 (P<0.01) and NL41 (P<0.01). Drought stressed N2 and N7 were also larger than F52 (P<0.01) and NL41 (P<0.05). W181 was also larger than NL41 (P<0.05). The F52 reduced significantly after DS by 26% from its WW control.

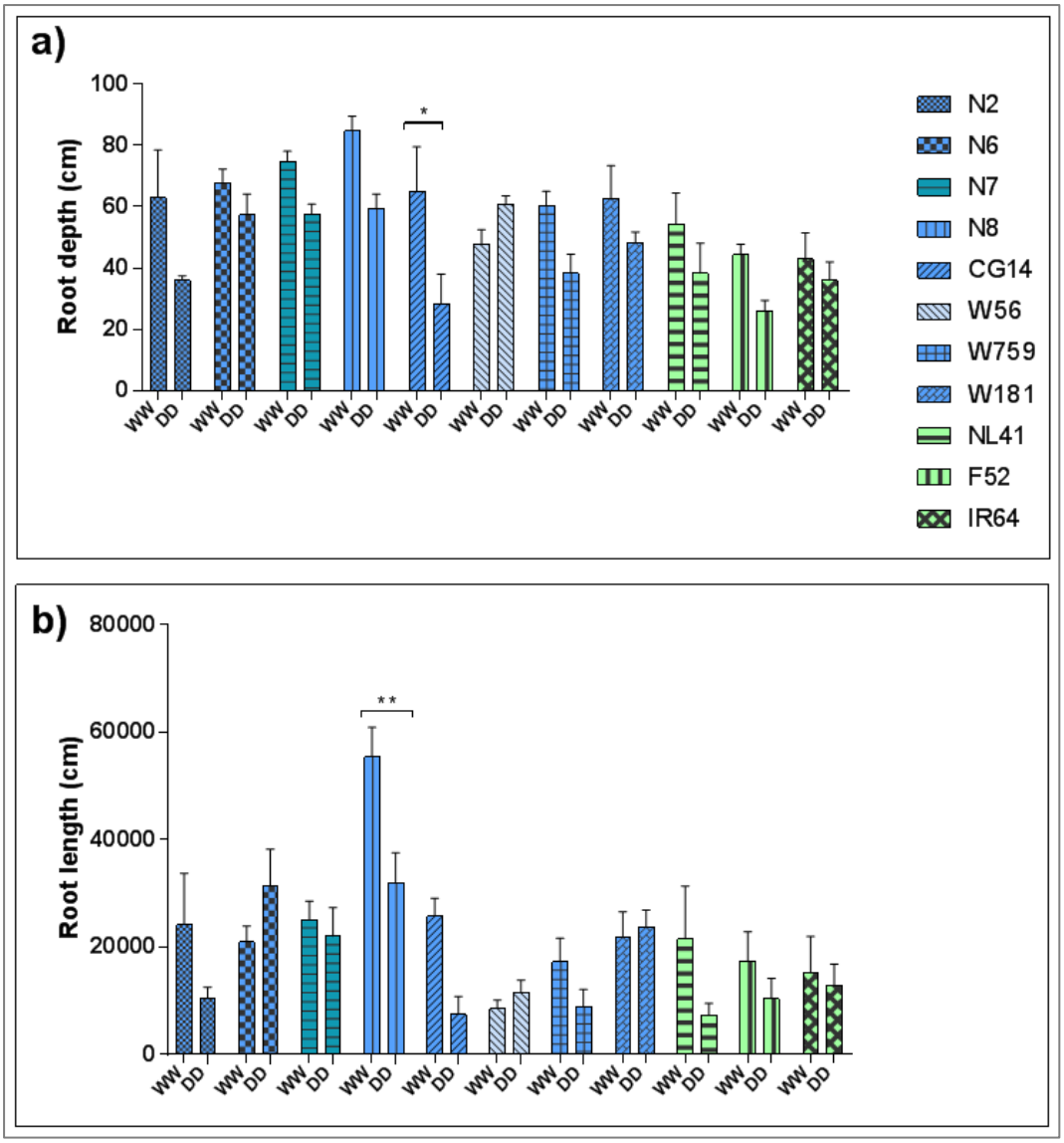

Figure 3.13. Root phenotypic differences among the African genotypes in well-watered and drought stressed conditions. A. The root depth. B. Root length. The asterisks represent the significant difference between the two treatments of the same genotype. (*=P≤0.05, **= P≤0.01). Error bars indicate the Standard Error of the Mean (±SEM)

The root average diameter of the entire roots in WW treatment revealed N2 was significantly ($P<0.05$) higher than N8, CG14 and W759. N6 was also higher than CG14. After the DS, N6 showed significant ($P<0.05$) decrease in the RAD by 25% from its WW treated. The N8 has shown a significantly higher root volume than N6 ($P<0.05$), W56 ($P<0.01$), W769 ($P<0.05$), NL41 ($P<0.01$), and IR64 ($P<0.01$) in well-watered condition. Similarly, N7 has significantly higher root volume than F52 ($P<0.01$). The differences were only observed between the genotypes, but no differences observed after the drought stress.

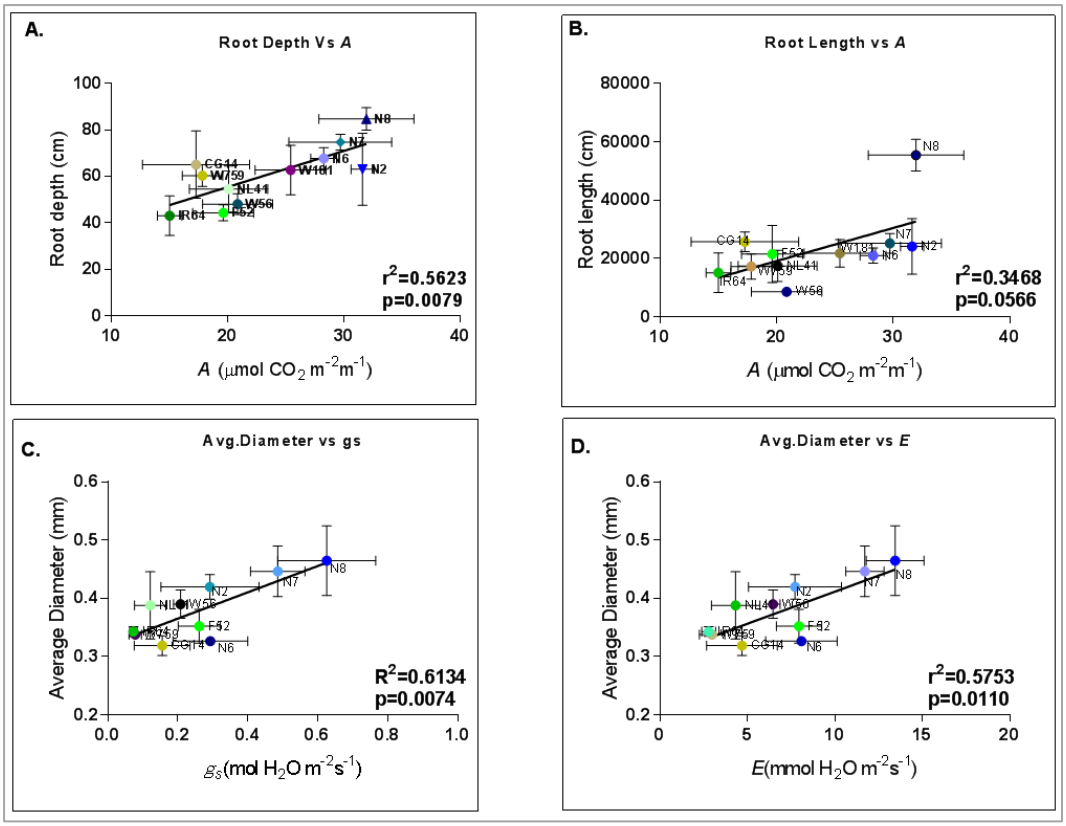

Figure 3.14. The relationship between the root morphological traits and the leaf gas exchange parameters (at 35 DAS) showing evidence that roots morphology is needed to support high photosynthesis. **A** Root depth vs CO_2 assimilation, **B**. Root length vs CO_2 assimilation rate. **C**. Average root diameter vs stomatal conductance, **D**. Average diameter vs transpiration. Error bars indicate ±SE on either side of the mean.

There were strong positive relationships between the root morphology and the gas exchange parameters (Figure 3.14). Between the root depth and the *A*, there was a significant correlation (r^2=0.5623, P=0.0079) between them. The average root diameter was also significantly (r^2=0.6134, 0.5753 and P=0.0074, 0.0110 respectively) correlated with gs and *E.* This, therefore, provides good evidence that root morphology is needed to support high photosynthesis via increased water access across diverse genotypes

3.4.2.1 Root Anatomy

Among the various anatomical traits present in roots, the metaxylem number has shown greater influence in the internal capture of CO_2, gs, and enhancement of water use efficiency in drought stress during the reproductive stage through hydraulic conductance. When the plant

opens their stomata to achieve high gs, to capture CO_2 for *A*, water is loss by transpiration. The water evaporating from the air spaces is replaced from cell walls, in turn drawing water from the xylem of leaf veins, stem and roots (Sack and Scoffoni, 2012). The root anatomical study was carried out with the assistance of John Vaughan Hirsch (UoN) on 7-day old primary roots of the plants used in the current study. In this study, the central metaxylem (CMX) differs among the genotypes (see figure 3.15 A). The lowland generally showed the lower area of CMX than most uplands. N7 had shown a significantly higher area of CMX than W759 ($P<0.001$), W56 ($P<0.001$), N2 ($P<0.01$), N8 ($P<0.01$), Kaybonnet ($P<0.01$), IR64 ($P<0.001$) and F52 ($P<0.001$). The CG14 had also shown significantly higher CMX than F52 ($P<0.01$), IR64 ($P<0.05$) and W759 ($P<0.05$). The F52 of the lowland had the lowest area of CMX and was significantly lower than NL41 ($P<0.05$) and W181 ($P<0.01$). The W759 had the lowest among the uplands and was significantly lower than W181 ($P<0.05$) and NL41 ($P<0.05$).

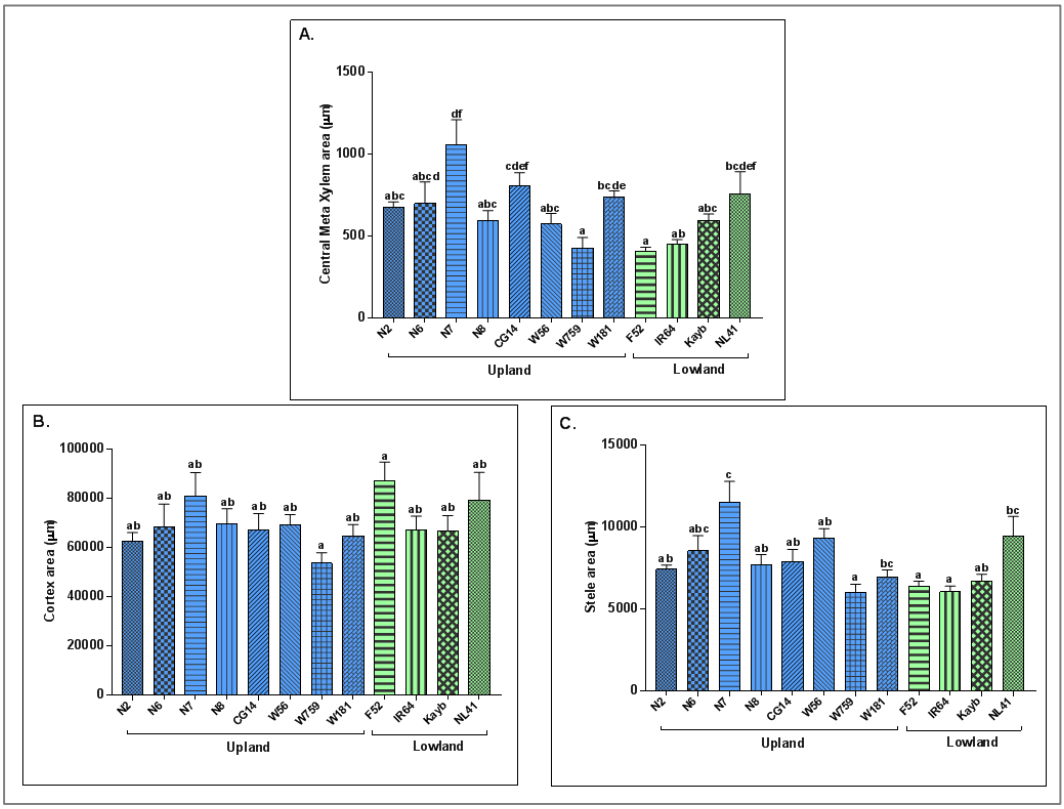

Figure 3.15. Anatomical traits of the upland (blue) and lowland (green) of the 7-day old seedling. A. Central metaxylem. B. Cortex area. C. Stele area. Different letters indicate significant differences. Error bars indicate the Standard Error of the Mean (±SEM)

The high stomatal density and the area of CMX found in N7 can be attributed to the high stomatal conductance and transpiration showed by the genotype in well-watered condition. It can also be linked to the high water use efficiency showed by N7 in drought condition. There was a strong positive relationship between the canopy temperature (in figure 3.5) and the CMX ($P<0.05$) at $R^2=0.5747$ (Figure 3.15) indicating an underlying relationship between whole plant water movement and xylem morphology among these lines.

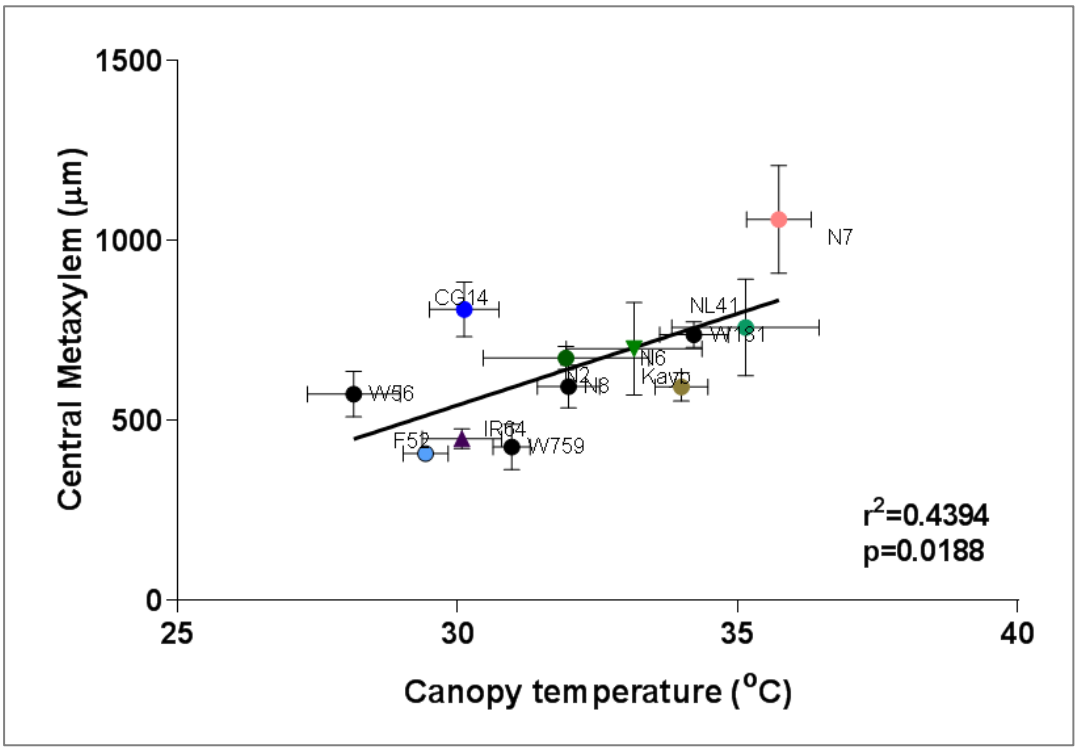

Figure 3.16. The relationship between the central metaxylem and the canopy temperature under well-watered. Plot show means ±SE.

There were no much differences in cortex area among the genotypes, except F52 with significantly higher than W759 ($P<0.05$). The stele area where all vessels are located (see Figure 3.15 C) also reveals N7 with significantly larger area than CG14 ($P<0.05$), N2 ($P<0.001$), N8 ($P<0.05$), W759 ($P<0.001$), W181 ($P<0.001$), F52 ($P<0.001$), IR64 ($P<0.001$) and Kaybonnet ($P<0.001$). The W759 however, showed a significantly smaller area than W56 ($P<0.01$), NL41 ($P<0.05$). The W56 and NL41 were larger than F52 and IR64 ($P<0.05$).

3.4.2.2 Biomass Analysis

The fresh shoot weight at the end of the experiment in the well-watered revealed N8 was significantly higher than the N2, W56 and F52. N7 had also shown significantly higher fresh weight than F52 (Table 3.2). Between the droughts treatment, no difference in fresh weight was observed. Between the treatments, N7, N8, CG14 and NL41 had significantly dropped their fresh weight by 53%, 54%, 73%, and 66% respectively. The Two way ANOVA reveals there was a strong interaction ($P<0.01$) between the genotypes and the treatment. Two upland genotypes had shown outstandingly higher dry weight than any of the genotypes used (Table 3.2). N7 had significantly higher dry weight than N2, N6, CG14, W56, W759, W181 and NL41 at $P<0.001$, then significantly higher than F52, and IR64 at $P<0.05$. Similarly, N8 dry weight was significantly higher than N2, NL41, F52, W56 and W759 at $P<0.001$, then CG14 ($P<0.001$) and W181 ($P<0.05$) level of significance. No difference between genotypes was observed in the drought treatment. Between drought and well-watered control, N7, N8 and IR64 have shown a significant loss in dry weight by 65%, 58% and 58% respectively. The total leaf area examined at the end of the experiment (Table 3.2) reveals no statistical differences between the genotypes in the well-watered condition as well as in the drought stress condition. This suggests that despite the significantly higher number of tillers (at the end of the experiment) formed by most of the lowland genotypes (F52, and IR64), the uplands varieties, however, (particularly N7 and N8) were able to compensate the differences with large sized leaves, sheath, and stalk. However, between the two treatments, N8 had significantly reduced ($P<0.05$) total leaf area after drought stress by 24%.

GENOTYPE	WELLWATERED			DROUGHT STRESS		
UPLAND	**Fresh weight (g)**	**Dry weight (g)**	**Leaf Area (cm^3)**	**Fresh weight (g)**	**Dry weight (g)**	**Leaf Area (cm^3)**
NERICA 2	38.4±6.0^{a}	6.4±0.3^{a}	894.5±104.1^{a}	22.7±2.2^{ab}	2.7±0.3^{a}	508.5±40.7^{a}
NERICA 6	83.7±8.8^{a}	14.5±4.6^{ab}	1298±48.4^{a}	63.9±1.4^{c}	5.0±1.5^{a}	753.3±21.9^{a}
NERICA 7	104.8±6.3^{a}	38.0±1.7^{c}	858.4±151.8^{a}	48.9±4.2^{abc**}	13.3±1.3^{a****}	439.6±85.0^{a}
NERICA 8	111.7±4.4^{a}	29.9±1.2^{bc}	956.7±138.8^{a}	50.4±8.8^{bc**}	12.3±2.3^{a***}	724.0±123.3^{a*}
CG-14	85.5±8.2^{a}	10.4±4.5^{a}	938.5±45.1^{a}	26.9±4.0^{ab**}	3.0±1.8^{a}	330.0±90.5^{a}
WAB 56	59.9±11.6^{a}	5.9±2.3^{a}	573.2±66.6^{a}	35.3±4.3^{abc}	5.4±2.3^{a}	445.4±55.1^{a}
WAB 759	75.8±14.6^{a}	6.2±1.0^{a}	1291.8±194.6^{a}	35.7±8.6^{abc}	3.4±0.7^{a}	679.9±155.3^{a}
WAB 181	93.3±19.0^{a}	8.0±0.7^{a}	935.8±260.8^{a}	53.1±6.1^{bc}	4.9±1.5^{a}	628.1±158.1^{a}
LOWLAND						
FARO 52	45.6±14.3^{a}	7.5±1.8^{a}	873.7±267.0^{a}	18.2±6.9^{a}	8.6±5.1^{a}	410.0±149.9^{a}
NERICA-L41	78.5±16.5^{a}	9.7±5.2^{a}	1195.0±140.1^{a}	26.9±4.0^{ab*}	6.1±1.1^{a}	511.3±122.6^{a}
IR64	70.7±24.5^{a}	20.6±5.1^{ab}	1176.1±438.8^{a}	27.4±6.4^{ab}	8.5±1.9^{a*}	507.7±78.9^{a}

Letter groups (vertically) indicates significant differences. The asterisks represent the significant differences between well-watered and drought stressed. (*=P≤0.05, **= P≤0.01, ***= P≤0.001, ****= P≤0.0001)

Table 3.3. Summary of the total biomass: Fresh weight, Dry weight and leaf area. Different letters indicate significant differences and the asterisk indicate the significant difference between the two WW and DS. The ± represents the Standard Error of the Mean (SEM).

3.4.3 POT EXPERIMENT:

3.4.3.1 The response of potted drought stressed African genotypes to measurement under Low and High relative humidity

Based on data from the column experiments, a smaller number of upland and lowland genotypes were selected for this study. The selection was based on the variability of their responses to gas exchange, stomatal density and canopy temperature and root morphology under drought stress. Plants were grown in compost, and drought stress followed. The gas exchange was carried out in two different relative humidity conditions controlled at the time of measurements in the IRGA.

3.4.3.2 Instantaneous gas exchange measurement at different RH (P_{max})

At 5 to 6 weeks after sowing (WAS), gas exchange measurements were taken at two RH levels controlled within the IRGA. High relative humidity (>55 %< 65) and low relative humidity (28±1%) as described. This was carried out to explore the effect of RH to gas exchange and the extent it may have influenced the previous experiment in the columns.

Between the genotypes, no statistical differences in *A* and *E* were observed in both the two RH levels. The response to the *gs* to high RH was however different as the N7 was significantly higher than the N2, W759 and NL41.

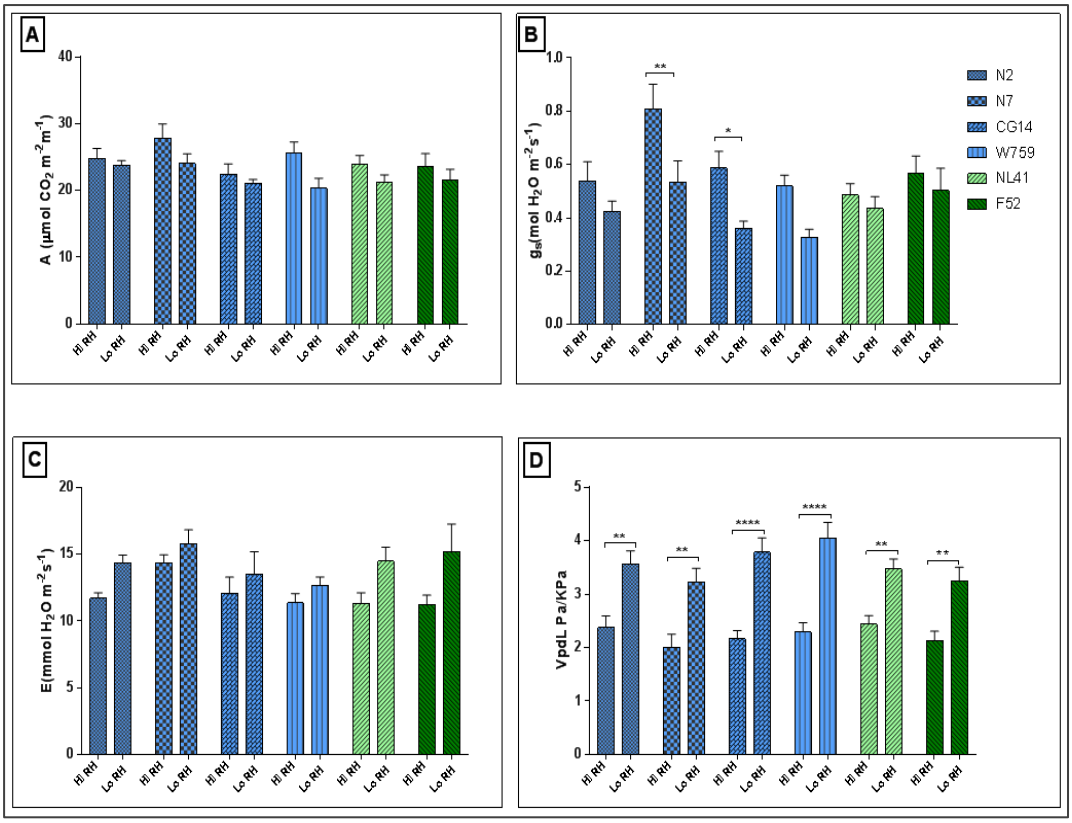

Figure 3.17. Leaf gas exchange in high and low cuvette relative humidity (Hi vs Low RH) levels. **A**. CO_2 assimilation rate at steady state (*A*). **B**. stomatal conductance (gs). **C**. transpiration (*E*) and **D**. Vapour pressure deficit (VPD). All values are means with ± SEM error bars. Asterisk indicate level of significant difference between the two relative humidity (*=P≤0.05, **= P≤0.01, ***= P≤0.001, ****= P≤0.0001).

Similarly, between the two RH levels, *gs* was strongly influenced. The N7 and CG14 showed a significant decline of *gs* in low RH by 34% and 40% (Figure 3.17). There was a compensation in the leaf to air vapour pressure (VPD) which has direct bearing to stomatal regulation. Low RH is driven by the atmospheric demand from a region of higher water potential to a lower potential. Hence, low RH showed a significant increase on VPD in all the genotypes.

3.4.3.3 Drought stress

After 5 days of drought stress, measurement at Hi RH revealed no significant difference in the mean of *A* between the well-watered and the drought stressed (Figure 3.18 A). The stomatal conductance was reduced by the drought stress in lowland F52 by 69.8% (P≤0.01). Similarly, the F52 showed a decline in their *E* by 69.4% (P≤0.05) in the

same condition. The VPD remain almost unchanged in Hi RH between drought stressed and well-watered in all the genotypes.

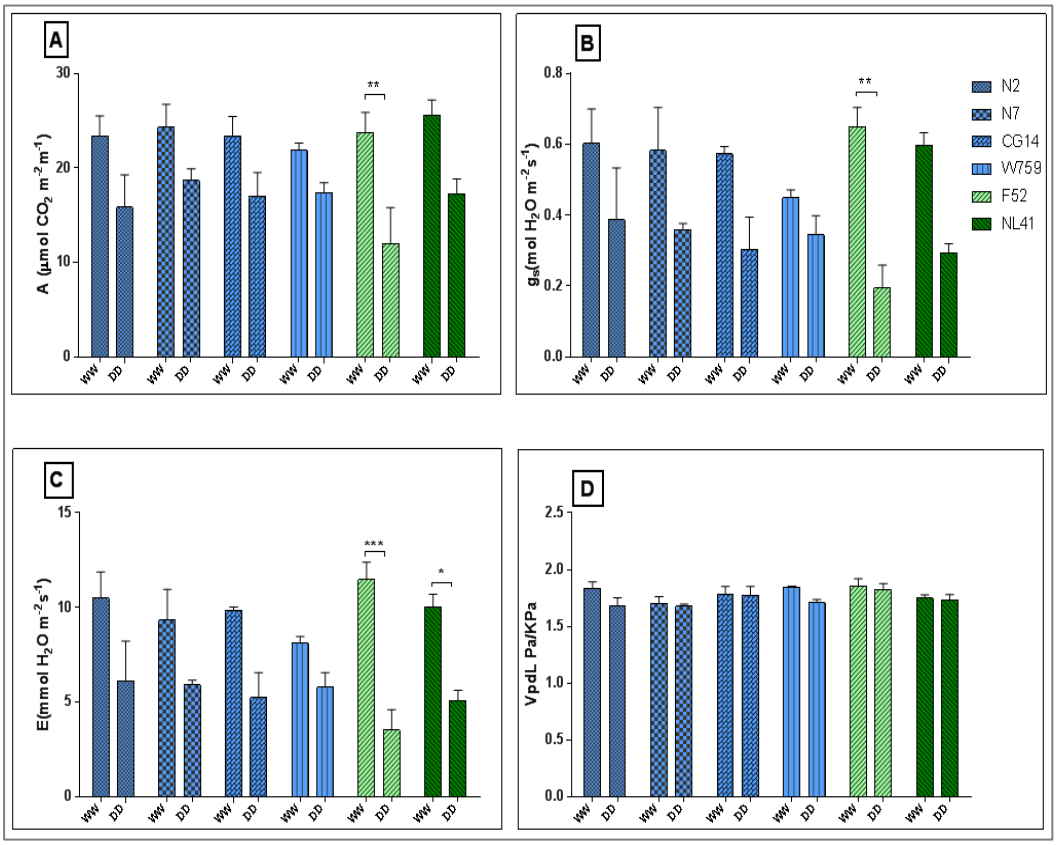

Figure 3.18. Leaf gas exchanges in high cuvette relative humidity under drought stress. **A**. CO_2 assimilation rate at steady state (*A*). **B**. stomatal conductance (gs). **C**. transpiration (*E*) and **D**. Vapour pressure deficit (VPD). All values are means with ± SEM error bars. Asterisk indicates the level of significant difference between the two relative humidity (*=P≤0.05, **= P≤0.01, ***= P≤0.001).

On the same 5th day of drought, measurement at low RH (Figure 3.19) showed a decline in *A* under drought for the lowland F52 by 46.2% at the P≤0.01 level of significance. The *gs* of the lowland F52 at low RH showed significant (P≤0.001) declined in drought by 77%. The other lowland genotype; NL41 also showed a significant (P≤0.01) decline after the drought by 63.8%.

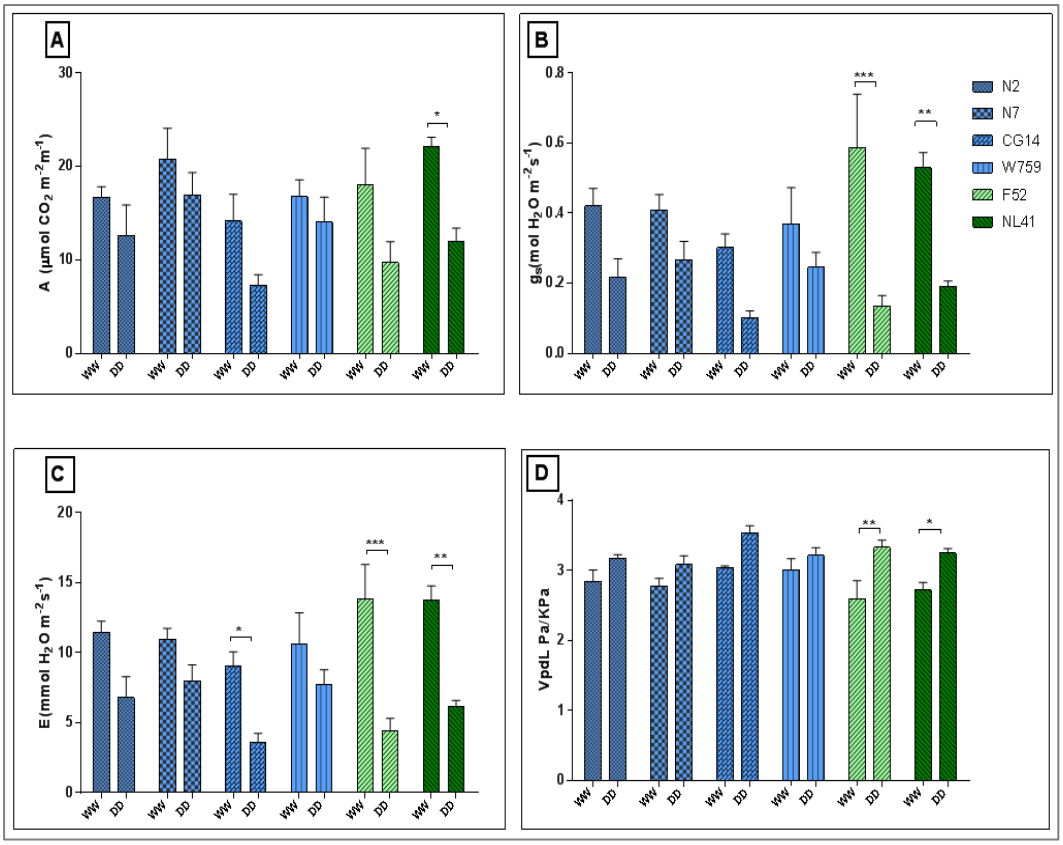

Figure 3.19. The response of the African lines to gas exchanges measurement in low relative humidity under drought stress. . **A**. CO_2 assimilation rate at steady state (*A*). **B**. stomatal conductance (gs). **C**. transpiration (*E*) and **D**. Vapour pressure deficit (VPD). All values are means with ± SEM error bars. Asterisk indicates the level of significant difference between the two relative humidity (*=P≤0.05, **= P≤0.01, ***= P≤0.001).

A similar trend in the *E* was observed with the lowland F52, and NL41 showed a significant decline in their loss of water after drought by 68% (P≤0.001) and 55.2% (P≤0.01) respectively. There was a compensation in the leaf to air vapour pressure (VPD) which has direct bearing to stomatal regulation. VPD has shown to increase with a decrease in RH in Fig 3.19 D, drought condition has further increased the VPD in all the genotypes, but it was significantly increased with the F52 and NL41 by 21.9% (P≤0.01) and 16.3% (P≤0.05) respectively.

3.4.3.4 Analysis of responses to Light (PAR)

Changes to *A* in response to varying light levels of Photosynthetic Active Radiation (PAR), was used to quantify the efficiency of the absorption of light energy into Photochemistry. Light response to *A* of the upland and

lowland rice genotypes in Figure 3.20 showed no differences among the genotypes at all the light levels including the point at saturated photon flux (A_{max}) in non-water stress condition. This may suggest that between all the genotypes, no sign of stress or genetic photoinhibition can be linked.

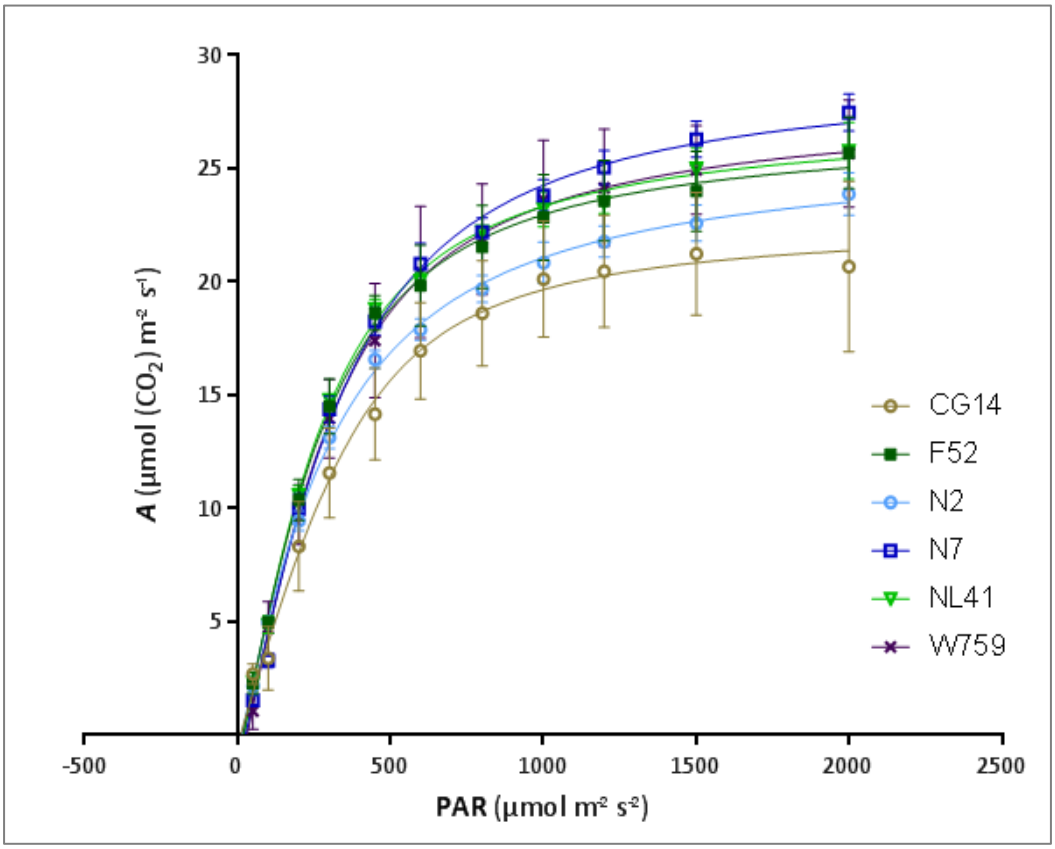

Figure 3.20. The Light response to assimilation rate on a fully expanded non stressed rice leaves. All data point are means with ± SEM error bars Values are means and standard errors. n= 3-4

Figure 3.20 shows light-saturation curves for the African genotypes measured at 28% relative humidity level. At 400µmol^{-1} CO_2, the photosynthesis was saturated at 2000 µmol $m^{-2}s^{-1}$ for both the genotypes. The chlorophyll fluorescence measured in the light state for the maximum quantum efficiency of open PSII reaction centres (Fv'/Fm') and the photochemical quenching (qP, the driving energy for *A*) reveals no significant differences were observed among the genotypes in a non-drought stress condition (data not shown).

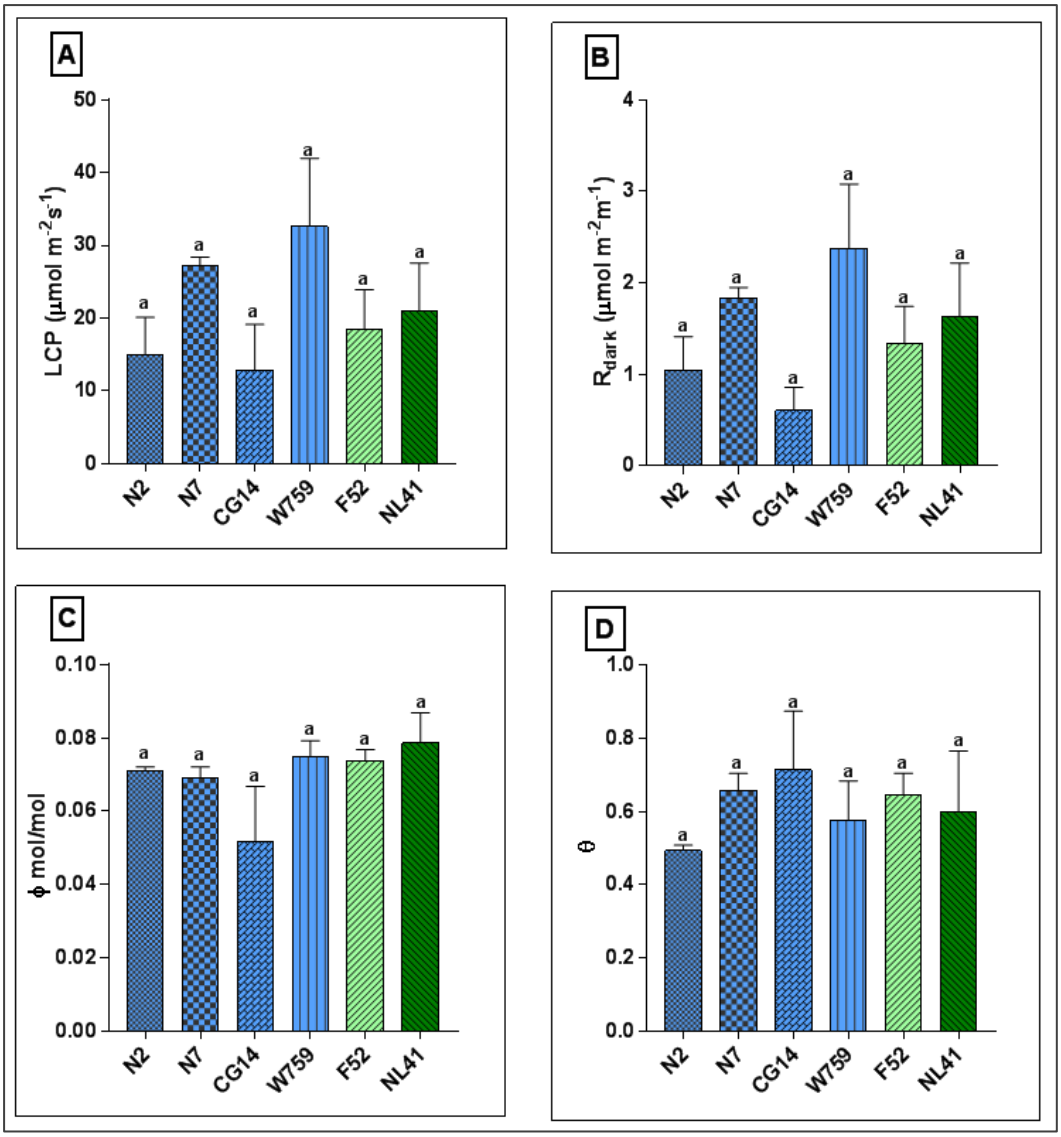

Figure 3.21. Simulated results estimated from the Light response curve. **A**. Light compensation point (LCP). **B**. Dark respiration rate (R_d). **C.** apparent maximum quantum yield (ϕ). **D**. Convexity of the curve (θ). All values are means with ± SEM error bars. Different letters denote significant differences among the genotypes.

The estimated parameters in Figure 3.21 were derived from the four parameters non-rectangular hyperbola fitted curves. The result revealed that there were no significant differences in their compensation points (incident light at A=0), the mitochondrial respiration in the light or dark respiration (R_d), the apparent maximum quantum yield (mol/mol), and curve convexity (θ). This may, therefore, eliminate the presence of photoinhibition among the genotypes.

3.5 DISCUSSION

3.5.1 Choice of growth medium

In this study, the genotypic variability in responsiveness to drought on both shoots and roots in terms of physiology, morphology and anatomy were analysed. As mentioned, the NERICA (New Rice for Africa) varieties were developed from the crosses between the *Oryza sativa* (W56) and *Oryza glaberrima* (CG14).

The rice genotypes used in this study had been previously characterised with varying drought tolerance, and this study aimed to determine whether the drought tolerance trait is associated with root traits, stomatal traits or whether there is evidence of both. To achieve this, tractable artificial growing condition to look at both the roots and the shoot in a controlled condition is required and could be very challenging. Pots experiments may compromise root study unless the size and depth of the root are taken into account. Soils can make the separation of root and shoots difficult. The hydroponic condition cannot be considered for drought experiment because physical touch also stimulates roots. However, expanded clays beads (Hydroleca) that are commonly used for horticultural and landscaping practices were used in a long PVC column because they are light and does not hold water, and they provide the advantage for the easy separation of the roots after the experiment. However, there were many limitations involved with this method, for example; the volumetric water content could not be monitored due to its size and nature of its water holding capacity. The nature of the hydroleca does not necessarily fit well for crops as it does not retain either water or nutrients for long periods. Thus, water with nutrients supplement was used for irrigation every day for well-watered treatment and with intervals in the drought treatment. The use of the clay beads for the experiment was to provide easy extraction of the roots in both drought and non-drought condition at the end of the experiment as soil can be very challenging to deal with.

3.5.2 Photosynthetic gas exchange

The plant response to gas exchange in the hydroleca and the compost differs slightly (e.g. Figure 3.2 and 3.19), but high responsiveness to drought was observed in the hydroleca. Among all the genotypes examined in this study, the upland N7 and N8 has shown a particular responsiveness regarding the gas exchange. N7 and N8 had shown very high and consistent stomatal conductance and high transpiration rates in well-watered condition, greater than most of the genotypes; including their parents (W56 and CG-14). The response was observed when the measurement used 600µmol $CO_2 mol^{-1}$ as the reference CO_2 concentration. The artificial growing medium (hydroleca in columns) was very similar to hydroponic and thus, was not ideal because it limits the effects of root-soil interaction (Price et al., 2002a). More so, the plants responded physiologically differently each time water was added to the drought-stressed treatment. Meaning, the stomatal conductance increases with increase in water supply, this changes the state of stress incurred by the drought, and consequently, it was difficult to show the time course changes of the gas exchange in response to the drought. However, at the onset of drought stress, the remarkable sensitivity in the stomatal closure observed in N7 and N8 may suggest an improved physiological adaption to drought condition, since the plants have shown a substantial CO_2 assimilation rate with the reduced stomata. In the fluctuating natural environment, the stomata and *A* responds continually to change in environmental condition. In such a situation, the response is not always synchronised. Therefore, the rapid stomatal response in the N7 and N8 may also associate with the stomatal kinetics in a way to improve the synchrony with mesophyll CO_2 demand when the condition changes (Lawson and Blatt, 2014). Therefore, with the poor water holding capacity of the expanded clay, the N7 and N8, unlike the rest of the African genotypes, were believed to rapidly shut their stomata to control the water loss by transpiration in limited water condition. Thus, the calculated intrinsic water use efficiency (A/gs), revealed that with the rapid stomatal closure in N7 and N8 following the 'watering-drying' treatment of the hydroleca, they were able to achieve a substantial

photosynthetic rate. Hence, they had significantly high water use efficiency, which suggests a potential for drought tolerance (Webster et al., 2016). This was interesting, considering the diversity of the habitat of distribution of the N7 and N8, they are hybrid with improving drought tolerance in an upland condition where rapid drought and high humidity may demand a faster stomatal response. They displayed great photosynthetic potentials which are all attributed to high yielding potentials. In drought condition, their response suggests a specialised drought signalling mechanism that enforces rapid stomatal closure for the utilisation of the limited available water. The importance of rapid opening and closure of stomata in dynamic conditions was shown in recent work of Lawson and Blatt (2014). The rapid stomatal movement responds to multiple signals integrated and sometimes hierarchical manner. However, the short-term stomatal response, similar to N7 and N8 are often considered to be related to water status, and they respond to changes in VPD (often related to change in temperature). The intrinsic water use efficiency (A/gs) is the simple experiment that demonstrates the impact of the rapidity of stomatal responses to changes in water loss on carbon gain (Lawson and Blatt, 2014). This supports the increased intrinsic WUE observed in N7 and N8. Meaning, improvement in WUE occurs if stomata respond rapidly and in synchrony with mesophyll demands for CO_2.

In response to photosynthesis at 400µmol $CO_2 mol^{-1}$ of ambient CO_2 concentration, all the Upland NERICA's (N2, N6, N7 and N8) and one of their parent (CG14) displayed a remarkably high *A* and *E* in well-watered condition, despite the potential resilience to stress. The chlorophyll fluorescence measurements indicated that the genotypic differences between the NERICA's do not indicate major differences in the PSII photochemistry as evident by the quantum efficiency of PSII photochemistry (ϕPSII) values which are nearly identical. However, between their parents; CG14 and W56, the latter was significantly higher. The biochemical components of photosynthesis; V_{cmax} and J_{max} derived from the *A vs Ci* relationship revealed no differences between the genotypes. Despite the sensitivity of Rubisco activity to stress, the stress level of the genotypes at which the *ACi* was examined, was not

severe as no differences were observed in V_{cmax} and J_{max} between drought and well-watered treatments in all the genotypes.

To fully understand the varietal differences in their response to gas exchange and their potential to drought tolerance as seen in the two of the upland genotypes, the stomatal density was examined. Stomatal density and size can govern maximum potential conductance values (Franks et al., 2009, Doheny-Adams et al., 2012). The N7 has shown a significantly higher stomatal density on both the abaxial and the adaxial leaf surfaces than CG16, W759, N2, F52 and IR64. This differences may be linked to the high photosynthetic rates (*A, gs* and *E*) observed in well-watered condition on both hydroleca and compost. However, differences in the above ground alone may not be sufficient enough to explain why the genotype showed remarkable gas exchange potentials. Perhaps due to hydraulic conductance and efficiency of water extraction at depth. In fact, in hydroleca the root system will find it more difficult to extract water during drought treatment

3.5.3 Root morphology and water extraction

It is hypothesised that genetic variation in root structure and morphology exists among the lines tested here. Hence the adaptive advantage of improved root system would result in some attributes that may affect water uptake in some of the genotypes during drought. It was confirmed that the depth to which the roots travels down the column differs among the genotypes (e.g. Figure 3.13 A). Differences in root depth between upland and lowland rice are well-documented in the literature (Fukai and Cooper, 1995, Gowda et al., 2011b). The upland NERICAs generally had a longer maximum root depth that travels very deep in upland regions for water acquisition, for example, N8 reaching close to 100cm in the present study. The effect of the drought had not caused many differences in the root depth except in the CG14 which had been previously described as a drought resistant cultivar. However, drought had significantly reduced its depth by almost half. The root depth represents the potential for water and nutrients absorption from the soil in deeper soil layer. It is argued here that the root morphology reflected the gas exchange characteristics of CG14 in drought stress. Hence the longer

root length may also have determined the rate of water and nutrient uptake in N8. The N8 showed a remarkable high root length under well-watered and drought conditions. With high maximum root depth and root length. This means N8 went deeper to extract more water from the bottom of the column as seen in Figure 3.12. This suggests N8 among other upland genotypes has greater ability to extract water from the deep soil layer. Similarly, N8 has shown higher root volume and surface area in both well-watered and drought conditions. Even though, root volume and surface area may not be reliable in this setup, since the medium used was not soil (Dupuy et al., 2010). However, the root surface area and volume at the first 10cm below the soil, N8 and N7 were high. There was a decrease in the root length in N8 under drought. Generally, under drought stress, the adjustment of the osmotic gradient enables the loosening ability of the cell wall and reduced average root thickness. Hence roots continue growing under low water stress. However, the significant decrease in the root length in N8 under drought stress may be associated lack of reduced root diameter and root volume that compensates need for increased length under DS. Furthermore, the root depth was not statistically reduced.

Interestingly, the root average diameter which is associated with the potential for soil penetration ability, branching and hydraulic conductivity, was almost indifferent among the genotypes in both drought and non-drought condition, except in N6 that was significantly reduced by drought stress. At the first 10 cm root depth, it revealed N7 and N2 with larger root diameter. This, therefore, has compensated the water uptake ability to which root depth was unable to reach.

3.5.4 Root Anatomy

Water from the roots to the transpiring leaves passes through series of cell layers. These layers are root epidermis, exodermis, schlerenchyma layer, cortex cells, endodermis, pericycle, and xylem vessels. Once it reaches the xylem, it moves to the aerial part of the plants. Through different water transport channels (apoplastic, symplastic and transcellular), water exchange between the pathways can help the root to adjustment of water uptake ability through transpiration demand of

leaves (Gowda et al., 2011a). Root anatomy (which has a genetic basis) interaction with other factors affects water uptake potentials. The central metaxylem area influences internal capture of CO_2, improved *gs* and, enhances water use and uptake under drought stress (Prince et al., 2017). Other traits like large stele area and cortex area near the root tip in deeper have been reported to facilitate water and nutrient utilisation within the plant system until flowering through hydraulic conductance (Kadam et al., 2015). Previous studies have shown a relationship between the canopy temperature and deep rooting in drought stress (Pinto and Reynolds, 2015). In this study, the root anatomy has revealed the common genetic basis for adaptation to water stress. A 7-day old root of N7 had shown high CMX, stele and cortex area than any of the genotype used in the experiment (see Figure 3.14). A strong relationship between canopy temperature and the central metaxylem has been identified in this study. Thus, this clearly explained how N7 differed from the rest of the upland genotype in terms of the high *gs, E* and WUE.

3.5.5 Conclusion

Based on the results of this study, it can be proposed that N7 and N8 of the first generation of NERICA have displayed different drought tolerance/avoidance strategy that enabled them to have high photosynthetic productivity during drought stress. The high stomatal conductance observed in N8 suggests an effective water extraction by the roots at depth. Therefore, high root depth and root length have enabled N8 to combat drought tolerance. Thus, its drought tolerance strategy can be considered root based. While, stomatal density, large metaxylem area, large stele and cortex area had contributed to the drought tolerance and water use efficiency of N7. Therefore, the drought tolerance strategy of N7 can be considered both stomatal and root based. The stomatal sensitivity is yet to be understood. More detail research may be needed to be able to fully characterise the adaptive drought traits that exist within the African lines.

CHAPTER FOUR: TRANSGENIC MANIPULATION OF STOMATAL DENSITY IN RICE FOR THE CONTROL OF WATER LOSS AND IMPROVEMENT OF WATER USE EFFICIENCY

4.1 INTRODUCTION

Water use efficiency is determined by relative levels of photosynthesis, transpiration and stomatal conductance. An increase in photosynthetic CO_2 assimilation rate coupled with a relative decrease in the transpiration amounts to increase in the plant WUE, as a strong determinant of the rate of both CO_2 and H_2O stomatal conductance plays a crucial role in affecting the rate of WUE in plants (Medrano et al., 2015).

Different plant species have evolved to possess a different form of stomata with great differences in size, density, and shape. Two known types of stomata are the dumb-bell shaped and the kidney-shaped stoma. The former is often found among the monocotyledons (e.g. *Oryza sativa*), while the latter is usually found among the dicotyledons (e.g. *Arabidopsis thaliana*). Interestingly, the monocot stoma is considered more evolutionary advanced over the dicot because of more rapid alteration of the aperture when the guard cells sense changes in environmental conditions (Hetherington and Woodward, 2003).

Stomatal movement, density, size, and distribution strongly determines the plant rate of photosynthesis and transpiration. Exchange of both H_2O and CO_2 are essential for plant survival. Photosynthesis assimilates CO_2 into photosynthates while transpiration is needed for nutrients movement and absorption as well as maintaining low leaf temperature by transpirational cooling. Hence, through stomata, exchange of CO_2 and water occurs between the plant and its environment. The plant closes stomata or reduces stomatal aperture which restricts water by restricting gas exchange and consequently, negatively affects the rate of photosynthesis and transpiration. In addition to the aperture which occurs over a short timescales, it is becoming clear that plants also evolved morphological adaptations (and plasticity in these traits) to

compromise the balance between the photosynthesis and transpiration by altering the stomatal properties such as density, size, and arrangement to control gas fluxes with changes in the condition. How stomatal density affect gas exchange has received little attention in comparison with aperture. There are two key aspects: first the genetic differences in stomatal morphology between species and varieties. The second is the plasticity in response to environmental variation in relation to key environmental factors such as light, water status and CO_2 (Lake et al., 2001, Xu and Zhou, 2008, Franks et al., 2009, Hubbart et al., 2012, Ohsumi et al., 2007). Ohsumi et al. (2007) suggested that decrease in the stomatal size and stomatal density with water deficit were found to have a positive correlation with *gs, A,* and *WUE*. Flexas and colleagues suggest that the effective screening and analysis of gas exchange and photosynthetic characteristics of rice under stress conditions may identify the functional traits associated with effective utilisation of water use efficiency (WUE) and the maintenance of yield and photosynthesis under water deficit (Flexas et al., 2013).

Recently, several genes were identified affecting the stomatal behaviour and development.(Hara et al., 2009, Hunt et al., 2010, Hunt and Gray, 2009). This strategy has, therefore, became a focus of intensive research to alter environmental condition to study the stomatal behaviour or the application of genetic manipulation of stomata to improve WUE in plants (Franks et al., 2015, Doheny-Adams et al., 2012).

4.1.1 Stomatal development

Stomata evolved over 400 million years ago soon after the first land plants evolved (Vatén and Bergmann, 2012). Plants adapted to dry atmospheric conditions through the protection against desiccation and maintenance of hydration that permits gas exchange necessary for photosynthesis.

Interestingly, stomatal distribution is not randomised but tightly regulated in all parts of the epidermal surfaces of the plant by the endogenous developmental mechanisms that control their density and pattern in different part of the plant (Hunt and Gray, 2009). This, therefore, ensures effective, consistent gas exchange properties on

every surface within the plant. The spacing and distribution of the stomata have the one-cell-spacing rule between each stoma. Between each stoma, there is at least one pavement cell which does not bear guard cells. This complex one cell rule improves spacing between stomata to avoid crossover of diffusion 'shells', proper opening and closure of the stomata, as well as an efficient exchange of water and ion to the neighbouring non-stomatal cells within the plants (Peterson et al., 2010).

This can be modulated by the environmental factors. The stomatal density of plants was significantly influenced by the fluctuation of the atmospheric CO_2 concentration with time. Fossil records show that from the ancient Devonian to the Carboniferous era, the stomatal density had increased by up to 100 fold in response to a gradual decline in the atmospheric CO_2 concentration (McElwain and Chaloner, 1995). This resulted in the morphological advancement in the formation of planate leaves in vascular plants such as *Rhynia* and *Cooksonia* which are very different from the modern land plants (Franks and Beerling, 2009, Peterson et al., 2010). Yet their stomata have a striking resemblance with the modern land plants such as *Arabidopsis thaliana* (here referred to as Arabidopsis)

4.1.2 Molecular mechanism of stomatal distribution

The genetic and molecular studies in Arabidopsis, have shed light in the understanding of the mechanisms influencing stomatal differentiation, patterning, distribution and clustering in plants (Gray et al., 2000, Hunt et al., 2010, Hunt and Gray, 2009). Stomata are developed through asymmetric cell division in which each stoma has a smaller and two larger neighbouring cells developing from the asymmetric division within the stomatal lineage. During stoma morphogenesis in Arabidopsis, the differentiation pattern from a protodermal cell to a fully matured symmetrical guard cells (stomata) and the coordination of the cell spacing and density were all regulated by a complex network of signalling pathways associated with the interplay between positional signalling peptides and transmembrane receptor kinases. In the

beginning, a cell population that initiates the stomatal lineage called the protoderm, decides between two fates; either to develop to a pavement cells or follow the stomatal lineage. Three basic-Helix-Loop-Helix (bHLH) transcription factors regulate the major transition of cell-state during stomatal differentiation; *SPEECHLESS (SPCH*), *MUTE* and *FAMA*. These three transcription factors operate distinctly in a sequential way to regulate the cell identity from each step of the stomatal development process (Pillitteri et al., 2007, MacAlister et al., 2007).

The *spch* mutants exhibit an entire absence of stomatal lineage cells with only maze shaped pavement cells interconnected on the entire shoot surface (MacAlister et al., 2007). The *mute* mutants developed no functional stomata (Pillitteri et al., 2007). The *fama* mutants have stomatal precursor interrupted at the guard mother cells state resulting in the excessive zig-zag symmetrically divided cells with no true guard cells.

The protoderm divides asymmetrically into a stomatal precursor called a meristemoid (MMC, Figure 4.1). This step is controlled by the *SPCH* which controls the initiation asymmetrical cell division that initiates the stomatal lineage line. The meristemoid repeatedly divides asymmetrically one to three times usually, creating large sister cells called the Stomatal Lineage Ground Cells (SLGCs) and small meristemoid cells which decrease in size at every round of division. *MUTE* plays the role of stopping the meristemoid's asymmetric division and regulate the meristemoid differentiation into a guard mother cell (GMC). The guard mother cell (GMC) divides symmetrically once to form a pair of cells that developed thick walls of characteristic stomatal guard cells (GC)(Pillitteri et al., 2007). The third paralog controls the final step of switching from GMC to GC; *FAMA*. The SLGCs eventually differentiates into pavement cells (Peterson et al., 2010).

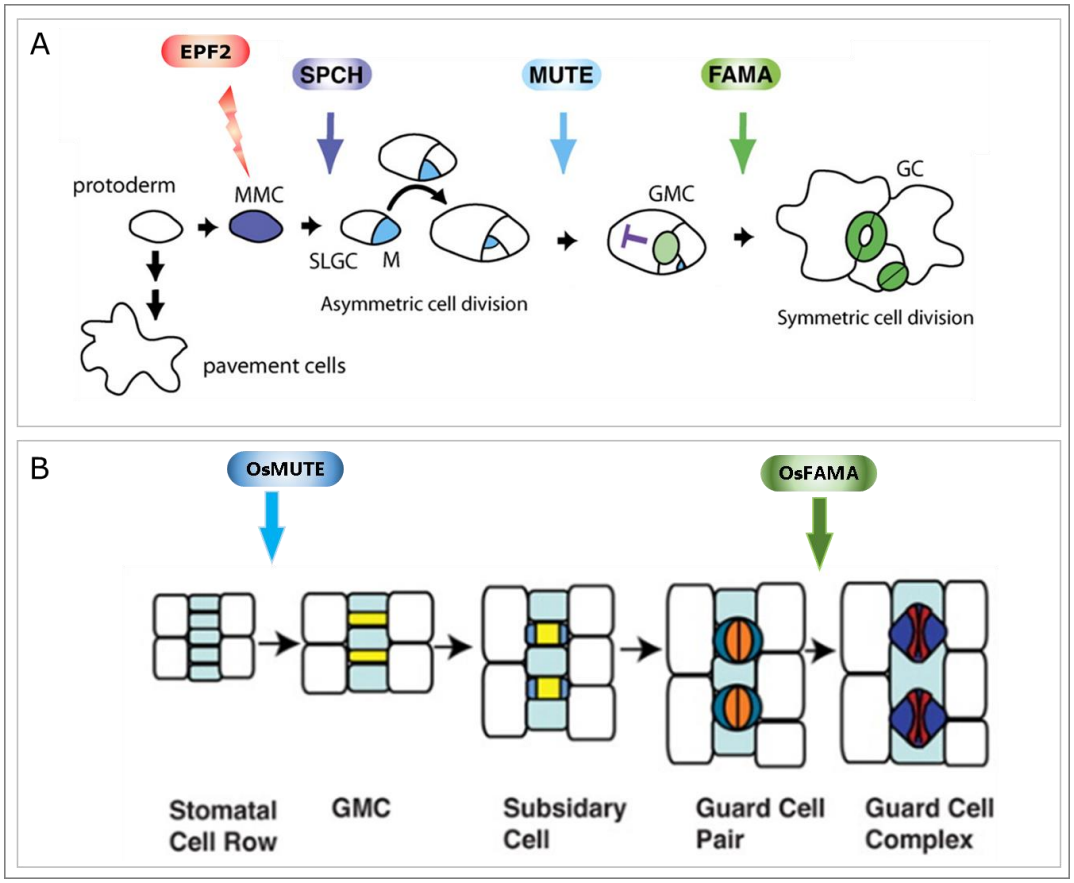

Figure 4.1. A. schematic description of stomatal development in Arabidopsis. The sequential cell developmental steps are driven by the three paralogous bHLH TFs at each point of a function. In the diagram, the protodermal cell decides between entering into stomatal lineage or differentiates into pavement cells. The putative ligand *EPF2* is proposed to be expressed in the MMC, which then through different signals block the protoderm to *MMC* transition. B. The stomatal developmental stages in rice with the bHLH TFs site of actions. *SPCH* is believed to act very early in rice before the illustrated stages in the stomatal lineage. Figures modified from (Liu et al., 2009, Rychel et al., 2010)

4.1.3 Patterning and Signaling: Epidermal patterning factor (EPF)

Stomatal development is regulated by both the environmental and developmental factors. Several signalling components characterised in the regulation of the stomatal development have been discovered (Lake et al., 2001). The one-cell stomatal spacing is regulated through the interaction of the secretory signalling peptides *EPIDERMAL PATTERNING FACTOR* (Like) family (*EPFL*) and the transmembrane receptors that comprises the three leucine-rich repeat receptor Kinases (*LRR-RLKs), ERECTA (ER), ERECTA-LIKE1* and 2 and one LRR-receptor-like protein,

TOO MANY MOUTHS (TMM) (Hunt and Gray, 2009, Vatén and Bergmann, 2012). The TMM and ER family play role as receptors for EPF peptides to initiate a signal cascade for stomatal development (Takata et al., 2013). Evidence suggests that an intracellular mitogen-activated protein kinase cascade (*MAPKKK*) became activated by the ligand binding to the receptor that then phosphorylates and destabilizes the bHLH TFs required in early leaf development and for a cell to begin the stomatal lineage (Doheny-Adams et al., 2012).

Unlike Arabidopsis, the positioning of the stomata in grasses is almost fixed at the early stages of the leaf development, which therefore eliminates the amplifying division in the group. The only step similar to Arabidopsis in grasses is the differentiation of GMC to guard cells. However, the paralog bHLH TFs (*SPCH, MUTE,* and *FAMA*) were all identified in *Oryza sativa* (Liu et al., 2009). Evidence has shown that genes in Arabidopsis shares function with their grass homologs particularly the bHLH. A slight difference in the time of expressions like the *OsSPCH* (1/2) which are expressed very early and possibly before the production of stomatal lineage. While *OsMUTE* is expressed later during stomatal development in Arabidopsis than in its grass counterparts that express earlier. Finally, the *OsFAMA* which is highly conserved in terms of expression pattern and changes in phenotype in both rice and Arabidopsis during stomatal development (GMC to GC) (Liu et al., 2009).

4.1.4 The Putative EPIDERMAL PATTERNING FACTOR

The EPF gene family is a cysteine-rich family of 11 putative secretory peptides that contains six conserved cysteine residue at their C-terminus (Figure 4.3). They encode plant-specific secretory peptides, several of which play a role in controlling stomatal density and patterning.The members include the mostly known *EPF1* and *EPF2* that are known to inhibit stomatal formation. The additional nine members are known as the EPF-like peptides from 1-9 (*EPFL1-EPFL9*). Among the nine *EPFL* peptide member, *EPFL4* and *5* have been categorised with the *EPF1* and *2* in the inhibitory function of stomatal development when ectopically

overexpressed. Hara and colleagues suggest that since these peptides are not expressed in the cell of the stomatal lineage, they are not likely to be implicated in the control of stomatal development (Hara et al., 2009).

The expression of *EPF2* in the protodermal cells regulates the decision that impacts on both the stomatal and the ground cell proliferation (Hara et al., 2009). Thus, the overexpression of the *EPF2* entirely inhibits asymmetric cell division of the MMCs into the stomatal lineage by the promotion of pavement cells formation at the expense of the GCs (Hunt and Gray, 2009). The expression of *EPF2* in the protodermal cells regulates the decision that impacts on both the stomatal and the ground cell proliferation (Hara et al., 2009). The phenotype of the *EPF2* overexpression (Figure 4.2) relied on the functional *TMM* and at least one of ER-family (*ERL1* and *ERL2*) and *YDA* because evidence has shown that the *EPF2* function upstream of the TMM (Hara et al., 2009).

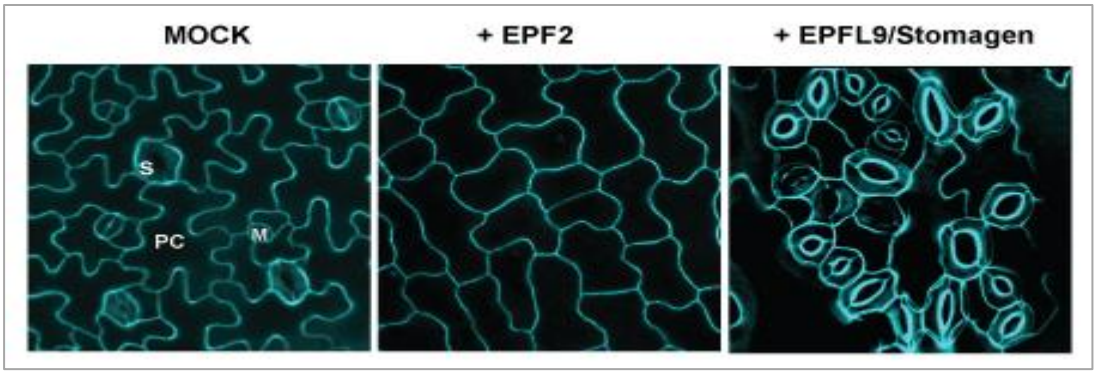

Figure 4.2. Confocal images of cotyledon epidermis of Arabidopsis seedlings grown; wild-type (left), in the presence of recombinant *EPF2* (middle) and *EPFL9* (right). (Lee et al., 2012)

EPFL9 unlike the other member of the *EPFL* secretory peptides, is commonly called *STOMAGEN* and was recently identified as a positive regulator of stomatal development. *EPFL9* has a role that antagonises the function of the *EPF1* and *EPF2*. The *EPFL9* is expressed in the leaf mesophyll layer of immature leaves and not in the epidermal tissues where stomata develop (Sugano et al., 2010, Katsir et al., 2011). The overexpression of *STOMAGEN* increases both the stomatal density and

clustering. It is predicted to prevent the inhibitory *EPF2* peptide from binding to their receptor that prevents stomatal development. *EPFL9* like EPF2 both requires functional *TMM* to exert its cell fate since overexpression of both *EPF2* and *EPFL9* on *tmm* mutants fail to alter their stomatal development. Similarly, STOMAGEN fails to increase the stomatal density of *epf1* and *epf2* mutants. Thus suggesting *STOMAGEN* and *EPF2* compete for the same receptor (Kondo et al., 2010).

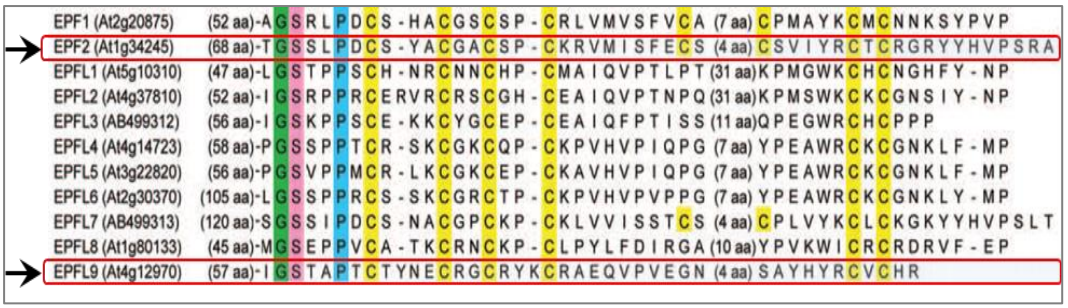

Figure 4.3. The alignment of the C-terminal regions of the EPF family protein. Conserved amino residues sequences are highlighted in colours (cysteine – Yellow, glycine, serine and proline marked in green, pink and blue respectively. The black arrow is indicating the *EPF2* and *EPFL9* sequence with a similar number of amino acid residues preceding and interrupting indicated in a bracket. (Hara et al., 2009)

The *OsEPF2* and *OsEPFL9* genes are believed to have very close relationship with Arabidopsis *EPF2* and *EPFL9* respectively. Here in Figure 4, a phylogenetic analysis has shown a close relationship between the two genes in the two species.

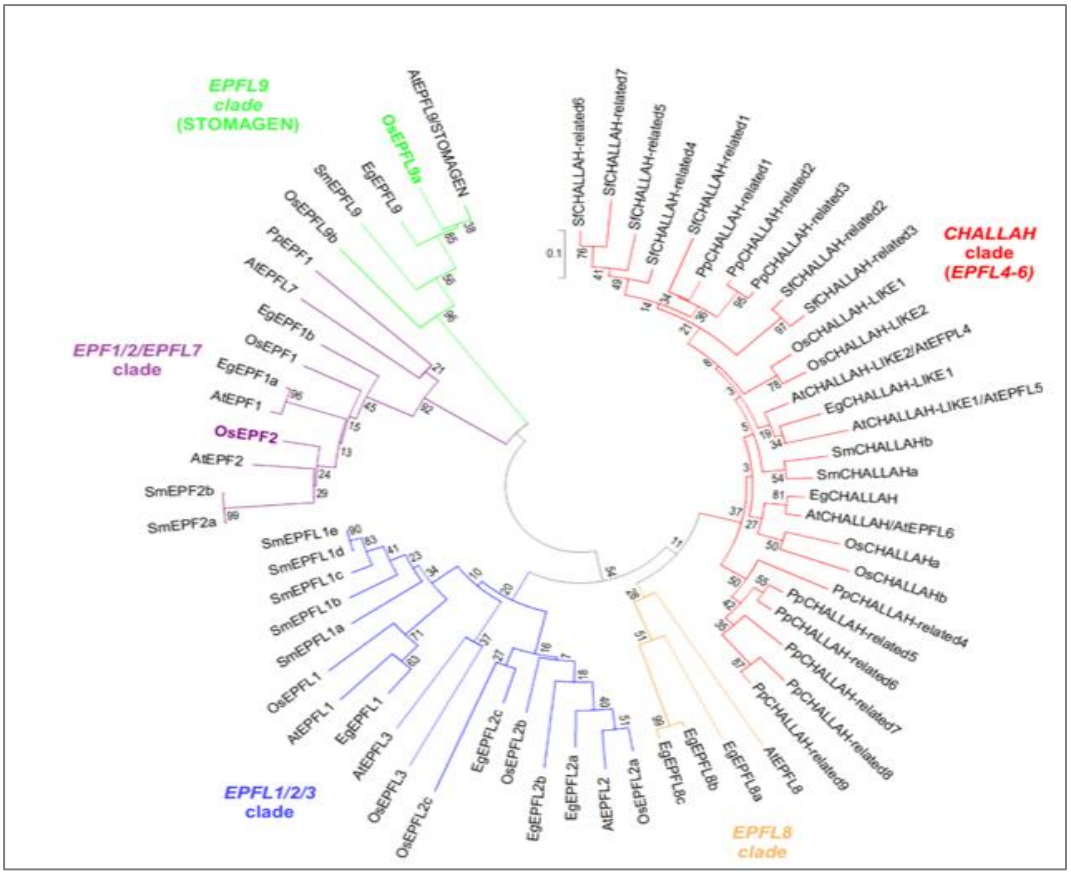

Figure 4.4. Phylogenetic analysis shows the close relationship between the rice secretory peptides (*OsEPF2* and *OsEPFL9*) and the Arabidopsis's (*EPF2* and *EPFL9*). (Caine R.S unpublished data)

In the present study, overexpression of the rice homolog of the *EPF2* and *EPFL9* through the optimised *Agrobacterium* rice transformation protocol developed in this study using the *Oryza sativa*. L Japonica background, Nipponbare. It has been shown that the *OsEPF* genes were able to change the stomatal patterning in the economic crop (rice). Here, effect of the EPF genes in rice was investigated, and how its transpirational control may affect carbon gain and water use efficiency. This is a step towards understanding the integrated mechanism of rice to acclimate itself to environmental stresses. Here, it has shown how leaf gas exchange parameters were influenced by the alteration of stomatal size and density. Also, in this chapter, it was shown how the excision, water loss and dehydration work showing that rice leaves can more efficiently 'buffer' rapid changes in leaf water content if stomatal density is lowered. Hence, it was hypothesised that reduction of stomatal density in rice has potential to acclimatise with the climatic changes (drought) through

reduced water loss by transpiration and increase biomass without loss of carbon gain (improved water use efficiency).

4.2 METHODS

4.2.1 Plant material and growth condition

The rice material used for this study are the *OsEPF* overexpression lines generated for the study under the *Oryza sativa* L. japonica Nipponbare background (transformation method was described in chapter 2, section 2.6). T0, T1 and T2 generations were used for this study. The lines were *OsEPF2* and *OsEPFL9* overexpression lines and the Nipponbare WT. The experiment was performed in 3L pots in the growth chamber (conditions described in Chapter 2 section 2.2).

4.2.2 Stomatal density and size

The stomatal impressions were carried on each plant (1 – 2 leaves per plant) on both the adaxial and abaxial (as described in chapter 2). The impressions were carried out at 2, 5, and 8 weeks after sowing. The stomatal density (mm^{-2}) was calculated as the number of stomata per 0.3216μm^2 field of view at X200 magnification. The stomatal size (μm^2) was calculated as the guard cell length × guard cell pair width from images collected at X400 magnification. More details in chapter 2

4.2.3 Gas exchange

Steady state photosynthetic measurements (P_{max}) and photosynthesis-light response curves (LRC) were measured using the infra-red gas analyser (IRGA) Licor 6400XT. All leaf gas exchange measurements were taken on the plant flag leaf. The block temperature was maintained at 28^oC for the experiment. The flow rate of 500ml min^{-1} and the cuvette humidity was set to ~28%. The CO_2 concentration used for the steady state measurements is 400 $\mu mol\ mol^{-1}$. The photosynthetically active radiation (PAR) was set at 1500 $\mu mol\ m^{-2}\ s^{-1}$. Measurements were taken at 4 weeks, 6 weeks and 8 weeks. More description for LRC in Chapter 2.

4.2.4 Leaf dehydration assay

Two leaf dehydration methods were used to determine the rate of water loss by a leaf.

4.2.4.1 Dehydration by stomatal conductance

The steady state photosynthetic measurement of a fully expanded leaf at 8 week old was obtained using IRGA (Licor 6400XT). The IRGA was programmed to take gs measurement after every 30 seconds and the cuvette condition was 28^{o}C leaf temperature, 28% relative humidity, 400 μmol mol^{-1} of ambient CO_2 was supplied, and 1500 μmol m^{-2} s^{-1} of PAR. Immediately after the first steady state measurement was obtained, the leave was excised from the plant at about 5 mm away from the chamber. The time point gs values obtained were converted to a percentage using Microsoft excel 2013. The values obtained were normalised.

4.2.4.2 Dehydration by weight

The rate of water loss per leaf was measured by the weight of leaf loss after excision per unit time. A leaf of specific leaf area (5cm^2 in young and 7cm^2 in matured, worked out) of a fully expanded leaf was excised and immediately weighed every 15 seconds for 10 minutes. The data collected were converted to a percentage and compared over time.

4.2.5 Statistical analysis

Analysis of variance (ANOVA, one-way and two-way) was carried out using GraphPad Prism 7.01 for Windows (La Jolla, CA, USA) and was verified with GenStat for Windows, 17th Edition (VSN International Ltd.) to investigate the effect of the stomatal density and size between the two overexpression lines (*OsEPF2* and *OsEPFL9*) and the WT. When an effect was detected, a Tukey's HSD (Honest Significant Difference) test was used to determine the level of significance.

4.3 RESULTS

4.3.1 Cloning and creation of the osEPF2 and osEPFL9 overexpression lines

EPF2 and EPFL9 were identified for the rice stomatal study. The two genes have been studied extensively in Arabidopsis with regards to the role they play epidermal cell divisions. The rice homologs of *EPF2* and *EPFL9* genes were kindly provided by Prof Julie Gray (University of Sheffield) in Gateway entry reaction. They were PCR amplified (Figure 4.5 A) and sub-cloned in to Gateway entry vector pCR-8/gw/TOPO, and created pCR8-EPF2 and pCR8-EPFL9.

A colony PCR was done to confirm the presence of the inserts (Figure 4.5 B)

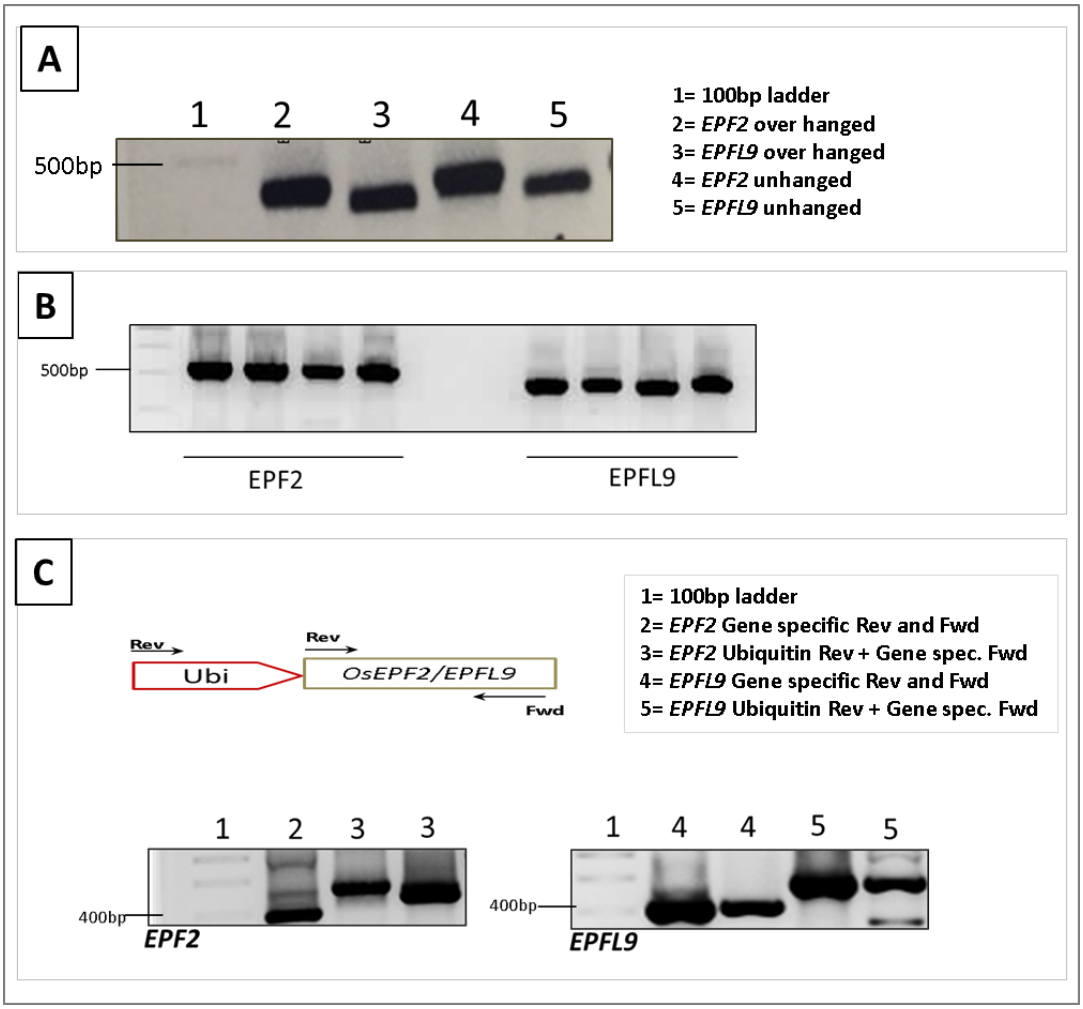

Figure 4.5 PCR amplification and restriction digest of OsEPF2 and OsEPFL9. **A**. A comparison between the 'A' over-hanged and non-over hanged of *OsEPF2* (408bp) and *OsEPFL9* (372bp). **B**. PCR Amplified colonies of *OsEPF2* and *OsEPFL9* in pCR-8/gw/TOPO with the gene specific primers. **C**. PCR amplified *OsEPF2* and *OsEPFL9* plasmids in pBRACT 214 destination vector with gene specific primers (Fwd and Rev) and Ubiquitin Rev combination with the gene specific Fwd.

The plasmids of four positive colonies from each gene were extracted and checked on PCR (Figure 4.5 B).

Once validated, the plasmid were sequenced to rule out PCR errors. The successful EPF2 and EPFL9 entry vectors were then used for LR cloning in Gateway Destination vector pBRACT 214. Few colonies were checked by colony PCR and the positive colonies each were used for plasmid extraction. The plasmid was checked again by PCR by Ubiquitin reverse primer and gene specific forward primer (Figure 4.5 C).

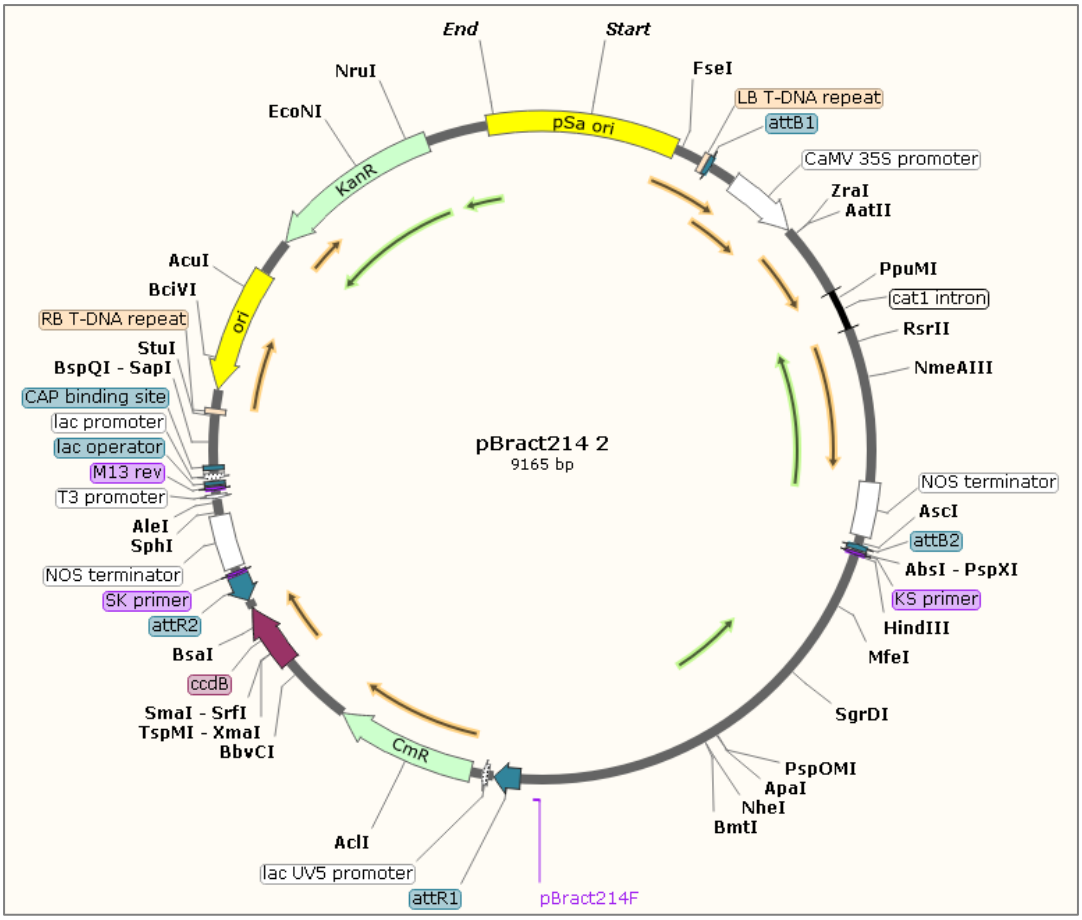

Figure 4.6. Schematic representation of the *pBRACT 214* gateway compatible vector used as a destination vector in the overexpression of the *EFP2* and *EPFL9* in rice.

Positive destination clones were then electrophoresed into *Agrobacterium AgL*1 *strained* (nonaggressive) and selected on Kanamycin and Rifampicin plates. The positive colonies were confirmed by PCR and for rice transformation.

4.3.2 Rice transformation.

The two genes construct *OsEPF2* and *OsEPFL9* constitutively driven by maize ubiquitin promoter were transformed into *Oryza sativa* L. Japonica (Nipponbare) using the rapid and efficient *Agrobacterium*-mediated rice transformation method developed in this study (Figure 4.7, See detail rice transformation in Chapter 7). After the successful rice transformation, a large number of independent overexpression lines were regenerated.

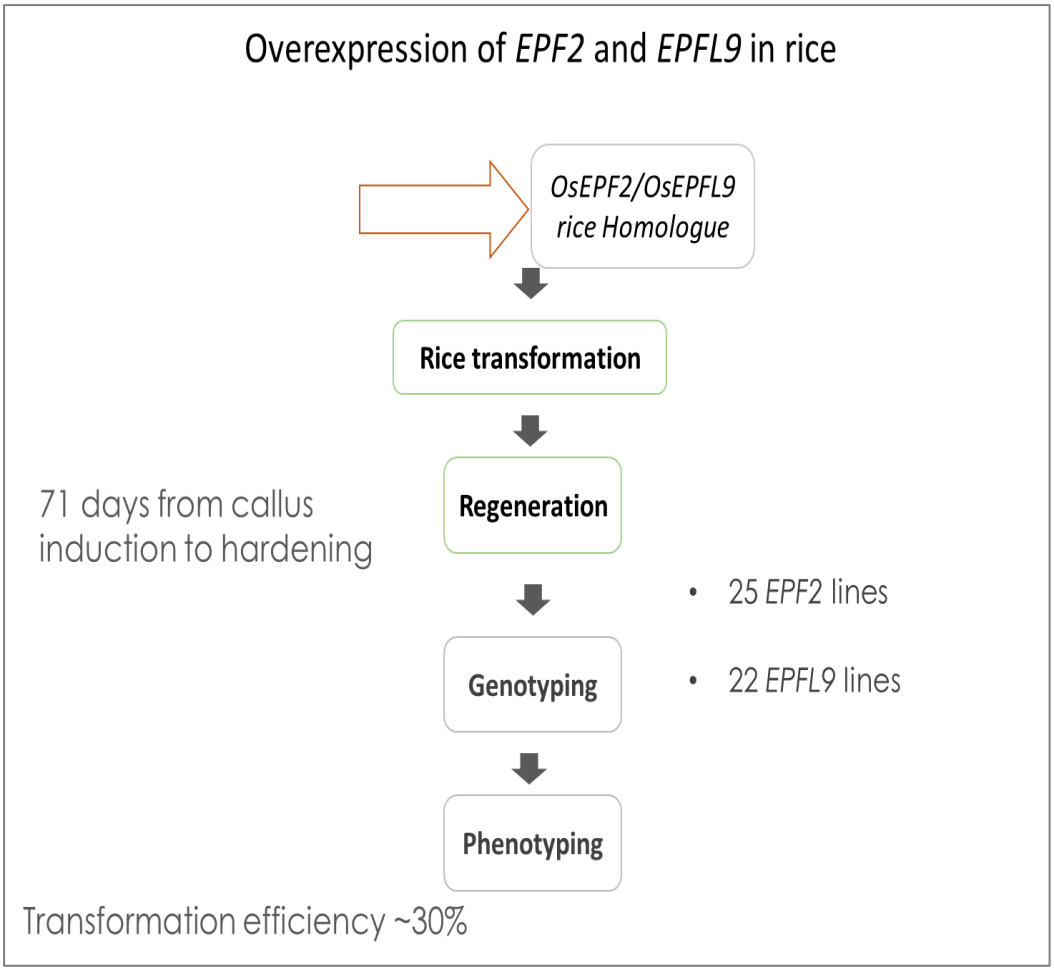

Figure 4.7. Schematic representation of the rapid and efficient Agrobacterium mediated rice transformation method developed. The steps and the total number of days in the creation of the transgenic *EPIDERMAL pattering factor 2* and *EPIDERMAL patterning factor-Like 9*.

4.3.3 Molecular evaluation of the transgenic status of the regenerated plants

The transgenic plants were genotyped by PCR that showed 21 out of 24 EPF2 plants and 17 out of 21 EPFL9 plants were transgenic positive. Four positive lines, two from each were then checked for transgene expression analysis by RT-PCR that confirmed the expression of the two transgenes in all four lines tested (Figure 4.8 A)

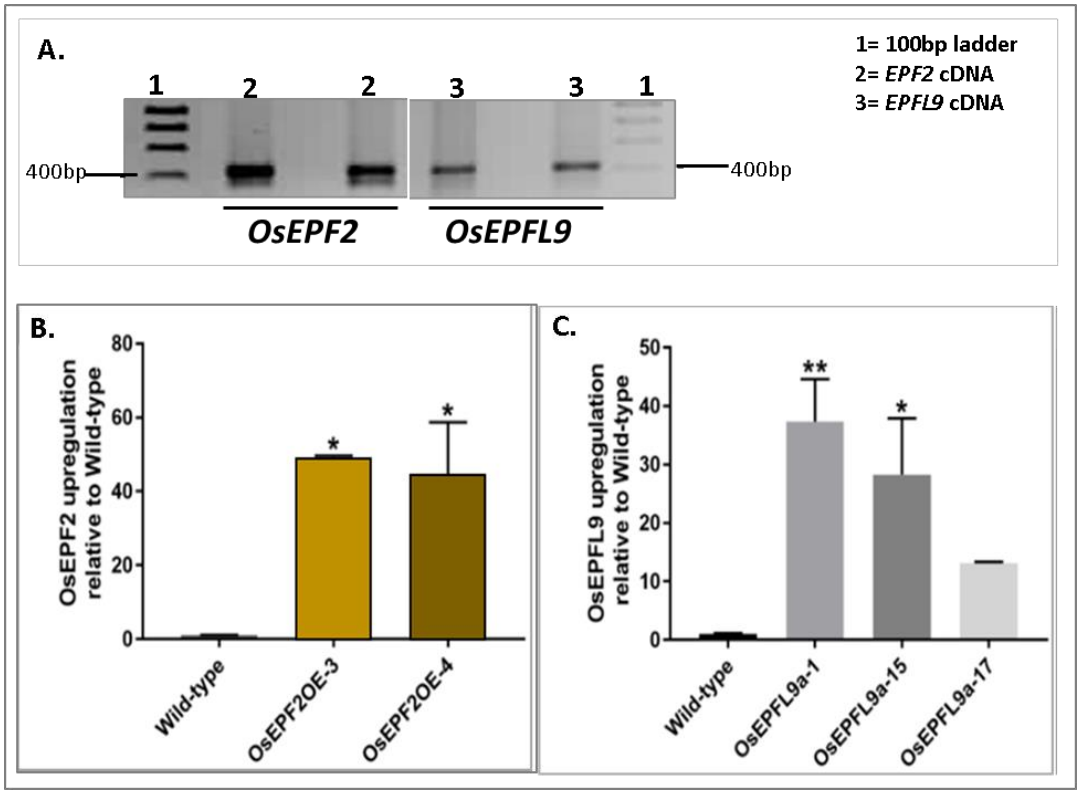

Figure 4.8. The OsEPF2 and OsEPFL9 expression from the leaf tissue. **A.** The reverse transcription analysis (RT-PCR) of two positive lines from each gene. The fragments sizes were; *OsEPF2* (408bp) and *OsEPFL9* (372bp) and 1kb hyper ladder. **B** and **C**. The expression analysis from the real-time qPCR of some T3 line from *OsEPF2* and *OsEPFL9* respectively.

The qRT-PCR was done on a few lines in collation with Julie Gray group at Sheffield University. The results show that the expression level in the *OsEPF2* lines (3 and 4) were significantly higher than the WT by about 50 fold. Whereas the *OsEPFL9* lines were significantly higher than the WT by about 35 fold.

4.3.4 EPF overexpression results in altered Density and Size

To explore the phenotypic effect that resulted from the overexpression of the two secretory peptides in developing rice leaves, the stomatal density and size were measured in the lines. The phenotype shows that the *EPF2* overexpression resulted in a reduction of stomatal density whereas, *EPFL9* overexpression results in the increase in the stomatal density (see Figure 4.9).

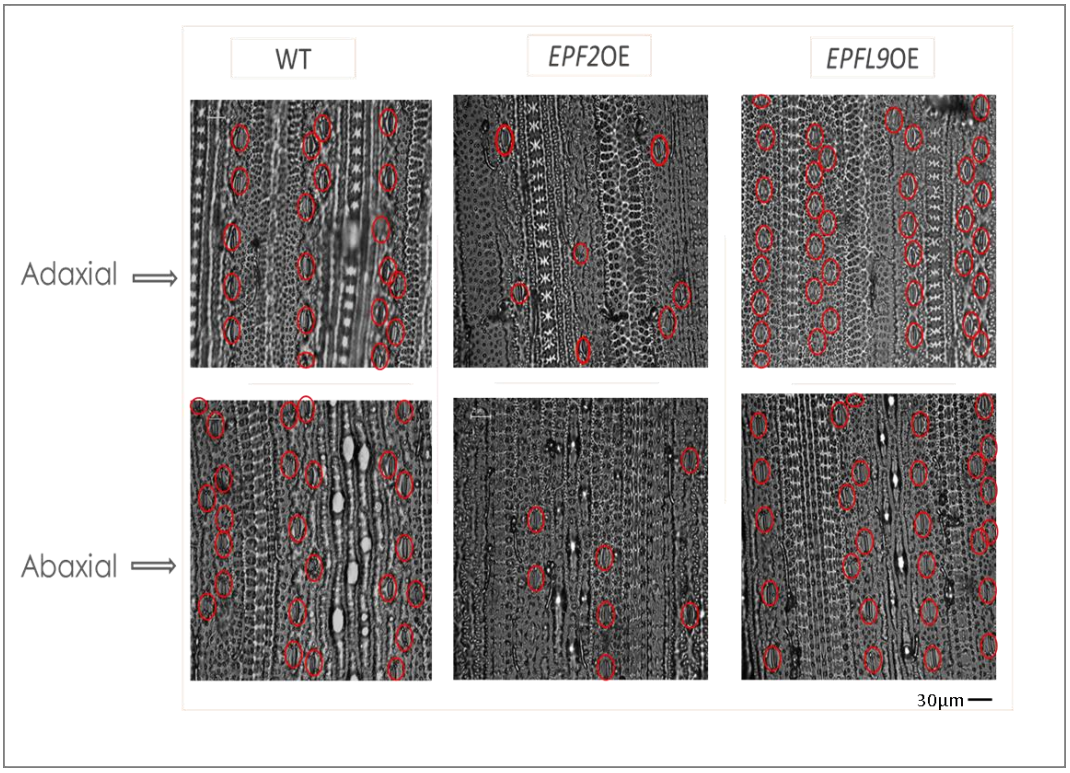

Figure 4.9. The effect of the overexpression of EPF2 and EPFL9 from the epidermal development. The stomatal distribution from adaxial and abaxial sides of the leaves marked in red. The bar represents 30µm.

From a large number of the transgenic lines regenerated, *EPF2 OE lines*_1, 2, 3 and 4 were selected at random while for *EPFL9OE lines* 1, 3 and 4 were chosen for this studies. The WT and the azygous were used as a control.

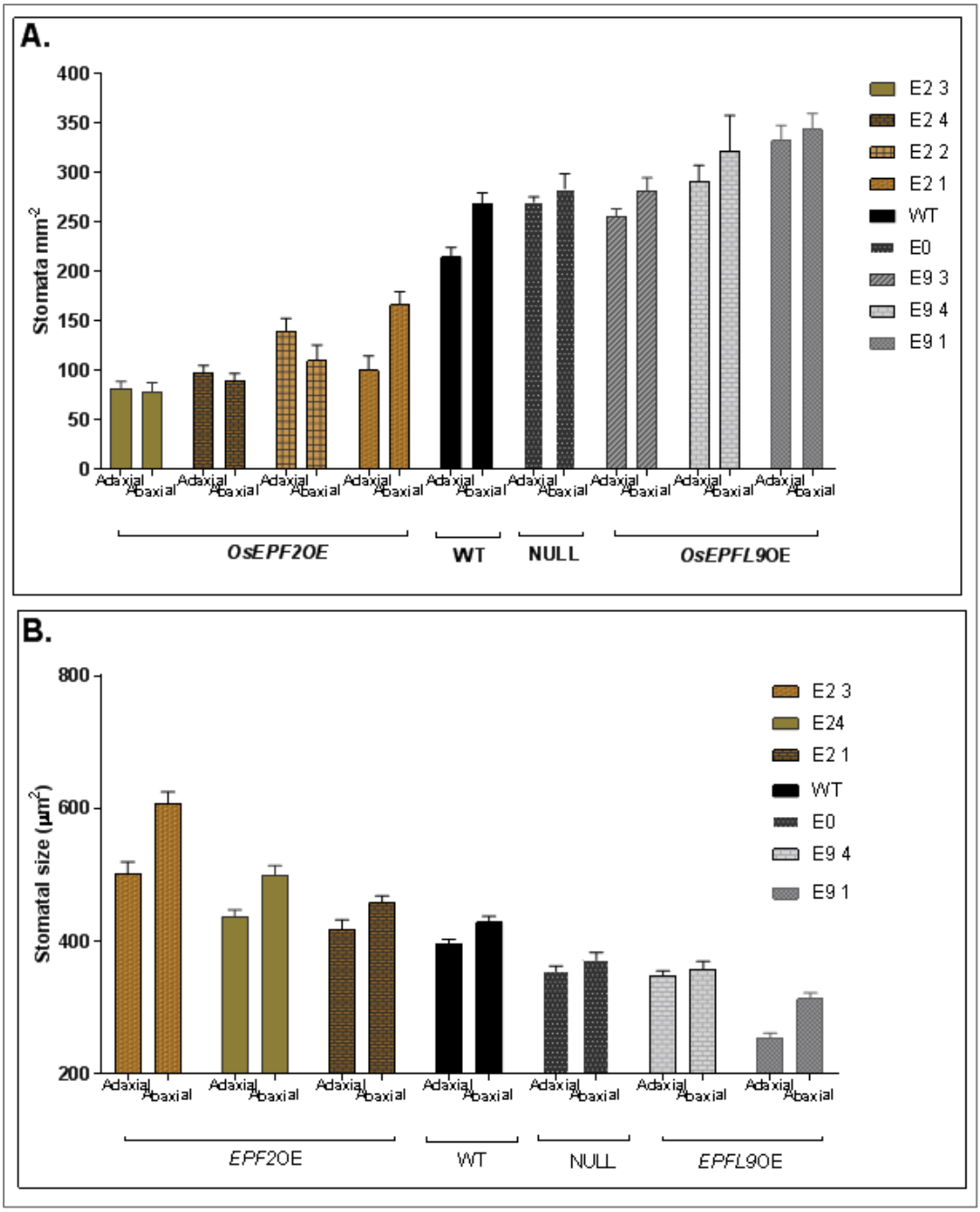

Figure 4.10. The effect of the overexpression of *EPF2* and *EPFL9* has caused a major alteration in the epidermal cell development in different individual OE lines. **A.** stomatal density (D). **B**. Stomatal size (S). The EO is the (azygous) line regenerated with no transgene and WT is the Wild type. All values are means with ± SEM error bars.

4.3.5 Relationship between the mean density and size of stomata

The mean stomatal densities in the 5 week old EPF2 overexpression lines displayed a significant reduction in the stomatal density on both the adaxial (top) and abaxial (bottom) surfaces of the leaves compared to the azygous control (E0) and WT.

The ANOVA result revealed the EPF2 OE line (E2 3) had shown a 67% reduction in stomatal density (62% on the adaxial surface and 73% of the abaxial surface). Other EFP2OE lines tested also showed a significant reduction in stomatal density with E2 4, showing a reduction by 61%, E2 2 by 48% and E2 1 by 44% (Figure 4.10).

The overexpression of the EPFL9 increased stomatal density. The EPFL9_1 (E9 1) line displayed the greatest increase in the stomatal density of the three EPFL9 lines examined by 28% (35% increase on the adaxial and 22% increase on the abaxial). The mean of E9 4 on both surfaces showed an increase by 22%. Surprisingly the stomatal density of the E9 4 did not show any significant increase in the stomatal density in T1 and was then discarded.

A characteristics compensation effect was observed among the two overexpression lines with their stomatal sizes (S) (Figure 4.10 B). A significant increase in the size of the stomata at both the adaxial and the abaxial was observed among the *EPF2OE* lines in comparison to the WT. Interestingly, the sizes of stomata at the abaxial surface appeared much larger than the adaxial surface in some of the *EPF2OE* lines. The mean of the stomatal size of *E2* 3 increased significantly on both the leaf surfaces at the $P \leq 0.0001$ level of significance. Similarly, the mean of *E2* 4, showed a significant increase in the size at their abaxial surface from the WT abaxial surface at $P=0.0011$. Also, an increase in the size was observed on the abaxial surface of *E2* 4 from its adaxial at $P=0.0284$.

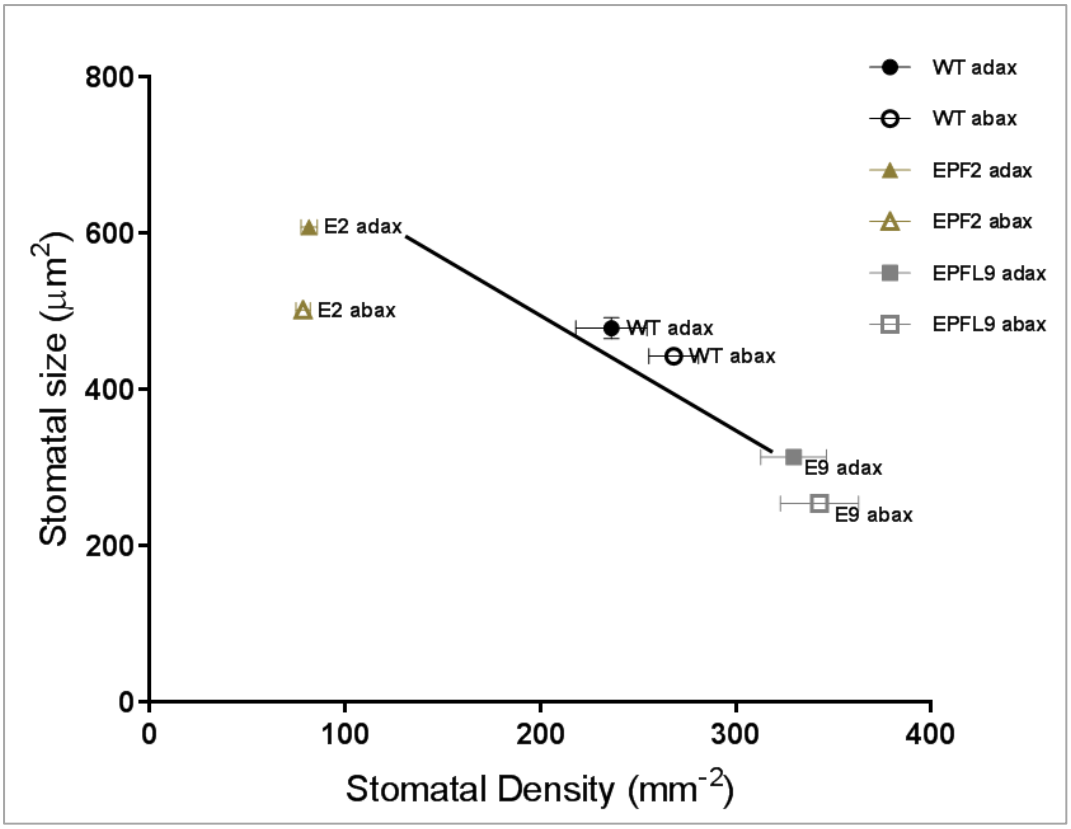

Figure 4.11. The relationship between the mean stomatal sizes and mean of stomatal densities of the adaxial and abaxial surfaces of the WT, EPF2OE and EPFL9OE. All data points (open symbols, abaxial surface; closed symbols, adaxial surface) are means ± SE of both vertical and horizontal points.

Interestingly, the *EPFL9OE* showed a reduced size on both the leaf surfaces from the mean of the WT. The adaxial and abaxial surface of *E9* 1 and the abaxial surface of *E9* 4 had displayed a significant reduction in their stomatal size at $P \leq 0.0001$. The *E9* 4 adaxial was therefore also increased at $P < 0.01$. The *E9* 1 like the *EPF2OE* lines had larger stomatal size at the abaxial than the adaxial. Quite the opposite of the stomatal density, *EPF2OE* lines were larger than the WT, while the *EPFL9* were smaller than the WT. Thus, a strong inverse relationship between the stomatal density and the stomatal size was readily seen in this experiment (Figure 4.11).

After the initial studies, one line each for the EPF2 (E2 3) and EPFL9 (E91) were selected for more detail physiology characterisation.

4.3.6 The instantaneous leaf gas exchange on the overexpressed lines with altered stomatal densities and size.

As shown above, the constitutive overexpression of the *OsEPF2* and *OsEPFL9* led to significant decrease and increase of the stomatal densities in rice respectively. It was also shown that the two genes; *EPF2* and *EPFL9* lead to an increase and decrease of the stomatal sizes respectively. In the second part of this experiment, the physiological responses were compared among the transgenic lines in both the T0 and T1 generation, with E0 (for T0) and WT (for T1) as control respectively.

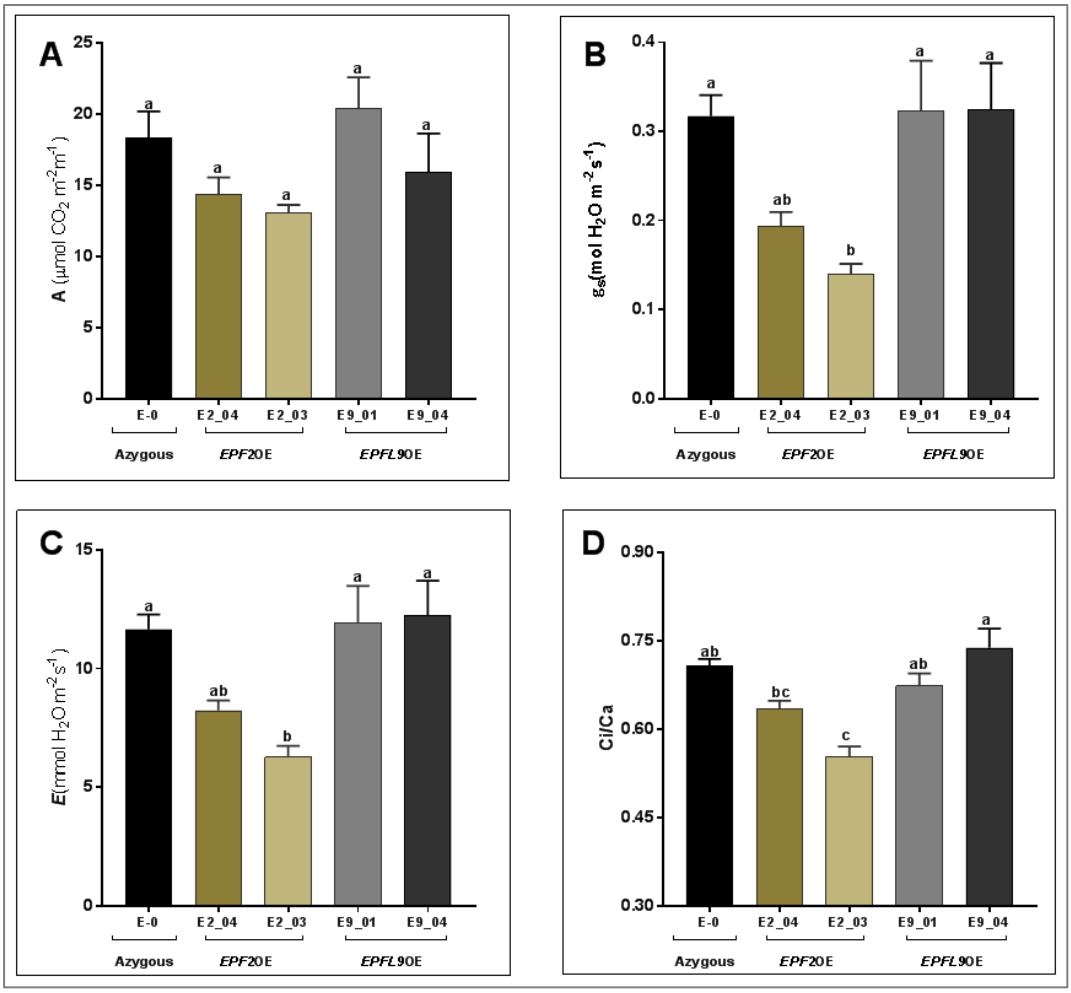

Figure 4.12. The response to gas exchange on genotypes with different stomatal densities (similar plants as in Fig 4.10) **A**. CO_2 assimilation rate (*A*), **B**. Stomatal conductance (*gs*), **C**, Transpiration rate (*E*), **D**. ratio of leaf intercellular to ambient CO_2 concentration (C_i:C_a). All values are means ±SE. Different letters represent significant differences among the genotypes.

The steady state photosynthetic data at light saturation, 28% relative humidity and 28^{o}C leaf temperature of the 4-week old plants revealed a significant decrease in the stomatal conductance (*gs*) among the *EPF2OE* line (*E2* 3) when compared to the control. The decline in the gs (Figure 4.12 B) reflects the stomatal density in *EPF2OE*. As anticipated, the differences in the *gs* between the *E2* 3 and the two *EPFL9OE* lines used (*E9* 1 and *E9* 4) was significant (P=0.00355 and 0.0331 respectively). However, there were no statistical differences between *EPFL9OE* lines and the WT control. Interestingly, with low gs in the *EPF2OE* lines, the drop in the maximum CO_2 assimilation (P_{max}) was not significant comparing mean of the azygous (E0) and *EPFL9OE* lines. Hence the effect of stomatal density does not appear to have had a significant effect on *A* in this experiment. The transpiration rate (*E*) had reduced significantly with reduced *gs* in the *EPF2OE* lines. A similar response was not observed between the *EPFL9OE* lines and the E0. The significant low ratio of the internal CO_2 concentration (*Ci*) to ambient CO_2 concentration (*Ca*) (*Ci*:*Ca*) in the *EPF2OE* lines (P=0.0007) observed, suggest a higher leaf-level water use efficiency than the E0 and the E9. Remarkably, a significantly high computed instantaneous and intrinsic water use efficiency was observed in the *E2* 3 (P=0.0427 and P=0.0006 respectively). Thus, this may have a direct link to the drop in *gs*, *Ci:Ca* ratio but with a substantial rate of *A*.

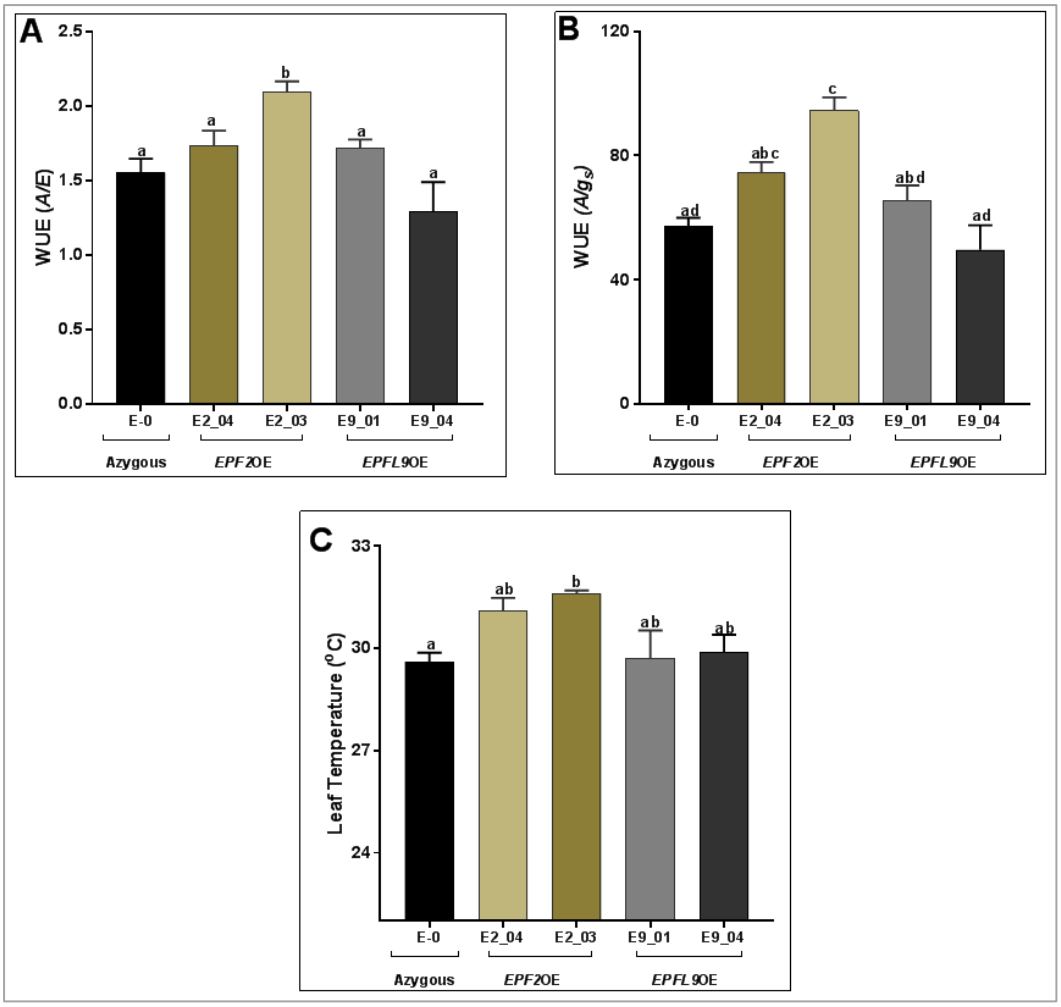

Figure 4.13. The response to gas exchange on genotypes with different stomatal densities (similar plants in Figure 4.10) **A**. Intrinsic water use efficiency (*A/gs*) **B**. Instantaneous water use efficiency (A/E), **C**. Relative leaf temperature All values are means ±SE. Different letters represent significant differences among the genotypes. n= 4 – 5. Cuvette condition: RH = 28%, leaf temperature 28°C, light saturation (1500µmol^{-2}s^{-2})

Among the two leaf-level water use efficiency estimations; intrinsic (*A/gs*) and instantaneous (*A/E*), the intrinsic WUE (*A/gs*) is considered more realistic and comparable between studies, as it is not influenced by the change in a leaf to air VPD in the leaf chamber. Importantly, both instantaneous (Figure 4.13 A) and intrinsic WUE (Figure 4.13 B) were significantly increased in *E2* 3 from the control. Furthermore, the increase in the leaf temperature of E2 3 (P=0.00416, figure 4.13 C) may have direct consequences from the decrease in the rate of transpiration of the *EPF2OE* lines.

The gas exchange responses in the T1 and T2 generations was very similar and consistent in *EPF2OE* but not with *EPFL9OE*, whose phenotypic characteristic wears after every generation (data not shown).

4.3.7 A rapid dehydration leaf assay reveals the influence of stomatal density in rice.

To determine the rate of water loss by a leaf bearing the *OsEPF2* and *OsEPFL9* overexpression using a relatively simple and fast method, a leaf dehydration assay was employed. Two approaches were used. The first measured the stomatal conductance (gs) of an excised leaf over time with the aid of an infra-red gas analyser (Licor 6400XT). The second approach was the loss of weight from an excised leaf over time. The major assumption to this experiment was that water loss occurs primarily through the stomata and when the stomata are shut the water loss becomes limited. Water loss through cuticle or the cut is usually considered negligible.

4.3.8 Dehydration in an excised leaf measuring stomatal conductance

The Two-Way ANOVA revealed a highly significant interaction between the lines and the time it takes for the stomatal decline at $P \leq 0.0001$. The Tukey's posthoc test, revealed that the mean of *EPFL9OE* showed a highly significant decline in the *gs* ($P \leq 0.0001$) and a marginal decline in WT ($P < 0.05$) compared to the *EFP2OE* at the first 120 seconds. At 180 seconds, there was a highly significant decline of the mean of both WT and *EPFL9OE* and the mean of *EPF2OE* ($P \leq 0.0001$ and 0.0176 respectively) (Figure 4.14)

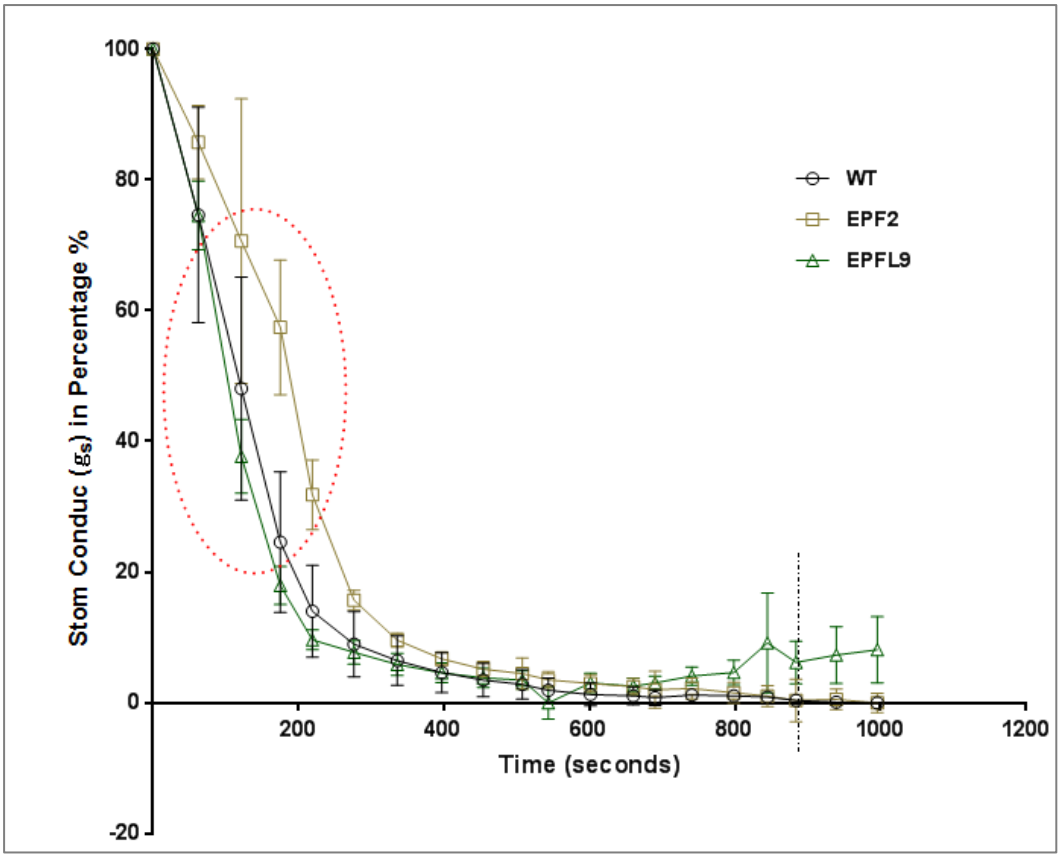

Figure 4.14. The stomatal sensitivity to dehydration in the two overexpressed lines (E2 and E9) and the wild type all with different stomatal density. The dehydration assay by stomatal conductance decline over time. The *gs* values are normalized to a percentage. Each data point represented as the mean ± SEM. The region surrounded by the red dots are the points of significant differences. N= 3 – 6, Cuvette condition: RH = 28%, leaf temperature 28°C, light saturation (1500μmol^{-2}s^{-2})

It appeared that the first four (4) minutes (red cycle) was a very critical point at which water retention in the *EPF2OE* leaf was superior to that of WT and *EPFL9OE*.

This analysis, therefore, indicated that *EPF2OE* lines were either responding very fast to dehydration by closing its stomata and/or size played a role in slowing down the water loss, assuming all the water loss was from the stomata at 700 seconds.

4.3.9 Rate of dehydration by weight loss

The second approach determined the rate of water loss by the loss of weight over time. The data collected (weight) were converted to a percentage (similar to Figure 4.14). Therefore, The ANOVA results

indicated highly significant effects of time (P≤0.0001) and genotype (P=0.0009). At 30 and 60 seconds (Figure 4.15), there was a significant loss of weight from the mean of WT compared to *EPF2OE* (P=0.00458 and P=0.0446 respectively). One possible explanation for the differences in the rate of water loss was that the leaf from each line had differences in their stomatal density.

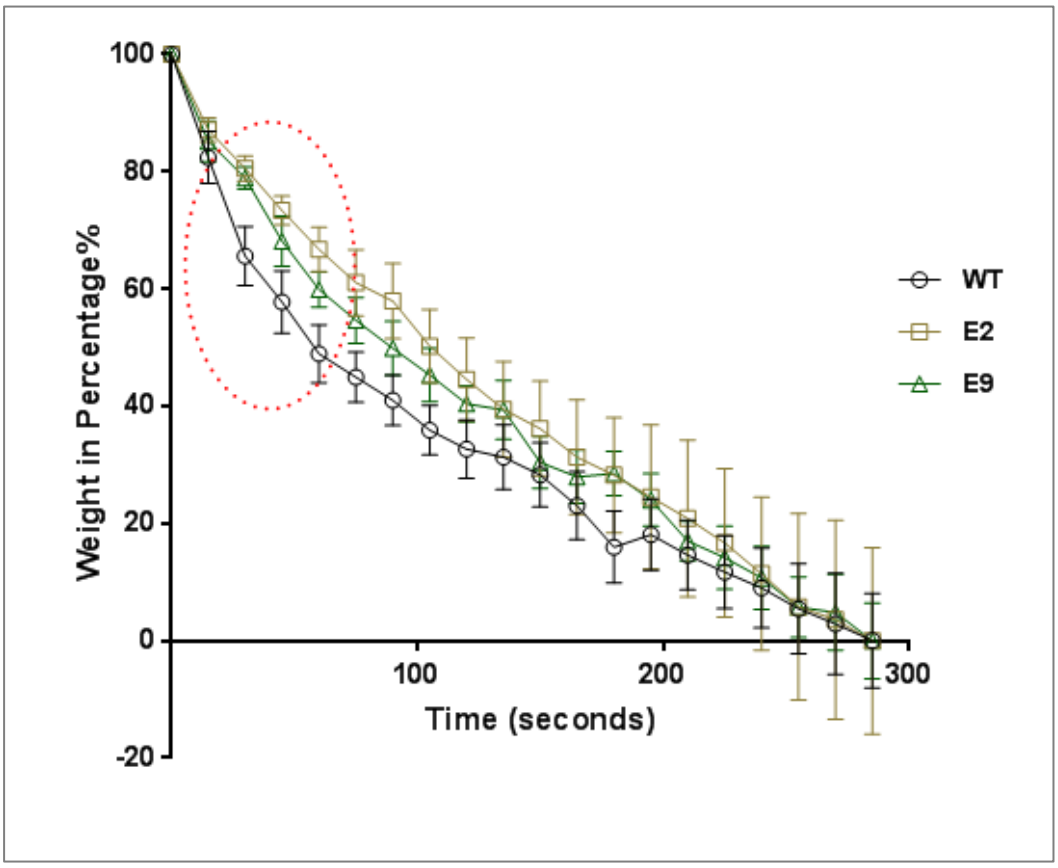

Figure 4.15. The rate of water loss from each line with different stomatal density in weight over time. Each data point represented as the mean ± SEM. The region surrounded by the red dots are the points of significant differences. N= 3 – 6.

4.3.10 The responses of CO_2 assimilation to Photosynthetic Active Radiation (PAR): The light response curve

The changes in the CO_2 assimilation (*A*) to varying levels of light (PAR), measures the quantum efficiency of the absorption of light energy into photosynthesis in fully expanded leaf 7 of *OsEPF2, OsEPFL9* and WT (Nipponbare). This relationship is commonly called the Light Response Curve (LRC). From the result obtained in Figure 4.16, it showed clearly that resonses of photosynthesis PAR do not show any statistical

differences between the two overexpressed lines with altered stomatal densities and the WT supporting the above (P_{max}) response in the three rice lines.

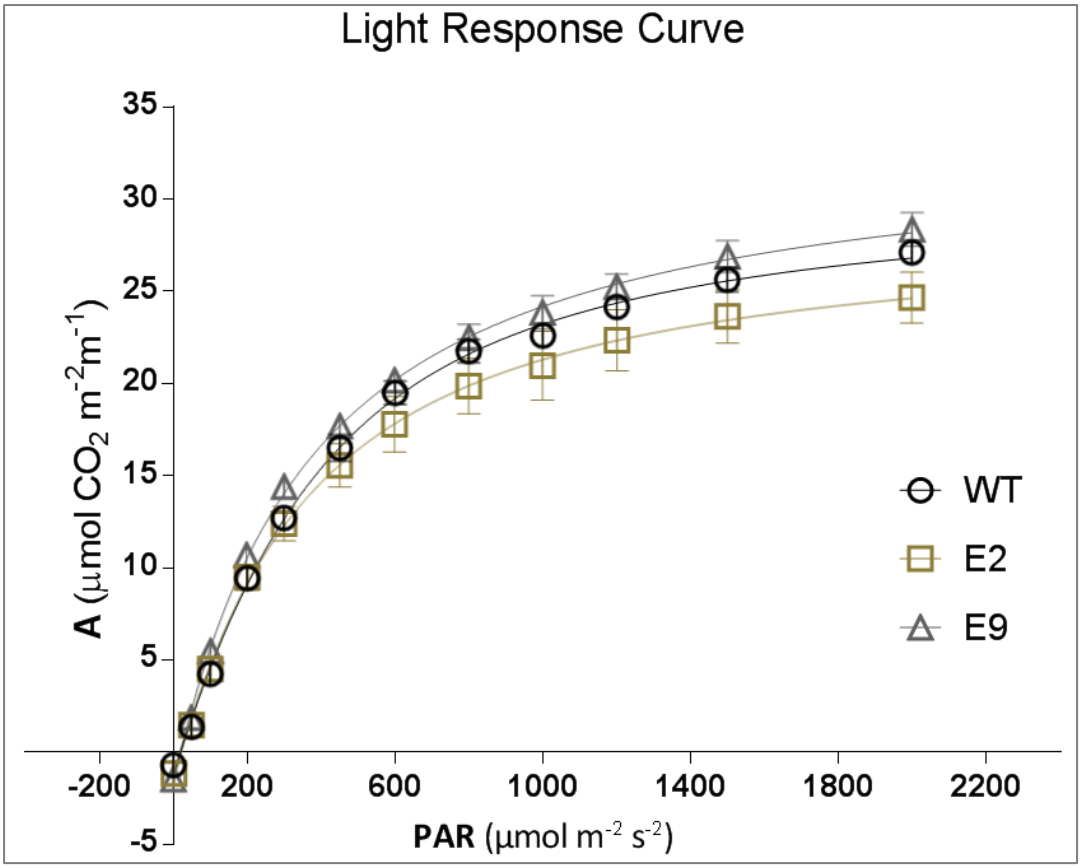

Figure 4.16. The effect of stomatal density on net photosynthetic rate (A) response to photosynthetically active radiation (PAR). Each data point represented as the mean ± Standard Error of the Mean (SEM). N= 3 – 4.

From the response of *A* vs PAR curve, estimated parameters were derived from the fitted light response curve (LRC) as described by a four-parameter non-rectangular hyperbola. The estimation revealed that the maximum CO_2 assimilation rates at saturating photon flux (A_{sat}/A_{max}) for WT, E2 and E9 were all remarkably high 31.87(0.63), 30.25(1.79) and 34.83(1.17) µmol CO_2 $m^{-2}m^{-1}$ respectively but with no statistical differences between them (Figure 4.17 A). The analysis of the Light compensation point (incident photon flux where A=0) which was calculated from the linear portion of the LRC at lower PAR, indicated that there was no significant difference between the two overexpression lines and the WT (Figure 4.17B). The mitochondrial respiration in the light or

dark respiration (R_d) was calculated from the LRC and there was no significant difference between all the three lines. The curve convexity (θ) of the two genes were also not significantly different with the mean of the WT. This was despite the decrease in the stomatal density in the E2.

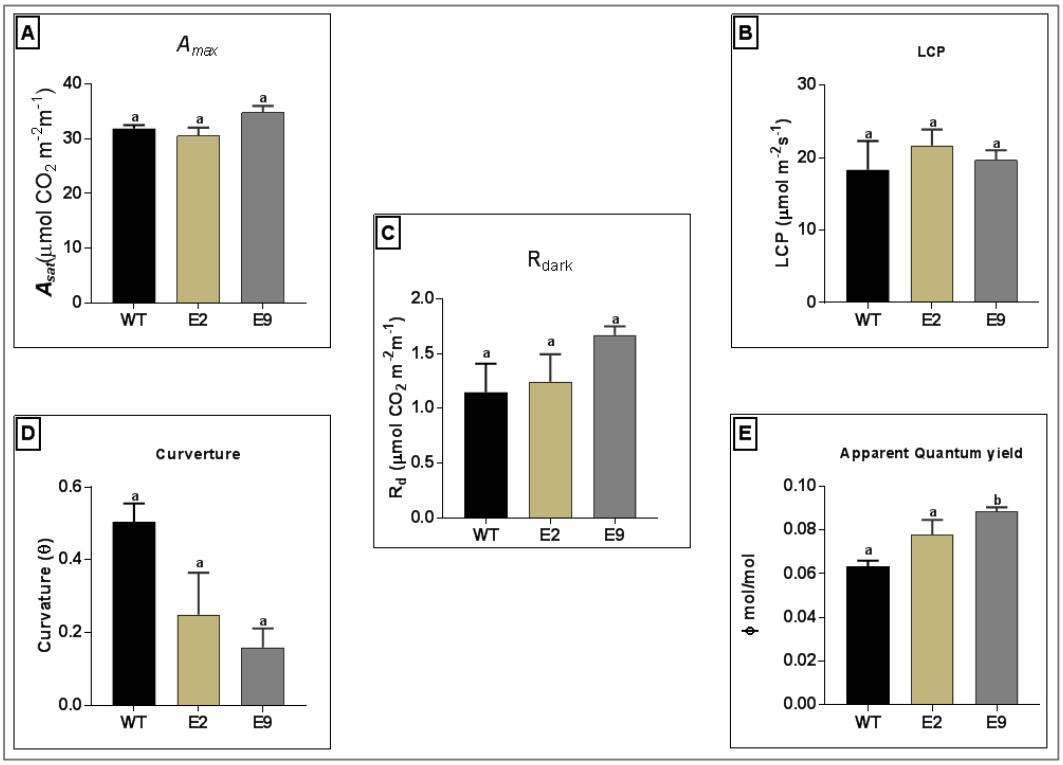

Figure 4.17. Simulated results derived from the Light response curve of the rice lines with difference stomatal densities. **A**. The net assimilation rate at saturated light (A_{max}). **B**. Light compensation point (LCP). **C**. Mitochondrial dark respiration rate (R_d). **D** Convexity (curvature) of the curve (θ). **E**. Apparent quantum yield. All values are means ±SE. Different letters represent significant differences among the genotypes. N=3-4

The apparent maximum quantum yield mol/mol (ϕ) were calculated from the linear portion of the light response curve at lower PAR flux and shows that E9 was only significantly higher than the mean of the WT (P=0.0144). The results may suggest that photosynthetic (quantum) efficiency had not been uncoupled due to the alteration of the stomatal density and sizes of the lines from the WT. The relationship between the stomatal conductance and internal CO_2 versus the photon flux on E2 and WT in Figure 4.17 revealed E2 response was lower than the WT. The stomatal conductance started from the high rate as opposed to the conventional scaling with *A* from low to high. This occurrence may be as

a result of two factors; the timing for the acclimation of the new light condition in the gas chamber was not enough to impose the closure of the stomata or because the measurement was carried out from low to high. The response of *gs* in WT began to increase with increasing light flux from at 300 $\mu molm^{-2}s^{-1}$ then became largely scaled with *A*. The E2 however, responded mildly to the increasing light flux and the *gs* was at its lowest at 200 $\mu molm^{-2}s^{-2}$ of light. The ANOVA result tested between the WT and E2 at each light level reveals significant differences between their mean at 0 (P=0.0059), 50 (P=0.0343), 1200 (P=0.0448), 1500 (P=0.0075) and 2000 $\mu molm^{-2}s^{-1}$ (P=0.0003). The decrease in the number of stomata among the E2 lines may account for the low gs observed in the gs vs PAR curve (Figure 4.19, opened symbols) as it has been shown from the P_{max} values at steady state (Figure 4.12).

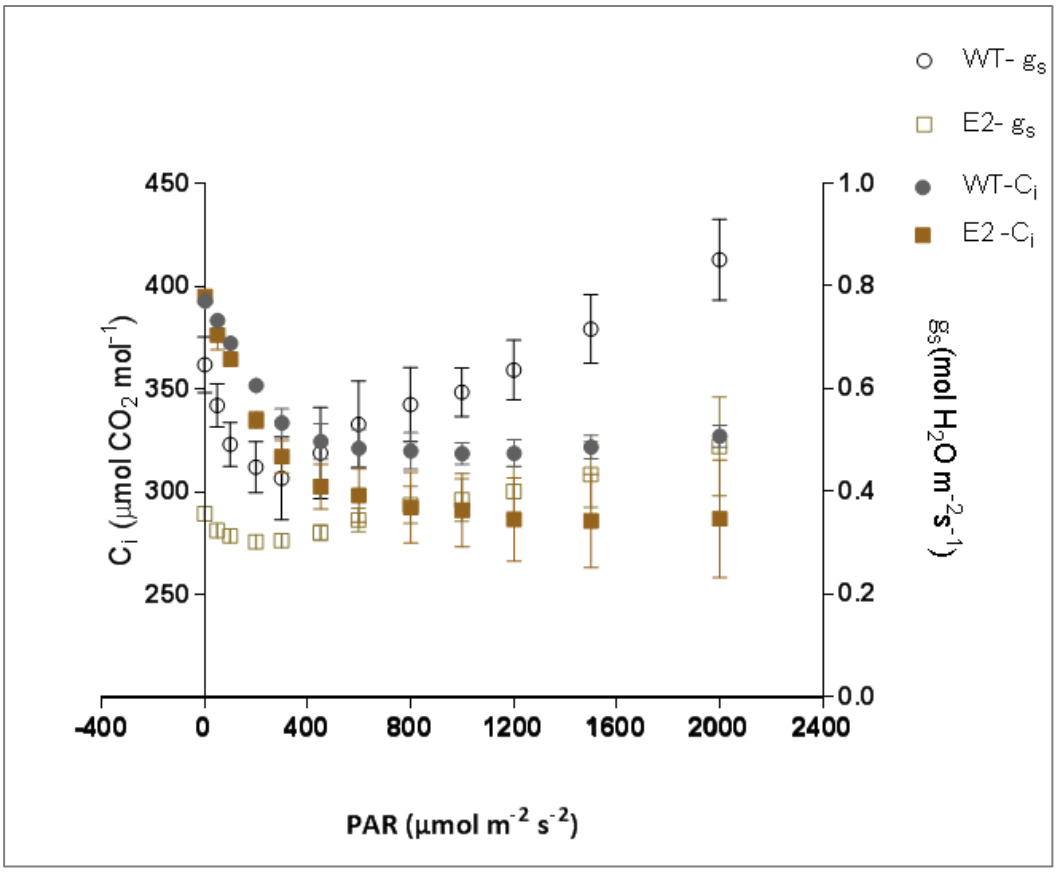

Figure 4.18. The effect of stomatal density on intercellular CO2 (Ci) and stomatal conductance (gs) responses to photosynthetically active radiation (PAR) in rice. Each data point represented as the mean ± Standard Error of the Mean (SEM).

The shape of the *Ci* response here displayed the principles of CO_2 utilization during photosynthesis. As light increasingly become available, *A* increases with increasing demand for CO_2. The available CO_2 will, therefore, reach a threshold where it can no longer diffuse into the leaf as before. Hence, the *Ci* begin to decrease to a point that *A* become limited and no longer increase with increasing light. From the *Ci* vs PAR curve (Figure 4.18, closed symbols), the *Ci* of the WT reached a plateau above 600 $\mu molm^{-2}s^{-1}$ while E2 only reached a plateau from above 1500 $\mu molm^{-2}s^{-1}$. This may suggest, due to the small number of stomata in E2, the loss of *Ci* increase continuously with the increasing demand to fix *A* from the increasing light. Thus, there was an insignificant difference in *A* observed among the genotypes.

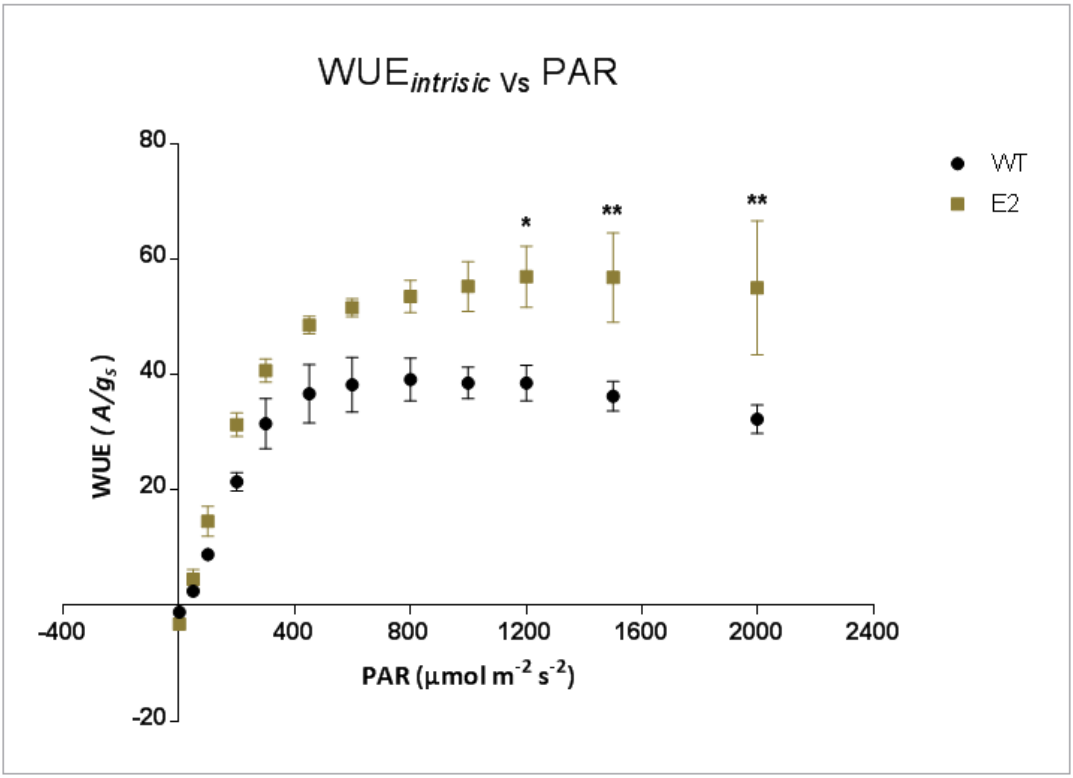

Figure 4.19. The response of intrinsic water use efficiency (WUE_{intrin}) to photosynthetically active radiation (PAR). Each data point represent the mean ± Standard Error of the Mean (SEM). N=3. Asterisk represent statistical differences at each light point (*= P<0.05, **=P<0.01).

Responses of the intrinsic WUE (significantly high in E2 in Figure 4.13 B) and the PAR is shown in Figure 4.19. The ANOVA conducted between the two lines at each PAR point revealed E2 with significantly (P=0.0262, 0.0087 and 0.0027) higher iWUE at 1200, 1500 and 2000 μmol $m^{-2}s^{-2}$ respectively. This therefore confirmed in the increased iWUE observed in E2 at steady state.

4.4 DISCUSSION

4.4.1 Stomatal Architecture

It is predicted that the temperature increase due to global warming is resulting to less water and thus increased drought problems in most tropical countries. Increased in population coupled with the demand for water, the supply for irrigation becomes limited. Thus, there is need for more sustainable agriculture in the development of plants with reduced water requirements. Over the recent years, studies on stomatal plasticity had indicated the prospect of improving plants photosynthetic performance and the regulation of water loss. Work in Arabidopsis has shown that altering the expression level of the *EPIDERMAL PATTERNING FACTOR* family members can cause alteration in stomatal density in Arabidopsis (Hunt et al., 2010, Hunt and Gray, 2009, Sugano et al., 2010). In Arabidopsis, it has been reported that *EPF2* and *EPFL9* genes antagonistically regulate stomatal architecture by interfering with the asymmetric cell division on either the MMCs or in the leaf mesophyll layer. In this study, similar approach has been exploited to reduce water loss to improve drought tolerance in rice. Here, the homologous rice genes were overexpressed in rice. The result shown that *OsEFPL9* overexpression results in increased stomatal density whereas, the *OsEPF2* overexpression caused reduction of the stomatal densities on both two leaf surfaces in rice. Even though, the epidermal cells in rice are difficult to examine compared to Arabidopsis but the *OsEPF2* overexpression lines shows very few guard cells with epidermal pavement cells covering almost all the leaf. This suggests that the protodermal cells were interfered from acquiring the meristemoid mother cell (MMC) fate, hence only a few cells had entered the stomatal lineage. Thus it may also suggest that more cells had animate the stomatal lineage but differentiated into pavement cells (Hunt and Gray, 2009). The *OsEPFL9*, therefore, prevents the *EPF2* function.

Interestingly, the changes in the stomatal density have always been accompanied by the changes in size. The results of this study showed

the inverse relationship between stomatal density and size holds true across the lines used for the study. As the density increases the size decreases. This nature of the relationship has been, since the stomatal evolution over 400 million years ago when the changes in atmospheric CO_2 effect to the inverse relationship between size and density. As the density changes, consequently, the size changes negatively with the density (Vatén and Bergmann, 2012). However, the pathways controlling the two characters (density and size) may have a strong link. It is thought that the density will be fully compensated with the size with respect to photosynthesis as previously reported in the *SDD1* mutants in *Arabidopsis* (Büssis et al., 2006). Similarly, it may also be assumed that the alteration of the stomatal density and size at the same time may not significantly alter the maximum possible pore area per unit leaf for gas exchange, particularly for rice with small sized stomatal compared to other plant species. Hence, the size may compensate the density in gas exchange (Yu et al., 2015) but that depends on species and leaf anatomy (Lawson and Morison, 2006). The decrease in the stomatal density and increase in the stomatal size (vice versa) was in the form of negative power function which is very consistent across various species. Franks and Beerling (2009) explained the long standing argument between the negative relationship of the stomatal density and size in term of the maximum stomatal conductance to water vapour (gs_{wmax}) and CO_2 (gs_{cmax}). They concluded that the occurrence was as a result of the improved economy of space allocated on leaf surface to stomata, and that smaller number of stomatal density with larger sized is a better strategy for conditions in which lower gs_{wmax} is sufficient. One fact yet to be established is the relationship of *EPF* signalling pathway and size, whether the effect is directly or indirectly. The size and shape of rice stomata are small compared to many other plant species (Terao and Yamashita, 1983). This supports my claim in the present study, which confirmed that the overexpression of the *OsEPF2* in Nipponbare does show the inverse relationship between density and size but the density was unable to be fully compensated with size in terms of gas exchange. This claim was supported by the examination of the rate of leaf desiccation per unit time (Figure 4.14 and 4.15), where *EPF2OE* lines

shown delay loss of water by desiccation as revealed by its loss in gs and leaf weight per unit time. A similar approach was previously reported in grapevine leaf (Hopper et al., 2014). An observation was made during these experiments (Figure 4.21), where the three lines were grown hydroponically until maturity. The water top up was suspended after the grain filling stage. With 22 days without water added into the hydroponic tubs, WT and *EPLF9OE* dried out with no single drop of water in their tubs, leaving the *EPF2OE* fresh with enough water to support the growth. This clearly illustrates the impact of reduced water loss by transpiration in the *EPF2OE* lines compared to the WT.

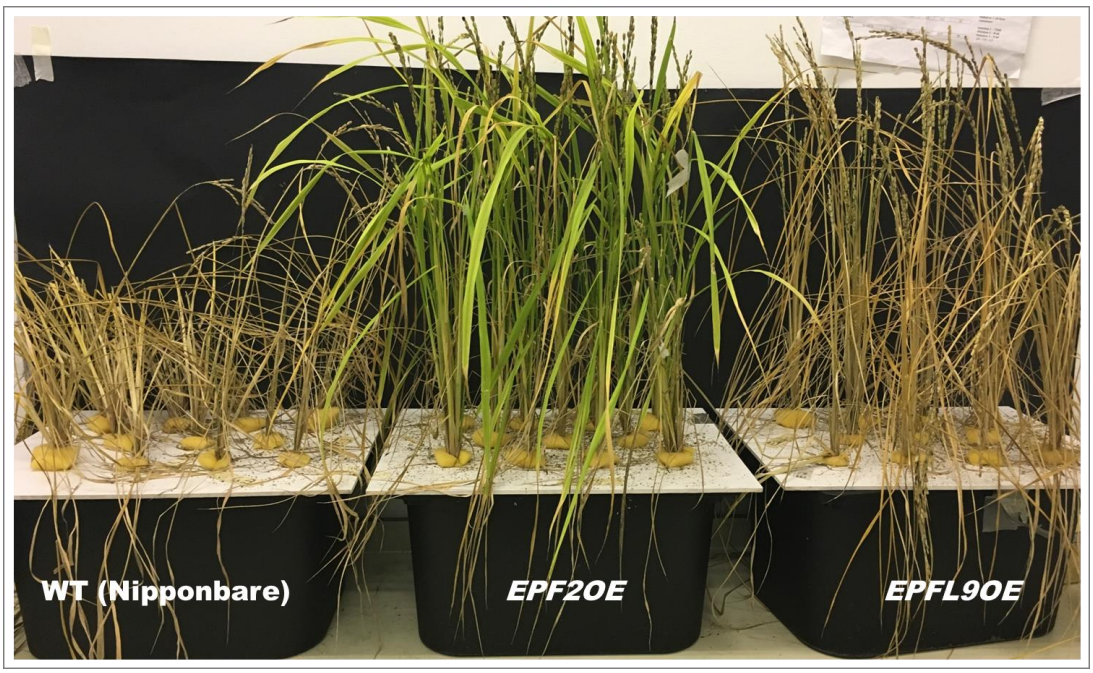

Figure 4.21. The three lines with different stomatal densities grown hydroponically until maturity. Water top up was suspended for 22 days.

4.4.2 Stomatal conductance and leaf-level Water Use Efficiency

A significantly lower gs and E was observed in *EPF2OE* in both steady state and the LRC when compared to the *EPFL9OE* and WT plants. No consistent changes in the Amax, LCP and R_d were observed. The low gs in the *EPF2OE* was responsible due to the constitutive reduction of the stomatal density. The *EPF2OE* lines responded differently to many published values in rice where low stomatal densities often result to low

photosynthetic values in many studies. The result also suggests that reduced stomatal density in rice has some agronomic advantages, particularly the water use efficiency as similarly shown in Arabidopsis (Franks et al., 2015). WUE has been used by breeders in screening for drought tolerance in crops. The emphasis in this study was to present the consistent intrinsic or instantaneous water-use efficiency that could be used by breeder as an approach to create rice varieties that can grow in sub optimal condition without the loss in productivity. The rice plants bearing the *OsEPF2* had shown a substantial CO_2 assimilation rate with reduced stomatal conductance and transpiration rate. Despite the higher leaf temperature resulted from the low transpiration rate, the plant biochemistry has not shown any dysfunctionality. More so, the result had shown that the reduced *gs* and *E* does positively benefit the plant against rapid leaf desiccation, which a limited water stress can induce. The results provide preliminary insights into the influences of the manipulation of stomatal density in responses to drought stress.

A constraint associated with this experiment was the use of rice plants from the T0 and T1 generation due to insufficient timing. Before every single plant was examined, genotyping was conducted on leaf tissue of every plant to validate the presence of the transgene and stomatal count to determine whether the phenotype has reached the expected density or not. The *EPFL9OE* lines had not been very consistent with their genotypes due to a loss in phenotypic expression resulting after every generation. It may be hard to be of interest in the drought experiment.

The significant reduction in the stomatal conductance with conservation of the photosynthetic rate in the *OsEPF2* lines resembles the natural adaptation of the plants growing under elevated CO_2 concentration without loss of J_{max} (result shown in next chapter) (Franks et al., 2013). The relative decline of the gs resulted to reduced transpiration rate per unit CO_2 assimilation, and ultimately resulted to improved WUE in rice without a cost to carbon gain

In this study, *EPF2OE* lines have achieved high photosynthetic rate with reduced stomatal conductance. Photosynthesis is limited not only by gs but by Rubisco activity, whereas transpiration is regulated almost entirely by gs in combination with differences in leaf temperature. This

means that if gs declines under well-watered conditions then photosynthesis may not decline proportionally, leading to an increase in WUE.

4.5 CONCLUSIONS:

Through the leaf excision, water loss and dehydration analysis showing that rice leaves can more efficiently 'buffer' rapid changes in leaf water content if stomatal density is lower

The *WUE* under fully hydrated conditions which is caused by the reduced stomatal conductance relative to CO_2 assimilation rate. Therefore, altering stomatal density in rice could be a beneficial approach to improve drought tolerance without loss in carbon yield.

CHAPTER FIVE: IMPROVEMENT OF DROUGHT TOLERANCE BY THE MANIPULATION OF STOMATAL DENSITY IN RICE

5.1 BACKGROUND

The relationship between the uptake of CO_2 for photosynthesis and stomatal conductance strongly varies in nature, due to the large number of environmental and genetic factors that affect the stomatal number and aperture (Büssis et al., 2006, Xu and Zhou, 2008). The role of stomatal regulation to gas exchange varies with plant species. In rice, for example, the stomatal conductance (*gs*) is often strongly correlated with CO_2 assimilation (*A*) (Jarvis and Davies, 1998, Kusumi et al., 2012, Yu et al., 2015). However, photosynthesis in rice is also influenced by other factors such as leaf nitrogen, photoinhibition (Chen et al., 2003), Rubisco content, but *gs* is co-dominantly correlated with *A*. Taylaran et al. (2011) reported that one of the high yielding rice (*indica*) variety in Japan, Takanari, has shown high rates of leaf photosynthesis, which has resulted from higher content of leaf nitrogen, that caused the elevated capacity for nitrogen accumulation associated with higher *gs*. Similarly, Koshihikari (*indica*) another high yielding variety in Japan with very high leaf photosynthesis has also shown high stomatal conductance (Adachi et al., 2011). Other factors, such as leaf boundary layer and a relative increase of cuticular conductance (Flexas et al., 2004) also contributes to whole leaf conductance. However, under drought stress, stomatal conductance declines with reduced stomatal aperture that resulted due to loss of water. This ultimately reduces the rate of photosynthesis during drought stress. In C3 plants, Flexas and Medrano (2002) suggests that stomatal closure is the first response to drought and the dominant limitation to photosynthesis at mild to moderate drought. The further progression of drought stress leads to decrease in the Rubisco activity

and content, which becomes increasingly limiting during severe drought stress and consequently inhibits photosynthesis further.

Stomatal aperture and density can in some circumstances serve as a proxy for stomatal conductance. Over a decade, studies have reported the successful reduction of the stomatal density in *Arabidopsis* through the interruption of the stomatal asymmetric division (Hunt and Gray, 2009, Hara et al., 2009). It was, therefore, suggested, that reducing stomatal conductance on the plant could be a breakthrough in generating drought tolerant varieties for economic crops (Xu and Zhou, 2008). Büssis et al. (2006), therefore, believed the reduction in the stomatal density in *Arabidopsis* does not reduce either *A, gs* or *E* since the reduction of stomatal density is always accompanied by increase in the stomatal size (Doheny-Adams et al., 2012) and the differences created by reduced density is fully compensated with increased size. Conversely, Franks et al. (2015) have shown that the genetic manipulation of stomatal density led to a significant decrease in stomatal conductance, which ultimately reduced the transpiration rate in *Arabidopsis*. They also observed that the CO_2 assimilation rate was reduced with the decrease in the stomatal conductance. However, the decline in the CO_2 assimilation observed has not caused any dysfunctionality in the photosynthetic biochemistry. Doheny-Adams et al. (2012) therefore, used similar lines to show reduced stomatal conductance has led to a significant improvement in the drought tolerance, through reduced water loss without causing any deleterious effect on nutrient uptake.

Therefore, in this study, a rice generated with reduced stomatal density (*EPIDERMAL PATTERNING FACTOR 2* over expressed) was characterized based on photosynthetic physiology under drought stress. In the previous chapter, phenotypic observations and measurement of gas exchange in response to the rate of transpiration and stomatal conductance, suggest that the rice with reduced stomatal density could as well act in drought tolerance strategy for rice during drought stress.

5.2 AIMS AND OBJECTIVES

- To determine the impact of manipulating stomatal development on drought tolerance.
- To evaluate the limitation imposed on *A* by the stomata in both drought and non-drought condition.
- To determine the impact of *EPF2OE* lines in biomass and yield production under drought

5.3 METHOD

5.3.1 Plant material and growth condition

Similar plant materials with Chapter 4 but only *OsEPF2* overexpression line and the WT were used for this chapter. Seeds were pre-germinated in the module trays for 10 days before they were transferred to the 3L pots containing the compost mix (details in chapter 2). The pots were randomized to a complete randomized design (CRD) on many trays.

5.3.2 Drought experiment

The drought experiment method was similar with experiment 2 of chapter 3. In this study, irrigation was suspended at week 5 and week 8 after sowing. In drought treatment for 5-week old plants, no water was added for 8 days. While in the drought treatment for the 8-week old plants, irrigation was suspended for 7 days but with addition of 5ml of water at day 5 of the DS to delay rapid wilting.

5.3.3 Recovery

On day 8 of drought stress for the 5-week old, and day 7 for the 8- week old, after all measurement were collected, the pots were flooded with water to determine the rate of recovery between the two lines over time.

5.3.4 Gas exchange

Steady state photosynthetic measurements (P_{max}) and photosynthesis vs. Ci (leaf internal CO_2 concentrations, AC_i) curve were measured using

the infra-red gas analyser (IRGA) Licor 6400XT with similar condition in Chapter 4. Measurements were taken more frequently in week 5 than week 8 old during the drought stress. More description for AC_i in Chapter 2 section 2.4.3.4.

5.3.5 Statistical analysis

The Student T-test was carried out using the GraphPad prism 7.01 for Windows (La Jolla, CA, USA) and verified with GenStat for Windows, 17th Edition (VSN International Ltd.) to investigate the effect the response of drought stress between *OsEPF2* and the WT.

5.4 RESULTS

5.4.1 The enhancement of drought tolerance from genetic manipulation of stomatal density

This chapter investigates the role of the *EPF* peptide in drought tolerance using the over expressor lines described in the previous chapter. A drought experiment was conducted to monitor growth and development under stress. Chapter four showed that the *EPF2OE* lines had significantly decreased their stomatal density (D) at the abaxial and adaxial surface by 72 and 63% respectively. It also showed a significantly lower transpiration rate and stomatal conductance at steady state (P_{max}) than its wild type (WT). The *EPFL9OE* lines were not used in this chapter. Drought stress was imposed on the *EPF2OE* and the WT at two growth stages and their recovery rate was also observed.

5.4.2 Effects of drought on relative growth rate (RGR) / Growth assessment from leaf and tiller development

Drought stress was imposed on 5-week old *EPF2OE* (*EPF2OE*) and wild type (WT) lines and height and tillers number were collected over the 7-8 days of water stress. A time-course was used to show the pattern of development between the two lines were under the two water regimes. In Figure 5.1 shows that the time course of the plant height in well-watered condition ran parallel between the WT and *EPF2OE* with no

significant differences between the two in all the time-points. The plant height and the tiller number in the WT was slightly higher than the *EPF2OE* before the drought stress. Under drought stress, only a 4.5% increase in height was observed from day 1 to day 5 in WT, whereas in *EPF2OE*, there was an increase in height by 11.4% from day 1 to day 5 of the drought stress.

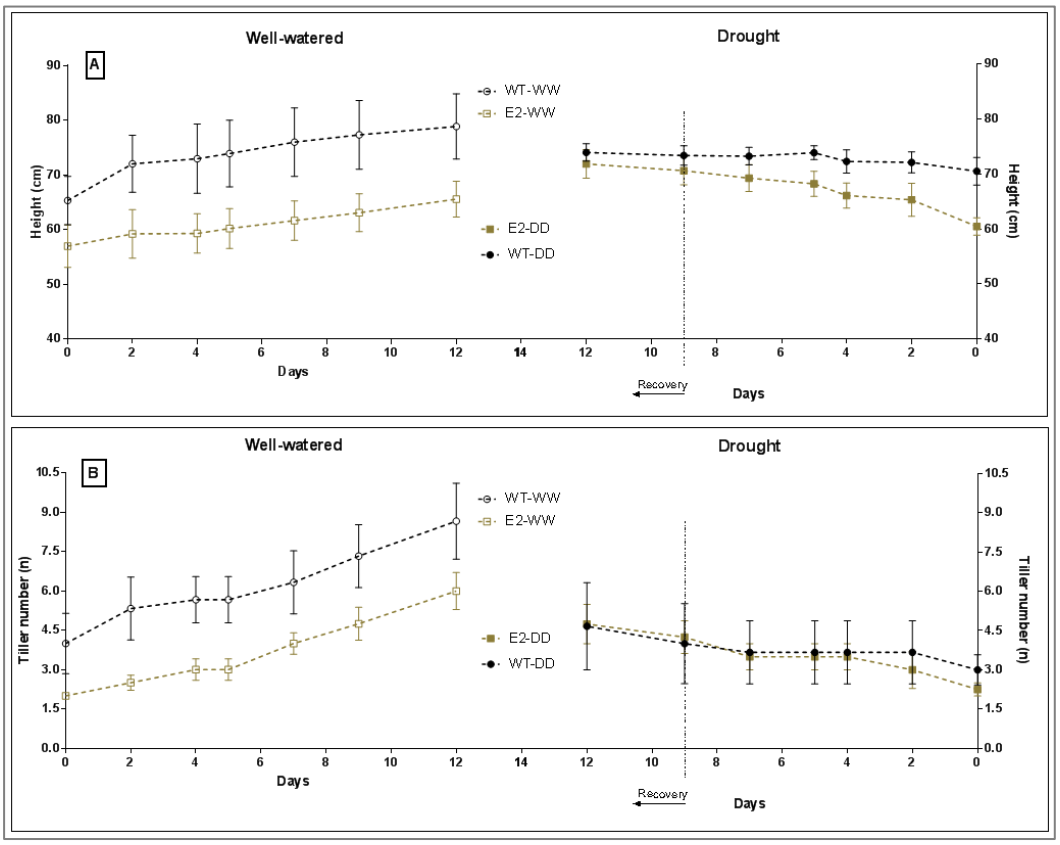

Figure 5. 1. A time-point comparison between well-watered and drought stressed WT and EPF2OE over 12 days. A, change in plant height. **B** changes in tiller development. All values are means with SEM error bars. DD= Drought, WW = Well-watered.

In the case of tillers, the time-course revealed a parallel but non-significant pattern under well-watered condition. Under drought condition, time reveals a non-parallel pattern, with *EPF2OE* closing on WT. This means that tillering slowed down in WT just 2 days into the drought stress. The mean of *EPF2OE* showed improved tillering in drought condition. Even though other signals may be involved in tiller development, high water retention linked to the *EPF2OE* may also play part in this condition.

5.4.3 Soil and Plant water status

From the beginning of the drought treatment, soil water content (SWC) was measured using the theta-probe (as described in chapter 2 section 2.4.2). A time course of the soil water loss in Figure 5.2 shows the gradual decline in the SWC over the period of drought. On day 2 of the drought stress, the SWC of the WT declined by 18.8% of its starting water content which was significantly higher (P=0.0315) than the water loss incurred by *EPF2OE* (5.8%). The decline in the two lines showed soil water loss continued in parallel with no significant differences between them.

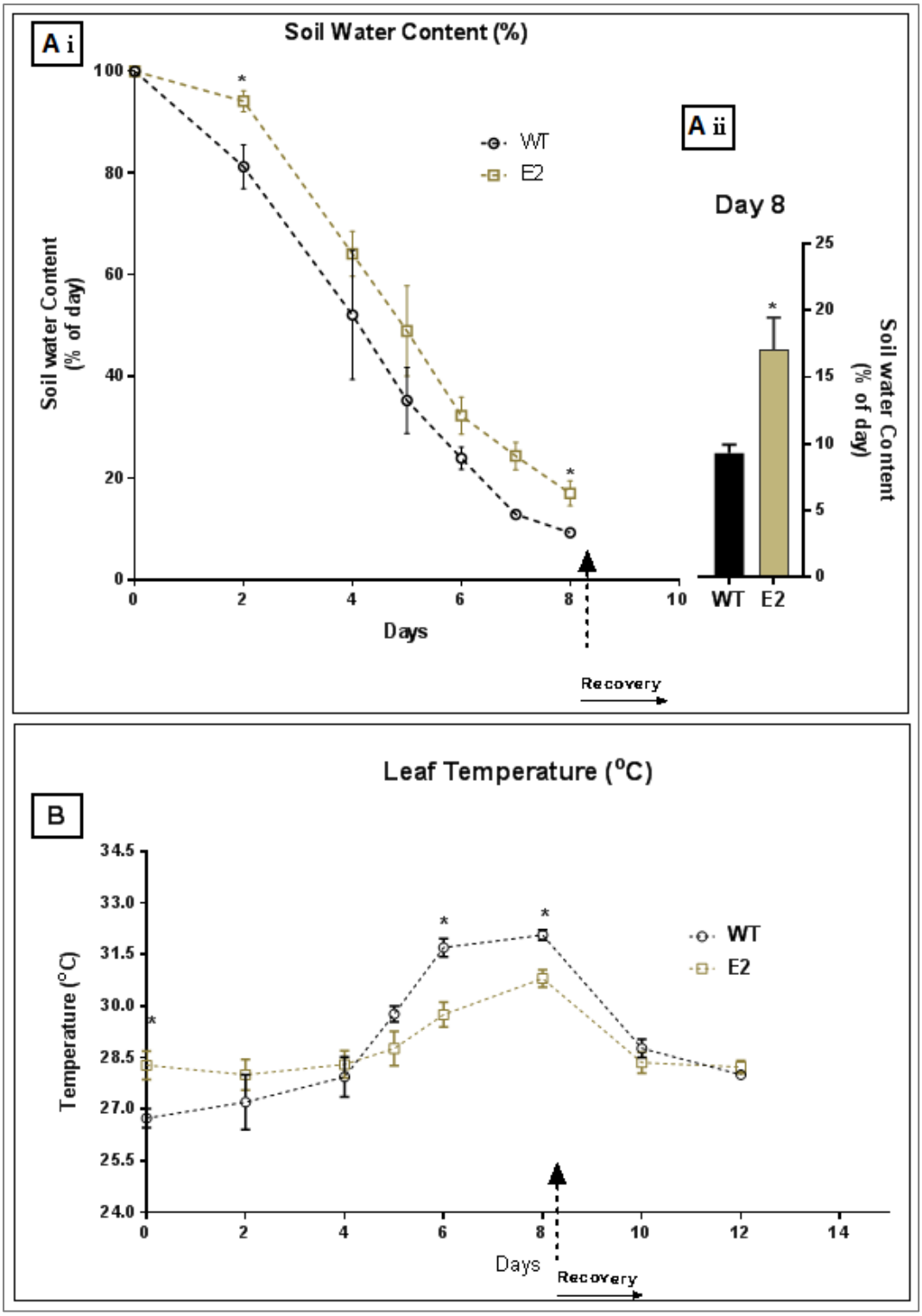

Figure 5.2 Reduced stomatal density improves drought tolerance form the 5-week old experiment. **Ai,** Changes in soil water content over the period of 8-day drought stress, compared to soil water at saturated state at 0 day (left Y-axis %). **Aii**, Differences in soil water content between WT and *EPF2OE* at the final day of the drought (day 8). **B.** A time-course mean leaf temperatures during the drought stress. Each point represented as the mean ± SEM. N= 4-5.

On day 7 of the drought stress when the mean SWC of the WT became significantly (P=0.0161) lower than the mean of the *EPF2OE* with a 11.5% difference. Similarly, on the final day of the drought stress (day 8), the mean of the WT was also significantly (P=0.0474) lower than the mean of the *EPF2OE* with 7.7% differences between them. Although the difference between the WT and *EPF2OE* was small (~10%) in terms of the soil water loss, it can be proposed that the low transpiration rate in the *EPF2OE* directly caused the slower decline in the SWC and thus links rate of soil water loss with reduced stomatal density.

The leaf temperature was measured which is determined by the level of leaf evaporative cooling owing to transpiration and provides a proxy measurement for transpiration. This was evident in the previous chapter when *EPF2OE* with low stomatal density showed higher leaf temperature due to low transpiration rate. The time-point changes in mean leaf temperature of *EPF2OE* was significantly (P=0.0360) higher than WT at day 0 of drought stress. On day 4 of the drought stress, the mean leaf temperature of the WT increased and level with mean *EPF2OE*. This indicates stomatal closure and loss of evaporative cooling by transpiration due to the limited water availability.

5.4.4 Water status in the leaf

The soil drying in Figure 5.2 A directly resulted in a reduction in leaf relative water content (RWC). In this part of the experiment, the well-watered plants maintained approximately 95% of leaf RWC. The RWC of the drought treated plants was examined on day 6 of the drought stress (Figure 5.3 A). The RWC of the drought stressed WT on day 6, was 38.8% lower than it's well-watered. Differences in *EPF2OE* between the treatments showed the RWC of the drought stress was 15.5% lower than the mean of the well-watered. Importantly, the drought stressed WT was significantly lower (P=0.0156) than the mean of the drought stressed *EPF2OE* (Figure 5.3 B). Thus, the high-water retention in the leaf of *EPF2OE* may be linked to the low stomatal density which evidently reduced its transpiration rate (not shown).

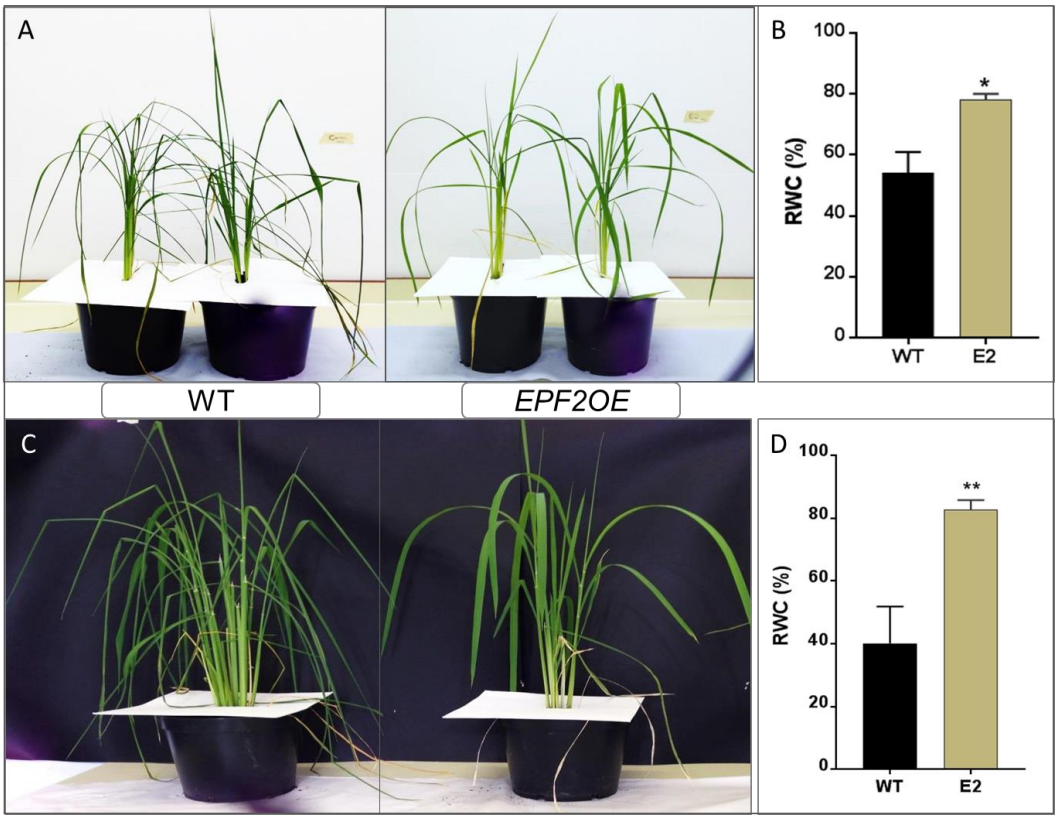

Figure 5.3 Reduced stomatal density improves drought tolerance in both 5-week and 8-week old rice plants. **A.** photographs of a representative of 5-week old plants (WT and *EPF2OE*) on day 6 of drought stress. **B.** Relative water content (of Fig 5.3A) at day 6 of drought stress.**C.** Photographs of a representative of 8-week old plants (WT and *EPF2OE*) on day 6 of drought stress. **D.** relative water content (of Fig 5.3C) at day 6 of drought stress. The asterisks represent the significant differences between the two treatments of the same (*=P≤0.05 and **=P≤0.01) and error bars indicate the SEM.

The other experiment (8-week-old plant), it was mentioned in the method that at day 5 of the drought stress, 5ml of water was added directly to the soil around the tiller of the 8-week old plants. This was aimed to slow down the rapid loss of turgor observed among the genotypes (see Figure 5.3 C) and to stretch the drought period for 8 days as done in the 5-week old plants. On day 6 of the drought stress and a day after 5ml of water was added, the RWC of the drought stressed 8-week old WT leaf had declined by 54.4% compared to its well-watered control. Conversely, the mean of the drought stressed *EPF2OE* showed only 14% loss of leaf water content on day 6 of the drought stress from its well-watered control. The differences between the mean of the two droughts stressed lines was significantly different at P=0.0058. Thus,

the RWC of the drought stressed *EPF2OE* was 51% more than the drought stressed WT. (see Figure 5.3 D)

5.4.5 Changes in Leaf gas exchange characteristics under drought stress

Gas exchange was recorded over the 8 days of drought stress and recovery to establish the relationship between the stomatal density and the dynamics of stomatal conductance, transpiration and water use efficiency in water restricted condition. As mentioned, drought stress was imposed on young plants (5-week old) and the matured plants (8-week old) for a period of 8 days and 7 days respectively. A time-course gas exchange for the 5-week old was observed over the period of the drought stress. The responses to CO_2 assimilation (*A*) and stomatal conductance (gs) in Figure 5.4 revealed that both the two lines; WT and *EPF2OE* (*EPF2OE*) generally showed a decline on each day over the period of the drought. it was not a surprise that on day 0 the *gs* and *E* of *EPF2OE* were significantly lower than WT. After four days of the drought stress, the gs (Figure 4 A) and *E* (not shown) of the WT had shown 43.7% and 38.7% drop from its rate on Day 0 respectively. The *gs* and *E* of the *EPF2OE* however, only declined by 14.2% and 17% respectively from day 0, consistent with the soil water, RWC measurements above. Interestingly, on day 4 of the drought stress, the *A* of the two lines both declined by ~15% (Figure 5.4 B).

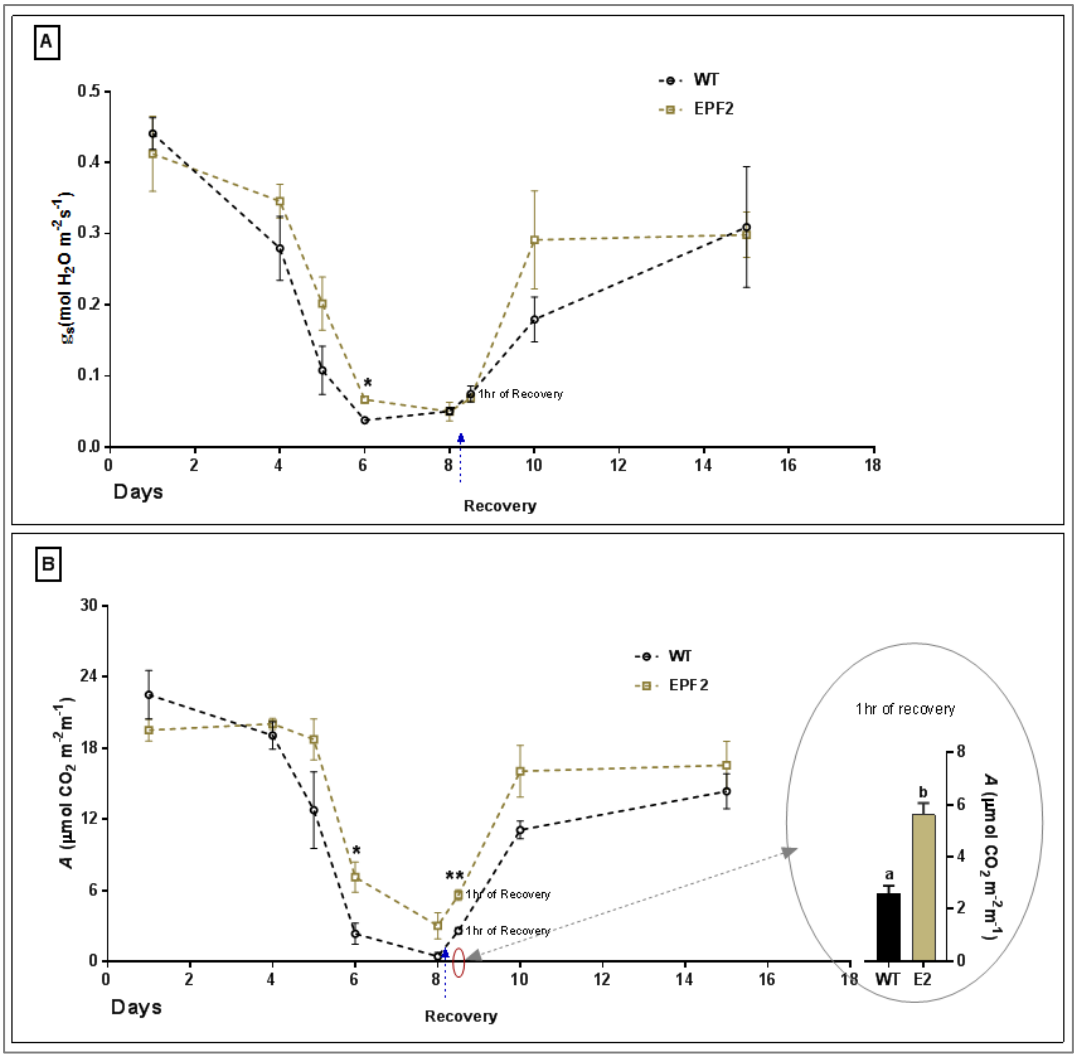

Figure 4. Time-course effect of the mean drought stress between the WT and the *EPF2OE* of the 5-week old. **A**. stomatal conductance (*gs*). **B**. CO_2 assimilation rate (*A*). The asterisks represent the significant differences between the two treatments at the same time-point. (*=P≤0.05, **= P≤0.01). Error bars indicate the Standard Error of the Mean (SEM). N= 3 - 5

On day 6 the loss in the *gs* and *E* of the WT had reached 92.4% and 88% from day 0 respectively. The *EPF2OE*, therefore, had a loss of 83.4% (P=0.0043) and 78% (P=0.0046) *gs* and *E* from day 0 respectively. Thus, the gs and *E* of the *EPF2OE* were significantly higher than the WT. Interestingly, the *A* of the WT at this stage has dropped significantly (P=0.0372) by 89.5% from day 0, while *EPF2OE* dropped 69.7% of day 0. Due to drop in the rate of transpiration in the WT, the mean leaf temperature at this stage (Fig 5. 2 B) exceeded the mean leaf temperature of *EPF2OE* significantly (P=0.0103) by ~1.95°C. The rise in the mean leaf temperature of the WT at this point which resulted in the

loss of turgor and stomatal closure are likely to have a direct link to the number of the stomata. Interestingly, day 6 became a critical point in which the amount of *E*, the g_S and the *A* of *EPF2OE* were all higher than WT during the stress. The drought stress lasted for 8 days. At the day 8 of drought, both the WT and *EPF2OE* showed lower gas exchange rates with *A* dropped by 98% and 87.2%, g_S dropped by 89.8% and 87.6%, E by 84.3% and 83.1% respectively. However, the mean leaf temperature of the WT which was significantly higher (P=0.0105) than the mean of the *EPF2OE*, there were no significant differences in g_S, *A* and *E* between the mean of WT and *EPF2OE* at this stage.

In 8-week old plants (mature), just 2 days after the water was added (at day 5, as mentioned earlier), the mean of *A* of the WT has declined significantly low (P<0.0001) to 0.17 μmol CO_2 $m^{-2}s^{-1}$ by 99.3% from the mean of the well-watered WT (see Figure 5.5). While in *EPF2OE* the mean of *A* was at 8.7 μmol CO_2 $m^{-2}m^{-1}$ making a significant (P=0.0002) 57.4% declined from its well-watered control. There was also a significant difference between the mean of drought stress *EPF2OE* and WT at P=0.0019 at the same time. On the same day 7 of drought stress, the CO_2 assimilation rate of *EPF2OE* was 39.8% higher than the mean of the WT. The g_S and *E* of the WT have significantly declined by 87.3% at and 84% at P<0.0001 from the mean of its well-watered control respectively. Similarly, *EPF2OE* showed a significant decline in the g_S by 72.3% at P=0.0006 and *E* by 67.9% at P<0.0001 level of significance. Low C_i*:Ca* in genotype act as a proxy to potentially high leaf water use efficiency. Thus, Ci:Ca was significantly low in *EPF2OE* drought stressed compared to the mean of the WT drought at P=0.0005 by 39.6% (see Figure 5.5 D) at day 7 of DS. Therefore *EPF2OE* had significantly higher intrinsic WUE than WT at P=0.0019 by 98%.

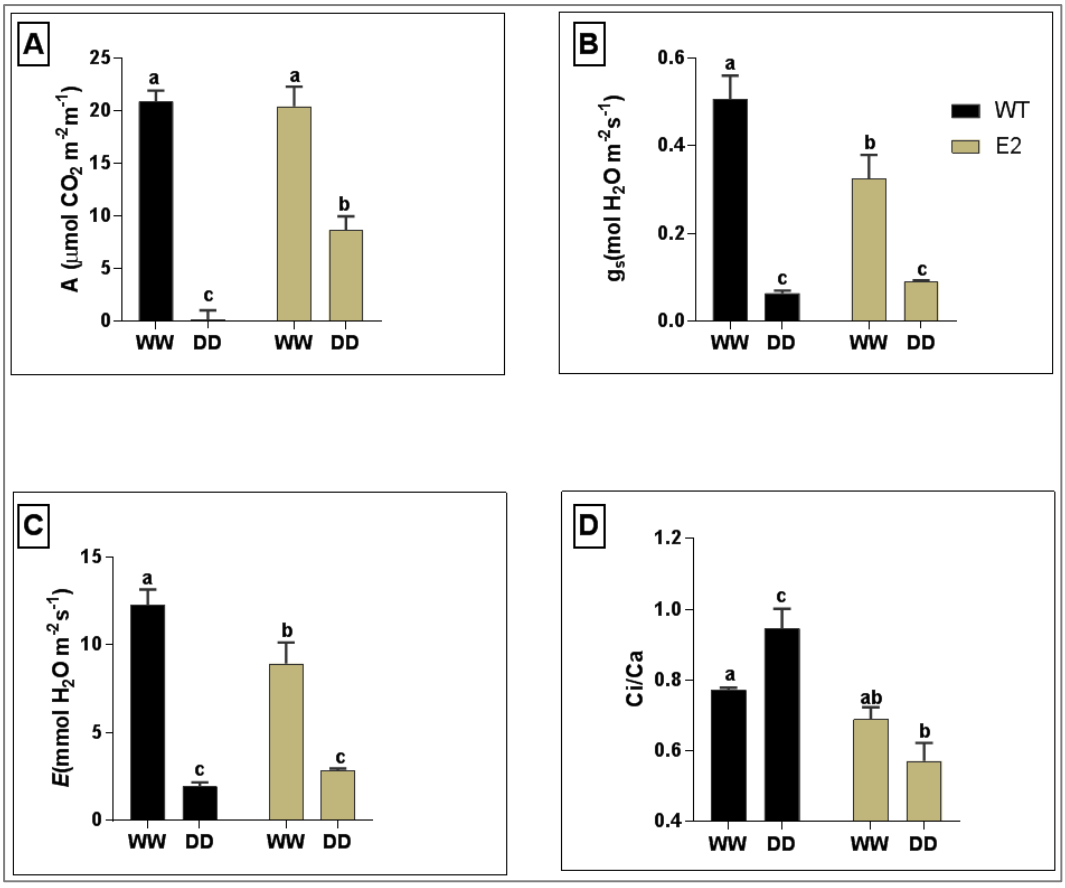

Figure 5.5. The leaf gas exchange parameters of the 8-week-old (matured) plants on the day 7 of the drought stress (2 days after 5ml of water was added) between the two lines and the well-watered control **A**. Carbon assimilation rate (*A*). **B**. Stomatal conductance (*gs*) **C**. Transpiration rate **D**. Ci:Ca ratio which by proxy reveals the level of leaf water use efficiency. Different letters group indicates significant differences. All values are means with SEM error bars. n= 4 – 5. Cuvette condition: RH = 28%, leaf temperature 28^{o}C, light saturation (1500μmol^{-2}s^{-2})

5.4.6 The analysis of response of CO_2 assimilation to intercellular CO_2 concentration under drought stress (A C_i Curve)

The relationship between the changes in the CO_2 assimilation (*A*) as a function of the intercellular CO_2 concentration (*Ci*) (A*Ci* curve) was used to determine the relative influence of stomatal density to photosynthesis. The ACi model was also used to determine the limitations imposed to photosynthesis by the stomata (Farquhar et al., 1980). The measurement was carried on day 4 of drought stress of the 5-week old plants and well-watered control. The carbon assimilation rates of WT and *EPF2OE* with higher and lower D respectively were measured at a series

of CO_2 concentrations and plotted *A* against *Ci*. The net photosynthetic rate increased with increasing CO_2 concentration in both *EPF2OE* and WT. The *A* at the operating point (ambient CO_2) of CO_2 (400 µmol/mol) derived from the *A* vs *C*i curve was not significant between the WT and *EPF2OE* in both drought and well-watered condition. The differences between means of *E*, gs and *Ci* at the operating point were not significant under drought condition between WT and E2. However, in well-watered there was a significant difference in *E, gs* and *Ci* between the two lines.

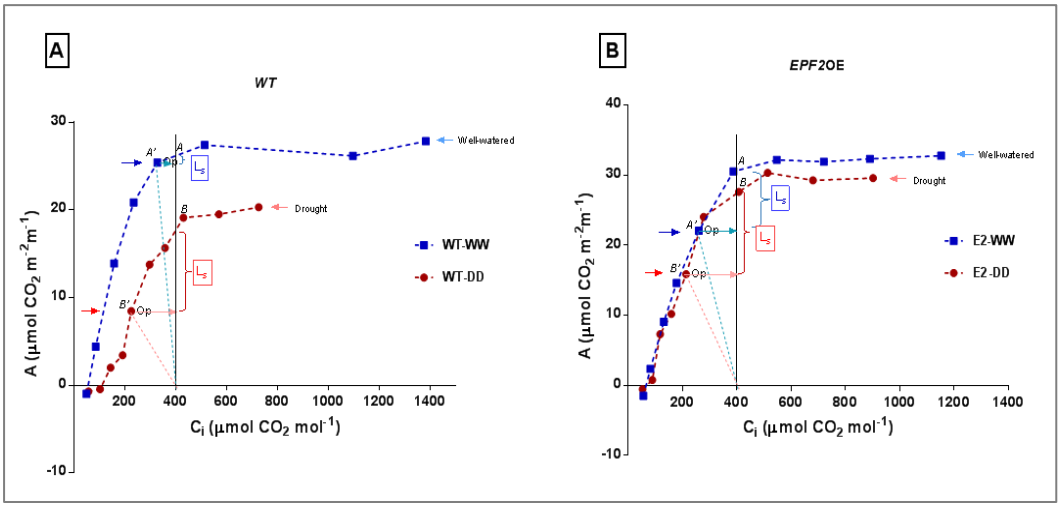

Figure 5.6. Example: *ACi* Single point A*Ci* curve and the stomatal limitation principle in both well-watered and drought stress measured at saturated light (PAR = 1500µmol $m^{-2}s^{-1}$). **A**. Single plant WT well-watered vs drought. **B**. Single plant *EPF2OE* well-watered vs Drought. n= 3-4 per line per treatment.

The limitation imposed on photosynthesis by the stomata (L_s) was derived from the A/Ci curve as described in Figure 5.6 (Long and Bernacchi, 2003). The L_s can be viewed as the proportion of the value of photosynthesis that results from stomatal resistance rather than other factors such as Rubisco activity or electron transport. L_s increased under drought condition in both the lines. Interestingly, with large differences in the stomatal densities (data not shown) on both leaf surfaces among the two lines, no significant differences were observed in the L_s of the WT (0.087±0.016) and *EPF2OE* (0.081±0.041) in well-watered treatment (Figure 5.7 C). This is somewhat expected given the data in previous chapter. The L_s in WT had increased by 81.7% after 4 days for drought stress while the *EPF2OE* increased by 75.6% after 4 days of

drought stress. Therefore, between the treatments, there was a significant increase in L_s in A, in both WT and *EPF2OE* at P=0.0095 and P=0.0087 level respectively. The differences between the drought stressed lines revealed 30.7% higher Ls than *EPF2OE*, even though, no significant difference was observed between the two lines. Generally, at a moderate drought stress, there is an increase in the diffusional limitations of carbon uptake imposed by the water stress. This may suggest that the rate of carbon assimilation was impaired as the stomata began to close due to loss of water in the both the lines. The lack of a difference in Ls is consistent with the statistical lack of control of stomatal resistance over photosynthesis in well-watered conditions but not with the water loss experiments described

In addition to the L_s, the biochemical components of photosynthesis, V_{cmax} (maximum carboxylation rate of Rubisco), J_{max} (maximum rate of RuBP regeneration) and leaf dark respiration were estimated from the curve fitting model of Farquhar's (Farquhar et al., 1980) modified by Bernacchi (Bernacchi et al., 2001) using a nonlinear regression technique. This was used to examine whether the manipulation of the stomata has any effect on the biochemical factors that contribute to the decrease or increase in the carbon assimilation. These observations were made under controlled leaf temperature, however, due to their varying level of transpiration rate, hence the leaf temperature varies with the lines. Therefore, the analysis was normalized to equal temperature (25^{o}C) to limit the temperature dependent variations in enzyme kinetics so as to have equal representation based on an equal amount of leaf temperature as suggested by Sharkey et al. (2007). Under both drought well-watered condition, no statistical differences in V_{cmax} and J_{max} were observed between the WT and *EPF2OE* (see Figure 5.7).

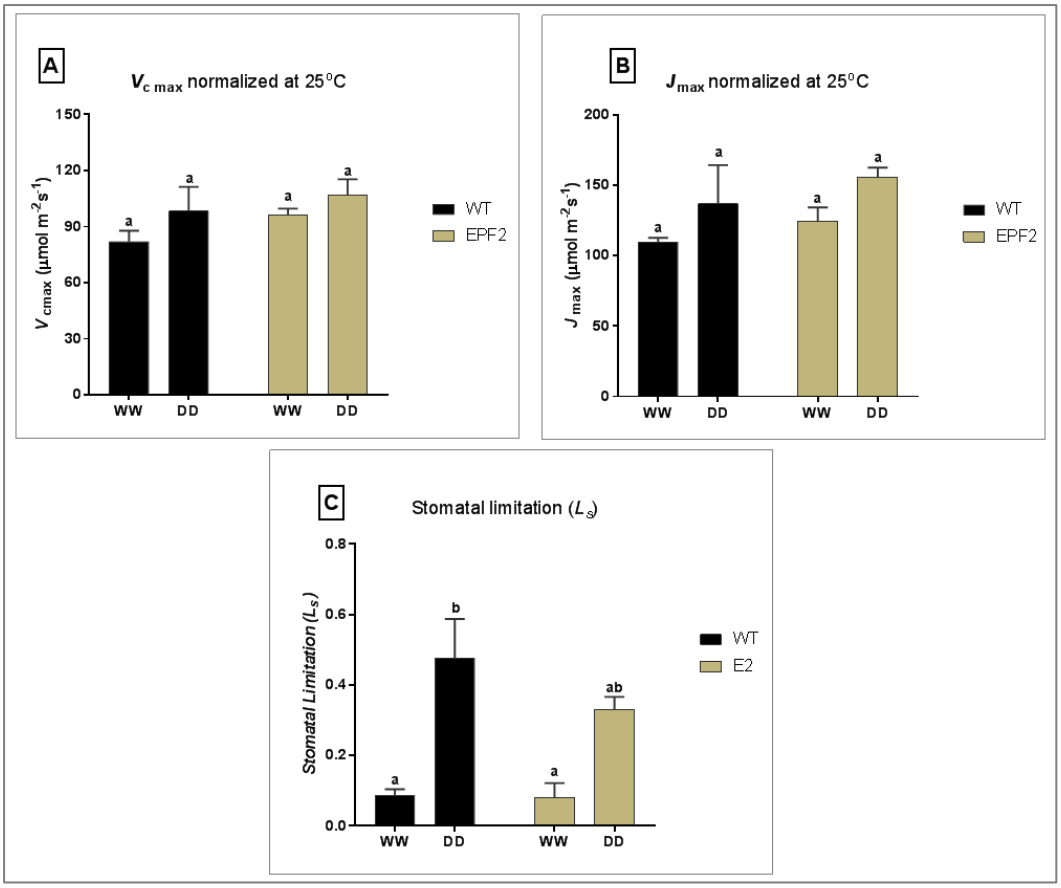

Figure 5.7. Summary of the ACi curve estimates of the photosynthetic biochemical components and non- biochemical component between drought and non-drought. **A.** The maximum carboxylation rate of Rubisco (V_{cmax}). **B**. The maximum rate of RuBP regeneration (J_{max}). **C**. The stomatal limitation imposed on *A* (L_s). Different letters group indicates significant differences. All values are means with SEM error bars.

It can, therefore, be predicted that the insignificant differences in photosynthetic potentials (V_{cmax} and J_{max}) of the WT and *EPF2OE* in non-stressed condition reveals that the genetic alteration of stomata in *EPF2OE* from WT does not affect or uncouple its photosynthetic biochemistry.

The responses to the photosynthetic biochemistry in a drought condition may only be linked to the water availability for Rubisco activity in the plant.

5.4.7 Recovery from the drought stress

Re-watering of the young stressed plants (5-week old) was immediately followed by measurements on the 8th day of the drought stress. After re-watering, the leaf gas exchange parameters (*A,* gs and *E*) recovered gradually, but the extent of their recovery varied greatly between the WT and *EPF2OE*. An hour after re-watering, there was a dramatic response among the two lines. The *EPF2OE* regained 11% of the *A* within an hour and this was significantly (P=0.0033) higher than the 9.6% regained by the WT see in Figure 5.4. The gs and *E* at this stage were not very responsive in both WT and *EPF2OE*, they regained less than 5 and 7% respectively.

After two days of re-watering, the *A* of the WT restored to 11 μmol CO_2 $m^{-2}m^{-1}$ and 47.6% from its lowest rate 0.446 μmol CO_2 $m^{-2}s^{-1}$ incurred on the final day of the drought stress. While the *A* of the *EPF2OE* was restored to 16.06 μmol CO_2 $m^{-2}s^{-1}$ and 55.5% from the rate at day 8 of drought stress. The gs and *E* of the WT restored to 0.180 mol H_2O $m^{-2}s^{-1}$ and 5.8 mmol H_2O $m^{-2}s^{-1}$ and 25.9 and 32.5% respectively. The gs and *E* of the *EPF2OE* restored to 0.291 mol H_2O $m^{-2}s^{-1}$ and 8.4 mmol H_2O $m^{-2}s^{-1}$ and regained almost the double of the WT with 59.8% and 62.5% of the rate at day 8 of drought stress.

Seven days after re-watering, *A* of WT and *EPF2OE* was restored to 14.4 and 15.8 μmol CO_2 $m^{-2}m^{-1}$ making them regained 62.1 and 54.3% of their rate at day 8 of drought stress. The WT at this point was not able to recover the high gs and *E* which was significantly higher than *EPF2OE* prior to the drought, instead, they restored 0.310 mol H_2O $m^{-2}s^{-1}$ and 8.1 mmol H_2O $m^{-2}s^{-1}$, making them 52.1 and 51.3% more from the rate at the end of the drought. The *A* of the recovered WT was significantly (P=0.0250) lower than the mean of the well-watered control by 35.6%. The gs and E of the WT were 27.5 and 25.3% less than the mean of the well-watered control respectively. Conversely, the *A* of the *EPF2OE* was only 10.5% less than the well-watered control and the gs and *E* of the recovered appeared to increase by ~13% each over the well-watered control respectively.

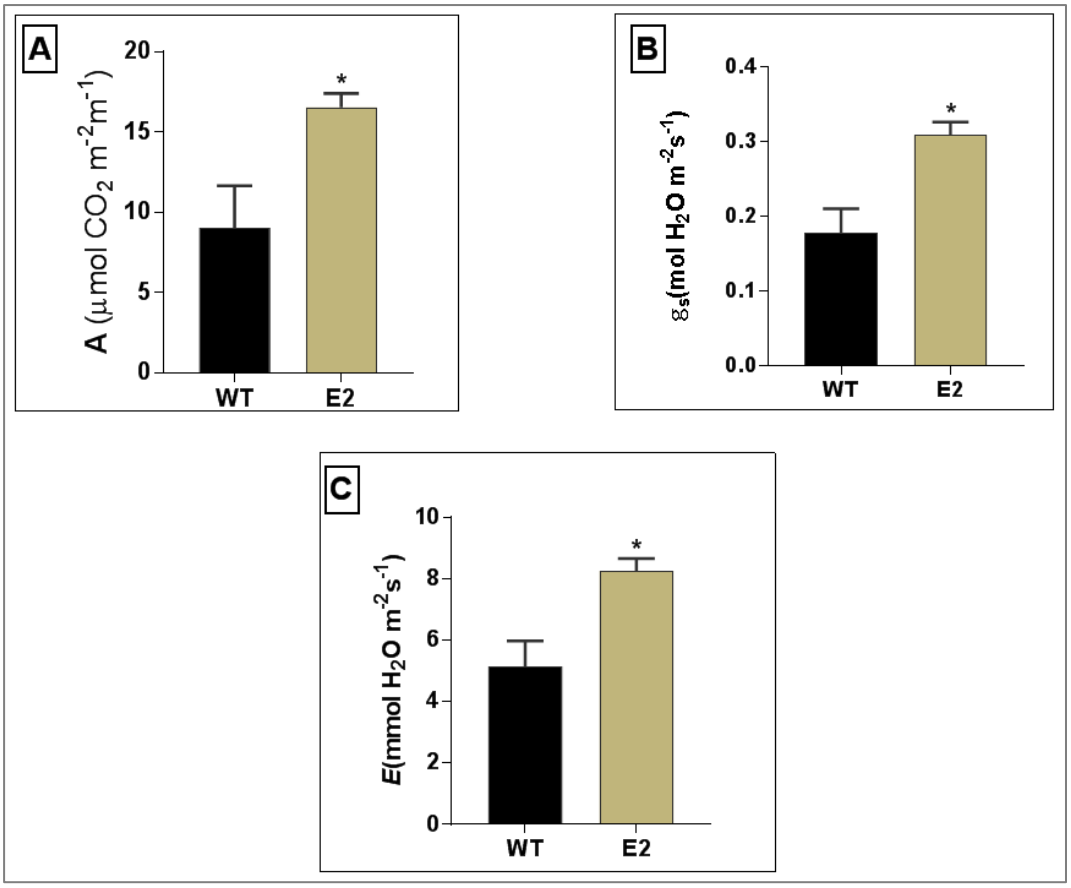

Figure 5.8. Leaf gas exchange of the 8-week of plants at 2 days of re-watering. **A**. Carbon assimilation rate (*A*). **B**. Stomatal conductance (*gs*) **C**. Transpiration rate. Asterisk represents significant differences (*P≤0.05). All values are means with SEM error bars. n= 4 – 5. Cuvette condition: RH = 28%, leaf temperature 28°C, light saturation (1500μmol^{-2}s^{-2})

Re-watering of the 8-week old (matured) plants was followed after 7 days of drought stress. 2 days after the recovery, the mean of the *A* of the two lines recovered at a different rate. WT had a mean of 9.05 μmol CO_2 m^{-2}m^{-1} which regained 98.1% of its lowest drought rate (0.168). *EPF2OE* regained 47.5% from its rate at day 7 of the drought stress. Therefore, the *A* mean of WT was significantly lower than the rate of *EPF2OE*. This may suggest the proper utilization and quick recovery of *EPF2OE* after the two days of re-watering. *E* and gs of WT regained 64 and 61% from the rate at day 7 of the drought stress respectively. Whereas, *EPF2OE* regained 70.7 and 65.2% of gs and *E* from its rate at the end of the drought. It was therefore revealed the gs (P=0.0119) and *E* (P=0.0139) of *EPF2OE* were significantly higher than the WT after two days of re-watering (Figure 5.8). This suggests that the *EPF2OE* showed

greater tendencies of recovery from drought due to its higher RWC at the point of re-watering which may have a direct bearing on the low rate of transpiration imposed by its low stomatal density.

Five days after the re-watering, the mean of *A*, g_S and *E* of the WT were 11.7 μmol CO_2 $m^{-2}s^{-1}$ and, 0.373 mol H_2O $m^{-2}s^{-1}$ and 9.9 mmol H_2O $m^{-2}s^{-1}$, While for *EPF2OE* are 13.1 μmol CO_2 $m^{-2}s^{-1}$, 0.214 mol H_2O $m^{-2}s^{-1}$ and 5.9 mmol H_2O $m^{-2}s^{-1}$ respectively. Consequently, at 5 days of recovery, the *A* were slightly low particularly the WT but no significant differences were observed between the two lines. The g_S and *E* of *EPF2OE* were all significantly lower than the WT at P=0.0159 and 0.0212 respectively. The $C_i:C_a$ ratio of *EPF2OE* was significantly lower than the WT, hence, making the intrinsic water use efficiency of *EPF2OE* significantly higher than the WT (figure not show).

The recovery in the two growth stages showed that the photosynthetic potentials of the two lines was greatly affected by the severity of the drought stress. Even so, the WT failed to recover fully to its potential. This may suggest the high possibility of Rubisco impairment and increased Rubisco oxygenation.

5.4.8 The Biomass

At the end of the two drought experiments carried out at two different plant ages. The information on the biomass data was collected at the end of the harvest period, after going through 7-8 days drought stress followed by re-watering (recovery) until harvest. The inducement of the drought stress at the early developmental stage of the rice has resulted in significant changes in the plant's biomass by the end of the harvest.

The effect of drought on the leaf area of WT and *EPF2OE* stressed/recovered at the 5-week old has revealed a significant (P=0.0035) decrease in the leaf area of the WT compared to the *EPF2OE* by end of the harvest. The recovered *EPF2OE* showed 35% higher leaf area than the recovered WT. As expected the leaf area of the non-stressed WT was significantly higher (P=0.0165) than the stressed WT, while the similar response was not observed between the non-stressed *EPF2OE* and the recovered *EPF2OE*, thus no statistical differences between them. Clearly, the stomatal alteration may have indirectly

altered leaf area indifference in the 5-week old. Differences in the leaf area among the 8-week old rice plants were not observed. Hence, no differences between non-stressed WT and non-stressed *EPF2OE* in terms of leaf area was observed. This means that the effect of stomatal alteration did not cause any significant changes to leaf area in the 8-week old plants.

S/N	Character	WW:	YOUNG			MATURED		
			RECOVERY:	WT:	*EPF2OE*:	RECOVERY:	WT:	*EPF2OE*:
		WT Vs *EPF2OE*	WT Vs *EPF2OE*	RECOV. Vs WW	RECOV. Vs WW	WT Vs *EPF2OE*	RECOV. Vs WW	RECOV. Vs WW
1	Number of Tillers (n)	22 ± 1.8 23.9 ± 3.3	13 ± 1.5 16.3 ± 3.4	13 ± 1.5 22 ± 1.8*	16.3 ± 3.4 23.9 ± 3.3	16.67 ± 2.963 18 ± 2.31	16.7 ± 3.0 22 ± 1.8	18 ± 2.3 23.9 ± 3.3
2	Fresh Weight (g)	42.4 ± 6.1 45.1 ± 6.3	18.2 ± 1.4 26.5 ± 0.8**	18.2 ± 1.4 42.4 ± 6.1*	26.5 ± 0.76 45.1 ± 6.3	25.64 ± 4.992 37.97 ± 5.967	25.6 ± 5.0 42.4 ± 6.1	38.0 ± 6.0 45.1 ± 6.3
3	Leaf Area (m^2)	914.9 ± 121.4 1094 ± 132.3	395.5 ± 34.1 609.4 ± 5.3**	395.5 ± 34.1 914.9 ± 121.4*	609.4 ± 5.3 1094 ± 132.3	619.8 ± 118.2 945.3 ± 125.5	619.8 ± 118.2 914.9 ± 121.4	945.3 ± 125.5 1094 ± 132.3
4	Dry Weight (g)	9.8 ± 1.5 11.2 ± 1.6	4.9 ± 0.5 7.2 ± 0.2*	4.9 ± 0.5 9.8 ± 1.4*	7.15 ± 0.15 11.17 ± 1.56	5.9 ± 1.3 9.1 ± 1.6	5.9 ± 1.3 9.8 ± 1.4	9.1 ± 1.6 11.2 ± 1.6
5	Yield (g)	7.8 ± 2.3 1.7 ± 0.6**	0.92 ± 0.17 0.22 ± 0.09*	0.92 ± 0.17 7.8 ± 2.3*	0.15 ± 0.05 1.7 ± 0.6	2.45 ± 0.19 0.15 ± 0.05***	2.5 ± 0.19 7.8 ± 2.3	0.15 ± 0.05 1.70 ± 0.59

Table 5.1: Summary of the total yield and biomass of the EPF2OE and WT after drought and recovery versus the well-watered control. The asterisks represent the significant differences. (*=P≤0.05, **= P≤0.01, ***= P≤0.001). Standard Error of the Mean (SEM) are indicated with the ±. WW=well-watered, RECOV= Plants recovered from drought stress. The table only compares the top data with the below data of every parameter.

There were no significant differences in the number of the total tillers at the end of the experiment between WT and *EPF2OE* of the plant stressed at 5-week old (young). Likewise the well-watered *EPF2OE* and the recovered *EPF2OE*. Conversely, the non-stressed WT has significantly (P=0.0147) higher number of total tillers than the recovered WT by 69.3%. This clearly suggests the development of the WT has been severely impaired by the drought and the recovery was not enough to close the gap with the *EPF2OE*. No difference was observed in the plants stressed at 8-weeks (matured). Usually, at that stage, plants are very close to flowering. Assimilates are generally channelled to flowering and most of the developmental growth stops when the plant began to initiate flowering.

Differences in fresh weight were observed between the recovered plants. Recovered young *EPF2OE* showed significantly (P=0.0064) higher fresh weight than the recovered WT by 31.5%. Similarly, the non-stressed WT also showed significantly higher fresh weight than the recovered WT. Interestingly, no differences were observed between the well-watered and the recovered. No significant changes were observed in terms of fresh weight among all the matured plants. The dry weight of the recovered young *EPF2OE* was significantly (P=0.0129) higher than the recovered young WT plants by 31.7%. The well-watered young WT was also significantly (P=0.0372) higher than the recovered young WT by 49.9%. The mature plants also don't show any significant differences in dry weight among both the genotypes and the conditions.

The result revealed that alteration of stomata (EPF2 OE) has a significant negative effect on the yield. This is part of ongoing research on why the stomatal alteration has a serious effect on the yield by groups in Universities of Nottingham and Sheffield. The result showed (Table 5.1) that the recovered WT had significantly (P=0.0213) higher yield than the recovered young *EPF2OE* by 75%. Interestingly, drought has caused an effect in the yield of young WT, as the non-stressed WT has significantly (P=0.0499) higher yield than the young recovered WT but the two *EPF2OE* plants did not show any significant differences in terms of yield.

The matured plants here displayed a significantly (P=0.0003) higher yield in the recovered WT than the recovered *EPF2OE* by 93.7%. Similarly, the non-stressed WT had significantly (P=0.0057) higher yield than the recovered matured WT. Surprisingly, the non-stressed *EPF2OE* and WT had no significant differences in terms of yield. This suggests that drought has a tremendous effect on the yield. The yield of the WT significantly dropped after drought stress at both early and late drought (young and mature) stress. However, the effect is very much high when the drought is imposed at the flowering stage.

5.5 DISCUSSION

In the previous chapter, it was revealed that the change in the stomatal density caused by the overexpression of the EPF family has resulted in a compensation effect on the size of the stomata. The decrease in the stomatal density caused an increase of the stomatal size in an inverse relationship (Franks et al., 2009, Doheny-Adams et al., 2012). A similar relationship has been reported in Arabidopsis where density was fully compensated with size were no differences in terms of gas exchange and chlorophyll fluorescence were observed between WT and *AtEPF2* (Büssis et al., 2006). However, in the present study, the stomatal density of Os*EPF2OE* was not able to fully compensate the changes in gas exchange with the increased stomatal size. Improvement of leaf water use efficiency accompanied by the reduced transpiration rate and stomatal conductance resulted by the genetic manipulation of stomatal density has been shown by the constitutive overexpression of the *OsEPF2* in *Oryza sativa* L. Japonica Nipponbare. Specific experiments using the two rice genotypes with varying stomatal density reveals physiological characteristics that could explain the sensitivity and tolerance to drought, as well as the biomass and yield after drought treatments. Five (5) week old *EPF2OE* plants with reduced stomatal density in rice has shown a slower time-point decline in the gs, *E* and *A* than the WT. *EPF2OE* was able to show higher performance over the period of 8 days water stress with effective utilization of the limited available water present in the soil. This was supported by the time-point examination of the soil water content and it suggests that *EPF2OE* has a considerable water conservation, which was significantly higher than the WT by the end of the water restriction period. This claim can also be supported by the gradual rise in leaf temperature of WT plants. In the period of water restriction, the loss of cooling by transpiration in WT lead to a significantly higher leaf temperature than *EPF2OE*. The retarded soil water loss among the *EPF2OE* may explain the reason why gas exchange was slightly higher in the *EPF2OE* than its WT over the period of water restriction. These differences in drought sensitivity were related to their

response to leaf desiccation treatment earlier showed in the previous chapter, where WT lost water more quickly than *EPF2OE*.

The analysis of the response of *A* to *Ci* demonstrated the decline in the *A* in both *EPF2OE* and WT during the period of water restriction stress may have a direct association with the limitation imposed by the stomata (stomatal limitation). At that moderate drought stress (4 days of drought stress), the decline in *A* at the operational point was accompanied with the low *gs* and *E* (not shown) which suggests stomatal limitations dominates irrespective of any metabolic impairment. The relative contribution of the L_s to *A* varied with the lines and the duration of the drought stress. This limitation is particularly important for *A* at the early stage of the drought and from this study, the results showed that the limitation imposed on stomata in non-drought condition was similar in both the two lines but that has since changed after 4 days of drought stress. The effect of the drought stress on WT shown a limitation on *A* by the stomata after 4 days of stress, whereas *EPF2OE* with relatively higher RWC does not show any changes in the L_s after 4 days of drought stress. Other photosynthetic components (V_{cmax}, J_{max}) did not change in response to the mild drought of 4 days among all the lines. Without sufficient evidence, it is hard to call the possibility of photorespiration which can be attributed to the decline in J_{max} and or increase in qP during a drought period. This is a common characteristic of C3 plants when stomatal closes, it increases the chances of oxygenation of Rubisco due to low intra leaf partial pressures of CO_2. The effect of drought stress in the decline of the photosynthetic parameters such as gs has been reported in many plant species and are usually result in the decline of A_{max} at severe drought stress (Flexas et al., 2004, Lawlor, 2002). The present study suggests that the reduction in the *A* in both *EPF2OE* and WT at day 4 of drought stress was due to reduced stomatal aperture resulting to low *Ci*. This relationship indicates downregulation of the *A* to adjust the mesophyll containing capacity of the decreased ambient CO_2 (C_a) supply imposed by the closure of stomata and consequently the loss of Rubisco activity follows (Lawlor and Cornic, 2002). It is worth mentioning that at a certain stage of the drought stress (after the 4^{th} day of drought), an increase in the C_i was observed in the drought stress

treated plants (young) which were lower at the beginning of the drought. The suggested reason is that at severe stress, C_i cannot be calculated accurately due to heterogeneous stomatal closure, cuticular conductance etc. that tend to overestimate the C_i. In a situation like this, when the gs was at the lowest end, yet the C_i increases, such indicates the predominance of the non-stomatal limitation imposed on photosynthesis (Flexas and Medrano, 2002). That point when the C_i began to increase is called the C_i inflexion point.

The reduced stomatal density served as a benefit to the *EPF2OE* plants in the period drought stress that enables rapid restoration of *A* by rehydration. The WT may need longer time for *A* restoration because, at 7 days after rehydration, it was still about 65% of its original *A*. This may suggest an irreversible impairment of Rubisco, whose activity can be easily affected by moderate or severe stress.

The result in this study revealed how low stomatal density under drought stress improved biomass (fresh weight, dry weight and leaf area) after recovery from 8 days restricted water stress imposed at 5-weeks. It was clear that the *EPF2OE* showed significantly higher fresh and dry weight as well as the leaf area than the WT. However, the yield in the *EPF2OE* was strongly compromised as the plants partitioned more into biomass production than in yield. No clear link with the drop-in yield and low stomatal density was established. However, it can be suggested that the transpiration rate which is affected by the alteration of the stomatal density affects the water uptake and increase canopy temperature. As temperature increases during the flowering time, such plants undergoes hastened maturity and consequently can leads to seed abortion (Matsui et al., 2000). The canopy temperature in the *EPF2OE* was evidently higher than the WT. Thus, temperatures effects on plants development depend on the genotype.

Generally, the exposure of plants to high or extreme temperatures at the beginning of the reproductive stages has a profound impact on grain or fruits production across all species. This can be supported with the known fact that the effect of increased temperature causes great impact during the reproductive stage than in the vegetative stages (Matsui et al., 2000). This is also associated with increased senescence, which

impairs the ability of the crop to fill in grain (Guilioni et al., 2003, Hays et al., 2007, Hatfield and Prueger, 2015). Dennis et al (unpublished) discovered that the *EPF2OE* in Arabidopsis and wheat does not bear stomata in the anthers at all (whereas in the WT there are). Hence, fertility was significantly reduced in both Arabidopsis and wheat overexpressing *EPF2*. This can, therefore, suggest that the *EPF2OE* has a physiological connection to the anthers opening (dehiscence). Studies in the literature have shown that anther dehiscence is a highly regulated process that is sensitive to abiotic stress, particularly the increased temperature (Wilson et al., 2011). Thus, *EPF2OE* with no stomata in the anthers (Dennis *et al*. unpublished) exhibits a severely delayed dehiscence in Arabidopsis and wheat.

5.6 CONCLUSION

It is clear that rice stomatal arrangement can be genetically manipulated to enhance drought tolerance capacity through the minimization of water loss by transpiration. This will have a beneficial effects for crops in suboptimal environments without loss of carbon gain, but it must be weighed against the evidence that *EPF2* overexpression have a cost that could limit yield in regardless of the water condition. However, more detailed studies are necessary to fully understand how reducing stomatal density with *EPF2* overexpression leads to massive loss of yield. Otherwise, this gene be will very beneficial to horticultural crops, where biomass is needed more than grain such as lettuce, basil, coriander etc.

CHAPTER SIX: REDUCED STOMATAL DENSITY IN ASSOCIATION WITH AN INCREASE IN LYSIGENEOUS AERENCHYMA IN RICE

6.1 BACKGROUND

6.1.1 Aerenchyma formation in cereal crops

Flooding is one of the major problems to crop production world because most crop species are susceptible to flooding stress. The complex situation largely associated with submergence is the different forms of stresses that can hinder growth and survival of crops. Namely, the low light (for gas exchange and photosynthesis), limited gas diffusion (Armstrong and Drew, 2002), the loss of soil nutrients, tissue rupture or mechanical damage, and increased exposure to pest and disease susceptibility (Nishiuchi et al., 2012). The major cause of damage is the insufficient supply of oxygen to the flooded tissues. Water, which preferentially displaces air from soil pore is what affects the flux of air diffusivity into the soil. The diffusivity of oxygen in water is ~10,000 times slower of that in the air, and when the soil pores are filled with water, the flux of oxygen into the soil in that condition is ~320,000 lower than in air (Armstrong and Drew, 2002). In addition, the rapid depletion of oxygen from the soil by microorganisms and fauna triggers the shift of microbial processes from aerobic to anaerobic (Shiono et al., 2011). This lead to the reduction of oxidised compounds and the production of phytotoxic ions such as the Fe^{2+}, $Mn^{2+}$and S^{2-} (Colmer and Flowers, 2008) within hours in some conditions.

Rice (*Oryza sativa* L.), unlike many other cereal crops, is highly tolerant to flooding stress. Rice grows well in a paddy field of either submergence condition (part or all the plants is under water) or waterlogging (in excess water in the soil that limits oxygen diffusion (Nishiuchi et al., 2012)). Therefore, a rice may be a good model for mechanisms that can supply air to the root zone for root respiration under long-term flooding

that will be beneficial for productivity and survival. One of the adaptive strategies for tolerance in submergence (partial or complete) is the longitudinal interconnection of gas spaces, in the cortical cells that enable the internal flow of air from the shoots to the roots (Armstrong and Drew, 2002). Tissue formed from such morphological changes are termed Aerenchyma. Aerenchyma development occurs in plants under flooded or submergence condition to enhance the internal diffusion of atmospheric and photosynthetic oxygen from the aerial part down to the flooded roots for the maintenance of the aerobic root respiration (Armstrong and Drew, 2002, Colmer et al., 2006). Some of the importance of aerenchyma includes; the contribution of oxygen supply from the shoots to roots, reduction of O_2 consuming cells, as a ventilator of gases such as CO_2 and methane from the roots to shoots, and provision of photosynthetic benefits by concentrating CO_2 from root respiration (Constable and Longstreth, 1994).

Two types of aerenchyma have been identified; primary aerenchyma (cortical) and secondary (spongy). The former forms in the roots of cereal crops such as rice, maize (*Zea mays*), barley (*Hordeum vulgare*) and wheat (*Triticum aestivum*). The latter is a spongy tissue filled with air spaces that form in the stem, hypocotyl, tap root, adventitious roots (roots that arise directly from the stem), root nodules of legumes such as soybean (*Glycine max*) (Yamauchi et al., 2013a). The cortical aerenchyma is divided into lysigenous and schizogenous aerenchyma. The schizogenous aerenchyma creates gas spaces in the cortical cells through cell separation and differential cell expansion. In the schizogenous type of aerenchyma, cell death is not involved. Conversely, lysigenous aerenchyma forms air spaces in the cortical cells through cell death and subsequent lysis of some cells among the cereal crops (Yamauchi et al., 2013a). They are formed specifically in the root cortex, where the content of the cells that form the lysigenous aerenchyma gets partially digested, leaving the cell wall surrounding the gas spaces (Evans, 2004). However, not all the cortex gets digested, some cells remain intact to provide shape, nutrient transport (apoplastic and symplastic) and form a radial bridge that gives structural integrity to the roots.

In rice unlike other cereals, lysigenous aerenchyma is constitutively formed under drained and aerated conditions (aerobic), and the formation can be inductively enhanced in response to oxygen deficiency (e.g. waterlogged soil) (Colmer et al., 2006, Shiono et al., 2011, Abiko and Obara, 2014). The aerenchyma formation in rice usually initiates at the apical parts of the roots and gradually expands to the basal part of the roots during root elongation (see Figure 6.1) (Ranathunge et al., 2003). Whereas, in a stagnant condition, rice roots develop lysigenous aerenchyma in all part of the roots. Rice is well adapted to low oxygen either by flood or submergence, which could be the main reason it adapts to flooding more than maize, wheat and barley (Colmer, 2002).

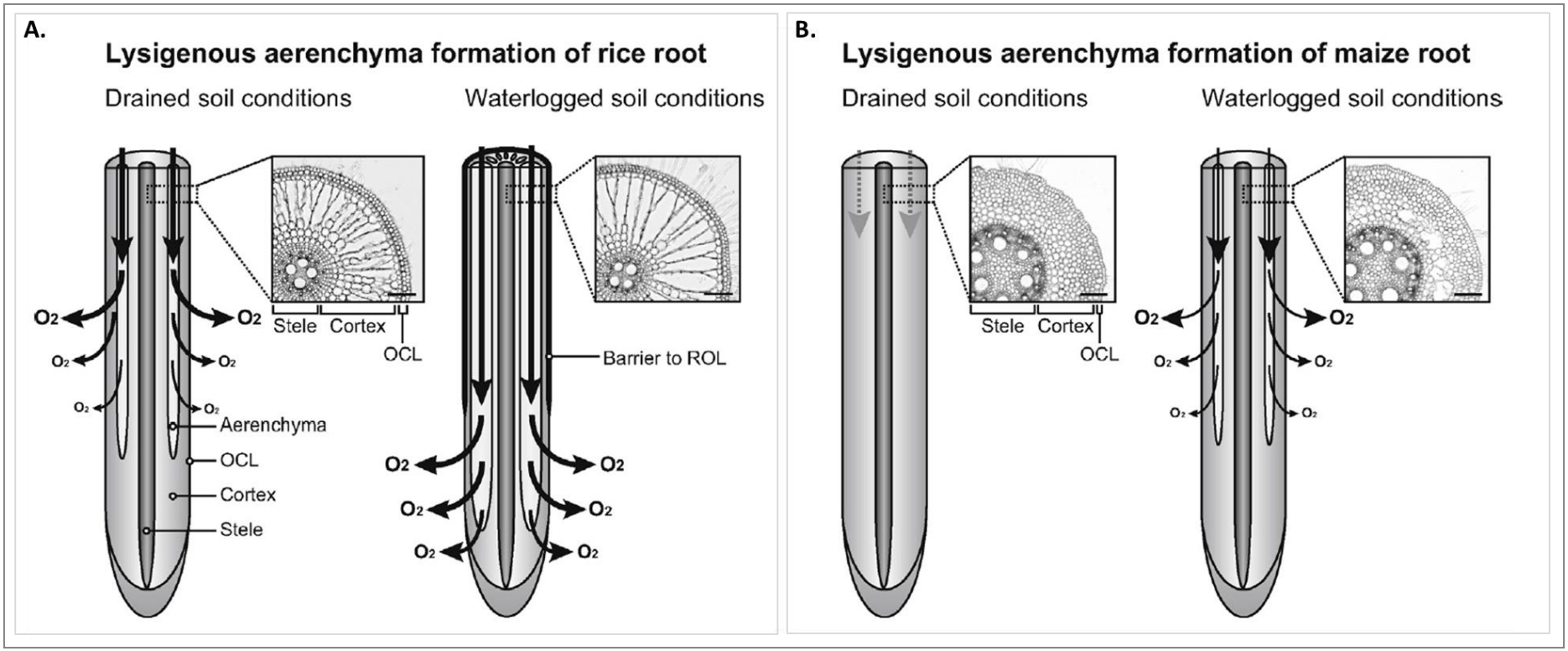

Figure 6.1. Lysigenous aerenchyma formation in cereal crops. **A.** In rice, lysigenous aerenchyma is formed constitutively in waterlogged condition and also inductively in drained condition. **B**. In maize and other dryland cereal crops, no formation of lysigenous aerenchyma under drained condition but is induced by soil waterlogging. Scale bar: 100μm. (Yamauchi et al., 2013a)

6.1.2 Signalling of lysigenous aerenchyma formation

Three different mechanisms have been reported for sensing oxygen deficiency (hypoxia); haemoglobin gene expression linked to increased activity of *Alcohol Dehydrogenase Activity* (ADH), changes in the concentration of cytosolic Ca^{2+} and ethylene.

Ethylene is strongly implicated in the formation of lysigenous aerenchyma in rice and maize. Study has shown that the treatment of ethylene to roots resulted in further increase in the formation of lysigenous aerenchyma in the rice under aerated conditions (Colmer et al., 2006). Where as a treatment with ethylene perception inhibitor (e.g. silver ions) decreases the formation of the aerenchyma under stagnant conditions (WIENGWEERA et al., 1997, Yukiyoshi and Karahara, 2014). Similarly, in maize, He et al. (1996) showed that ethylene biosynthesis is stimulated by enhancing the activity of two enzymes; 1-aminocyclopropane -1- carboxylic acid (ACC) *oxidase* and ACC *synthase* at the beginning of lysigenous aerenchyma formation. However, the treatment of the wheat (Yamauchi et al., 2013b) and maize roots with ethylene biosynthesis inhibitors such as amino ethoxy vinyl glycine, amino-oxyacetic acid, and cobalt chloride blocks the formation of the aerenchyma in anaerobic condition (Jackson et al., 1985). Hence, ethylene is therefore considered as a trigger to aerenchyma formation.

The chemical inhibitors and stimulators of programmed cell death (PCD) and other signalling pathways such as phospholipase C, G- protein, Ca^{2+} dependent signalling pathways, affects the formation of ethylene induced aerenchyma (He et al., 1996). It has been suggested that in hypoxic condition, Ca^{2+} is released from the mitochondria into the cytosol, the elevated gradient of the cytosolic Ca^{+2} concentration triggers subsequent activation of kinases and phosphatases during aerenchyma formation. Other inhibitors of protein phosphatases include okadaic acid which is repressed by K252a and an inhibitor of kinases (He et al., 1996). PCD is strongly regulated by activation of a specific biochemical pathway, not under the genetic control of the cell. Therefore PCD is different from necrosis. Necrosis occurs from an uncontrolled accidental cell death

without the involvement of biochemical or signalling pathways (Drew et al., 2000).

Nutrient deficiency (independent of ethylene synthases) has recently been reported to induce aerenchyma in rice roots. Abiko and Obara (2014) showed the effect of nitrogen deficiency in the formation of inducible lysigenous aerenchyma through spatiotemporal screening. They discovered that N deficiency extensively induced aerenchyma in rice roots to a greater extent than oxygen deficiency induced it.

I can, therefore, hypothesize that the difference in potential biomass production between the transgenic lines and the WT under drought and rehydration are strongly due to their genetic differences in altered stomatal density and may also have a root adaption ability to changes in water availability. Hence, the present study will focus on the evaluation of the lysigenous aerenchyma formation in three different rice lines with different number and sizes of stomata.

6.2 AIMS AND OBJECTIVE

- To establish the growth condition that will enable the evaluation of inducible aerenchyma by differences in stomatal density.

- To clarify the spatiotemporal pattern of the lysigenous aerenchyma formation induced by alteration of stomatal density.

6.3 METHODS

6.3.1 Plant material and growth condition

The rice material used for this study were similar to Chapter 4 but T2 and T3 generations were used. The experiment was performed in hydroponic media in the growth room chamber (details of growth condition in Chapter 2, section 2.2.2). Seeds were germinated in the 9cm diameter petri dish for 5-7 days and were transferred into the 20L

tubs containing hydroponic media (chapter 2) for 10 days to reach about 10cm in height. At that point, plants were either transplanted in aerated or non-aerated hydroponic solution.

6.3.2 Stagnant condition (non-aerated)

Seedling were transferred in a fresh hydroponic media in black 20L tubs (as described in chapter 2, section 2.2.2). More than one seedling inserted into a single hole to facilitate dissolved oxygen accumulation. Parcel tape was used to seal the light-proof plastic support that held the plants to the tub to minimise water loss. Unless the water was low by about 30%, no water was added into the tubs in order to maintain the low dissolved oxygen level.

6.3.3 Aerated condition

Seedlings were transferred into a fresh hydroponic media in black 20L tubs (as described in section 2.2.2). An aquarium air pump used to supply continuous air into the hydroponic media. Using a stone, the pipe was pushed down to pump air from the bottom. One pump per tub was used for this study.

6.3.4 Dissolved oxygen measurement

The dissolved oxygen in the hydroponic media was measured using the YSI portable dissolved oxygen meter (YSI Pro20 Xylem Inc, USA). Using the manufacturer's guide, the DO and the water temperature were monitored before each sample collection.

6.3.5 Aerenchyma measurements

The lysigenous aerenchyma on adventitious roots was evaluated as described in Chapter 2 from 15, 30 and 60-day old roots. With the help of the agarose embedded roots, it was easy to identify the length where root section will be taken with the vibratome. Sections were taken from 2cm, 6cm and 12cm from the root apex. The images obtained from the confocal microscopy were converted to black and white using IMAGEJ software. The Root Scan v2.0 software (Penn State, College of Agricultural Science, USA) was used to estimate the aerenchyma.

6.3.6 Morphological Root analysis

The maximum root length was measured by a ruler from the crown of the root to the tip of the root expressed in cm. Others such as the root total length, average root diameter, root surface area and root volume were all examined using the WinRHIZO (see Chapter 2 for details).

6.3.7 Gas exchange

Steady state photosynthetic measurements (P_{max}) was measured using the infra-red gas analyser (IRGA) Licor 6400XT with similar cuvette condition in Chapter 4.

6.3.8 Statistical analysis

Analysis of variance (ANOVA, one-way and two-way) was carried out using GraphPad Prism 7.01 for Windows (La Jolla, CA, USA) to investigate the effect of the stomatal density and size in the formation of lysigenous aerenchyma. When an effect was detected, a Tukey's HSD (Honest Significant Difference) test was used to determine the level of significance.

6.4 RESULTS

6.4.1 Overexpression of OsEPF2 and OsEPFL9 reduced stomatal density in hydroponic media

As discussed in the previous chapter, the over-expression of the two secretory peptides; *EPIDERMAL PATTERNING FACTOR 2* (EPF2 or E2) and *EPIDERMAL PATTERNING FACTOR- like 9* (*EPFL9* or E9) had resulted in the alteration of the stomatal density in rice. E2 and E9 have antagonising functions between each other, the *OsEPF2OE* that resulted in reduced stomatal density has shown a significant reduction in their transpiration rates (E) and stomatal conductance (g_s) when grown in compost. The *OsEPF2OE* lines have also shown greater drought tolerance and leaf water retention. It is likely that these changes are consequences

of reduced water loss by transpiration which was exerted due to the reduced number of stomata as has been shown in the previous chapters. Here, the effect of reduced stomata on roots morphology was investigated using hydroponic systems to allow manipulation of oxygen access to roots and permits ease of root analysis.

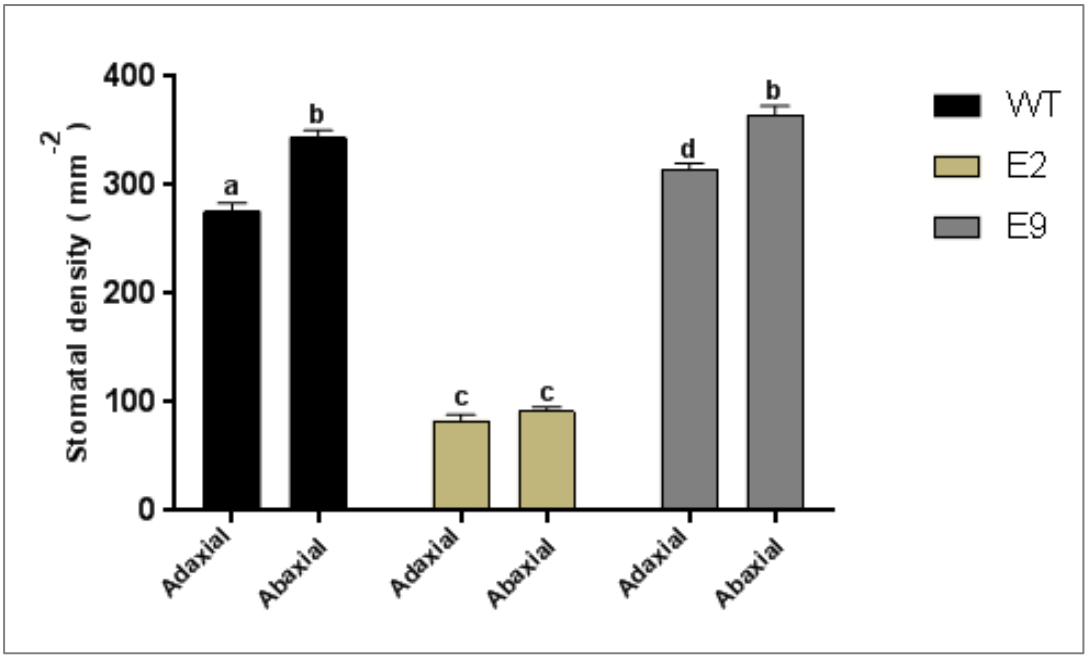

Figure 6.2. Overexpression of EPF genes (*OsEPF2* and *OsEPFL9*) results in alteration of stomatal density. This shows the stomatal densities for the plants used for this chapter has grown using the hydroponics system and measured at leaf 5 stage. Letters of the different group indicate significant differences. Error bars indicate the standard error of the mean (SEM)

In this experiment, however, the effect of reduced stomatal number has revealed a profound effect on the formation of aerenchyma in rice.
Due to the weak nature of the E9 lines in a T3 generation, T2 lines were used. The ANOVA reveals that the stomatal density on the abaxial surfaces were all significantly higher than the adaxial in both the WT and the E9 (Figure 6.2). Notably, the stomatal density of E2 lines were approximately 72% less the number of the wild type (abaxial and adaxial combined) at $P<0.0001$. The stomatal density on the adaxial surface of the E9 was significantly higher than the adaxial surface for WT ($P<0.001$). The stomatal density of E9 was also higher than that of E2

(P<0.0001). The stomatal differences found in this study (hydroponic) was slightly higher than the rate found in soil between E2 and WT.

6.4.2 Reduced stomatal number facilitates lysigenous aerenchyma at the early stage of root organogenesis

To test the role of altered stomatal density on aerenchyma formation, the adventitious roots of the *OsEPF2* and *OsEPFL9* transgenic lines and the WT were evaluated. Plants were grown hydroponically and adventitious roots of 15, 30 and 60 days old plants were examined for aerenchyma formation. Two positions 2cm and 13 cm from the roots tips were used in the spatiotemporal evaluation of the effect of stomatal density (Figure 6.3). Aerenchyma were observed in all the three lines tested and in all the three growth stages, but it was more spread in EPF2OE. However, no statistical differences in the estimated aerenchyma formed were observed between them.

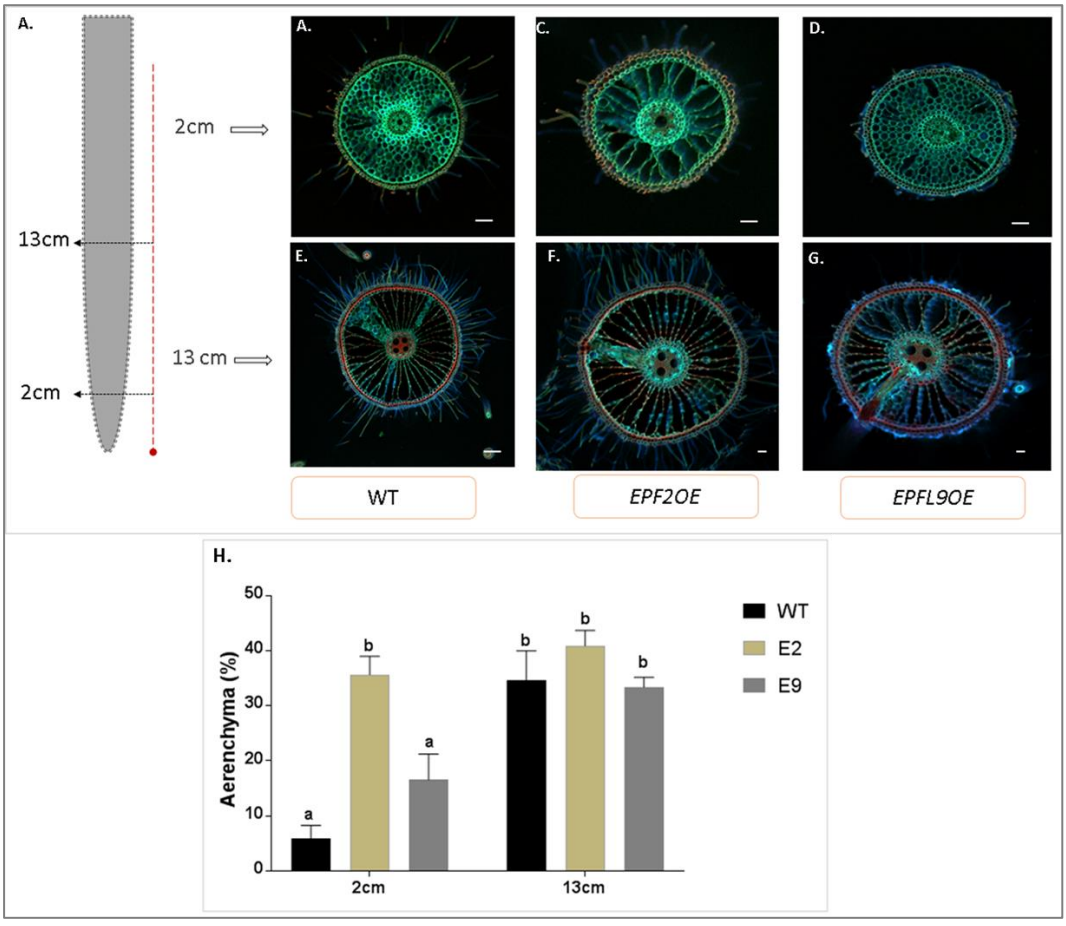

Figure 6.3 Spatiotemporal formation of aerenchyma induced by a constitutive reduction in stomatal density of 30-day old. **A**. Spatial aerenchyma formation compared in two

positions, illustrated along the adventitious roots of plants with three different stomatal densities. **B-D** are the root sections collected at 2cm of WT, E2 and E9 respectively. **E-G**. Root sections at 13cm from the root tip of WT, E2, and E9 respectively. **H.** the estimated aerenchyma formed in the two root regions (2cm and 13cm). Different letters above the columns indicate significant differences between lines and sampling region at P-value of 5% (Tukey's test). All values are represented as the mean ± SEM Mean. Scale bar in the picture indicates 50μm.

At 2cm from the root tip (Figure 6.3 H), 35.7% of the cortical cells in the *EPF2OE* lines were lysigenously broken, forming an aerenchyma. The *EPFL9OE* and the WT in the similar region had 16.5% and 5.8% of aerenchyma formed respectively (expressed as a % of total cortical area). The differences, therefore, reveals that *EPF2OE* had significantly more aerenchyma at the apical region (2cm) by 83.5% ($P<0.0001$) than the mean of the WT, and 53.6% ($P<0.0057$) more aerenchyma than in the *EPFL9OE* lines. This clearly suggests that the lysigenous aerenchyma in E2 lines with reduced stomata, constitutively formed at the early stage of root organogenesis than the WT and E9 (Figure 6.3 H). Interestingly, at 13cm from the root tip, the aerenchyma was fully established in all the three lines, and there were no statistical differences observed between them. Between the two E2 sampling regions there were not differences in the aerenchyma. In contrast to WT and E9, there was a significant ($P<0.0001$) difference in the estimated aerenchyma formed. The differences in the estimated aerenchyma formed by WT between 2cm to 13cm was by 83% at $P<0.0001$ level of significance. While for E9, there were a 50% difference between the two regions (2cm and 13 cm) increased. Thus, in WT and E9, the lysigenous aerenchyma was highly developed in the basal part of the roots between the region of elongation and the region of maturation.

6.4.3 The effect of oxygen level in the root vicinity in determining the formation of lysigenous aerenchyma in rice plants with altered stomatal density

It is believed that some or all of the degenerated cortical cells is caused by necrosis, and necrotic cell death is usually initiated by oxygen starvation (anoxia) and acidification of the cytoplasm which then results

in the lysigenous aerenchyma formation. To fully understand how aeration can influence the formation of aerenchyma, the two different transgenic lines and WT with different stomatal densities were grown under levels of dissolved oxygen. This was to examine if stomatal density can influence the cortical cells degeneration in the two growing conditions (figure 6.4 A). The plants were densely grown hydroponically under two treatments; aerated and non-aerated. In the aerated tubs, the air was constantly supplied into the hydroponic water solution to maintain high dissolved oxygen (DO) level. At week five the adventitious root sections were sampled at 6cm from the root tip.

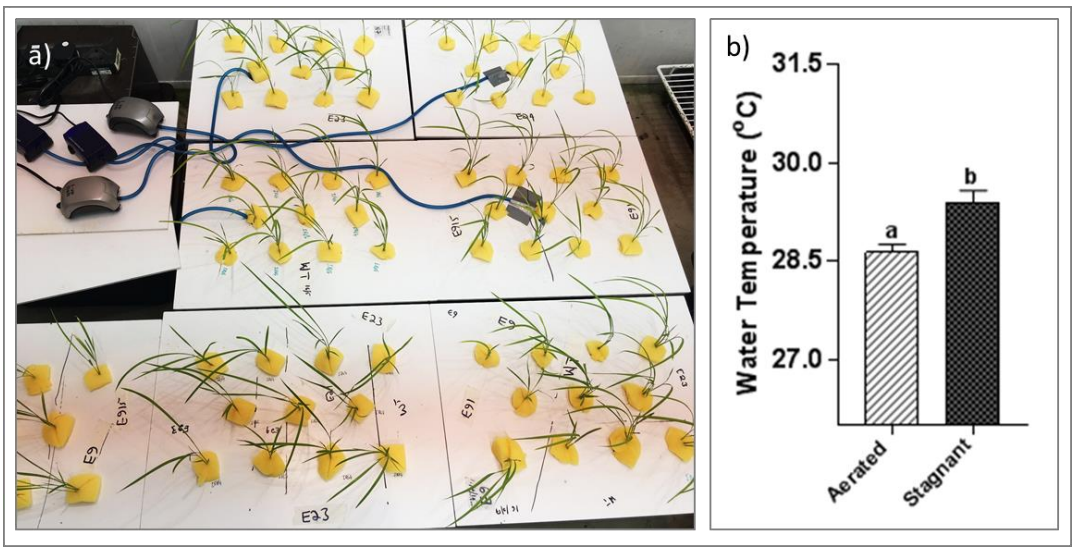

Figure 6.4. Aerated and non-aerated hydroponic system. **A**. Pictorial representation of the two treatments; aerated and non-aerated hydroponic solutions. **B.** The mean of the water temperature between aerated and non-aerated solutions. Different letters above the columns indicate significant differences between treatments. All values are represented as the mean ± SEM Mean.

The temperature of the hydroponic liquid solution maintained a consistent level throughout the tissue sampling period. However, in the aerated hydroponic tubs, the mean temperature (28.7°C±0.1) was significantly lower at P=0.0109 than the mean temperature of the stagnant condition (29.4°C±0.2) by 2.5% (Figure 6.4 B).

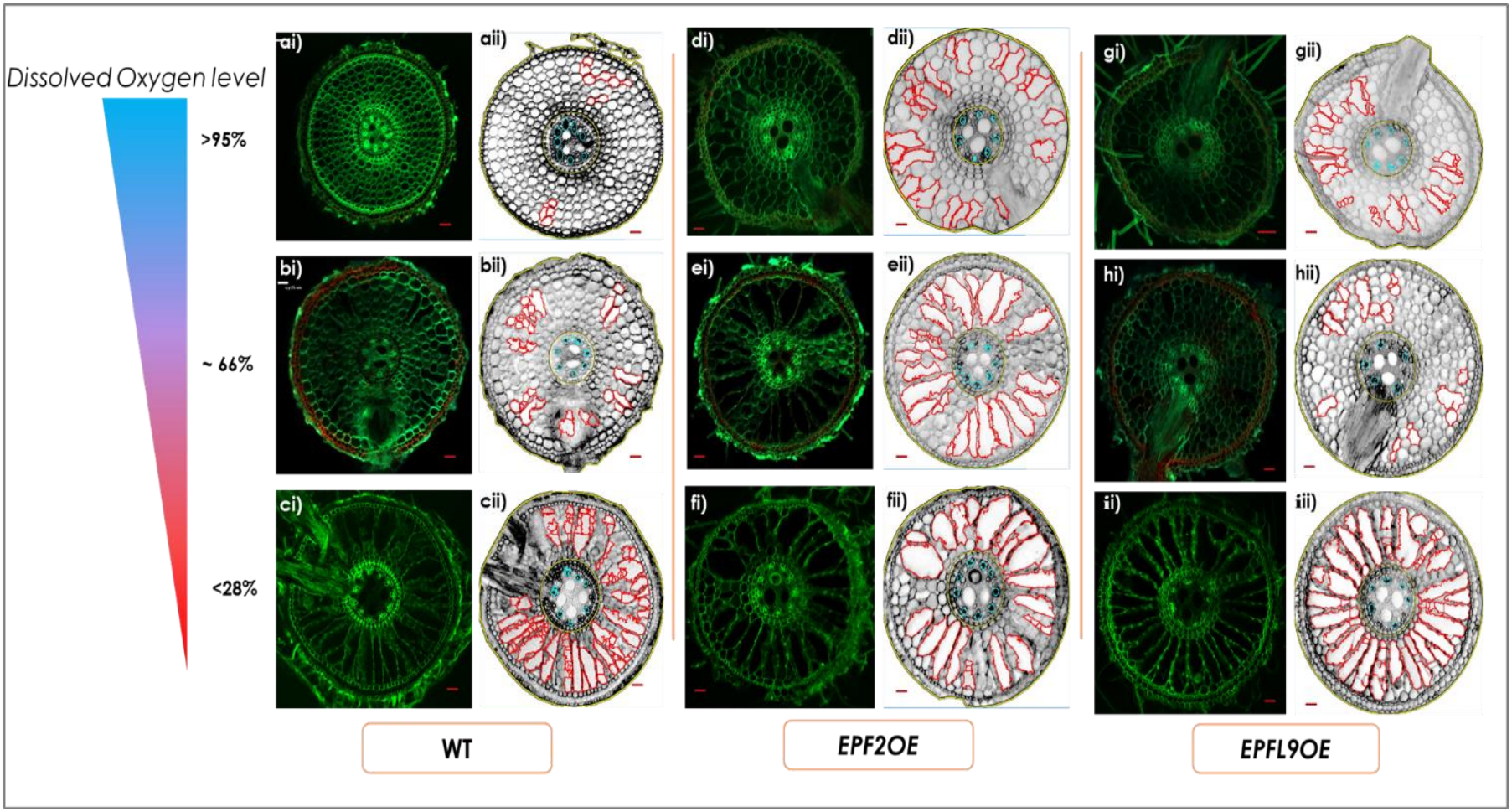

Figure 6.5. The formation of aerenchyma in three lines with different stomatal density grown under three dissolved oxygen levels (95%, 66%, and 28%). **a-c** are the WT cross-section in decreasing D.O levels. **d-f**. E2 cross-sections in decreasing D.O levels. **g-j**. E9 cross-sections in decreasing D.O levels. **i**. confocal image of the cross-section. **ii**. Aerenchyma estimation of '**i**' with the Rootscan2 software. Scale bar represent 50μm.

The mean of the dissolved oxygen level in the aerated water remained at 95(±2) % throughout tissue sampling while the dissolved oxygen level in the stagnant liquid solution dropped gradually with time. The mean of the DO level at week 5 in the stagnant liquid solutions was 65(±5) %. Naturally, the rate of cellular oxygen consumption during respiration, particularly at warm temperatures, exceeds the oxygen supply rates to the respiring cells. As such, increase in temperature may also be implicated in the aerenchyma formation in non-aerated growing condition.

In well-oxygenated condition (aerated), the mean of the estimated aerenchyma formed in the WT roots was 56.7% lower than the aerenchyma formed in E2 roots at P=0.0169 (Figure 6.6). In non-aerated condition (with ~65% DO level reveals) the E2 roots have significantly higher aerenchyma on both WT and E9 (69 and 71% respectively). Surprisingly, E2 roots has no significant differences in the estimated aerenchyma between the two conditions of 95 and 66% DO levels. Furthermore, between the 95 and 66% DO levels, no increase of aerenchyma was observed in all the lines.

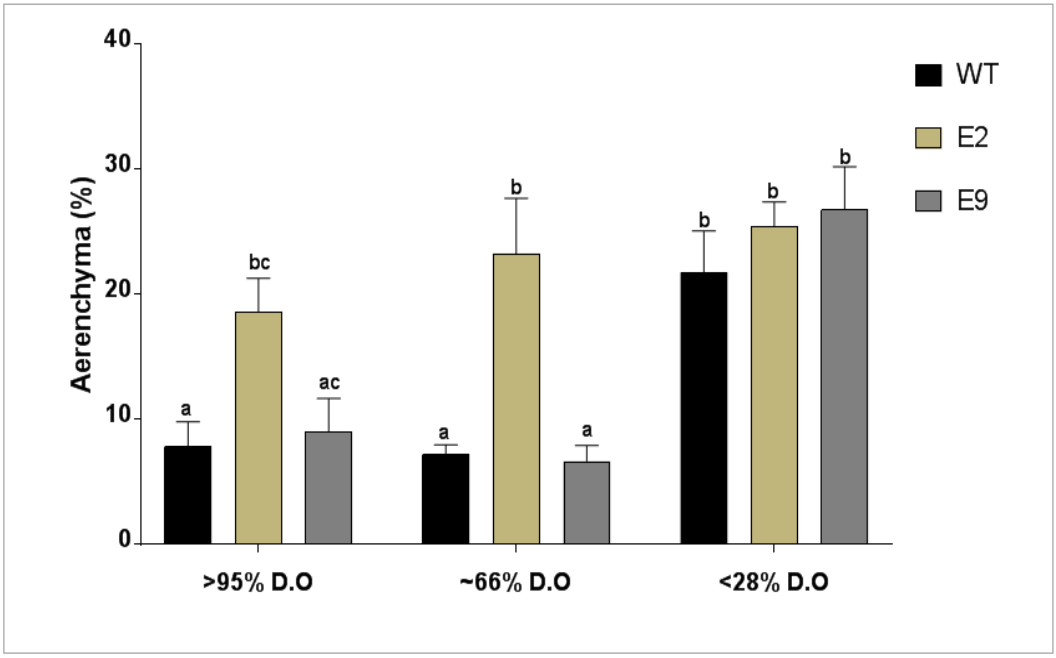

Figure 6.6. The estimated aerenchyma formed by WT, E2 and E9 in three dissolved oxygen level (95%, 66% and 28%). Different letters above the columns indicate significant differences between lines and sampling region at P-value of 5% (Tukey's test). All values are represented as the mean ± SEM Mean.

A week after the root examination at 66 and 95% DO level, water was not added the tubs with 66% D.O, which lead to further depletion of DO level to 28%. The water temperature did not change significantly in both treatments from the previous work. While the aerated tubs remain unchanged due to the constant supply of air. This interestingly, reveals that both the WT and E9 showed improved aerenchyma formation by 66.7% and 75% of the previous week respectively. Thus, the depleted DO (28%) has brought the estimated aerenchyma of WT and E9 level with E2 with no statistical differences. Most importantly, in all the three DO levels, no statistical difference was observed in the mean of aerenchyma formed by E2.

Figure 6.7 shows that the stomatal density have negative relationship to aerenchyma formation in rice.

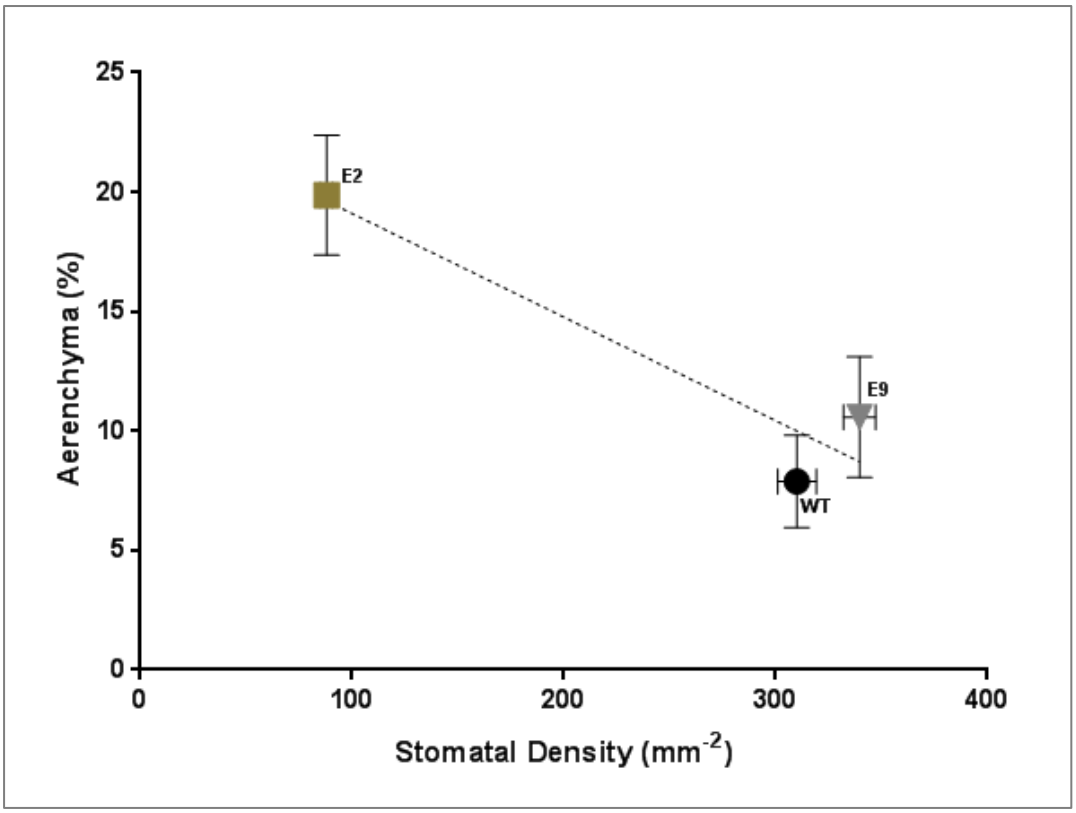

Figure 6.7. The relationship between the mean of aerenchyma and the mean of the stomatal density of the WT, E2, and E9 at 95% DO level. All data points are means ± SEM on both vertical and horizontal points

6.4.4 The interaction of the gas exchange with the aerated and non-aerated growth condition and altered stomatal density

It was reported that aerenchyma in addition to other functions might be beneficial photosynthetically, by concentrating CO_2 from root respiration and supplying it to the aerial part intercellular spaces in young aquatic plants growing in anoxic condition (Colmer et al., 2011).

In the current study the steady state CO_2 assimilation (*A*) at light saturation of the three lines in the stagnant/non-aerated condition reveals some similar responses to previous results chapters. The response to CO_2 assimilation rate does not differ among the genotypes grown in the stagnant hydroponic condition (Table 6.1). However, the mean of E9 in aerated hydroponic condition displayed a significantly higher *A* than WT and E2 by 27% and 31% respectively. Stomatal conductance showed a different response. E2 had a significantly reduced stomatal number (figure 6.2) again consistent with a significantly lowered gs in the stagnant condition by approximately 40% in both WT and E9. Interestingly, gs in the aerated conditions showed a different pattern with no difference between WT and E2 but a higher gs in E9 compared to WT (~1.01mol H_2O $m^{-2}s^{-1}$) with 46% and 55% higher than WT and E2 respectively. A similar response was observed in their transpiration rates where E9 displayed a significantly higher rate than WT and E2. The low transpiration rate in the E2 lines resulted in significantly high leaf temperature and consequently an elevated vapour pressure deficit than the E9.

		TREATMENT					
		Aerated			Stagnant		
S/N	Parameters	WT	*EPF2OE*	*EPFL9OE*	WT	*EPF2OE*	*EPFL9OE*
1.	**Stomatal Conductance (gs)**	0.55±0.03 [a]	0.45±0.06 [a]	1.02±0.05 [b]	0.44±0.02 [a]	0.27±0.05 [b]	0.45±0.03 [a]
2.	**Transpiration (*E*)**	11.6±0.4 [a]	11.1±0.8 [a]	18.6±0.6 [b]	7.6±0.2 [a]	5.5±1.2 [a]	7.9±0.3 [a]
3.	**Photosynthesis (*A*)**	15.5±1.9 [a]	14.6±1.9 [a]	21.3±1.0 [b]	23.9±0.6 [a]	20.4±4.1 [a]	20.6±1.0 [a]
4.	**Leaf Temperature**	26.2±0.3 [a]	27.5±0.5 [a]	24.7±0.2 [b]	29.2±0.1 [a]	30.0±0.1 [b]	29.2±0.2 [a]
5.	***Ci:Ca***	0.85±0.0 [a]	0.83±0.0 [a]	0.88±0.0 [b]	0.75±0.0 [a]	0.66±0.0 [b]	0.78±0.0 [a]
6.	**WUE *intrinsic***	37.2±3.4 [ab]	59.6±5.5 [a]	32.9±0.9 [b]	28.2±2.6 [a]	32.4±2.9 [b]	21.2±0.6 [a]

Table 6.1 Summary of the Leaf gas exchange on lines with different stomatal density. Stomatal conductance (gs), CO_2 assimilation rate (*A*), Leaf temperature (°C), Ci:Ca ratio and intrinsic WUE. Different (same colour) letters indicate significant diffences between genotype of the same treatment. Different letters represent significant differences among the genotypes. Cuvette condition: RH = 28%, leaf temperature 28°C, light saturation (1500µmol^{-2}s^{-2})

6.4.5 The changes in root development induced by the effect of the EPIDERMAL PATTERNING FACTOR (EPF2 and EPFL9) overexpression

Changes in the root development in response to the differences in stomatal densities were examined in the hydroponic solution just before the plants entered their reproductive stage. The roots were harvested from the interface between shoots and roots. The root length measured was approximately 40cm in both WT and E2 (Figure 9 B). Whereas, the E9 line, had significantly shorter roots than either WT or E2. (Figure 6.8 a). Interestingly, however, the root lengths of E2 was similar to WT, and root density was severely reduced compared to both WT and E9 (Figure 6.8 a)

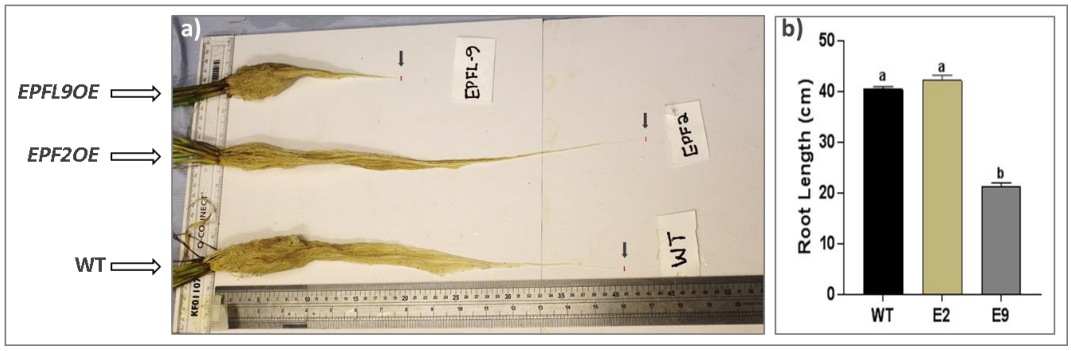

Figure 6.8 Shows a) The image of the harvested roots of the two transgenic lines (*EPF2OE* and *EPFL9OE*) and the WT at 65 days. b) Maximum root length. All values are means ±SE. Different letters represent significant differences among the genotypes. n= 5-7

More detailed root analysis using WinRHIZO revealed that the WT plants have significantly larger computed total root length compared to both E2 and E9 by 39.5% and 32.8% respectively (Figure 6.9 A). No statistical differences were observed in their average root diameter (Figure 6.9 C), root volume (Figure 6.9 D) and root surface area (Figure 6.9 E) between the three lines. WT had significantly higher root length density (RLD) than E2 and WT by 50% and 32.5% respectively (Figure 6.9 B). WT showed higher values for critical features that determine the potential for water and nutrient uptake. This, therefore, gives the WT an edge over the E2 and E9 regarding fresh weight (Figure 6.10 A). Additionally, the higher cortical cells degeneration that resulted in the aerenchyma

gas spaces formation could also contribute to the loss of fresh weight. No differences in dry weight were observed among 3 lines.

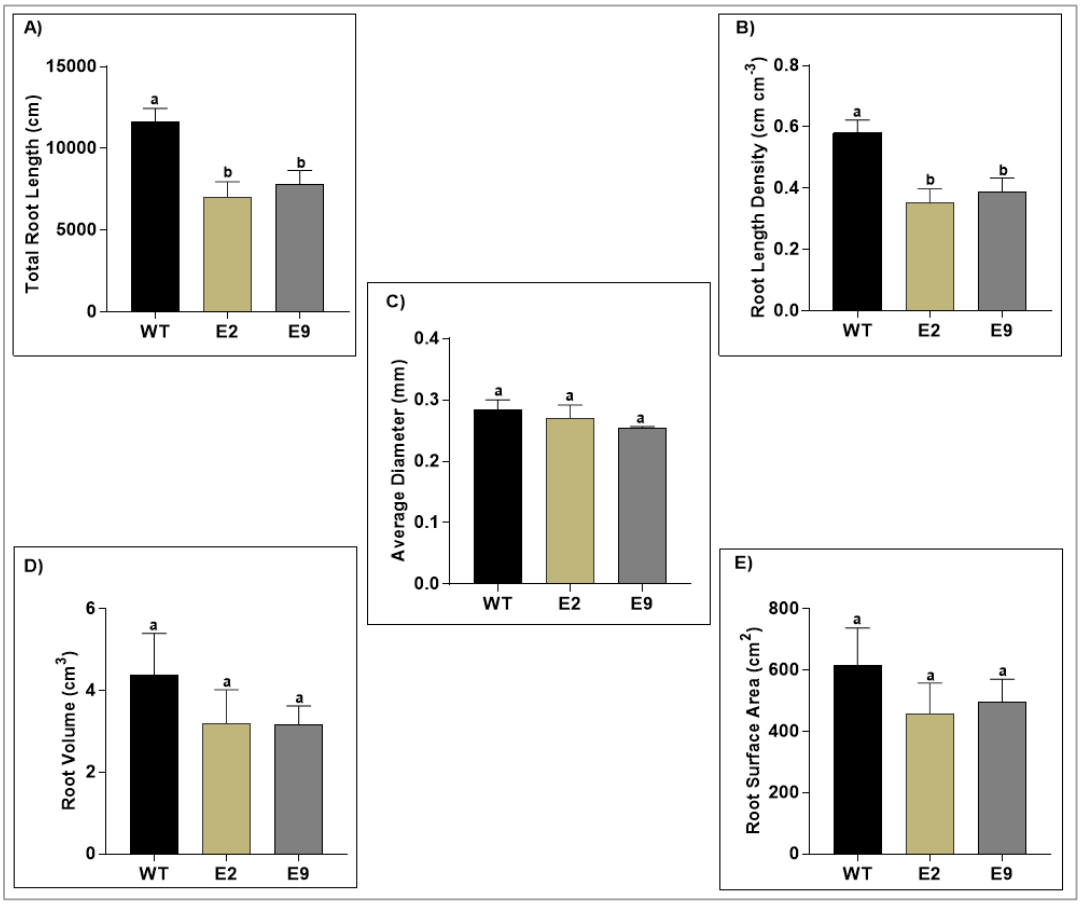

Figure 6.9. The differences in root characteristics between the three lines. **A**. Total root length. B. Root length density (RLD). **C**. Average diameter. **D.** Root volume. E. Root surface area. Different letters above the columns indicate significant differences between lines at P-value of 5% (Tukey's test). All values are represented as the mean ± SEM Mean. N=5 - 7

However, it may be difficult to associate WT with higher potential to water acquisition, because the plants were grown hydroponically. Furthermore, in soil condition (from the previous chapter) E2 with low stomatal density had shown higher drought tolerance by improved water use efficiency, reduced transpiration rate and consequently a retarded soil water loss over the WT.

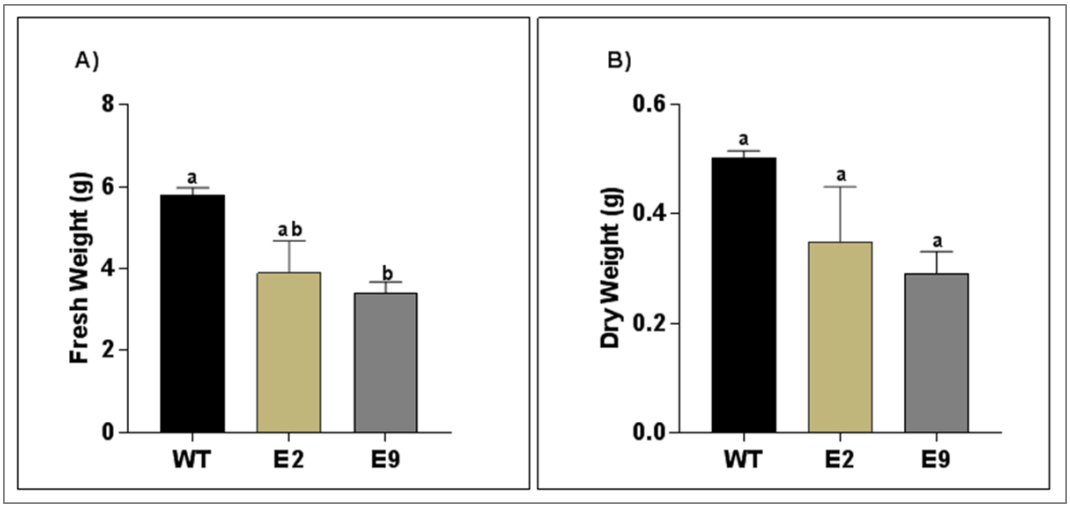

Figure 6.10. Total root biomass of the three lines grown hydroponically. A. Fresh weight. B. Dry weight. Different letters above the columns indicate significant differences between lines at P-value of 5% (Tukey's test). All values are represented as the mean ± SEM Mean. N= 4 - 6

6.5 DISCUSSION

In principle, the general cause of damage in plants growing in the flooded environment is the inadequate supply of oxygen to the flooded tissue. As such, growth and development becomes increasingly affected by plants growing in the waterlogged conditions. Plants such as rice have demonstrated outstanding adaptation mechanisms to the wetland.

This study has shown how reduced stomatal density in leaf either caused or was at least associated with a compensating effect in the root. It was shown in the previous chapter that the *EPF2OE* lines had a significantly reduced stomatal density and they have shown a profound decrease in water loss by transpiration. It has also been shown that the decrease in the number of stomata prepared the plants to withstand a long period of water stress, possibly by the retarded soil water uptake. In other words, with the decrease in the number of stomata, the plant regained better drought tolerance through multiple mechanisms. This has all been shown in *EPF2OE* without causing any negative effect to its photosynthetic apparatus or loss of carbon gain.

The calculated average diameter, root volume and root surface area were all unchanged in E2 comparing to WT (Figure 6.8 B). However, the computed root length density of the WT suggested enhanced root length area and has better potential for water and nutrient acquisition in the hydroponic condition. This may not necessarily be the case in the soil because E2 has shown higher biomass in soil comparing to WT (in chapter 5). Importantly, the E2 revealed higher drought recovery with the significantly higher number of tillers, fresh weight, leaf area and dry weight (Table 5.1).

Under the hydroponic condition, higher aerenchyma formation has been observed with *EPF2OE* lines more than its WT. A spatiotemporal trend in the formation of the inducible aerenchyma resulting from the differences in the stomatal number differs among the genotype, suggests that stomatal density can play a role in the formation of the aerenchyma in rice. At 15, 30, and 60 DAS, the inducible aerenchyma was found in all the positions along the roots except at the apical meristem region where

elongation begins. At the apical region, very few lacunae from aerenchyma formation were observed among the WT and the E9. While E2 formed significantly high aerenchyma at the apical region. This observation was made in oxygen depleted condition.

This study, however, demonstrates the physiological mechanisms of aerenchyma formation caused by oxygen deficiency in rice which forms at the root tip when oxygen is severely depleted (Shiono et al., 2011). The enhance aerenchyma in stagnant condition effectively facilitated atmospheric O_2 diffusion to the roots. It was reported that high O_2 accumulation was shown in plants with their shoots excised and the cut was sealed, which was made to obstruct the air conduit of atmospheric O_2 supply in the plant. This consequently facilitates induced aerenchyma in the roots (Suralta and Yamauchi, 2008). Suralta and Yamauchi (2008) also explained that the constitutive aerenchyma formed in rice under drought condition, could not transport O_2 into the roots when exposed to sudden low O_2 deficiency. This was due to resistance to O_2 diffusion and needed enhancement of aerenchyma for longitudinal gas movement. This may support the hypothesis of this study, that the constitutive lysigenous aerenchyma commonly formed in rice, was not sufficient enough for *EPF2OE* lines due to the low aerial gas outlet (stomata), in both aerated and stagnant condition. Hence, it induced a rapid plastic response for aerenchyma formation to meet the O_2 demand in the submerged tissues. Enhanced root elongation and aerenchyma have been identified with waterlogged roots to facilitate atmospheric O_2 diffusion as similarly known to plant in transient drought conditions (Maricle and Lee, 2007, Suralta and Yamauchi, 2008). Higher root elongation was also observed in the *EPFL2OE* (both at 5-weeks, Figure 6.11 and at 65 days, Figure 6.5) lines.

Figure 6.11. 5-week old rice roots

The data may first, suggest that E2 has a very high sensitivity to low O_2 not only from the root environment but from the internal longitudinal O_2 diffusion which may be construed by the limitation imposed by the number of gas exchange pores. Furthermore, there is a possibility of reduced respiration by root, which is a possible physiological function that results in inducible aerenchyma formation. Also, lysigenous aerenchyma does not only provide the internal pathway for O_2 movement but also reduces the amount O_2 consuming cells. Recently inducible aerenchyma formation has been reported in nutrient deficiency. As such significant reduction in respiration has been reported in phosphorus deficient roots (Lynch and Brown, 2008).

Unlike maize, wheat or barley, aerenchyma formation is constitutive in some rice varieties which do not require hypoxia or ethylene. However, cell death occurs in response to ethylene or hypoxia. This is because rice possessed unique cellular adaptive traits that enable them to minimise O_2 loss to the surrounding soil by conserving more O_2 at the apical meristem for respiration (Nishiuchi et al., 2012). A higher continuous oxygen supply was pumped into the hydroponic solution where E2, E9 and WT and were also compared in non-aerated hydroponic solution. The result demonstrates the sensitivity of the E2 roots to cell lysis, where aerenchyma formation was detected in both the aerated hydroponic solution with near 100% dissolved oxygen level and in condition with ~25% DO level. Interestingly, no significant difference in aerenchyma

formation was observed with E2 in the two different oxygen level conditions. The case was different with WT and E9 which complies with the existing studies on the effect of aeration to aerenchyma formation.

Rapid O_2 consumption outpaces the supply with the increased temperature around the root. Therefore, it can be suggested that the increased temperature has contributed to the high inducible aerenchyma, coupled with the depleted O_2 observed in among all the genotypes in non-aerated condition. However given the very small change in temperature, it is considered unlikely that temperature was a major factor.

As mentioned in the literature, ethylene signalling has been implicated in inducible aerenchyma formation in rice (Colmer et al., 2006). Thus ethylene usually accumulates in low oxygen condition, and it strongly induces more aerenchyma in both the apical and the basal regions (Shiono et al., 2011). As mentioned in the introduction the EPF peptide signals are key regulators of the stem-cell-like divisions used in the stomatal development and are known to influence both the frequency and orientation of asymmetric division of epidermal cells. There is no known link to ethylene signalling associated with the EPF family. Hence, the high frequency of the aerenchyma formation in E2 regardless of the O_2 level may clearly support the claim that the E2 has very high sensitivity to aerenchyma formation solely due to limited diffusion of oxygen access of the root tissue to O_2 and thus aerenchyma formation is exacerbated by the low O_2 condition.

The E2 lines has shown a remarkable water use efficiency and drought-tolerant characteristics (previous chapters). The high sensitivity to aerenchyma formation may also indicate the adaptation potential to submergences by reducing respiration, increasing porosity for O_2 movement, and reducing O_2 consuming cells for optimum utilisation of the limited O_2 supply for root respiration. Thomson et al. (1992) reported a positive correlation between the rate of aerenchyma formation and the tolerance to flooding among wheat and triticale cultivars. Thomson and colleagues suggest that the poor growth performance of wheat and triticale than the rice in flooded soil condition may have a strong relation to their differences in morphology and anatomy of the roots and

particularly to differences in aerenchyma formation and radial oxygen loss profile. Hence, E2 may present better ability in escaping transient conditions of hypoxia in the case of waterlogging.

Further studies are needed to determine the molecular mechanism surrounding the formation of aerenchyma by *EPF2* overexpression.

CHAPTER SEVEN: INVESTIGATION OF THE ROLE OF N-END RULE PATH WAY AS A SENSOR OF DROUGHT IN RICE

7.1 BACKGROUND AND LITERATURE REVIEW

7.1.1 Ethylene Responsive Factor (ERF) Family

Genes in the Ethylene Responsive Factor (ERF) family encodes the transcription and the regulation of many functions associated with plant development and physiological characteristics. They are also largely involved in the environmental responses and tolerance. This large gene family is characterised by the conserved *APATELA 2/ER*F DNA binding domain that consists of about 60 to 70 amino acid residue (Nakano et al., 2006). The AP2 domain was first described in a study on flowering in Arabidopsis as a class of plant regulatory protein (Jofuku et al., 1994). The ERF domain was described with a conserved motif in four DNA binding proteins, ethylene-responsive element proteins 1 – 4 (*EREBPs*) in tobacco. The domain binds to GCC box (AGCCGCC), which is a DNA sequence involved in *Ethylene Responsive*-transcription of the gene (Ohme-Takagi and Shinshi, 1995). The *ERF* family is subdivided further into the ERF and the C-repeat binding factor/dehydration responsive element binding protein (CBF/DREB), a subfamily based on common conserved amino acid sequence within their AP2 domains. The variation in the amino acid sequence of the two sub group members causes the differences in the DNA binding specificities to the transcriptions factors that regulate the responses to a different set of stress signalling genes (Nakano et al., 2006, Lata and Prasad, 2011). Interestingly, a monocot study on *ERF* family suggests that the mechanisms for the translation of ERF function and their downstream target genes are conserved between monocot and dicots (Dey and Corina Vlot, 2015).

A comprehensive study of genome-wide analysis reveals that there are about 139 and 122 *ERF* family gene in rice (*Oryza sativa* L*. japonica*) and *Arabidopsis* (*Arabidopsis thaliana*) which clustered into 15 and 12 subgroups respectively (Nakano et al., 2006). Others include barley

(*Hordeum vulgare*) with 53 and maize (*Zea mays*) with 184 (Zhuang et al., 2011, Du et al., 2014).

7.1.2 The role of N-end rule pathway in plants

The life span of a protein molecule in a cell ranges from few seconds to many days. The selectivity in regulating proteolysis is determined by timely recognition of specific degradation signals on substrates (Varshavsky, 2011). A proteolytic system where N-terminal residues of short-lived proteins are recognised by a proteolysis recognition component of degradation signals is termed the N-end rule pathway.

The N-end rule pathway of ubiquitin-mediated targeted protein degradation relates the half-life and stability of protein substrates to the identity of its N-terminus (N-degron) (Varshavsky, 1996). The N-terminal residue can be stabilising or destabilising, and that determines the fate of the protein. A substrate of N-end rule pathway containing destabilising residues in the N-terminals is targeted for proteasomal degradation by N-recognins (specific E3 ligases) via the 26S proteasome (Gibbs et al., 2011).

Substrate ubiquitination is carried out through the action of three different enzymes; activating enzyme (E1), a conjugating enzyme (E2) and ligase (E3) before the residue degradation is further carried out by the 26S proteasome (Varshavsky, 2011, Tasaki et al., 2012). The E3 ligases specifically identify target proteins with degradation signals at the N-terminus. Therefore, primary destabilising residues are identified by the E3 ligases termed as N- recognins. The E3 ligases (N-degrons) in *Arabidopsis* are *PROTEOLYSIS 1* and *6 (PRT1* and *PRT6*) (Gibbs et al., 2011).

7.1.3 Substrates of N-end rule pathway

Among the sub-group of the ERF family gene, members of the group VII ethylene responsive factors have been studied quite well over the years on the basis of the role they played in plant growth, development and stress responses. The group VII ERF transcription factors are characterised by the motifs of their various conserved sequences at the N-terminal. The encoded protein contained an N-terminal signature

sequence 'MCGGAI(I/L)' (Tournier et al., 2003, Nakano et al., 2006, Jung et al., 2007) (see Figure 7.1 B). The (MCGGAI(I/L) has a feature that is mostly conserved among the flowering plant's species (Gibbs et al., 2011).

Figure 7.1 A. The conserved motifs of amino acid sequences (in the red box) from rice Group VII AP2/ERF domain in the N-terminal region showed the conserved sequence ' MCGGAI(I/L) (Rashid et al., 2012)

7.1.4 Role of N-end rule pathway in hypoxia and submergence

The N-end rule pathway has emerged as a key regulator of diverse cellular responses in eukaryotes (Gibbs et al., 2011). It has been shown that members of the group *VII ERF* TF subfamily are substrates of the N-end rule pathway acting as homeostatic oxygen and nitric oxide sensors in plants (Gibbs et al., 2011, Gibbs et al., 2014b). TFs of the Group VII has shown enhance responses to hypoxia in *Arabidopsis*. Nakano et al. (2006) has shown that the characteristic feature of the Group VII ERF; MCGGAI(I/L) has been used extensively to demonstrate the relationship of the ERFVII TFs to N-end rule pathway in response to the environmental conditions. A sub-family of the ERFVII has shown homology to the famous rice ERFs *SUB1A* and *SNORKEL* by the presences of the initiating motif Met-Cyc at the N-terminus to which most of the group VII members shared along with the –GGAI(I/L). However, *SUB1A* is not a substrate of N-end rule pathway probably due to the absence of an optimally positioned lysine downstream of the N-degron. (Gibbs et al., 2011).

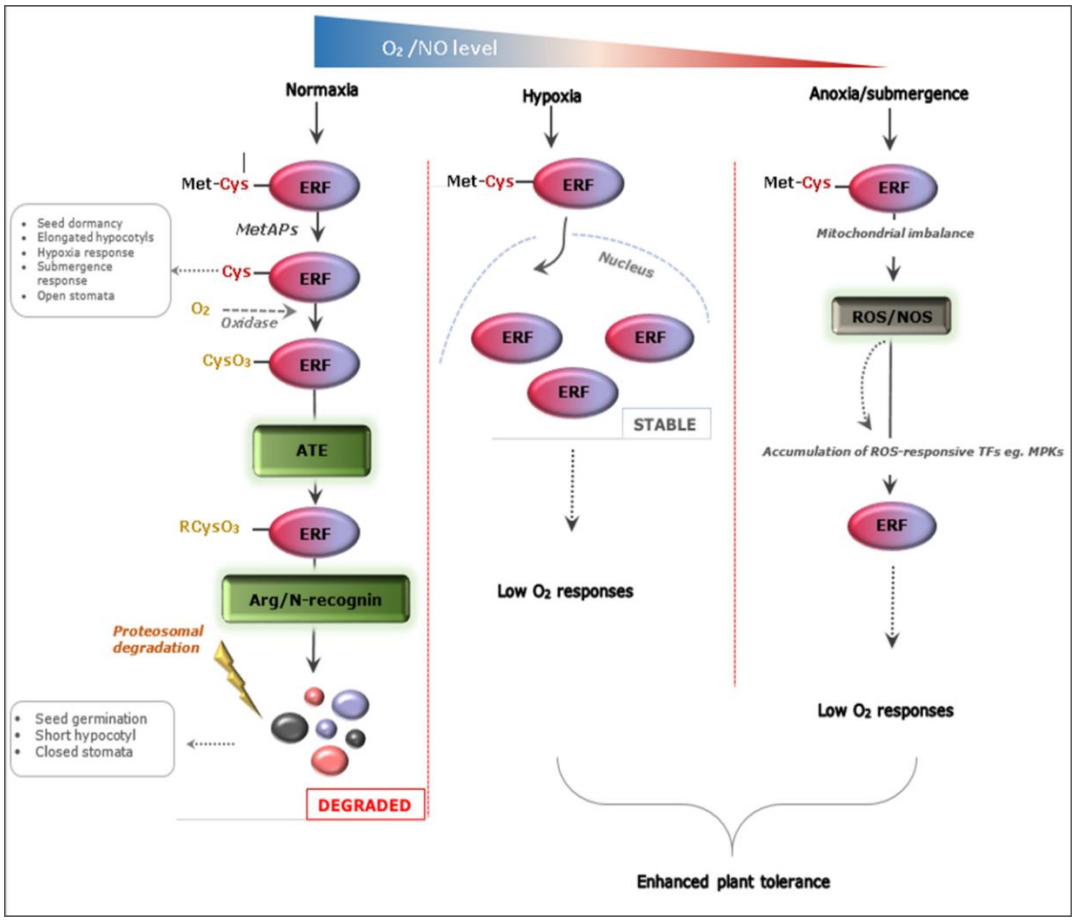

Figure 7.2 Under normoxia and re-oxygenation, ERFVII TFs are targeted to proteasomal degradation through the N-end rule pathway. The Nt-Met is cleaved from the Cys enzymatically by MetAPs which subsequently expose the *Cys to oxidation by a mechanism dependant on O_2 availability and may involve other factors like the cytosolic acidification, alteration of redox state, ROS/NOS and enzymatic activities. Under low O_2/NO (hypoxia), the ERFVII TFs at the N-terminus is stabilised and it migrates to the nucleus to activate the expression of hypoxia signalling genes. Under anoxia, a mitochondrial imbalance causes the production of ROS and promotes the activation of genes related to oxidative stress. Source: image created by author.

The conserved Met-Cys N-degron among group VII ERF TFs under normoxia is targeted for constitutive proteasomal degradation through the process of N-end rule pathway. This branch (Arg/N-end rule pathway) relies on the production of oxidised Cysteine (*Cys) which is made by the constitutive removal of 'Methionine' from 'Cysteine' by an enzyme called Methionine amino peptidase (*MetAPs*) to expose the N-

terminal Cys, a tertiary destabilizing residue (See figure 7.2). In the presence of both O_2 and NO, the Cys residue is oxidised to produce Cys-sulphinic acid (Cys^{O2H}) or Cys-sulphonic acid (Cys^{SO3H}); a secondary destabilising residue. The enzymes that catalyse NO degradation in this pathway is the nitrate reductases. The Cys^{SO3H} ($RCysO_3$) compound triggers the conjugation of the primary destabilising residue Arg by arginyl-tRNA transferases (ATEs) which is bound and ubiquitinated by N-recognin PRT6 (in *Arabidopsis*) before degradation by the 26S Proteasome. The degradation may, therefore, lead to a various set of responses such as seed germination, short hypocotyl, and stomatal closure (Banti et al., 2013, Gibbs et al., 2014a).

Under low gas (hypoxia) and zero gas (anoxia) condition (figure 7.2), the destructive Cys oxidation here lead to the stability of the protein and thus, control various sets of developmental responses. In *Arabidopsis,* for example, the impaired Cys oxidation allows *RAP2.12* stability. Under hypoxia or submergence, *RAP2.12* is released and relocated to the nucleus to activate the expression of anaerobic responsive genes. In the presence of aeration, the non-anchored *RAP2.12* is degraded via N-end rule pathway before relocation to the nucleus (Licausi et al., 2011).

Apart from the known functions of the Arg/N end rule pathway in ABA signalling through Proteolysis 6 (PRT6) (N-recognin in *Arabidopsis*), such as initiation of seed germination, control of leaf and shoot development and leaf senescence as previously mentioned (Gibbs et al., 2011). The over-expression of ERF augments ABA responsiveness, and that MC-ERF substrates mediate cross-talk between submergence and drought tolerance. This indicates that the MC-ERFs are central regulators of plant responses to water availability, and this regulation is integrated through the N-end rule pathway.

7.1.5 Relationship of N-end Rule Pathway with Submergence and Drought in rice

The group VII ERF has not been fully understood based on the evolutionary origin and classification, but the group has specifically been shown in various studies to have a role in the adaptation to flooding, hypoxia, salinity and drought e.t.c in both rice and *Arabidopsis*. Hattori

et al. (2009) has identified two genes; *SNORKEL1* and *SNORKEL2* whose molecular mechanism in the adaptation of deep water responses is to trigger ethylene signalling under water. These two *ERFVII* genes are transcriptionally induced underwater upon ethylene accumulation causing a remarkable internode elongation through gibberellin. Similarly, another *ERFVII* gene, *SUBMERGENCE 1 (SUB1A)* was found to confer submergence escape in rice through quiescence when submergence occurs, and enable the plant to return to its normal growth at re-oxygenation (Xu et al., 2006). The mechanism through which *SUB1A* gene functions is that it limits growth and induces anaerobic fermentation to reduce energy accumulation during the submergence. The gene is expressed at the base of the leaf sheath and collar regions which suppress leaf elongation under submergence (Fukao et al., 2006, Singh et al., 2010). Interestingly, there is a crosstalk between submergence and drought tolerance in rice, where the *SUB1A* gene has been shown to confer enhanced survival to rapid dehydration that follows re-oxygenation and water deficit. *SUB1A* prevent leaf water loss by increasing ABA responsiveness and lipid peroxidation that facilitates the expression of various drought associated genes such as *DEHYDRATION RESPONSE ELEMENT-BINDING PROTEIN 1 (DREB1)* and *LATE EMBRYOGENESIS ABUNDANT (LEA).* It also reduces the spread of reactive oxygen species (ROS) by neutralising the oxidative damage associated with dehydration using superoxide dismutases and catalases enzymes (Fukao et al., 2011).

In *Arabidopsis*, there hasn't been any clear quiescence or internode elongation under submergence, but there has been a fermentation process where O_2 availability is reduced for ATP production (Lee et al., 2011). During hypoxia condition, the transcript level of two members of the *ERFVII* namely, *HYPOXIA RESPONSIVE1* and 2 (*HRE1 and HRE2*) was increased. In the post-transcriptional regulation of the *ERF TFs*, the stability of *ERF* protein is regulated by many pathways that involve the 26S proteasome (Licausi et al., 2013).

Studies on ERFVII have revealed cysteine as a physiological residue that regulates responses to hypoxia and submergence in Arabidopsis and

Barley (Gibbs et al., 2014b, Mendiondo et al., 2015) and may serve as a breakthrough to understanding plants responses to stress such as the role of *SUB1* gene in rice. It will also be interesting to know whether specific structural or environmental changes can allow some proteins to escape degradation by the N-end rule pathway.

7.2 AIMS AND OBJECTIVES

- To develop a rapid and efficient rice transformation protocol
- To create transgenic lines (sensor lines) bearing the motif of the group VII ERF signature fused to GUS protein
- To show the activity of GUS in response to abiotic stress as a way of understanding whether the principle of N-end rule pathway applies to drought stress

7.3 METHOD

7.3.1 Plant material and growth condition

The rice seeds used for this study were created for the study through *Agrobacterium* mediated rice transformation in two different background, Nipponbare and Kaybonnet. All plants were grown in the glasshouse and growth room (details of the condition in Chapter 2, in section 2.2.2).

7.3.2 Hypoxia condition

The fully expanded rice leaf was excised from the ligule region of mature rice (60 DAS), and young leaf (21 DAS) which were covered and hydrated by dipping the ligule in water. The leaf tissue was then placed in 12cm x 12cm culture plates containing a small amount of water to keep the leaf hydrated. Two identical leaf preparations was made (with replicates) for treatment and control. The leaves tissues were mounted in the chamber, closed and followed by the released of the hypoxic gas (containing 1% of oxygen mixture) into the chamber. The controls were

placed in the similar chamber but with no gas or vacuum. After 6 hours leaf tissues were immediately transferred into X-gluc solution for GUS activity (see Chapter 2, section 2.9).

7.3.3 Submergence condition

A 3 leaf old rice plants in 250mL pots (soil compost) and 5- day old germinating seedlings were submerged in a 1L Casablanca jar filled with water. The bottled remained half closed but covered in the dark for 3 days. After 3 days in submergence, a leaf tissue (ligule) for the 3 leaf old, and the entire coleoptile and the endosperm of the 5 day old seedlings were immediately transferred into X-gluc solution for GUS activity.

7.3.4 Drought

Irrigation was restricted on the 2-3 week old rice seedlings growing in a 250mL pot containing soil compost or combination of Pilate and compost. The soil water content was monitored using the theta probe (Delta T-Cambridge, UK). At 70% soil water loss, the RWC of the leaf was taken to determine the leaf water content.

7.4 RESULTS

7.4.1 Creation of N-end rule pathway sensor lines

To investigate the role of N-end rule pathway (NERP) in drought stress, a reporter based approach was used. It has been previously shown that GUS reporter gene could be engineered to make it a substrate of NERP by adding the ERFVII signature motif MCGGAIL at the N-terminal. When the 7 amino acid sequences were fused to GUS reporter and gene driven under the control of the Ubiquitin promoter. Mutated constructs with cysteine were replaced with alanine 'MAGGAIL' was also kindly provided as a control construct (Mendiondo et al., 2015)(see Figure 7.3). These constructs were provided by Dr Guillermina Mendiondo (University of Nottingham)

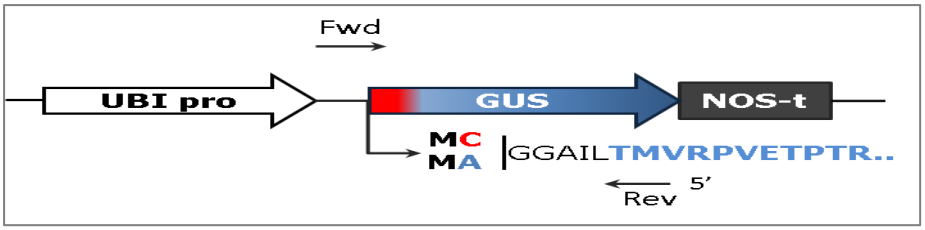

Figure 7.3 Schematic representation of the gene constructs transformed into rice via *Agrobacterium* transformation. The construct consists of group VII ERF motif with GUS promoter.

These constructs were introduced into rice using *Agrobacterium*-mediated transformation. Two different rice accessions were used; Kaybonnet and Nipponbare

7.4.2 Transformation of Kaybonnet and Nipponbare

An efficient rice transformation system was established in the laboratory using mature rice embryos. Typically, the protocol took 10 to 11 weeks, from the callus induction to the transfer of seedlings to the soil.

7.4.3 Callus induction

It started with the formation of callus from matured *O. sativa*. Hv *japonica* (Kaybonnet and Nipponbare) seeds. The seeds were surface sterilised and introduced on induction medium containing nutrients, growth regulating hormones (2,4-D) and proline as protection against stress (Toki et al., 2006). The seeds were incubated under light at 32°C for 10 days. Just after 3 days of induction, shoots began to grow in response to the rich content of the medium (N6D). At day 7-8, the shoots and roots that began to grow were aseptically removed, and the callus was transferred to a fresh induction medium (N6D). 2 days after the sub-culture, a genotype differences were observed between the calli of Nipponabare and Kaybonnet. The health of the calli from both the genotypes was remarkable. The Kaybonnet calli break into small friable pieces (see Figure 7.4A) at around day 12 in the callus induction medium. This, therefore, made the calli very suitable for the next step; *Agrobacterium* infection. The average number of calli obtained from Kaybonnet at day 12 was 16 per seed.

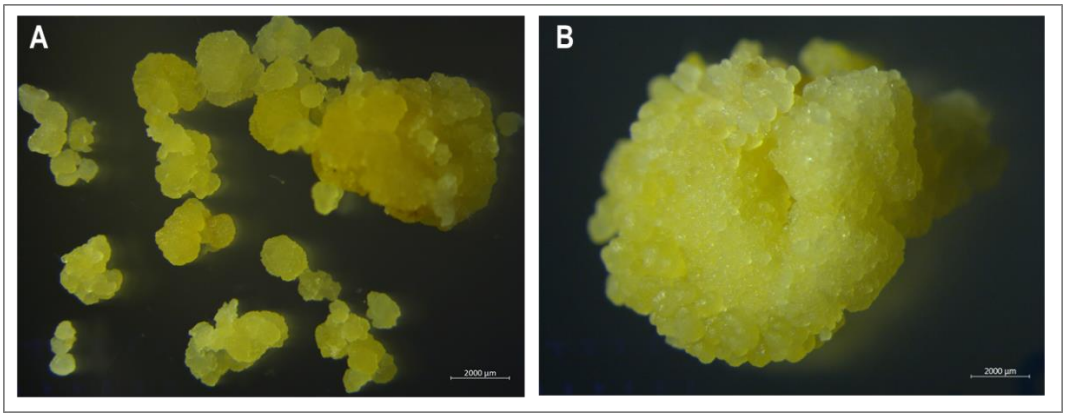

Figure 7.4 Calli produced by Kaybonnet and Nipponbare **A**. Finely dividing callus tissues of Kaybonnet rice genotype at 12 days on callus induction medium **B**. The large single expanded callus tissue of Nipponbare genotype at 12 days on callus induction medium. The scale bar was 2000µm

Hence this increased the chances of generating a higher number of independent lines from a fewer Kaybonnet seeds. The Nipponbare callus, therefore, doesn't break into pieces within 12 days as Kaybonnet. Instead, it expands to a single healthy callus which was easy to excise into 4 – 6 pieces (see Figure 7.4B) before the *Agrobacterium* infection (co-culture).

7.4.4 Co-culture: Agrobacterium infection

The next step after the callus induction was the callus *Agrobacterium* infection (co-culture). The co-cultivation with strain *Ag*L1 on the rice genotypes; Nipponbare and Kaybonnet were carried out with both high and low *Agrobacterium* densities (~1.0 and ≤~0.3 OD_{600}). As mentioned, the incubation period at this stage was shortened to ~48hrs to ensure minimum to less bacterial overgrowth. This was contrary to most protocols, where 3 days was reported as standard. However, the two cell densities were both used separately. After the two days of incubation at 25°C, the callus infected with higher *Agrobacterium* density had an occasional bacterial overgrowth on top and side of the calli despite the presence of the sterile filter paper laid between the calli and the medium. This prompted the post infection callus washing. The callus was washed with SDW and 200mg/L of Timentin. Whereas, the callus infected with

lower *Agrobacterium* density showed very little to no bacterial over growth. As such, they were transferred into the selection medium without washing. Within the first seven (7) days in the selection medium, plates containing calli infected with higher cell densities were sub-cultured 2-3 times due to bacterial over growth. Whereas, the plates containing the calli infected with low cell densities were only sub-cultured once. The sub-culturing however, was to minimize the genotoxicity of synthetic auxin (2, 4-D) (Filkowski et al., 2003) and high temperature (32^{o}C) employed in this protocol. Typically, sub-culturing was done at least 3-4 times during the selection period for efficient transformation rate.

Genotype	Low Cell density (~0.3 OD_{600})	High Cell density (~1.0 OD_{600})
Nipponbare Expt. 1 &2	29/42	6/27
Kaybonnet Expt. 1 & 2	37/54	7/33

Table 7.1. The effect of *Agrobacterium* cell density on the transformation efficiency of Nipponbare and Kaybonnet

However, the regeneration efficiency of those infected with high *Agrobacterium* density in table 1, showed lower percentage in both the genotypes; Nipponbare (22.2%) and Kaybonnet (21.2%) when compared to those infected with the low *Agrobacterium* density in Nipponbare (69%) and kaybonnet (68.5%). This may have a direct bearing on the over growth lead by the high *Agrobacterium* density used. Thus, over growth is thought to cause a decrease in a transformation efficiency. Therefore, from the result in table 1, it may suggest that the regeneration and transformation efficiency of rice callus significantly improved when callus washing was avoided. This can only be achieved when low Agrobacterium cell density was used for the infection, and the co-culture duration is shortened to only 2 days instead of the 3 days. There are some cases of Hygromycin-resistant callus infected with low

Agrobacterium density but failed to regenerate into shoots but remained in the same size with green undeveloped spots the never regenerate. However, for rapid and efficient rice transformation method with the *Ag*L1 strain on japonica, the use of low *Agrobacterium* density (≤~0.3 OD_{600}) had shown more reliability with a greater chance of generating positive transgenic rice lines than any other method used previously.

7.4.4 Regeneration

Regeneration was made as described by Toki et al. (2006) with some modifications

On the day 2 of the infected calli in the co-culture medium (at 25°C), the calli were transferred into a selection medium containing selection antibiotic (Hygromycin) and bacteriocide (Timentin). The Timentin served to kill the excess *Agrobacterium* remains around the calli. Different concentrations of hygromycin and Timentin were examined. For Hygromycin, 50mg/L, 30mg/L, and 0mg/L were used and for Timentin 160mg/L and 96mg/L (See table 2). The calli with 0mg/L hygromycin concentration were grown in 160mg/L Timentin concentration. Plants are usually more resistant to infection by *Agrobacterium* at a temperature above 32°C (Toki et al., 2006). Therefore, 32°C was used throughout selection to help in the stimulation of bacterial removal from the rice cells after co-culture. Thus, during the infection, calli are under very high stress of both temperature and antibiotics. Proline application, therefore, protects against the stress.

Timentin	Hygromycin			Regeneration Efficiency (%)		
	50mg/L	25mg/L	0mg/L			
160mg/L	6/12	9/13	9/10	50	69	90
98mg/L	8/13	11/14	10/11	62	79	91

Table 7.2 Different combination of the Hygromycin and Timentin concentrations used and the number of transgenic plants lines regenerated each combination. The regeneration efficiency was obtained from the ratio of Hygromycin concentration: Timentin concentration × 100.

It was observed that the embryogenic calli with no antibiotic regenerated much faster with about 90% regeneration efficiency. Green tissue in this stage began to proliferate after 13 days in the regeneration medium. However, not all the regenerated shoots were positive for the transgene. Also, there was a high rate of clonal where many tillers emerged from a single embryogenic callus. At 25mg/L of Hygromycin and 160mg/L Timentin, 69.2% regeneration efficiency was achieved, where as 78.6% efficiency was achieved from 160mg/L of Hygromycin and 98mg/L Timentin. Whereas, the standard concentration of 50mg/L of Hygromycin and 160mg/L of Timentin has showed delayed green shoot proliferation and regeneration efficiency of only 50%. Although with reduced Timentin (98mg/L) 61.5% was achieved.

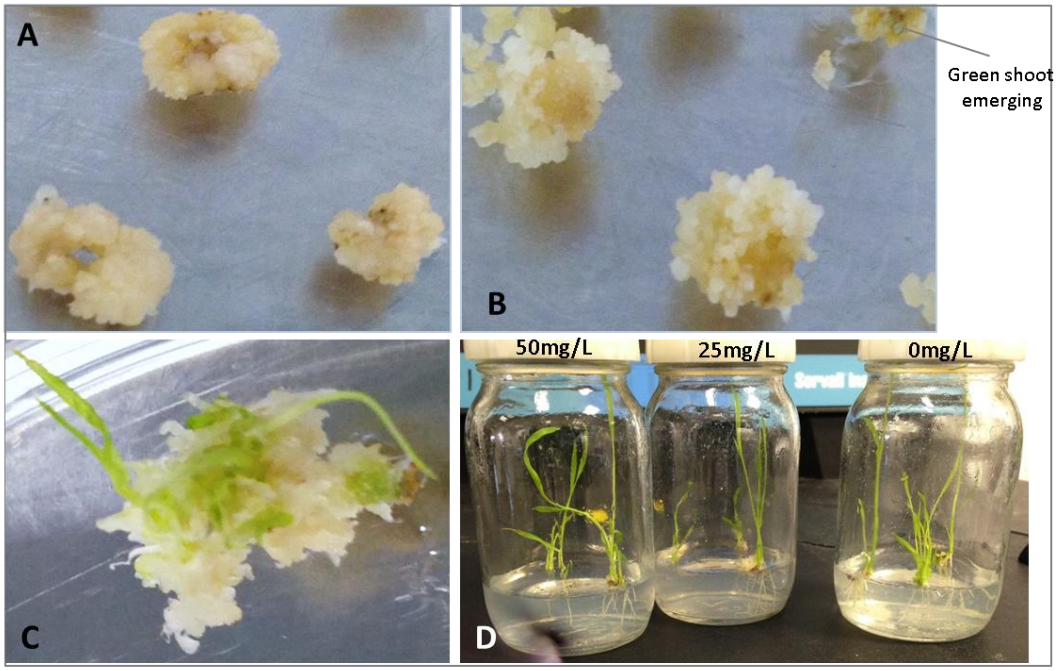

Figure 7.5 A. Embryogenic callus at 20 days in the regeneration medium containing 50mg/L Hygromycin and 160mg//L Timentin. A sign of a struggle in the regenerating green shoots. **B.** Embryogenic callus at 20 days on the regeneration medium containing 30mg/L hygromycin and 96mg/L Timentin. **C**. No antibiotic embryogenic callus is regenerating green tissues after 23 days on the regeneration medium. **D**. Root development among three young shoots regenerated under three different Hygromycin concentrations and 160mg/L Timentin.

At low Hygromycin and Timentin concentrations (25mg/L and 98mg/L), green shoot proliferation began between 18 to 20 days, and the effect of Timentin concentration in all Hygromycin concentrations does not appear to have any effect on the timing of the green shoot proliferation. However, growth was slower in higher concentration compared to the growth rate in low concentrations (see figure 7.5). All the regenerated shoots tested for histochemical GUS expression were positive

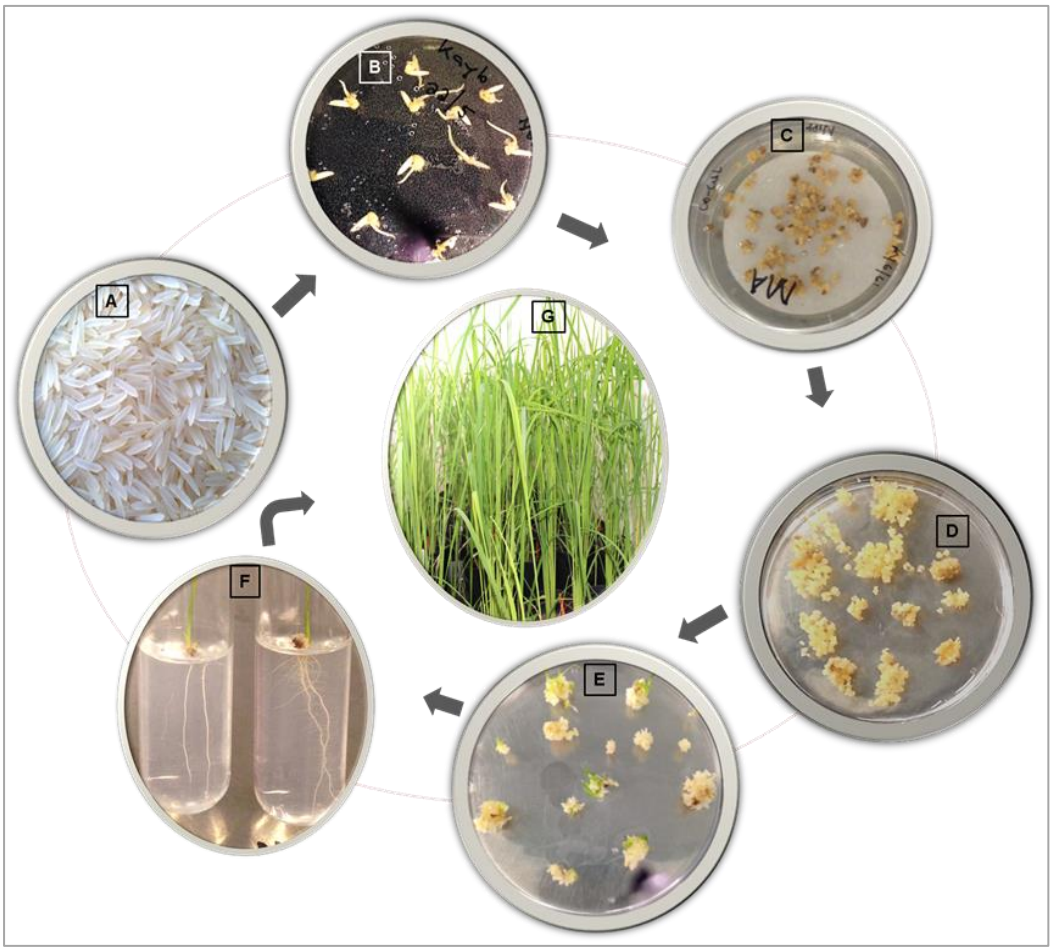

Figure 7.6. Stages of the rapid rice transformation method with AgL1 strain. **A.** Dehusked rice kernels which were surfaced sterilized before transfer to callus induction. **B.** rice seeds incubated in N6D callus induction medium for 10-13 days **C.** callus infected with Agrobacterium strain AgL1 containing the gene of interest growing in the co-culture medium for 2 days. **D.** Hygromycin resistant micro calli emerging from the *Agrobacterium* infected callus in the selection. This usually takes 14-18 days. **E.** Regeneration of green shoots from the Hygromycin resistant embryogenic calluses from the regeneration medium. This stage takes about 20-24 days. **F.** Roots emerged from the regenerated shoots in root medium. This stage usually takes 10 to 14 days for roots

to be ready for hardening. **G.** The hardening: transfer of the regenerated plants from into soil.

7.4.5 Selection and Validation of Transgenic plants

To confirm the transformation efficiency, the below formula was used:

$$Transformation\ Efficiency(\%) = \frac{Number\ of\ GUS/PCR\ positive\ plants}{Number\ of\ calli\ inoculated\ with\ Agrobacterium} \times 100$$

Equation 7.1. Transformation efficiency (Sahoo et al., 2011)

7.4.6 Molecular evaluation of the transgenic status of the regenerated plants

The transgenic status of the regenerated plants was tested using PCR (for MCGGAIL::GUS) and expression of GUS-assay (for MAGGAIL::GUS). It was found that 35 out of 49 (35/49) MAGGAIL::GUS tested lines were GUS positive and all the MCGGAIL::GUS lines tested by PCR were positive using the gene specific (forward and reverse) primers in Table 7.3.

Primer	Sequence (5′ – 3′)	Size	GC%	Tm °C
MC forward	ATGTGTGGTGGAGCGATCCTCATGGTACGTCCTGTA	~600bp	53	69
MA forward	ATGGCTGGTGGAGCGATCCTCATGGTACGTCCTGTA	~600bp	56	70
GUS reverse	TAGAGCATTACGCTGCGATG			
Ubi1_FWD	ATGATGGCATATGCAGCAGC	~400bp	50	57

Table 7.3. Primers used for the PCR genotyping

Few lines were selected from each gene for reverse transcription PCR (Figure 7.7 a). The RNA expression of the two genes was revealed in 9 of 11 MAGGAIL:: GUS construct and 7 of 8 MCGGAIL:: GUS construct

tested. See the reverse transcription analysis for two tested independent lines from each gene (Figure 7.7b).

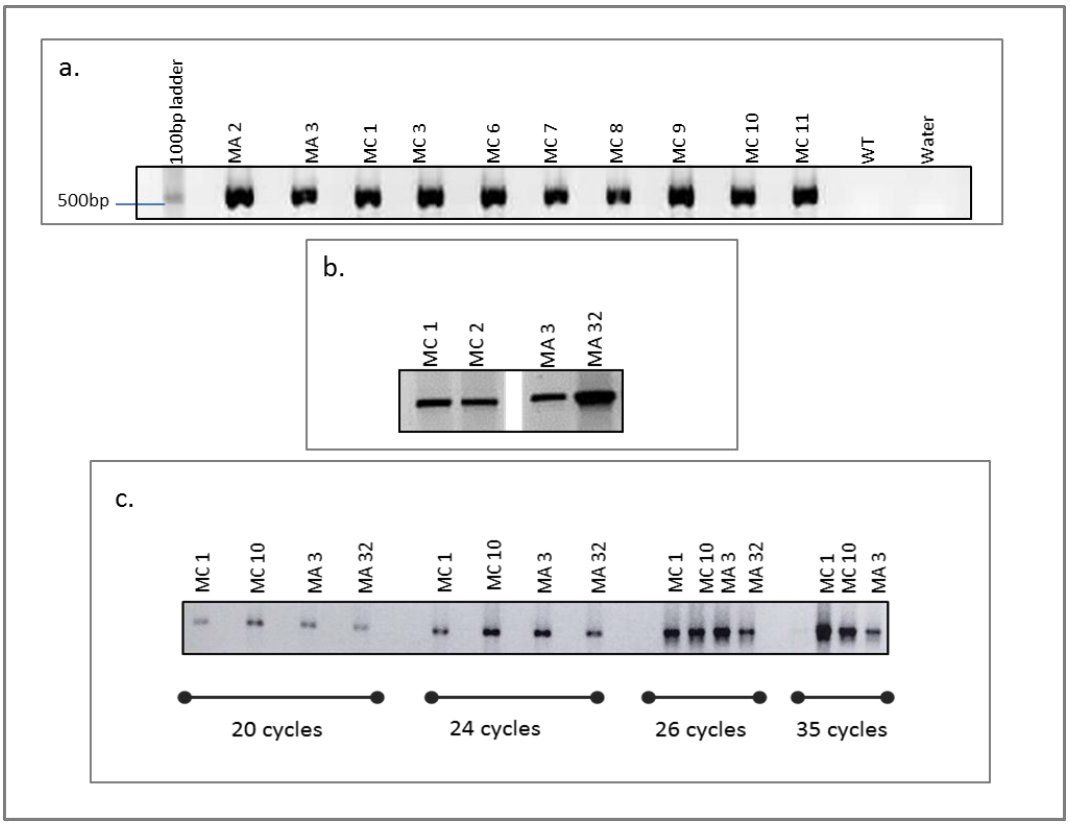

Figure 7.7 A. PCR genotyping of two MAGGAIL:: GUS and eight MCGGAIL:: GUS independent transgenic lines regenerated. Using the gene specific primers, all the samples tested shown the presence of the transgene **B.** GUS RNA expression in the transgenic rice assayed by Reverse transcription PCR of two MC/MAGGAIL:: GUS each. **C**. Semi-quantitative PCR conducted to determine the level of expression of two MC and tow MAGGAIL:: GUS in four PCR cycles.

To get some idea of the level of expression of the two genes, the cDNA synthesised for the reverse transcription-PCR which showed the gene expression at RNA level (Figure 7.7 b) was used for semi-quantitative PCR (semi-qPCR). The semi-qPCR was set and ran for 4 cycles; 20, 24, 26 and 35 (Figure 7.7 c). Expression, however, was comparable in each cycle tested.

Expt. number	Cultivar	Construct/ gene	Cocultivated (A)	Antibiotic resistant calli	Regenerated plantlets	Positive plants (B)	Transformation Efficiency (%) (B/A)	GUS positive	PCR positive	Rev-Trans PCR	Semi-qPCR
1	Kaybonnet (japonica)	MCGGAIL-GUS	~140	51	38	27	19.3	0/27	27/27	7/9	1/1
2	Kaybonnet (japonica)	MAGGAIL-GUS	~140	56	49	32	22.9	32/49	5/5	5/6	1/1
3	Nipponbare (japonica)	MCGGAIL-GUS	70	19	3	3	4.3	0/3	3/3	1/2	1/1
4	Nipponbare (japonica)	MAGGAIL-GUS	65	22	3	3	4.6	3/3	3/3	2/2	1/1

Table 7.4 Summary of the results obtained from the rice transformation so far from Kaybonnet and Nipponbare cultivar as well as MAGGAIL::GUS and MCGGAIL::GUS genes transformed.

7.4.7 The GUS- protein stability reveals the activity of the ERFVII

The motif of the ERFVII signature is conserved in most flowering plants (Gibbs et al., 2011, Rashid et al., 2012). They initiates with a motif Met-Cys followed by the long sequence –GGAI(I/L). In this study, the barley ERF sequence of the Group VII which had previously shown the conservation of the N-end rule pathway in barley with cysteine as a sensor for hypoxia in submergence (Mendiondo et al., 2015). The MCGGAIL::GUS construct consist of the 7 amino acid sequence fused to β-glucuronidase (GUS) reporter protein at the N- terminus. A similar sequence was mutated as control with the replacement of 'Cys' with 'Ala' to give MAGGAIL:: GUS. This was created to serve as a control, because the N terminal sequence is not an ERFVII and will not follow the process of NERP. The GUS activity of the MAGGAIL::GUS only help with the comparison to MCGGAIL::GUS protein stability. In all the two constructs (MC/MAGGAIL::GUS), their RNA expression was driven constitutively by the maize Ubiquitin promoter. The overexpression of the two construct was carried out on two *Oryza sativa*. Japonica rice varieties viz Nipponbare and Kaybonnet (as mentioned).

To probe at the stability of the protein with the N- terminal consensus sequence of the Group VII ERF TFs, the *Agrobacterium* infected callus tissue of the two genes were examined after 5 days in the selection stage with histochemical staining for GUS activity (Figure 7.8). The callus transformed with the native Cys-2 containing reporter (MCGGAIL::GUS) expressed no GUS activity under normal condition, whereas the callus transformed with the mutated alanine containing reporter (MAGGAIL:: GUS). This was because of the MCGGAIL::GUS protein stability strongly depends on the conditions that prevent the oxidation of Cys when exposed (Figure 7.2). The GUS activity of the calli were tested in normoxia (open air). Thus, the Cys became oxidised which then led to the subsequent processes of the protein degradation. The MAGGAIL::GUS as mentioned, does not have the component of the ERFVII (lacks Cys at the N-terminus) so the GUS activity was not hindered.

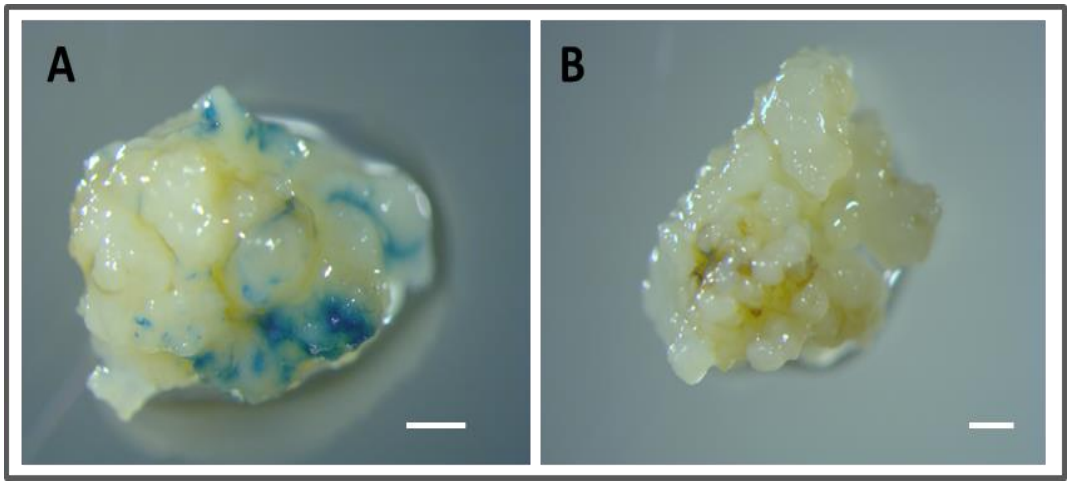

Figure 7.8. The histochemical activity of GUS on Hygromycin resistant calli. **A.** MAGGAIL:: GUS transformed calli expresses the GUS staining at normal condition. **B**. MCGGAIL::GUS transformed calli could not stabilize GUS activity despite the presence of the transgene. This was due to protein degradation followed by the N-end rule pathway. Scale bar is 2000μm.

7.4.8 Demonstration of N-terminal Cysteine function as Oxygen sensor in rice through N-end rule pathway.

It was shown previously that the group VII ERF transcription factor acts as an oxygen and nitric oxide (NO) sensor in Arabidopsis (Gibbs et al., 2014b), as well as submergence in Barley through hypoxia (Mendiondo et al., 2015). This was as a result of the ERFVII sequence signature encoded with Cysteine at the N-terminus which was then ubiquitinated through the channels of N-end rule pathway. As a proof of concept study, the stability of the ERFVII motif in rice was tested in under hypoxia condition. A fully expanded flag leaf of 63 DAS and a 15 DAS were treated for hypoxia, while the controls leaves were only dipped in water (to keep it hydrated) and kept in the normoxia chamber. After 6 hours treatment in the hypoxia or normoxia chamber, the leaf tissue were treated with X-gluc solution and incubated at 37^{o}C. After 4-6 days for mature leaf and 2 days for young leaf in the X-gluc solution, the result showed a low but a consistent pattern of the GUS activity on some portions of the leaf (see Figure 7.9). In comparison, MCGGAIL::GUS in the normoxia condition were unable to show any GUS activity despite prolonging incubation in the Gus solution. This, however, suggests that the N-terminal cysteine within the long group VII ERF consensus has the capability to act as a sensor to Oxygen in rice. It may also suggest that

the group VII ERFs accumulate to coordinate the transcriptional response to the O_2 limitation (Gibbs et al., 2011). The MAGGAIL:: GUS samples which do not conform to the N-end rule pathway, showed strong GUS signal around the leaf and the ligule. (Figure 7.9).

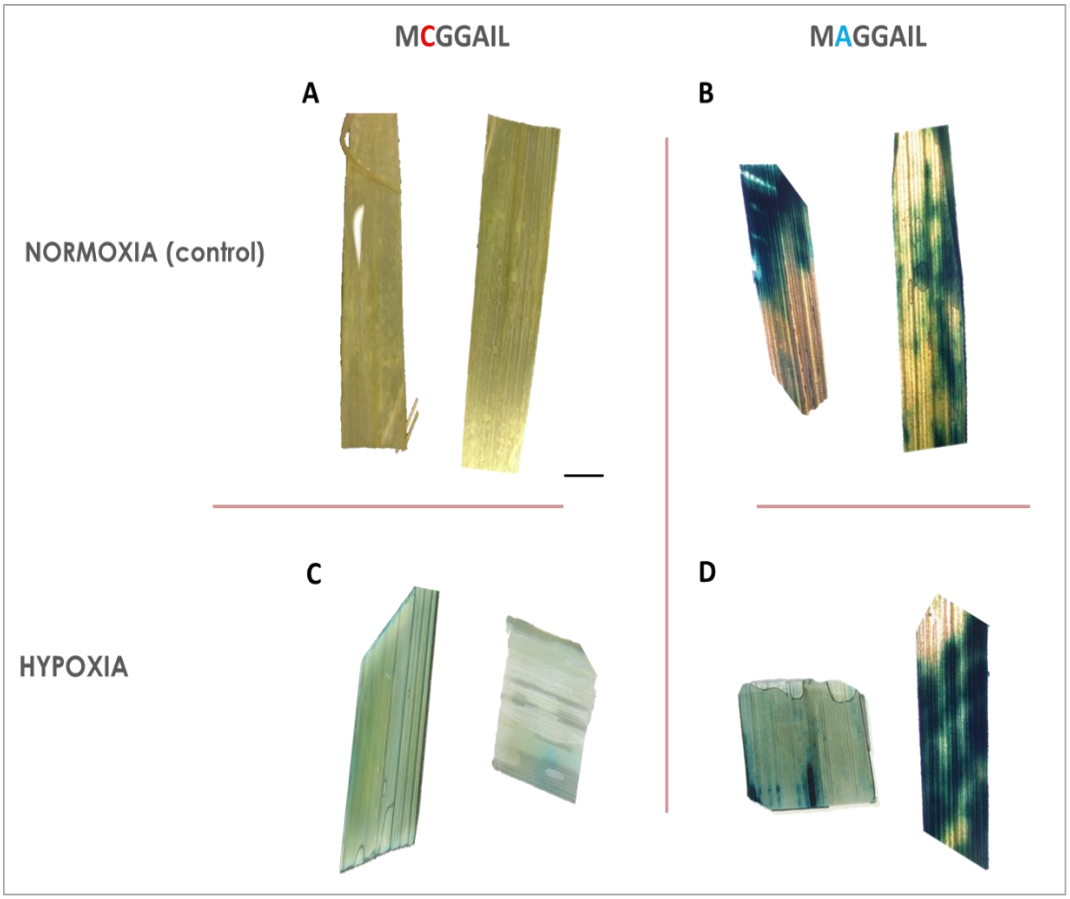

Figure 7.9 GUS staining of transgenic leave tissue stabilized after hypoxia treatment. A**.** Transgenic leaves tissue expressing MCGGAIL:: GUS in control condition; **B**. Transgenic leaves tissue expressing MCGGAIL:: GUS shows low but consistent staining. The MCGGAIL:: GUS protein is stabilized after 6 hours of hypoxia treatment. **C**. MAGGAIL:: GUS containing transgenic leaves showing GUS staining in normal condition and **D**. in hypoxic condition.

To test the activity of the MCGGAIL::GUS line under submergence condition, 3-leaf rice stage was growing in compost, and 5-day old rice seedling grown on wet filter paper were submerged in half - closed bottle filled with water covered in the dark for 3 days. The effect of the submergence caused the MCGGAIL::GUS lines to show GUS activity around the leaf region and the embryo portion of the seed (in the 5-day

old seedling). This, therefore, reveals the stability of the ERFVII in rice by submergence. (Figure 7.10).

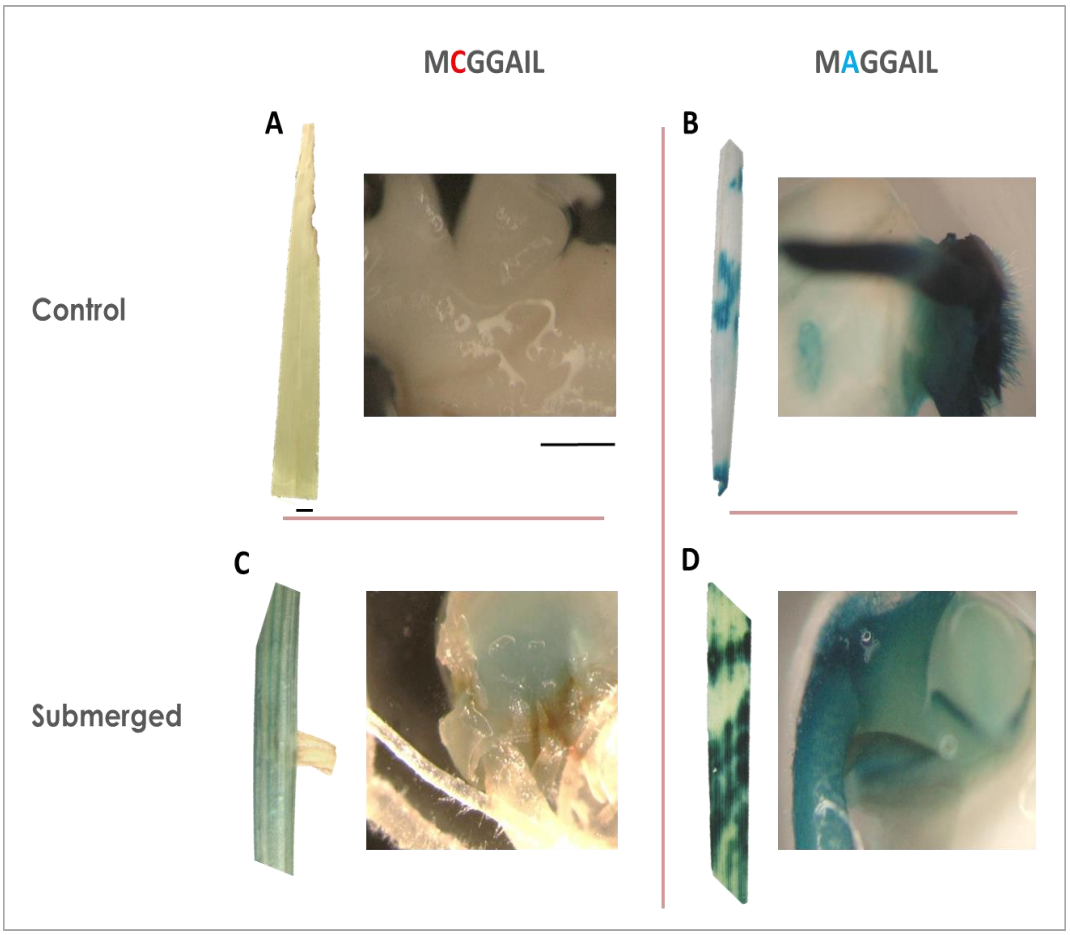

Figure 7.10 GUS staining of transgenic leave and embryo tissue stabilised after submergence treatment. **A**. Transgenic leaf and embryo tissue expressing MCGGAIL::GUS in control condition; **B**. Transgenic leaf and embryo tissue expressing MCGGAIL::GUS indicates the protein is stabilised after 3 days of submergence through GUS staining. **C**. Transgenic leaf and embryo tissue expressing MAGGAIL::GUS in control condition and **D**. MAGGAIL::GUS transgenic leaf and embryo after submergence treatment.

7.4.9 Stability of Group VII ERFs protein act as sensors of drought in rice

The effect of the hypoxia and submergence in response to the GUS stability may suggest that the ERFVII may also be involved in responses to drought, salinity and other abiotic factors that point to the presence of a complex signalling channels.

To test the effect of the MCGGAIL::GUS in drought, the transgenic rice lines were tested under drought treatment. 15 days old transgenic rice

seedlings (at 3 leaf old stage) were subjected to stress for 7 days, to the point of approximately 55% RWC. The soil water content was also dropped by approximately 76% (Figure 7.11)

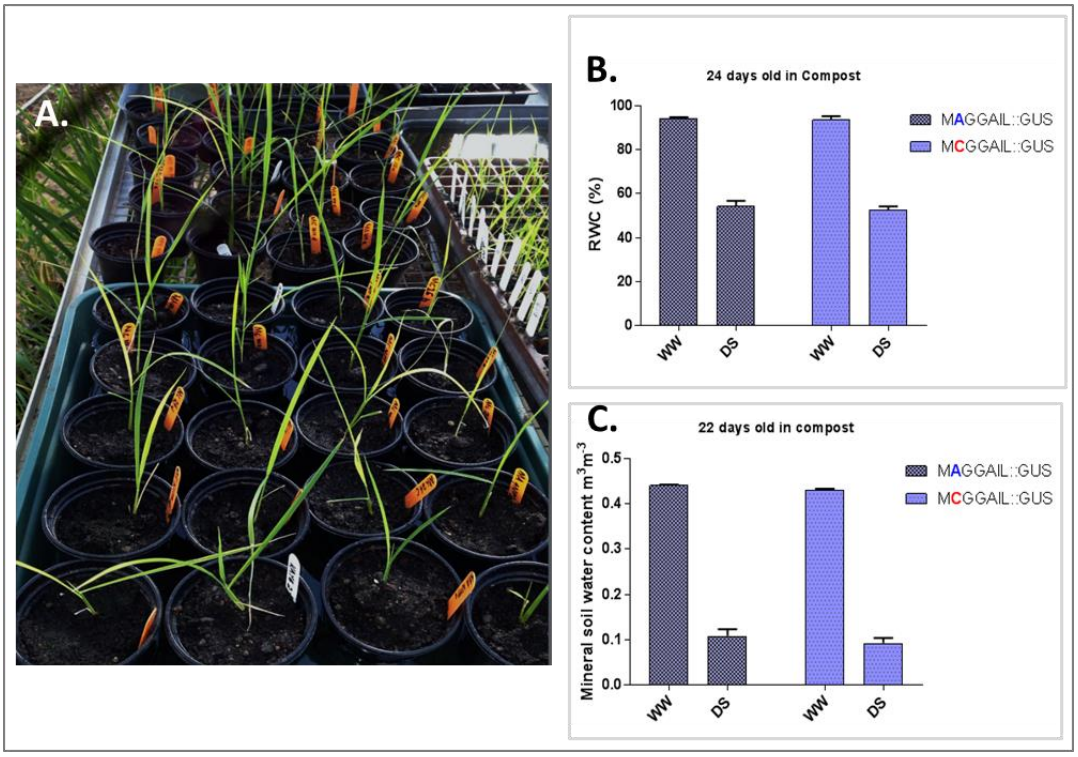

Figure 12. Drought experiment **A.** Water was suspended from the 15-day old seedlings for 7 days water stress alongside their controls growing in sufficient water (Well-watered) **B.** The relative water content (RWC) between the well-watered and drought stressed transgenic at the time of the GUS assay. **C.** Soil water content based on Mineral soil water content ($m^3/m\text{-}^3$)

The rice plants were grown in the compost, and the leaf tissues (particularly the ligule region of the flag leaf) were collected for histochemical GUS staining. There was a consistent GUS stain around the ligule region of the stressed MC-ERF rice of both the Kaybonnet and Nipponbare background but not in the MCGGAIL::GUS plants. The MAGGAIL::GUS line however showed consistent staining regardless of the condition (Figure not shown). This reveals the stability of the artificial N-end rule substrate reporter under drought stress.

7.4.10 GUS protein stability in root and leaf tissue.

To confirm the integrity of the GUS expression in drought stressed MCGGAIL:: GUS plants, rice plants were grown to 3-leaf old stage in a small 250 mL sized pot containing rice compost (top layer 1-1.5cm) and the white pilate (bottom layer 2-3cm, see Figure 7.12A). The choice of white pilate material was to simplify the root cleaning for harvest after the drought stress and to facilitate aeration in the root zone to avoid hypoxic response. At around 7 – 8 days after water stress, the RWC of the leaves was approximately 57% compared to the 96% in the non-stressed leaves (Figure 7.12 B).

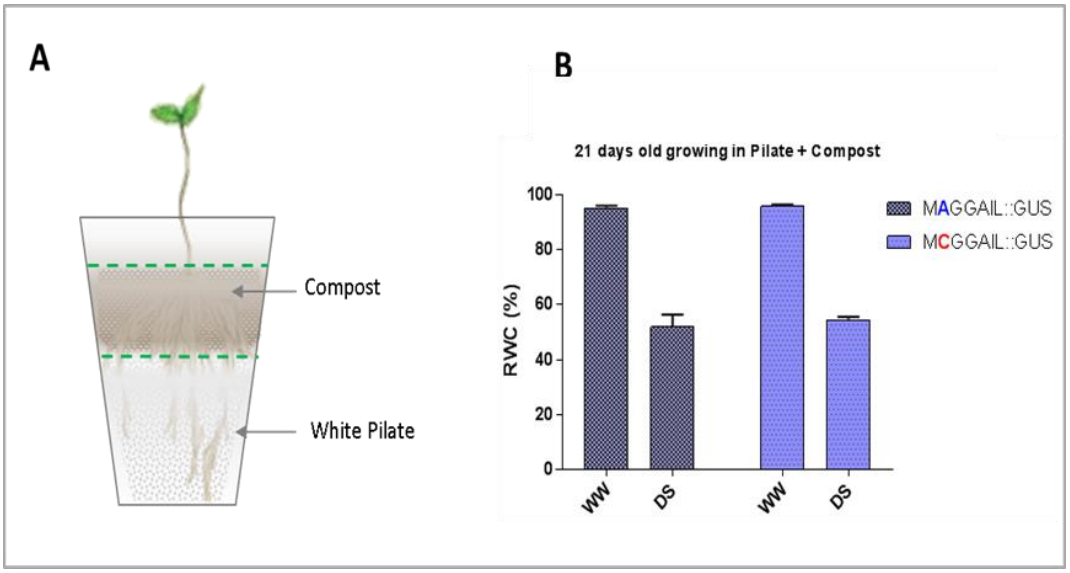

Figure 7.12. Drought treatment with compost and Pilates. **A** a schematic description of the two profile layers of rice compost and white Pilate with which the rice seedlings were grown, and water stressed. **B**. the relative water content of the leaves at the end of the 8 days drought stress. Bar charts pair represents well-watered and the drought. The Error bars indicate the Standard Error of the Mean (SEM) and n=7-9

At the end of the treatment, the rice leaves were GUS stained to investigate whether drought stress has an effect on the intensity and distribution of the GUS activity. Low activity of the GUS was observed at random patches around the leaf but was stronger at the ligule region of the leaf of both the genotypes (Figure 7.13 B). Typically younger MCGGAIL::GUS plants showed more consistent GUS expression under drought stress. The presence of the cuticle and wax in matured leaves

may hinder the penetration of the substrate solution. In contrast to the non-drought stressed MCGGAIL::GUS plants did not show any single GUS stain or patch on the entire leaf tissue (Figure 7.13 A). Suggesting that the stability of the ERFVII protein has been compromised (possibly due to protein degradation via the N-end rule pathway). In these plants, MAGGAIL::GUS line should show much stronger and consistent GUS staining under both drought and non-drought.

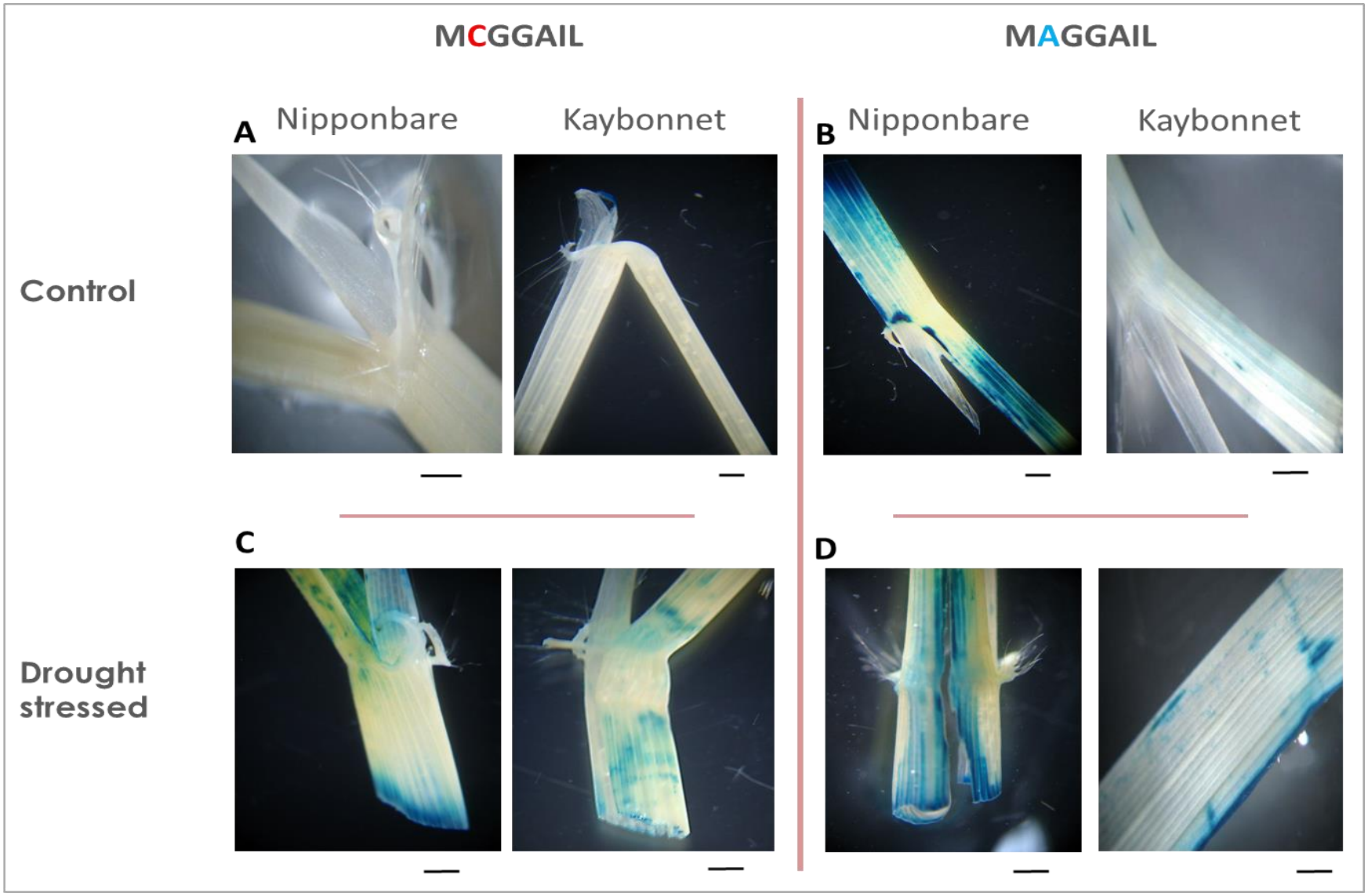

Figure 7.13. GUS staining of the transgenic leaf ligule of the drought stressed MCGGAIL::GUS and MAGGAIL::GUS under two different rice background; Nipponbare (Nipp) and Kaybonnet (Kayb). **A**. leaf ligules of MCGGAIL::GUS Nipp and Kayb from well-watered condition not showing GUS expression. **B**. MAGGAIL::GUS from Nipp and Kayb expressing GUS activity all-round the leaf. **C**. MCGGIAL::GUS leaves of Nipp and Kayb drought stressed for 7-8 days expressing the GUS activity from both ligule and other part of the leaf sheath. **D**. MA::GUS leaves of Nipp and Kayb expressing the GUS activity

GUS staining was also carried out in the root tissues. GUS activity was observed in the seminal and lateral roots of the young drought-stressed MCGGAIL:: GUS rice plants. The expression was much stronger and consistency around the tip of the root hairs (Figure 7.14 C). The intensity of the GUS expression in roots was broadly similar to that observed on the leaf of the same plant. Similarly, the non-drought stressed MCGGAIL:: GUS roots do not show the GUS activity at all.

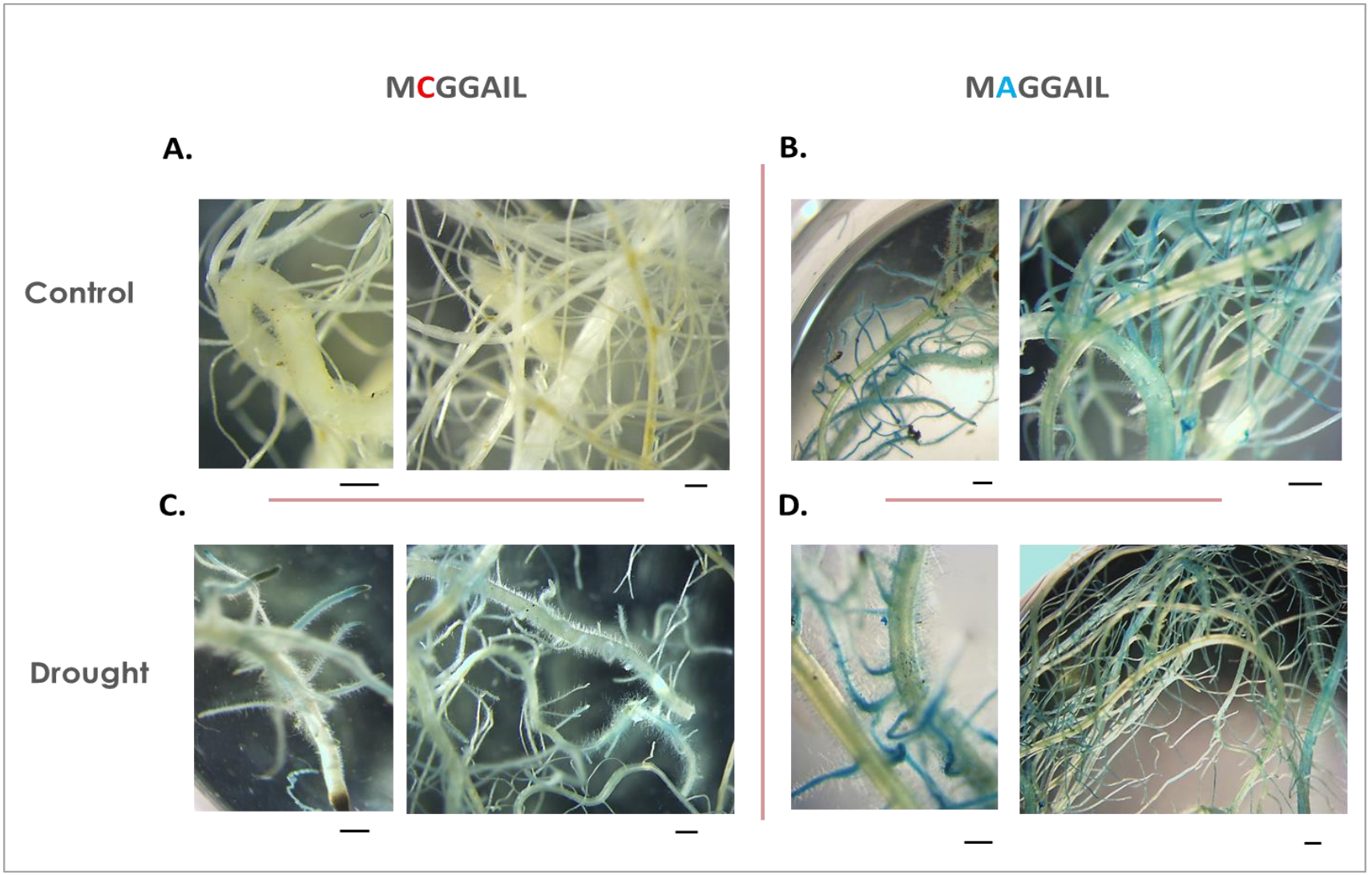

Figure 7.14. GUS staining on the transgenic roots of Nipponbare background after 7-8 days of drought stress in different magnification. **A** MCGGAIL::GUS grown in well-watered condition. **B** MAGGAIL::GUS grown in well-watered condition. **C.** MCGGAIL::GUS grown under drought stress. **D.** MAGGAIL::GUS grown under drought stress. Error bar represents 1mm.

MAGGAIL:: GUS roots showed GUS activity in both conditions. This, therefore, may suggest the role of the N-end rule pathway in rice as a sensor to abiotic stress as shown in both barley and the intensively studied Arabidopsis.

7.4.11 Validation of the stabilised GUS protein

To further validate the GUS assay results, the western immune blotting was used. The total protein extracted from the drought stressed, and non-drought stressed 3-leaf stage rice's leaves and root tissues of the MCGGAIL::GUS plants were used. The westerns revealed a band of about 70kDA in the drought stressed tissue. In contrasted, the non-drought stressed MCGGAIL::GUS tissues do not show this band (Figure 7.15). In some cases, very faints band can be detected in the control MCGGAIL::GUS tissues. It may not be clear what has caused the band but it is possible that there might be some weak stabilisation of GUS due to some unknown stress.

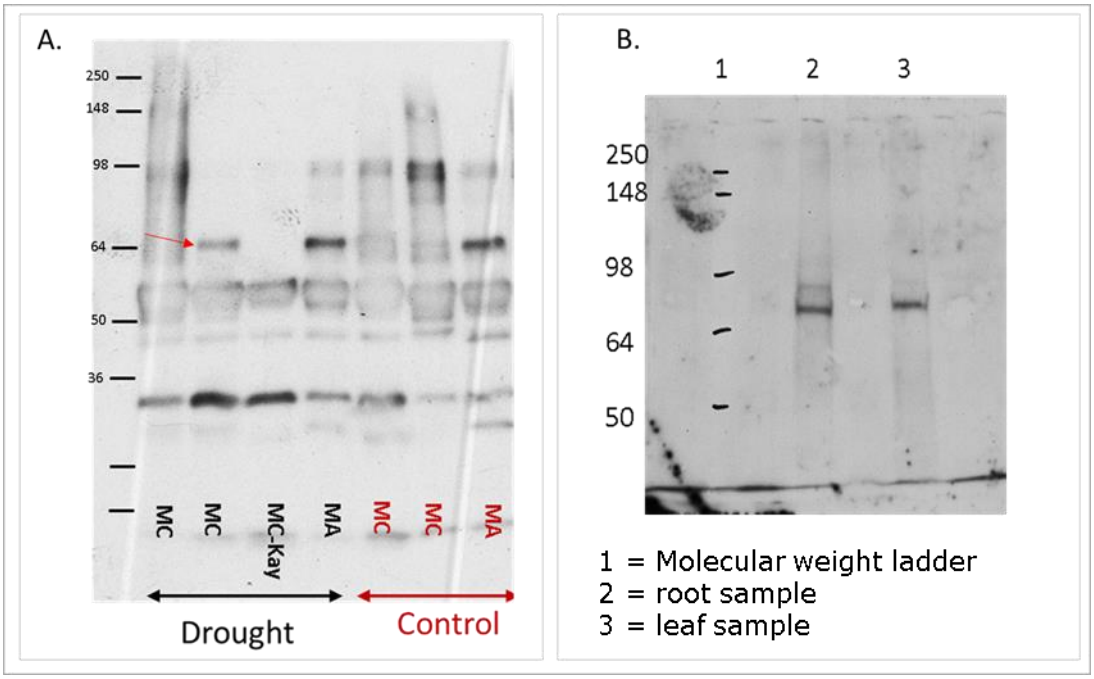

Figure 7.15. Western blotting showing enhanced stability in drought treatment. **A**. GUS protein signals between drought stress leaf tissues and well-watered leaf tissue of MCGGAIL::GUS and MAGGAIL::GUS. MC/MA represent MC/MA-Nipp. **B**. Positive GUS signals present in leaf and root tissues of drought treated MCGGAIL::GUS.

7.5 DISCUSSION

7.5.1 Tissue culture

The method of *Agrobacterium* rice transformation reported in this project aimed at eliminating the short comings associated with rice transformation efficiency previously reported. With this method, transgenic rice plants were not only regenerated rapidly, but it also assures high transformation efficiency. Over the period of optimisation, it was discovered that 5-day old callus could be used for infection (Toki et al., 2006) but the chances of regenerating transgenic plant are low, and the number of transgenics produced from a single seed is reduced. Therefore, this method has been used successfully on two different *Oryza sativa* L japonica varieties; Nipponbare and Kaybonnet more than ten times. It is important to note that seed quality and viability are key determining factor for a successful transformation. The healthier the seeds are, the more likely the chance of the embryo to see through all the transformation stages. The 9-12 days of the callus induction were to successfully develop a young healthy callus that can be excised into smaller fragments, yet escaping any genetic changes that are normally associate with *Agrobacterium* mediated transformation (Colombo et al., 2001). The *Agrobacterium* cell density used was low as well as the duration of co-cultivation. From the two cell densities compared in this experiment, low *Agrobacterium* cell density suggests a better chance of eliminating bacterial over growth as well as best suited for our rapid and efficient transformation method in a simple laboratory tissue culture setup. The high temperature adapted from Toki et al. (2006) with an addition of a substantial amount of stress protectant (proline) has improved this method in hastening callus growth and development as well as protection from stress that normally triggers the extrusion of phenolic compounds (darkening of the media). The proline was predicted to protect high temperature, Agrobactericide antibiotic Timentin as well as to facilitate recovery from *Agrobacterium* infection (Hare and Cress, 1997).

The method also targets the somaclonal variation which is a known problem with Agrobacterium mediated rice transformation that occurs after prolonged exposure to biostimulant during tissue culture, among other factors (Colombo et al., 2001, Hiei and Komari, 2008, Toki et al., 2006). Even though genomic analysis on retrotransposon was not carried out, however, the rapid method may have minimised the somaclonal variation as no phenotypic differences within the same line was observed among the transgenic plants.

The molecular evaluation of the transgenic plants reveals high regeneration (>75%) and transformation (~32%) efficiency.

7.5.2 Stability of Group VII ERF protein under stress

Plants have evolved several mechanisms to adapt and respond to biotic and abiotic stresses. Several recent studies on Arabidopsis indicates that group VII ERF TFs regulate the expression of hypoxia responsive genes for the survival in low oxygen stress (Gibbs et al., 2011) and submergence (Mendiondo et al., 2015). In the present study, the effect of drought stress on the stability of ERFVII protein has been studied using a GUS reporter plants. In this approach, MCGGAIL sequence was fused to GUS at the N-terminus sequence making it a potential substrate of NERP. The control mutated MAGGAIL was also fused to the GUS at the N-terminus. As a proof of concept study, the transgenic lines were first tested under hypoxia and submergence conditions. The results obtained from the hypoxia and submergence experiments demonstrated that MCGGAIL::GUS transgene was stabilised under hypoxia and submergence condition but there was no GUS stain under normal condition (non-stressed). In contrast MAGGAIL::GUS stained irrespective of condition. Thus it can be concluded that the stability of the GUS protein with ERFVII motif may have function through the NERP and that cysteine Arg/N-end rule also acts as a redox sensor in rice possibly through tertiary destabilisation.

7.5.3 The role of drought stress in the stability of ERFVII

The results presented in this study demonstrates the role of drought in the stabilisation of the ERFVII protein. It is important to note that the

response to drought stress is a complex network of various genes that interact in the signalling of the dehydration responses. ERF plays a functional role in the transcription regulation of acclimation responses and tolerance to drought (Narusaka et al., 2003). The mechanism behind the protein stability in this study may have close association with the ERF TFs that are involved in stress signalling among plants. One of them is the *SUB1A*, an ERF TFs found in limited rice accessions. Fukao et al. (2011) described the functional role of *SUB1A* gene in acclimation to dehydration. Studies have shown a *SUB1A* crosstalk between submergence and drought tolerance in rice, and it is believed to exert function through ABA, ethylene, and gibberellin signalling (Fukao and Bailey-Serres, 2008, Zhang and Li, 2015, Jung et al., 2010). Studies have shown *SUB1A* gene function through three conditions simultaneously, from the submergence to the simultaneous re-oxygenation after submergence and subsequent water deficit (Fukao et al., 2011). This is an ability of a species that quiescence during submergence, to act as a tolerance/adaptation to drought during water deficit. Therefore, the ERFVII motif signature in the N-terminus of the GUS promoter has revealed the protein stability through GUS activity in both submergence and in drought.

Importantly, the objective of the study was to demonstrate whether the motif of the ERFVII group could be used as a sensor for drought in rice. It is unclear, however, whether the MCGGAIL::GUS functioned in a similar way to the *SUB1A* gene but the finding in this study concur with the work on hypoxia (Gibbs et al., 2011), submergence (Mendiondo et al., 2015) and now drought stress. More detail study is required to understand the mechanism fully, and how NERP may be a useful approach in securing enhanced tolerance to abiotic stress in crops.

However, the 'abiotic sensor lines' created for this study may serve as a valuable material in the understanding in the protein modification that justifies submergence tolerance in rice. It can also help with the understanding of whether the manipulation of the Group VII ERF accumulation and turnover can act as an effective strategy to exert survival to flooding and submergence in crops.

CHAPTER 8: GENERAL DISCUSSION

The results obtained from this project (thesis) have been structured into five chapters (3, 4, 5, 6 and 7) and the relevant findings were profusely discussed in each chapter based on their general objectives. Therefore, the general discussion focuses on the conclusions in a broad context.

Global food security is one of the biggest challenges facing world agriculture and urgently needs to be addressed. Rice is an important crop that directly feeds more than half of the world population (Alexandratos and Bruinsma, 2012, Maclean et al., 2013). However, water-related stresses cause a severe threat to rice production. Drought among other abiotic stresses causes an extensive economic loss to agricultural products around the world with a threat to food sustainability reference. Furthermore, the continuously increasing global population places pressure on the supply of available water for agricultural production. Thus, the need for crop varieties that are highly adapted to dry and various other co-occurring sub-optimal conditions becomes necessary. Despite the general awareness of the economic implication of drought in rice, breeding for drought resistance has not been very successful as one can imagine. This is partly due to the unpredictability of the onset of drought stress and the physiological complexity of the response mechanisms of the stress. This makes it very difficult to characterise component traits that can help to improve performance without a compromise for crop yield and productivity (Serraj et al., 2011). The importance of rice in the global scale and its rise as a genetic model, the availability of physiological resources, availability of its genomic resources (such as its genome sequence project (Li et al., 2014)) and the development advanced analytical tools are believed to provide a basis for improving and understanding drought tolerance in rice. The present study has shown that improvement of drought tolerance in rice can be achieved by different approaches: transformation and exploiting natural variation. This chapter will discuss and critically assess these different approaches, integrating the findings for the different chapters.

8.1 REDUCED TRANSPIRATION RESULTS IN DROUGHT TOLERANCE

A large amount of water is lost from crops through transpiration (on a molar basis this is many times the amount of carbon fixed), and any means of reducing this water loss may serve as a potential approach to enhancement of water use efficiency and conserving soil water levels (Hepworth et al., 2015). Water loss from plants occurs through the stomata thus making these epidermal cellular structures a promising target in the control of plant water loss and conserving soil water. The present study has manipulated the expression of a rice *EPF* ortholog which results in the interruption of the stomatal development pathway. Consequently, a significantly enhanced leaf WUE, drought tolerance and soil water conservation properties were observed (chapter 6).

8.1.1 Why haven't breeding programs led to lower stomatal density for the improvement of water use efficiency?

There has been a long-standing argument to whether alteration of stomatal density could be utilised as important traits in a breeding program for the improvement of water use efficiency. Attempts started in the 70s and 80s in different crop breeding programs (Jones, 1977, Jones, 1987) but with limited success. The original hypothesis was that a genetically determined increase or decrease in the number of stomata would have a direct effect on stomatal conductance. Over the years, several studies have investigated? This hypothesis with the model dicot species Arabidopsis but with different outcomes. Several reports argued that increased stomatal aperture can compensate for reduced stomatal density. Therefore the selective pressure during breeding under water-limited or plentiful conditions may have been to alter aperture rather than morphology. Schlüter et al., 2003 indicated that mutants in SDD1 (stomatal density and distribution) gene that regulates stomatal density resulted in increased stomatal density and 30% increase in *A* and gs on *sdd1* mutants (Schlüter et al., 2003). In contrast, SDD1 revealed comparatively, Büssis et al. (2006) found that no differences in the gs or *A* was observed in the SDD1 overexpression lines. Their findings claimed that the manipulation of only the physical features of stomata

to gs could lead to counterbalance by changes in stomatal function (Franks et al., 2009). Recently, studies are beginning to report the stomatal manipulation from the overexpression of the *EPIDERMAL PATTERNING FACTOR (EPF*) secretory peptides; *EPF1, EPF2* and *EPFL9* (*STOMAGEN*). Reducing stomatal density with a reduction in the stomatal conductance and transpiration with a compromised decline in the CO_2 assimilation rate in both Arabidopsis (Hepworth et al., 2015, Franks et al., 2015, Doheny-Adams et al., 2012) and Barley (Hughes et al., 2017). The present study, however, has reported a successful ectopically overexpression of the *OsEPF2* in rice that led to a marked reduction in the stomatal density. The results revealed a decrease in stomatal conductance (*gs*) and transpiration rate (*E*) without loss of carbon gain or uncoupling of the photosynthetic biochemistry (Chapter 4, 5 and 6). Results also show that, with reduced *gs* and *E*, reduction of stomata number resulted in drought tolerance/avoidance through reduced water loss as discussed in the chapter. More importantly, the relative decline in *gs* compared to *A*, the *A* does not decline proportionally and has led to an increased leaf WUE (intrinsic and instantaneous). Under water stress, plants adjust the trade-off between water loss (by transpiration) and carbon gain (photosynthesis) through stomatal changes to sustain productivity and conserve resources. This mechanism enables proper functioning of the cells without tissue damage (Li et al., 2017).

Alternatively, there may have been a potential selective pressure to reduce stomatal density, but other genetic alterations may have conflicted. For example improvements to canopy photosynthesis in optimal conditions occurred by increasing nitrogen responsiveness, optimising architecture and leaf area index. Such changes were critical for yield potential and may have dominated the selection process by breeders. In water limited conditions there may have been alternative strategies that acted as a 'surrogate' for reduced stomatal density for example phenology. 'Earliness' is a trait found in some drought- tolerant rice cultivars and results in a greater likelihood of life cycle completion before terminal drought.

8.1.2 How beneficial is reducing stomatal density to the global food security?

These findings can contribute considerably to a breeding program for drought tolerant rice varieties by the alteration of stomatal density with *EPF* genes (*OsEPF2*), indicating that reducing the stomatal density could increase water use efficiency and survival of rice under certain drought conditions. In the current increase in the global temperature and diminishing water availability, particularly in the tropics, the utilisation of rice cultivars with reduced stomatal density could be a very attractive approach for ensuring food availability in sub-optimal conditions. This approach can give rise to the development drought tolerant cultivars with effective utilisation of low available water with the loss of photosynthetic efficiency.

8.1.3 What are the disadvantages of lower SD for other conditions?

The fact that stomata play a vital role in the plant's water use makes the function and physical attributes of stomata a potential target for manipulation to improve plant productivity. However, studies have reported the effect of the low stomatal conductance on crop yield, not only on the CO_2 diffusion but the impact on evaporative cooling of the leaf owing to reduced transpiration rate (Fischer et al., 1998). In the present study, a low yield was recorded (Table 5.1) in lines with reduced stomatal density when the *OsEPF2* gene was constitutively overexpressed. However, this observation could be attributed to multiple processes, not just those resulting from leaf processes. For example stomata in the wall of anthers (Dennis et al. unpublished) which are essential in the anther dehiscence process for the dehydration of the endothecium and epidermal cells during anthesis, essentially by evaporation (Keijzer et al., 1987). The Low stomatal density could increase anther temperatures, e.g. leading to delayed dehiscence and increased senescence that interferes with crop grain filling. High temperature has been linked to the reduction in the swelling of pollen, which has mechanical influence in anthers opening (Wilson et al., 2011) and changes in protein expression particularly those associated with

dehiscence (Jagadish et al., 2009). However, because the gene was constitutively overexpressed with the 35S promoter, this can be easily addressed by localising gene expression to the leaf epidermal tissue of the plant. A gene like *EPF2* with great drought tolerance potential may be hugely beneficial to horticultural plants where leaves are harvested and there is no reproductive process needed for commercial production e.g. lettuce, coriander.

8.2 THE POTENTIAL ADAPTATION TO FLOODING

In this study, the *OsEPF2* lines had indicated a crosstalk in terms of drought and flooding tolerance potentials (Chapter 5 and 6). Enhanced aerenchyma which can also have a wide-ranging advantage in flooded conditions was observed in rice when the stomatal density was reduced from *EPF2* overexpression (chapter 6) under hydroponic conditions. In addition to improving O_2 transport to roots, aerenchyma also reduces respiratory losses in flooded conditions (Ito et al., 1999).

8.2.1 Could this apply to aerobic and anaerobic soils?

The well-known *SUB1A* gene of *ERF* transcription factor that enhances rice survival under submergence has been reported to improve survival of rapid dehydration following de-submergence and water deficit during drought (Fukao et al., 2011). Thus there is a high possibility the *EPF2* lines can show a considerable drought and flooding resistance when grown in the field prone to flooding and drought. Therefore, the drought tolerant attributes and the flooding resistance potentials of rice with reduced stomatal density may as well be a big step to increasingly optimised Climate Ready Rice for the future. This is because the *EPF2* lines showed an early emergence of cortical aerenchyma at the apical meristem than the WT in anaerobic condition. This could suggest high sensitivity to reduced O_2 transport. This may allow continued growth and development of the plant with the potential to early readjustment of decreased O_2 supply for respiration by lysing the O_2 consuming cortical cells (aerenchyma). Whereas in the aerated condition, the lines with reduced stomatal density have shown a well-established lysigenous aerenchyma regardless of the aeration level of the growing condition.

This would be beneficial to the plant since the root respiration will be reduced, and it will benefit the plant against sudden changes in the aerobic condition without incurring the metabolic costs of anaerobic respiration.

This study has also laid a background study in the molecular as well as the physiological approaches to understanding the role of targeted protein modifications, in controlling functions of the ERFVII transcription factors that control the key components of abiotic stress tolerance in rice, e.g. *SUB1A* in submergence condition.

8.3 ROOTS ARE KEY ELEMENTS FOR DROUGHT TOLERANCE

One of the key focus of the research was to study root architecture in African rice varieties and correlate root architectural traits to above ground physiology. There have been several studies and reports that suggest that improvement in root architecture can have a profound impact in improving resource use efficiency. Leading world expert Jonathan Lynch has even suggested that next green revolution will be brought about by improving root architecture (Lynch, 2007). Over the years, researchers have developed an understanding of the traits responsible for crop productivity in infertile soil and other sub-optimal conditions. Root architectural traits under genetic control include basal root gravitropism, lateral root formation and branching are critically important in the nutrient acquisition (Uga et al., 2013). Others root traits such as topsoil foraging, length and root hairs density for the acquisition of immobile nutrients (such as phosphorus and potassium) and water in deep soil layers. Genetic variation in root cortical aerenchyma (RCA) are important in reducing the metabolic costs of root growth and soil exploration. Enhanced root anatomical traits, such as the vascular tissues improves nutrient and water transport (Prince et al., 2017).

Chapter 3 demonstrated the study on both the above ground physiology and root architectural traits and how they affect their drought tolerance (Figure 3.14).

8.3.1 Do the differences in RSA determine the differences in drought tolerance among the African accessions?

Rice is generally well adapted to irrigated and water-saturated soil with most ecotypes doing well in stagnant soil systems, but their physiological response to drought differs between their ecological habitat (lowland or upland). Very little is known about their exact mechanisms of water uptake. The understanding of their root attributes towards water uptake during drought condition will be very beneficial to the rice breeders in identifying the interactions of a rice genotype and the environment (G × E) (Serraj et al., 2011). Such interactions can help with identifying traits that can enable drought resistance in rice. Root characteristics associated with architecture (such as root branching and depth), function (water uptake per unit length of roots through hydraulic conductivity) (Henry et al., 2012, Comas et al., 2013) as well as the morphological attributes (root length, average diameter, volume, surface area and root length density) (Price et al., 2002a, Henry et al., 2011, Gowda et al., 2011b). Water uptake is determined by root length, root diameter, soil and root hydraulic conductance, and transpiration demands (Henry et al., 2011). The present study has unveiled the interaction of the above ground physiology and how it affects root attributes in African diversity panel of rice. As mentioned, the plants were grown in an expanded clay beads as growth media, and the maximum depth that root travels was genetically determined and differed among genotypes growing in the same condition. Furthermore, the maximum root depth is achieved only when the roots did not encounter physical obstruction that can limit growth (Comas et al., 2013). The results revealed some of the upland (NERICA's) genotypes with more depth. The results also revealed that root growth appears to depend directly on the type of media the plants were grown in. It has been reported that coarse roots have a direct role in drought resistance as their large diameter improves penetration ability and branching (Wang et al., 2006). However, Direct association with the root volume in successfully established root system could be misleading (Dupuy et al., 2010), because some plants may produce short but thicker roots in response to the growing media (e.g. resistance from compaction). Plants may, therefore, possess similar total root volume

with others with long and thinner roots. In contrast to soil-grown plants, when the plants were grown in the hydroponic media, there was no physical resistance to affect root volume and the root diameter. Therefore the extensive variation for drought tolerances among the African rice germplasm has been shown in Chapter 3. The results have also demonstrated the photosynthetic sensitivity to water stress could have been constrained by the stomatal conductance, which in turn was dependent on hydraulic rooting properties. An observation was made in the roots under drought treatment, small fine root diameters, with long specific root length, were observed in all the genotypes (except line N8). This is in agreement with previous reports that suggest that these are plants' strategies (root morphology) to increase crop productivity under drought conditions (Comas et al., 2013).

Root traits associated with the maintenance of crop productivity under drought are the morphological traits, however, in regions with late season water deficits, the xylem diameters is targeted for the maintenance of deep water for use during crop maturation (Comas et al., 2013). The current study had also looked at the differences in the roots anatomical differences in African lines. Central metaxylem diameter was identified to be larger in some upland genotypes that showed enhanced leaf water use efficiency. A strong relationship was obtained between the CMX and above ground physiology. Caution should be exercised when using correlations to attribute mechanistic relationships. Nonetheless the results of this study strongly suggest that improvement in both root and shoot structure and function is necessary in order to obtain enhanced yields in water limited environments. This has implications for phenotyping programmes which predominantly examine above ground parts. A solution could either be derived by developing below ground analysis techniques which is quite difficult (Bao et al., 2014, Mairhofer et al., 2013) (see X-ray CT imaging which requires large infrastructure, Figure 8.1) or by using above ground proxies. The latter has already been done, e.g. canopy temperature can be used to predict rooting depth (Lopes and Reynolds, 2010, Pinto and Reynolds, 2015)

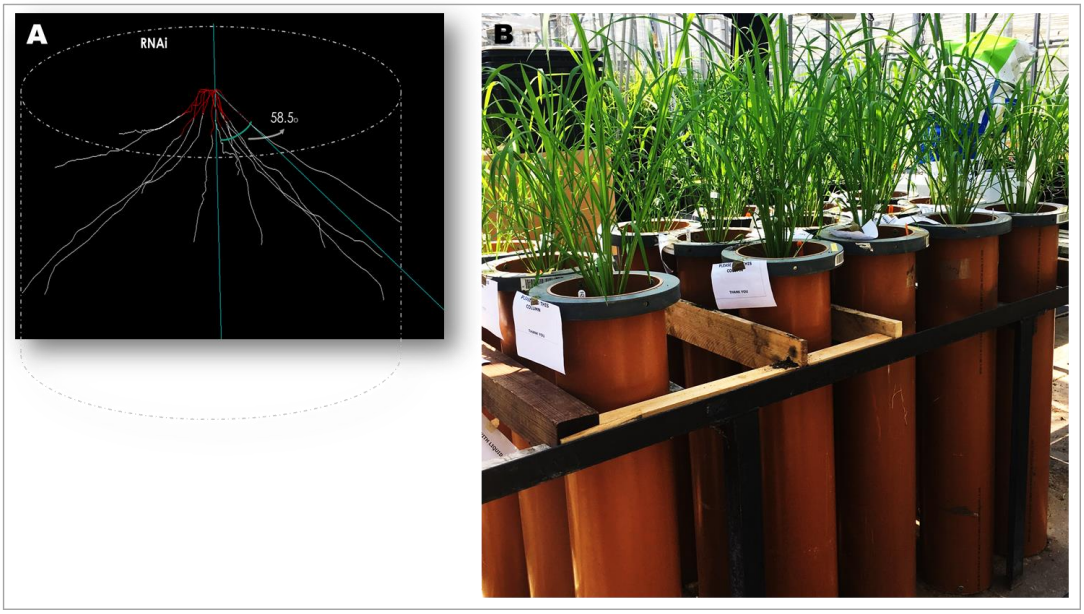

Figure 8.1 **A**. X-ray CT images constructed for root angle analysis. **B.** Drought experiment set-up for X-ray micro CT analysis.

This thesis presents different approaches to improving drought tolerance: transgenic as a result of reverse genetics approach (*OsEPF2* overexpression) and a screen for variation in shoot and root traits among a carefully selected set of African lines. A balanced conclusion would be that both approaches are promising in the quest to improve both water use efficiency and drought tolerance (2 different traits). The advantages of the transgenic approach are that it is rapid and has a precise phenotype targeting stomatal density. However, the aerenchyma observation, while interesting and potentially useful, has shown that there may be consequences beyond leaf functioning. From a physiological viewpoint this is not totally unexpected since stomata sit at a pivotal point, the interface between the atmosphere and the leaf primary photosynthetic processes. Most gasses will pass through stomata. Other disadvantages of this approach would be the acceptability of genetically modified (GM) crops. While there are no fundamental differences between GM crops and 'conventional' crops, this technology is in the process of recovery from an early bad press in European countries, and this still needs to be overcome (Phipps and Park, 2002, Nap et al., 2003). Crispr Cas offers the potential of making targeted alterations without being classed as GM. The advantage of using

existing genetic variation is the possibility of using conventional breeding alongside marker-assisted selection, and other advanced genotyping technologies (Collard and Mackill, 2008). It is probably advantageous to pursue both approaches and even combine them. Scientists are probably going to need every 'tool in the box' to reach the goal of a 50 % increase in yield per hectare in the next 30 years.

8.4 PROSPECT AND FUTURE WORK

- The evidence from the current study that root morphology and anatomy are essential to support high photosynthesis through increased water access across the genotype were all obtained from either hydroponic media or expanded clays. The use of soil column to study the alteration of the root system architecture will be preferential for the future and will represent the natural environment and more realistic in the screening of the genetic diversity and root plasticity under different soil water levels and to obtain good correlations to the photosynthetic parameters.

  From an uncompleted study conducted within the time of the PhD (but not completed at the date of submission), involved the use of the modern Three-Dimensional Micro-Computed Tomography (X-ray, Micro CT) facility here in the University of Nottingham (Hounsfield).
- More work is needed with a good number for statistical analysis to understand more details into the mechanisms with which the *EPF* lines used for the improvement of drought tolerance and water use efficiency without loss to carbon gain, unlike SDD1 and others (Büssis et al., 2006) that were previously reported with conflicting results.

  The unexpected but interesting finding on the on the effect of reduced stomatal density in the enhancement of lysigenous aerenchyma in rice will need more detail study to understand the physiological cause fully as well as to examine for the presence of any molecular signalling (if there is any. e.g. Ethylene involvement)

REFERENCES

ABIKO, T. & OBARA, M. 2014. Enhancement of porosity and aerenchyma formation in nitrogen-deficient rice roots. *Plant Science,* 215**,** 76-83.

ADACHI, S., TSURU, Y., NITO, N., MURATA, K., YAMAMOTO, T., EBITANI, T., OOKAWA, T. & HIRASAWA, T. 2011. Identification and characterization of genomic regions on chromosomes 4 and 8 that control the rate of photosynthesis in rice leaves. *Journal of Experimental Botany,* 62**,** 1927-1938.

ADACHI, Y., SUGIYAMA, M., SAKAGAMI, J.-I., FUKUDA, A., OHE, M. & WATANABE, H. 2015. Seed germination and coleoptile growth of new rice lines adapted to hypoxic conditions. *Plant Production Science,* 18**,** 471-475.

ADU, M. O., CHATOT, A., WIESEL, L., BENNETT, M. J., BROADLEY, M. R., WHITE, P. J. & DUPUY, L. X. 2014. A scanner system for high-resolution quantification of variation in root growth dynamics of Brassica rapa genotypes. *Journal of experimental botany***,** eru048.

AKINWALE, M., AKINYELE, B., ODIYI, A., NWILENE, F., GREGORIO, G. & OYETUNJI, O. Phenotypic screening of Nigerian rainfed lowland mega-rice varieties for submergence tolerance. Proceedings of the world congress on Engineering, 2012. 4-6.

AL-TAHIR, F. M. 2014. Flag leaf characteristics and relationship with grain yield and grain protein percentage for three cereals. *Journal of Medicinal Plants,* 2**,** 01-07.

ALEXANDRATOS, N. & BRUINSMA, J. 2012. World agriculture towards 2030/2050: the 2012 revision. ESA Working paper Rome, FAO.

ARAÚJO, W. L., FERNIE, A. R. & NUNES-NESI, A. 2011. Control of stomatal aperture: a renaissance of the old guard. *Plant signaling & behavior,* 6**,** 1305-1311.

ARMSTRONG, W. & DREW, M. 2002. Root growth and metabolism under oxygen deficiency. *Plant roots: the hidden half,* 3**,** 729-761.

ARO, E., SUORSA, M., ROKKA, A., ALLAHVERDIYEVA, Y., PAAKKARINEN, V., SALEEM, A., BATTCHIKOVA, N. & RINTAMÄKI, E. 2004. Dynamics of photosystem II: a proteomic approach to thylakoid protein complexes. *Journal of Experimental Botany,* 56**,** 347-356.

AROCKIASAMY, S. & IGNACIMUTHU, S. 2007. Regeneration of transgenic plants from two indica rice (Oryza sativa L.) cultivars using shoot apex explants. *Plant Cell Reports,* 26**,** 1745-1753.

BANDILLO, N., RAGHAVAN, C., MUYCO, P. A., SEVILLA, M. A. L., LOBINA, I. T., DILLA-ERMITA, C. J., TUNG, C.-W., MCCOUCH, S., THOMSON, M. & MAULEON, R. 2013. Multi-parent advanced generation inter-cross (MAGIC) populations in rice: progress and potential for genetics research and breeding. *Rice,* 6**,** 11.

BANTI, V., GIUNTOLI, B., GONZALI, S., LORETI, E., MAGNESCHI, L., NOVI, G., PAPARELLI, E., PARLANTI, S., PUCCIARIELLO, C. & SANTANIELLO, A. 2013. Low oxygen response mechanisms in green organisms. *International journal of molecular sciences,* 14**,** 4734-4761.

BAO, Y., AGGARWAL, P., ROBBINS, N. E., STURROCK, C. J., THOMPSON, M. C., TAN, H. Q., THAM, C., DUAN, L., RODRIGUEZ, P. L., VERNOUX, T., MOONEY, S. J., BENNETT, M. J. & DINNENY, J. R. 2014. Plant roots use a patterning mechanism to position lateral root branches toward available water. *Proceedings of the National Academy of Sciences,* 111**,** 9319-9324.

BATTS, G., ELLIS, R., MORISON, J., NKEMKA, P., GREGORY, P. & HADLEY, P. 1998. Yield and partitioning in crops of contrasting cultivars of winter wheat in response to CO2 and temperature in field studies using temperature gradient tunnels. *The Journal of Agricultural Science,* 130**,** 17-27.

BEERLING, D. J. & CHALONER, W. G. 1992. Stomatal density as an indicator of atmospheric CO2 concentration. *Holocene,* 2**,** 71-78.

BERNACCHI, C., SINGSAAS, E., PIMENTEL, C., PORTIS JR, A. & LONG, S. 2001. Improved temperature response functions for models of Rubisco-limited photosynthesis. *Plant, Cell & Environment,* 24**,** 253-259.

BERNIER, J., ATLIN, G. N., SERRAJ, R., KUMAR, A. & SPANER, D. 2008. Breeding upland rice for drought resistance. *Journal of the Science of Food and Agriculture,* 88**,** 927-939.
BISWAL, A. K. & KOHLI, A. 2013. Cereal flag leaf adaptations for grain yield under drought: knowledge status and gaps. *Molecular breeding,* 31**,** 749-766.
BISWAS, J., CHOWDHURY, B., BHATTACHARYA, A. & MANDAL, A. 2002. In vitro screening for increased drought tolerance in rice. *In Vitro Cellular & Developmental Biology-Plant,* 38**,** 525-530.
BLUM, A. 2000. *Drought tolerance-is it a complex trait.*
BOCCO, R., LORIEUX, M., SECK, P., FUTAKUCHI, K., MANNEH, B., BAIMEY, H. & NDJIONDJOP, M.-N. 2012. Agro-morphological characterization of a population of introgression lines derived from crosses between IR 64 (Oryza sativa indica) and TOG 5681 (Oryza glaberrima) for drought tolerance. *Plant science,* 183**,** 65-76.
BURGESS, A. J., RETKUTE, R., HERMAN, T. & MURCHIE, E. H. 2017. Exploring Relationships between Canopy Architecture, Light Distribution, and Photosynthesis in Contrasting Rice Genotypes Using 3D Canopy Reconstruction. *Frontiers in plant science,* 8.
BÜSSIS, D., VON GROLL, U., FISAHN, J. & ALTMANN, T. 2006. Stomatal aperture can compensate altered stomatal density in Arabidopsis thaliana at growth light conditions. *Functional Plant Biology,* 33**,** 1037-1043.
CAIRNS, J., AUDEBERT, A., TOWNEND, J., PRICE, A. & MULLINS, C. 2004. Effect of soil mechanical impedance on root growth of two rice varieties under field drought stress. *Plant and Soil,* 267**,** 309-318.
CATTIVELLI, L., RIZZA, F., BADECK, F.-W., MAZZUCOTELLI, E., MASTRANGELO, A. M., FRANCIA, E., MARE, C., TONDELLI, A. & STANCA, A. M. 2008. Drought tolerance improvement in crop plants: an integrated view from breeding to genomics. *Field Crops Research,* 105**,** 1-14.
CENTRITTO, M., LAUTERI, M., MONTEVERDI, M. C. & SERRAJ, R. 2009. Leaf gas exchange, carbon isotope discrimination, and grain yield in contrasting rice genotypes subjected to water deficits during the reproductive stage. *Journal of Experimental Botany***,** erp123.
CHAN, M.-T., CHANG, H.-H., HO, S.-L., TONG, W.-F. & YU, S.-M. 1993. Agrobacterium-mediated production of transgenic rice plants expressing a chimeric α-amylase promoter/β-glucuronidase gene. *Plant Molecular Biology,* 22**,** 491-506.
CHANDRA, B. R. 2010. Breeding for drought resistance in rice: an integrated view from physiology. *Babu R. Chandra,* 1**,** 9.
CHEN, E.-H., ZHANG, P., ZUO, S.-M., LI, A.-H., ZHANG, Y.-F., CHEN, Z.-X. & PAN, X.-B. 2004. Factors affecting Agrobacterium-mediated transformation efficiency in rice. *Rice Science,* 11**,** 181-185.
CHEN, J.-Q., MENG, X.-P., ZHANG, Y., XIA, M. & WANG, X.-P. 2008. Over-expression of OsDREB genes lead to enhanced drought tolerance in rice. *Biotechnology letters,* 30**,** 2191-2198.
CHEN, Y., MURCHIE, E. H., HUBBART, S., HORTON, P. & PENG, S. 2003. Effects of season-dependent irradiance levels and nitrogen-deficiency on photosynthesis and photoinhibition in field-grown rice (Oryza sativa). *Physiologia plantarum,* 117**,** 343-351.
COLLARD, B. C. & MACKILL, D. J. 2008. Marker-assisted selection: an approach for precision plant breeding in the twenty-first century. *Philosophical Transactions of the Royal Society of London B: Biological Sciences,* 363**,** 557-572.
COLMER, T. 2002. Aerenchyma and an inducible barrier to radial oxygen loss facilitate root aeration in upland, paddy and deep-water rice (Oryza sativa L.). *Annals of Botany,* 91**,** 301-309.
COLMER, T., COX, M. & VOESENEK, L. 2006. Root aeration in rice (Oryza sativa): evaluation of oxygen, carbon dioxide, and ethylene as possible regulators of root acclimatizations. *New Phytologist,* 170**,** 767-778.
COLMER, T. D. & FLOWERS, T. J. 2008. Flooding tolerance in halophytes. *New Phytologist,* 179**,** 964-974.

COLMER, T. D., WINKEL, A. & PEDERSEN, O. 2011. A perspective on underwater photosynthesis in submerged terrestrial wetland plants. *AoB Plants,* 2011**,** plr030.
COLOMBO, L., BARDINI, M. & SALA, F. 2001. Genomic changes in transgenic rice (Oryza sativa L.) plants produced by infecting calli with Agrobacterium tumefaciens. *Plant Cell Reports,* 20**,** 325-330.
COMAS, L., BECKER, S., CRUZ, V. M., BYRNE, P. F. & DIERIG, D. A. 2013. Root traits contributing to plant productivity under drought. *Frontiers in Plant Science,* 4.
CONSTABLE, J. V. & LONGSTRETH, D. J. 1994. Aerenchyma Carbon Dioxide Can Be Assimilated in Typha Iatifolia L. Leaves. *Plant Physiology,* 106**,** 1065-1072.
CORNIC, G. & FRESNEAU, C. 2002. Photosynthetic carbon reduction and carbon oxidation cycles are the main electron sinks for photosystem II activity during a mild drought. *Annals of Botany,* 89**,** 887-894.
DATTA, S. K. 2004. Rice biotechnology: a need for developing countries.
DEY, S. & CORINA VLOT, A. 2015. Ethylene responsive factors in the orchestration of stress responses in monocotyledonous plants. *Frontiers in plant science,* 6**,** 640.
DINGKUHN, M., JONES, M. P., JOHNSON, D. E. & SOW, A. 1998. Growth and yield potential of Oryza sativa and O. glaberrima upland rice cultivars and their interspecific progenies. *Field Crops Research,* 57**,** 57-69.
DIXIT, S., HUANG, B. E., CRUZ, M. T. S., MATURAN, P. T., ONTOY, J. C. E. & KUMAR, A. 2014. QTLs for tolerance of drought and breeding for tolerance of abiotic and biotic stress: an integrated approach. *PLoS One,* 9**,** e109574.
DOHENY-ADAMS, T., HUNT, L., FRANKS, P. J., BEERLING, D. J. & GRAY, J. E. 2012. Genetic manipulation of stomatal density influences stomatal size, plant growth and tolerance to restricted water supply across a growth carbon dioxide gradient. *Philosophical Transactions of the Royal Society of London B: Biological Sciences,* 367**,** 547-555.
DREW, M. C., HE, C.-J. & MORGAN, P. W. 2000. Programmed cell death and aerenchyma formation in roots. *Trends in plant science,* 5**,** 123-127.
DU, H., HUANG, M., ZHANG, Z. & CHENG, S. 2014. Genome-wide analysis of the AP2/ERF gene family in maize waterlogging stress response. *Euphytica,* 198**,** 115-126.
DU, H., WANG, N., CUI, F., LI, X., XIAO, J. & XIONG, L. 2010. Characterization of the β-carotene hydroxylase gene DSM2 conferring drought and oxidative stress resistance by increasing xanthophylls and abscisic acid synthesis in rice. *Plant Physiology,* 154**,** 1304-1318.
DUPUY, L., GREGORY, P. J. & BENGOUGH, A. G. 2010. Root growth models: towards a new generation of continuous approaches. *Journal of experimental botany,* 61**,** 2131-2143.
EVANS, D. E. 2004. Aerenchyma formation. *New Phytologist,* 161**,** 35-49.
FAGERIA, N. & MOREIRA, A. 2011. 4 The Role of Mineral Nutrition on Root Growth of Crop Plants. *Advances in agronomy,* 110**,** 251-331.
FAROOQ, M., WAHID, A., KOBAYASHI, N., FUJITA, D. & BASRA, S. 2009. Plant drought stress: effects, mechanisms and management. *Sustainable Agriculture.* Springer.
FARQUHAR, G. V., VON CAEMMERER, S. V. & BERRY, J. 1980. A biochemical model of photosynthetic CO2 assimilation in leaves of C3 species. *Planta,* 149**,** 78-90.
FILKOWSKI, J., BESPLUG, J., BURKE, P., KOVALCHUK, I. & KOVALCHUK, O. 2003. Genotoxicity of 2, 4-D and dicamba revealed by transgenic Arabidopsis thaliana plants harboring recombination and point mutation markers. *Mutation Research/Genetic Toxicology and Environmental Mutagenesis,* 542**,** 23-32.
FISCHER, R., REES, D., SAYRE, K., LU, Z.-M., CONDON, A. & SAAVEDRA, A. L. 1998. Wheat yield progress associated with higher stomatal conductance and photosynthetic rate, and cooler canopies. *Crop science,* 38**,** 1467-1475.
FLEXAS, J., BOTA, J., LORETO, F., CORNIC, G. & SHARKEY, T. 2004. Diffusive and metabolic limitations to photosynthesis under drought and salinity in C3 plants. *Plant Biology,* 6**,** 269-279.
FLEXAS, J. & MEDRANO, H. 2002. Drought-inhibition of photosynthesis in C3 plants: stomatal and non-stomatal limitations revisited. *Annals of botany,* 89**,** 183-189.

FLEXAS, J., NIINEMETS, Ü., GALLÉ, A., BARBOUR, M. M., CENTRITTO, M., DIAZ-ESPEJO, A., DOUTHE, C., GALMÉS, J., RIBAS-CARBO, M. & RODRIGUEZ, P. L. 2013. Diffusional conductances to CO2 as a target for increasing photosynthesis and photosynthetic water-use efficiency. *Photosynthesis Research,* 117**,** 45-59.

FRANKS, P. J., ADAMS, M. A., AMTHOR, J. S., BARBOUR, M. M., BERRY, J. A., ELLSWORTH, D. S., FARQUHAR, G. D., GHANNOUM, O., LLOYD, J. & MCDOWELL, N. 2013. Sensitivity of plants to changing atmospheric CO2 concentration: from the geological past to the next century. *New Phytologist,* 197**,** 1077-1094.

FRANKS, P. J. & BEERLING, D. J. 2009. Maximum leaf conductance driven by CO2 effects on stomatal size and density over geologic time. *Proceedings of the National Academy of Sciences,* 106**,** 10343-10347.

FRANKS, P. J., DRAKE, P. L. & BEERLING, D. J. 2009. Plasticity in maximum stomatal conductance constrained by negative correlation between stomatal size and density: an analysis using Eucalyptus globulus. *Plant, cell & environment,* 32**,** 1737-1748.

FRANKS, P. J., W DOHENY-ADAMS, T., BRITTON-HARPER, Z. J. & GRAY, J. E. 2015. Increasing water-use efficiency directly through genetic manipulation of stomatal density. *New Phytologist,* 207**,** 188-195.

FUKAI, S. & COOPER, M. 1995. Development of drought-resistant cultivars using physiomorphological traits in rice. *Field Crops Research,* 40**,** 67-86.

FUKAI, S., COOPER, M. & SALISBURY, J. 1997. *Breeding strategies for rainfed lowland rice in drought-prone environments*, Australian Centre for International Agricultural Research.

FUKAI, S., PANTUWAN, G., JONGDEE, B. & COOPER, M. 1999. Screening for drought resistance in rainfed lowland rice. *Field Crops Research,* 64**,** 61-74.

FUKAO, T. & BAILEY-SERRES, J. 2008. Submergence tolerance conferred by Sub1A is mediated by SLR1 and SLRL1 restriction of gibberellin responses in rice. *Proceedings of the National Academy of Sciences,* 105**,** 16814-16819.

FUKAO, T., XU, K., RONALD, P. C. & BAILEY-SERRES, J. 2006. A variable cluster of ethylene response factor–like genes regulates metabolic and developmental acclimation responses to submergence in rice. *The Plant Cell,* 18**,** 2021-2034.

FUKAO, T., YEUNG, E. & BAILEY-SERRES, J. 2011. The submergence tolerance regulator SUB1A mediates crosstalk between submergence and drought tolerance in rice. *The Plant Cell Online,* 23**,** 412-427.

FUKUTA, Y., KONISHO, K., SENOO-NAMAI, S., YANAGIHARA, S., TSUNEMATSU, H., FUKUO, A. & KUMASHIRO, T. 2012. Genetic characterization of rainfed upland New Rice for Africa (NERICA) varieties. *Breeding science,* 62**,** 27-37.

GALMÉS, J., FLEXAS, J., SAVÉ, R. & MEDRANO, H. 2007. Water relations and stomatal characteristics of Mediterranean plants with different growth forms and leaf habits: responses to water stress and recovery. *Plant and Soil,* 290**,** 139-155.

GHILDYAL, B. & TOMAR, V. 1982. Soil physical properties that affect rice root systems under drought. *Drought resistance in crops with emphasis on rice***,** 83-96.

GIBBS, D. J., BACARDIT, J., BACHMAIR, A. & HOLDSWORTH, M. J. 2014a. The eukaryotic N-end rule pathway: conserved mechanisms and diverse functions. *Trends in Cell Biology*.

GIBBS, D. J., LEE, S. C., MD ISA, N., GRAMUGLIA, S., FUKAO, T., BASSEL, G. W., CORREIA, C. S., CORBINEAU, F., THEODOULOU, F. L., BAILEY-SERRES, J. & HOLDSWORTH, M. J. 2011. Homeostatic response to hypoxia is regulated by the N-end rule pathway in plants. *Nature,* 479**,** 415-418.

GIBBS, D. J., MD ISA, N., MOVAHEDI, M., LOZANO-JUSTE, J., MENDIONDO, G. M., BERCKHAN, S., MARÍN-DE LA ROSA, N., VICENTE CONDE, J., SOUSA CORREIA, C. & PEARCE, S. P. 2014b. Nitric oxide sensing in plants is mediated by proteolytic control of group VII ERF transcription factors. *Molecular cell,* 53**,** 369-379.

GOWDA, V. R., HENRY, A., YAMAUCHI, A., SHASHIDHAR, H. & SERRAJ, R. 2011a. Root biology and genetic improvement for drought avoidance in rice. *Field Crops Research,* 122**,** 1-13.

GOWDA, V. R. P., HENRY, A., YAMAUCHI, A., SHASHIDHAR, H. E. & SERRAJ, R. 2011b. Root biology and genetic improvement for drought avoidance in rice. *Field Crops Research,* 122**,** 1-13.
GRAVOIS, K., MOLDENHAUER, K., LEE, F., NORMAN, R., HELMS, R., BERNHARDT, J., WELLS, B., DILDAY, R., ROHMAN, P. & BLOCKER, M. 1995. Registration of 'Kaybonnet'rice. *Crop Sci,* 35**,** 587-588.
GRAY, J. E., HOLROYD, G. H., VAN DER LEE, F. M., BAHRAMI, A. R., SIJMONS, P. C., WOODWARD, F. I., SCHUCH, W. & HETHERINGTON, A. M. 2000. The HIC signalling pathway links CO2 perception to stomatal development. *Nature,* 408**,** 713-716.
GUILIONI, L., WÉRY, J. & LECOEUR, J. 2003. High temperature and water deficit may reduce seed number in field pea purely by decreasing plant growth rate. *Functional Plant Biology,* 30**,** 1151-1164.
HARA, K., YOKOO, T., KAJITA, R., ONISHI, T., YAHATA, S., PETERSON, K. M., TORII, K. U. & KAKIMOTO, T. 2009. Epidermal cell density is autoregulated via a secretory peptide, EPIDERMAL PATTERNING FACTOR 2 in Arabidopsis leaves. *Plant and Cell Physiology,* 50**,** 1019-1031.
HARE, P. & CRESS, W. 1997. Metabolic implications of stress-induced proline accumulation in plants. *Plant growth regulation,* 21**,** 79-102.
HATFIELD, J. L. & PRUEGER, J. H. 2015. Temperature extremes: effect on plant growth and development. *Weather and Climate Extremes,* 10**,** 4-10.
HATTORI, Y., NAGAI, K., FURUKAWA, S., SONG, X. J., KAWANO, R., SAKAKIBARA, H., WU, J. Z., MATSUMOTO, T., YOSHIMURA, A., KITANO, H., MATSUOKA, M., MORI, H. & ASHIKARI, M. 2009. The ethylene response factors SNORKEL1 and SNORKEL2 allow rice to adapt to deep water. *Nature,* 460**,** 1026-U116.
HAYS, D. B., DO, J. H., MASON, R. E., MORGAN, G. & FINLAYSON, S. A. 2007. Heat stress induced ethylene production in developing wheat grains induces kernel abortion and increased maturation in a susceptible cultivar. *Plant Science,* 172**,** 1113-1123.
HE, C.-J., MORGAN, P. W. & DREW, M. C. 1996. Transduction of an ethylene signal is required for cell death and lysis in the root cortex of maize during aerenchyma formation induced by hypoxia. *Plant Physiology,* 112**,** 463-472.
HENRY, A., CAL, A. J., BATOTO, T. C., TORRES, R. O. & SERRAJ, R. 2012. Root attributes affecting water uptake of rice (Oryza sativa) under drought. *Journal of experimental botany*.
HENRY, A., GOWDA, V. R., TORRES, R. O., MCNALLY, K. L. & SERRAJ, R. 2011. Variation in root system architecture and drought response in rice (Oryza sativa): phenotyping of the OryzaSNP panel in rainfed lowland fields. *Field Crops Research,* 120**,** 205-214.
HEPWORTH, C., DOHENY-ADAMS, T., HUNT, L., CAMERON, D. D. & GRAY, J. E. 2015. Manipulating stomatal density enhances drought tolerance without deleterious effect on nutrient uptake. *New Phytologist,* 208**,** 336-341.
HERVÉ, P. & KAYANO, T. 2006. Japonica rice varieties (Oryza sativa, Nipponbare, and others). *Agrobacterium protocols.* Springer.
HETHERINGTON, A. M. & WOODWARD, F. I. 2003. The role of stomata in sensing and driving environmental change. *Nature,* 424**,** 901-908.
HIEI, Y. & KOMARI, T. 2008. Agrobacterium-mediated transformation of rice using immature embryos or calli induced from mature seed. *Nature Protocols,* 3**,** 824-834.
HIEI, Y., OHTA, S., KOMARI, T. & KUMASHIRO, T. 1994. Efficient transformation of rice (Oryza sativa L.) mediated by Agrobacterium and sequence analysis of the boundaries of the T-DNA. *The Plant Journal,* 6**,** 271-282.
HIMMELBAUER, M. 2004. Estimating length, average diameter and surface area of roots using two different image analyses systems. *Plant and Soil,* 260**,** 111-120.
HOPPER, D. W., GHAN, R. & CRAMER, G. R. 2014. A rapid dehydration leaf assay reveals stomatal response differences in grapevine genotypes. *Horticulture research,* 1**,** 2.

HOSHIKAWA, K. C. 1989. The growing rice plant. *Tokyo.: An anatomical monograph. Nobunkyo*.
HSIAO, T. C. & XU, L. K. 2000. Sensitivity of growth of roots versus leaves to water stress: biophysical analysis and relation to water transport. *Journal of experimental botany,* 51**,** 1595-1616.
HU, H., DAI, M., YAO, J., XIAO, B., LI, X., ZHANG, Q. & XIONG, L. 2006. Overexpressing a NAM, ATAF, and CUC (NAC) transcription factor enhances drought resistance and salt tolerance in rice. *Proceedings of the National Academy of Sciences,* 103**,** 12987-12992.
HU, L., WANG, Z. & HUANG, B. 2010. Diffusion limitations and metabolic factors associated with inhibition and recovery of photosynthesis from drought stress in a C3 perennial grass species. *Physiologia plantarum,* 139**,** 93-106.
HUBBART, S., AJIGBOYE, O. O., HORTON, P. & MURCHIE, E. H. 2012. The photoprotective protein PsbS exerts control over CO2 assimilation rate in fluctuating light in rice. *The Plant Journal,* 71**,** 402-412.
HUGHES, J., HEPWORTH, C., DUTTON, C., DUNN, J. A., HUNT, L., STEPHENS, J., WAUGH, R., CAMERON, D. D. & GRAY, J. E. 2017. Reducing Stomatal Density in Barley Improves Drought Tolerance without Impacting on Yield. *Plant Physiology,* 174**,** 776-787.
HUNT, L., BAILEY, K. J. & GRAY, J. E. 2010. The signalling peptide EPFL9 is a positive regulator of stomatal development. *New Phytologist,* 186**,** 609-614.
HUNT, L. & GRAY, J. E. 2009. The signaling peptide EPF2 controls asymmetric cell divisions during stomatal development. *Current Biology,* 19**,** 864-869.
IMOLEHIN, E. & WADA, A. 2000. Meeting the rice production and consumption demands of Nigeria with improved technologies. *International Rice Commission Newsletter,* 49**,** 33-41.
ITO, O., ELLA, E. & KAWANO, N. 1999. Physiological basis of submergence tolerance in rainfed lowland rice ecosystem. *Field Crops Research,* 64**,** 75-90.
JACKSON, M., FENNING, T., DREW, M. & SAKER, L. 1985. Stimulation of ethylene production and gas-space (aerenchyma) formation in adventitious roots of Zea mays L. by small partial pressures of oxygen. *Planta,* 165**,** 486-492.
JAGADISH, S., MUTHURAJAN, R., OANE, R., WHEELER, T. R., HEUER, S., BENNETT, J. & CRAUFURD, P. Q. 2009. Physiological and proteomic approaches to address heat tolerance during anthesis in rice (Oryza sativa L.). *Journal of experimental botany,* 61**,** 143-156.
JALEEL, C. A., MANIVANNAN, P., WAHID, A., FAROOQ, M., AL-JUBURI, H. J., SOMASUNDARAM, R. & PANNEERSELVAM, R. 2009. Drought stress in plants: a review on morphological characteristics and pigments composition. *Int J Agric Biol,* 11**,** 100-105.
JARVIS, A. J. & DAVIES, W. J. 1998. The coupled response of stomatal conductance to photosynthesis and transpiration. *Journal of Experimental Botany***,** 399-406.
JI, K., WANG, Y., SUN, W., LOU, Q., MEI, H., SHEN, S. & CHEN, H. 2012. Drought-responsive mechanisms in rice genotypes with contrasting drought tolerance during reproductive stage. *Journal of plant physiology,* 169**,** 336-344.
JIAN-JUN, M., XIU-FEN, Y., HONG-MEI, Z., JING-JING, Y. & DE-WEN, Q. 2009. Medium selection in tissue culture of japonica rice cultivar Nipponbare and preparation of transgenic plants with an elicitor-coding gene from Magnaporthe grisea. *Chinese Journal of Agricultural Biotechnology,* 6**,** 103-109.
JIANG, Q., ROCHE, D., MONACO, T. & HOLE, D. 2006. Stomatal conductance is a key parameter to assess limitations to photosynthesis and growth potential in barley genotypes. *Plant Biology,* 8**,** 515-521.
JNANDABHIRAM, C. & SAILEN PRASAD, B. 2012. Water stress effects on leaf growth and chlorophyll content but not the grain yield in traditional rice (Oryza sativa Linn.) genotypes of Assam, India II. Protein and proline status in seedlings under PEG induced water stress. *American Journal of Plant Sciences,* 2012.

JOFUKU, K. D., DEN BOER, B., VAN MONTAGU, M. & OKAMURO, J. K. 1994. Control of Arabidopsis flower and seed development by the homeotic gene APETALA2. *The Plant Cell,* 6**,** 1211-1225.
JOHNSON, G. & MURCHIE, E. 2011. Gas exchange measurements for the determination of photosynthetic efficiency in Arabidopsis leaves. *Chloroplast Research in Arabidopsis: Methods and Protocols, Volume II***,** 311-326.
JONES, H. 1977. Transpiration in barley lines with differing stomatal frequencies. *Journal of Experimental Botany,* 28**,** 162-168.
JONES, H. 1987. Breeding for stomatal characters.
JONES, H. G. 2007. Monitoring plant and soil water status: established and novel methods revisited and their relevance to studies of drought tolerance. *Journal of experimental botany,* 58**,** 119-130.
JONES, H. G., SERRAJ, R., LOVEYS, B. R., XIONG, L., WHEATON, A. & PRICE, A. H. 2009. Thermal infrared imaging of crop canopies for the remote diagnosis and quantification of plant responses to water stress in the field. *Functional Plant Biology,* 36**,** 978-989.
JONES, M. P., DINGKUHN, M., ALUKO, G. K. & SEMON, M. 1997. Interspecific Oryza sativa L. x O. glaberrima Steud. progenies in upland rice improvement. *Euphytica,* 94**,** 237-246.
JUNG, J., WON, S. Y., SUH, S. C., KIM, H., WING, R., JEONG, Y., HWANG, I. & KIM, M. 2007. The barley ERF-type transcription factor HvRAF confers enhanced pathogen resistance and salt tolerance in Arabidopsis. *Planta,* 225**,** 575-588.
JUNG, K.-H., SEO, Y.-S., WALIA, H., CAO, P., FUKAO, T., CANLAS, P. E., AMONPANT, F., BAILEY-SERRES, J. & RONALD, P. C. 2010. The submergence tolerance regulator Sub1A mediates stress-responsive expression of AP2/ERF transcription factors. *Plant Physiology,* 152**,** 1674-1692.
KADAM, N., YIN, X., BINDRABAN, P., STRUIK, P. & JAGADISH, K. 2015. Does morphological and anatomical plasticity during the vegetative stage make wheat more tolerant of water-deficit stress than rice? *Plant physiology***,** pp. 114.253328.
KARKI, S., RIZAL, G. & QUICK, W. P. 2013. Improvement of photosynthesis in rice (Oryza sativa L.) by inserting the C4 pathway. *Rice,* 6**,** 28.
KATO, Y., ABE, J., KAMOSHITA, A. & YAMAGISHI, J. 2006. Genotypic Variation in Root Growth Angle in Rice (Oryza sativa L.) and its Association with Deep Root Development in Upland Fields with Different Water Regimes. *Plant and Soil,* 287**,** 117-129.
KATO, Y., KAMOSHITA, A., YAMAGISHI, J., IMOTO, H. & ABE, J. 2007. Growth of Rice (Oryza Sativa L.) Cultivars Under Upland Conditions With Different Levels of Water Supply3. Root System Development, Soil Moisture Changeand Plant Water Status. *Plant Production Science,* 10**,** 3-13.
KATSIR, L., DAVIES, K. A., BERGMANN, D. C. & LAUX, T. 2011. Peptide signaling in plant development. *Current Biology,* 21**,** R356-R364.
KEIJZER, C., HOEK, I. & WILLEEMSE, M. 1987. The processes of anther dehiscence and pollen dispersal III. The dehydration of the filament tip and the anther in three monocotyledonous species. *New phytologist,* 106**,** 281-287.
KHUSH, G. S. 1997. Origin, dispersal, cultivation and variation of rice. *Oryza: From Molecule to Plant.* Springer.
KIM, T.-H., BÖHMER, M., HU, H., NISHIMURA, N. & SCHROEDER, J. I. 2010. Guard cell signal transduction network: advances in understanding abscisic acid, CO2, and Ca2+ signaling. *Annual review of plant biology,* 61**,** 561-591.
KONDO, M., MURTY, M. V. & ARAGONES, D. V. 2000. Characteristics of root growth and water uptake from soil in upland rice and maize under water stress. *Soil Science and Plant Nutrition,* 46**,** 721-732.
KONDO, T., KAJITA, R., MIYAZAKI, A., HOKOYAMA, M., NAKAMURA-MIURA, T., MIZUNO, S., MASUDA, Y., IRIE, K., TANAKA, Y., TAKADA, S., KAKIMOTO, T. & SAKAGAMI, Y. 2010. Stomatal Density is Controlled by a Mesophyll-Derived Signaling Molecule. *Plant and Cell Physiology,* 51**,** 1-8.

KUSUMI, K., HIROTSUKA, S., KUMAMARU, T. & IBA, K. 2012. Increased leaf photosynthesis caused by elevated stomatal conductance in a rice mutant deficient in SLAC1, a guard cell anion channel protein. *Journal of Experimental Botany,* 63**,** 5635-5644.

LAKE, J., QUICK, W., BEERLING, D. J. & WOODWARD, F. I. 2001. Plant development: signals from mature to new leaves. *Nature,* 411**,** 154.

LARTAUD, M., PERIN, C., COURTOIS, B., THOMAS, E., HENRY, S., BETTEMBOURG, M., DIVOL, F., LANAU, N., ARTUS, F. & BUREAU, C. 2014. PHIV-RootCell: a supervised image analysis tool for rice root anatomical parameter quantification. *Frontiers in plant science,* 5.

LATA, C. & PRASAD, M. 2011. Role of DREBs in regulation of abiotic stress responses in plants. *Journal of Experimental Botany*.

LAUTERI, M., HAWORTH, M., SERRAJ, R., MONTEVERDI, M. C. & CENTRITTO, M. 2014. Photosynthetic diffusional constraints affect yield in drought stressed rice cultivars during flowering.

LAWLOR, D. & CORNIC, G. 2002. Photosynthetic carbon assimilation and associated metabolism in relation to water deficits in higher plants. *Plant, Cell & Environment,* 25**,** 275-294.

LAWLOR, D. W. 2002. Limitation to Photosynthesis in Water-stressed Leaves: Stomata vs. Metabolism and the Role of ATP. *Annals of botany,* 89**,** 871-885.

LAWSON, T. & BLATT, M. R. 2014. Stomatal size, speed, and responsiveness impact on photosynthesis and water use efficiency. *Plant Physiology,* 164**,** 1556-1570.

LAWSON, T., KRAMER, D. M. & RAINES, C. A. 2012. Improving yield by exploiting mechanisms underlying natural variation of photosynthesis. *Current Opinion in Biotechnology,* 23**,** 215-220.

LAWSON, T. & MORISON, J. 2006. Visualising patterns of CO2 diffusion in leaves. *New Phytologist,* 169**,** 641-643.

LECKIE, C. P., MCAINSH, M. R., ALLEN, G. J., SANDERS, D. & HETHERINGTON, A. M. 1998. Abscisic acid-induced stomatal closure mediated by cyclic ADP-ribose. *Proceedings of the National Academy of Sciences,* 95**,** 15837-15842.

LEE, J. S., KUROHA, T., HNILOVA, M., KHATAYEVICH, D., KANAOKA, M. M., MCABEE, J. M., SARIKAYA, M., TAMERLER, C. & TORII, K. U. 2012. Direct interaction of ligand–receptor pairs specifying stomatal patterning. *Genes & development,* 26**,** 126-136.

LEE, S. C., MUSTROPH, A., SASIDHARAN, R., VASHISHT, D., PEDERSEN, O., OOSUMI, T., VOESENEK, L. A. & BAILEY-SERRES, J. 2011. Molecular characterization of the submergence response of the Arabidopsis thaliana ecotype Columbia. *New Phytologist,* 190**,** 457-471.

LEVITT, J. 1972. Response of plants to environmental stresses. *Water, radiation, Salt and other stresses,* 2.

LI, J.-Y., WANG, J. & ZEIGLER, R. S. 2014. The 3,000 rice genomes project: new opportunities and challenges for future rice research. *GigaScience,* 3**,** 8.

LI, X., ZHANG, L. & MA, L. 2011. Effects of Preconditioning on Photosynthesis of Rice Seedlings under Water Stress. *Procedia Environmental Sciences,* 11, Part C**,** 1339-1345.

LI, Y., LI, H., LI, Y. & ZHANG, S. 2017. Improving water-use efficiency by decreasing stomatal conductance and transpiration rate to maintain higher ear photosynthetic rate in drought-resistant wheat. *The Crop Journal,* 5**,** 231-239.

LICAUSI, F., KOSMACZ, M., WEITS, D. A., GIUNTOLI, B., GIORGI, F. M., VOESENEK, L. A., PERATA, P. & VAN DONGEN, J. T. 2011. Oxygen sensing in plants is mediated by an N-end rule pathway for protein destabilization. *Nature,* 479**,** 419-422.

LICAUSI, F., PUCCIARIELLO, C. & PERATA, P. 2013. New Role for an Old Rule: N-end Rule-Mediated Degradation of Ethylene Responsive Factor Proteins Governs Low Oxygen Response in PlantsF. *Journal of integrative plant biology,* 55**,** 31-39.

LIU, T., LONGHURST, A. D., TALAVERA-RAUH, F., HOKIN, S. A. & BARTON, M. K. 2016. The Arabidopsis transcription factor ABIG1 relays ABA signaled growth inhibition and drought induced senescence. *eLife,* 5**,** e13768.

LIU, T., OHASHI-ITO, K. & BERGMANN, D. C. 2009. Orthologs of Arabidopsis thaliana stomatal bHLH genes and regulation of stomatal development in grasses. *Development,* 136**,** 2265-2276.
LONG, S. & BERNACCHI, C. 2003. Gas exchange measurements, what can they tell us about the underlying limitations to photosynthesis? Procedures and sources of error. *Journal of Experimental Botany,* 54**,** 2393-2401.
LOPES, M. S. & REYNOLDS, M. P. 2010. Partitioning of assimilates to deeper roots is associated with cooler canopies and increased yield under drought in wheat. *Functional Plant Biology,* 37**,** 147-156.
LOPEZ, F., CHAUHAN, Y. & JOHANSEN, C. 1997. Effects of timing of drought stress on leaf area development and canopy light interception of short-duration pigeonpea. *Journal of Agronomy and Crop Science,* 178**,** 1-7.
LUAN, S. 2002. Signalling drought in guard cells. *Plant, cell & environment,* 25**,** 229-237.
LYNCH, J. P. 2007. Roots of the Second Green Revolution. *Australian Journal of Botany,* 55**,** 493-512.
MACALISTER, C. A., OHASHI-ITO, K. & BERGMANN, D. C. 2007. Transcription factor control of asymmetric cell divisions that establish the stomatal lineage. *Nature,* 445**,** 537-540.
MACLEAN, J., HARDY, B. & HETTEL, G. 2013. *Rice Almanac: Source Book for One of the Most Important Economic Activities on Earth*, IRRI.
MACLEAN, J. L. & DAWE, D. C. 2002. *Rice almanac: Source book for the most important economic activity on earth*, Int. Rice Res. Inst.
MAIRHOFER, S., ZAPPALA, S., TRACY, S., STURROCK, C., BENNETT, M. J., MOONEY, S. J. & PRIDMORE, T. P. 2013. Recovering complete plant root system architectures from soil via X-ray mu-Computed Tomography. *Plant Methods,* 9**,** 1-7.
MARICLE, B. R. & LEE, R. W. 2007. Root respiration and oxygen flux in salt marsh grasses from different elevational zones. *Marine Biology,* 151**,** 413-423.
MARSHALL, B. & BISCOE, P. 1980. A model for C3 leaves describing the dependence of net photosynthesis on irradiance. *Journal of Experimental Botany,* 31**,** 29-39.
MATSUI, T., OMASA, K. & HORIE, T. 2000. High temperature at flowering inhibits swelling of pollen grains, a driving force for thecae dehiscence in rice (Oryza sativa L.). *Plant Production Science,* 3**,** 430-434.
MCELWAIN, J. C. & CHALONER, W. G. 1995. Stomatal density and index of fossil plants track atmospheric carbon dioxide in the Palaeozoic. *Annals of Botany,* 76**,** 389-395.
MEDRANO, H., TOMÁS, M., MARTORELL, S., FLEXAS, J., HERNÁNDEZ, E., ROSSELLÓ, J., POU, A., ESCALONA, J.-M. & BOTA, J. 2015. From leaf to whole-plant water use efficiency (WUE) in complex canopies: limitations of leaf WUE as a selection target. *The Crop Journal,* 3**,** 220-228.
MENDIONDO, G. M., GIBBS, D. J., SZURMAN-ZUBRZYCKA, M., KORN, A., MARQUEZ, J., SZAREJKO, I., MALUSZYNSKI, M., KING, J., AXCELL, B. & SMART, K. 2015. Enhanced waterlogging tolerance in barley by manipulation of expression of the N-end rule pathway E3 ligase PROTEOLYSIS6. *Plant biotechnology journal*.
MOLDENHAUER, K. A. & GIBBONS, J. H. 2003. *Rice morphology and development*, Rice: Origin, History, Technology, and Production. Hoboken, NJ. John Wiley and Sons.
MURCHIE, E., HUBBART, S., PENG, S. & HORTON, P. 2005. Acclimation of photosynthesis to high irradiance in rice: gene expression and interactions with leaf development. *Journal of Experimental Botany,* 56**,** 449-460.
MURCHIE, E. H., ALI, A. & HERMAN, T. 2015. Photoprotection as a trait for rice yield improvement: status and prospects. *Rice,* 8**,** 31.
MURCHIE, E. H., CHEN, Y.-Z., HUBBART, S., PENG, S. & HORTON, P. 1999. Interactions between senescence and leaf orientation determine in situ patterns of photosynthesis and photoinhibition in field-grown rice. *Plant Physiology,* 119**,** 553-564.
MURCHIE, E. H., HUBBART, S., CHEN, Y., PENG, S. & HORTON, P. 2002. Acclimation of rice photosynthesis to irradiance under field conditions. *Plant Physiology,* 130**,** 1999-2010.

MURCHIE, E. H. & LAWSON, T. 2013. Chlorophyll fluorescence analysis: a guide to good practice and understanding some new applications. *Journal of experimental botany,* 64**,** 3983-3998.
MUTHAYYA, S., SUGIMOTO, J. D., MONTGOMERY, S. & MABERLY, G. F. 2014. An overview of global rice production, supply, trade, and consumption. *Annals of the New York Academy of Sciences,* 1324**,** 7-14.
NAKANO, T., SUZUKI, K., FUJIMURA, T. & SHINSHI, H. 2006. Genome-wide analysis of the ERF gene family in Arabidopsis and rice. *Plant physiology,* 140**,** 411-432.
NAP, J. P., METZ, P. L., ESCALER, M. & CONNER, A. J. 2003. The release of genetically modified crops into the environment. *The Plant Journal,* 33**,** 1-18.
NARUSAKA, Y., NAKASHIMA, K., SHINWARI, Z. K., SAKUMA, Y., FURIHATA, T., ABE, H., NARUSAKA, M., SHINOZAKI, K. & YAMAGUCHI-SHINOZAKI, K. 2003. Interaction between two cis-acting elements, ABRE and DRE, in ABA-dependent expression of Arabidopsis rd29A gene in response to dehydration and high-salinity stresses. *The Plant Journal,* 34**,** 137-148.
NISHIUCHI, S., YAMAUCHI, T., TAKAHASHI, H., KOTULA, L. & NAKAZONO, M. 2012. Mechanisms for coping with submergence and waterlogging in rice. *Rice,* 5**,** 2.
NWANZE, K. F., MOHAPATRA, S., KORMAWA, P., KEYA, S. & BRUCE-OLIVER, S. 2006. Rice development in sub-Saharan Africa. *Journal of the Science of Food and Agriculture,* 86**,** 675-677.
O'TOOLE, J. C. Rice and water: the final frontier. First International Conference on Rice for the Future, 2004. Rockefeller Foundation Bangkok, Thailand, 1-26.
OHME-TAKAGI, M. & SHINSHI, H. 1995. Ethylene-inducible DNA binding proteins that interact with an ethylene-responsive element. *The Plant Cell,* 7**,** 173-182.
OHSUMI, A., KANEMURA, T., HOMMA, K., HORIE, T. & SHIRAIWA, T. 2007. Genotypic variation of stomatal conductance in relation to stomatal density and length in rice (Oryza sativa L.). *Plant Production Science,* 10**,** 322-328.
OTENG, J. & SANT'ANNA, R. 1999. Rice production in Africa: Current situation and issues. *International Rice Commission Newsletter (FAO) Bulletin de la Commission Internationale du Riz (FAO) Noticiario de la Comision Internacional del Arroz (FAO)*.
PAEZ-GARCIA, A., MOTES, C. M., SCHEIBLE, W.-R., CHEN, R., BLANCAFLOR, E. B. & MONTEROS, M. J. 2015. Root traits and phenotyping strategies for plant improvement. *Plants,* 4**,** 334-355.
PETERSON, K. M., RYCHEL, A. L. & TORII, K. U. 2010. Out of the mouths of plants: the molecular basis of the evolution and diversity of stomatal development. *The Plant Cell,* 22**,** 296-306.
PHIPPS, R. H. & PARK, J. 2002. Environmental benefits of genetically modified crops: global and European perspectives on their ability to reduce pesticide use. *Journal of Animal and Feed sciences,* 11**,** 1-18.
PIERRET, A., DOUSSAN, C., GARRIGUES, E. & MC KIRBY, J. 2003. Observing plant roots in their environment: current imaging options and specific contribution of two-dimensional approaches. *Agronomie,* 23**,** 471-479.
PIETERS, A. J. & EL SOUKI, S. 2005. Effects of drought during grain filling on PS II activity in rice. *Journal of plant physiology,* 162**,** 903-911.
PILLITTERI, L. J., SLOAN, D. B., BOGENSCHUTZ, N. L. & TORII, K. U. 2007. Termination of asymmetric cell division and differentiation of stomata. *Nature,* 445**,** 501-505.
PINTO, R. S. & REYNOLDS, M. P. 2015. Common genetic basis for canopy temperature depression under heat and drought stress associated with optimized root distribution in bread wheat. *Theoretical and Applied Genetics,* 128**,** 575-585.
PLACIDO, D. F., CAMPBELL, M. T., FOLSOM, J. J., CUI, X., KRUGER, G. R., BAENZIGER, P. S. & WALIA, H. 2013. Introgression of novel traits from a wild wheat relative improves drought adaptation in wheat. *Plant physiology,* 161**,** 1806-1819.
PRICE, A., STEELE, K., GORHAM, J., BRIDGES, J., MOORE, B., EVANS, J., RICHARDSON, P. & JONES, R. 2002a. Upland rice grown in soil-filled chambers and exposed to contrasting water-deficit regimes: I. Root distribution, water use and plant water status. *Field Crops Research,* 76**,** 11-24.

PRICE, A. H., CAIRNS, J. E., HORTON, P., JONES, H. G. & GRIFFITHS, H. 2002b. Linking drought-resistance mechanisms to drought avoidance in upland rice using a QTL approach: progress and new opportunities to integrate stomatal and mesophyll responses. *Journal of Experimental Botany,* 53**,** 989-1004.

PRICE, A. H., YOUNG, E. & TOMOS, A. 1997. Quantitative trait loci associated with stomatal conductance, leaf rolling and heading date mapped in upland rice (Oryza sativa). *New phytologist,* 137**,** 83-91.

PRINCE, S. J., MURPHY, M., MUTAVA, R. N., DURNELL, L. A., VALLIYODAN, B., SHANNON, J. G. & NGUYEN, H. T. 2017. Root xylem plasticity to improve water use and yield in water-stressed soybean. *Journal of experimental botany,* 68**,** 2027-2036.

PUCKRIDGE, D. & O'TOOLE, J. 1980. Dry matter and grain production of rice, using a line source sprinkler in drought studies. *Field Crops Research,* 3**,** 303-319.

QUAN, R., HU, S., ZHANG, Z., ZHANG, H., ZHANG, Z. & HUANG, R. 2010. Overexpression of an ERF transcription factor TSRF1 improves rice drought tolerance. *Plant biotechnology journal,* 8**,** 476-488.

RAHBARIAN, R., KHAVARI-NEJAD, R., GANJEALI, A., BAGHERI, A. & NAJAFI, F. 2011. Drought stress effects on photosynthesis, chlorophyll fluorescence and water relations in tolerant and susceptible chickpea (Cicer Arietinum L.) genotypes. *Acta Biologica Cracoviensia Series Botanica,* 53**,** 47-56.

RANATHUNGE, K., STEUDLE, E. & LAFITTE, R. 2003. Control of water uptake by rice (Oryza sativa L.): role of the outer part of the root. *Planta,* 217**,** 193-205.

RASHID, M., GUANGYUAN, H., GUANGXIAO, Y., HUSSAIN, J. & XU, Y. 2012. AP2/ERF transcription factor in rice: genome-wide canvas and syntenic relationships between monocots and eudicots. *Evolutionary Bioinformatics,* 8**,** 321.

RAY, D. K., MUELLER, N. D., WEST, P. C. & FOLEY, J. A. 2013. Yield trends are insufficient to double global crop production by 2050. *PLoS One,* 8**,** e66428.

REBOUILLAT, J., DIEVART, A., VERDEIL, J., ESCOUTE, J., GIESE, G., BREITLER, J., GANTET, P., ESPEOUT, S., GUIDERDONI, E. & PÉRIN, C. 2009. Molecular genetics of rice root development. *Rice,* 2**,** 15-34.

REDILLAS, M. C. F. R., JEONG, J. S., KIM, Y. S., JUNG, H., BANG, S. W., CHOI, Y. D., HA, S.-H., REUZEAU, C. & KIM, J.-K. 2012. The overexpression of OsNAC9 alters the root architecture of rice plants enhancing drought resistance and grain yield under field conditions. *Plant Biotechnology Journal,* 10**,** 792-805.

RYCHEL, A. L., PETERSON, K. M. & TORII, K. U. 2010. Plant twitter: ligands under 140 amino acids enforcing stomatal patterning. *Journal of plant research,* 123**,** 275-280.

SACK, L. & SCOFFONI, C. 2012. Measurement of leaf hydraulic conductance and stomatal conductance and their responses to irradiance and dehydration using the Evaporative Flux Method (EFM). *Journal of visualized experiments: JoVE*.

SAGE, R. F. 2004. The evolution of C4 photosynthesis. *New phytologist,* 161**,** 341-370.

SAHOO, K. K., TRIPATHI, A. K., PAREEK, A., SOPORY, S. K. & SINGLA-PAREEK, S. L. 2011. An improved protocol for efficient transformation and regeneration of diverse indica rice cultivars. *Plant methods,* 7**,** 49.

SAIKA, H. & TOKI, S. 2010. Mature seed-derived callus of the model indica rice variety Kasalath is highly competent in Agrobacterium-mediated transformation. *Plant Cell Reports,* 29**,** 1351-1364.

SAMEJIMA, H. & TSUNEMATSU, H. 2016. Genotypic variation in rice varieties screened for deep rooting under field conditions in West Africa. *Plant Production Science,* 19**,** 181-192.

SAMSON, B. K., HASAN, M. & WADE, L. J. 2002. Penetration of hardpans by rice lines in the rainfed lowlands. *Field Crops Research,* 76**,** 175-188.

SCHLÜTER, U., MUSCHAK, M., BERGER, D. & ALTMANN, T. 2003. Photosynthetic performance of an Arabidopsis mutant with elevated stomatal density (sdd1-1) under different light regimes. *Journal of Experimental Botany,* 54**,** 867-874.

SEKI, M., KAMEI, A., YAMAGUCHI-SHINOZAKI, K. & SHINOZAKI, K. 2003. Molecular responses to drought, salinity and frost: common and different paths for plant protection. *Current opinion in biotechnology,* 14**,** 194-199.

SERRAJ, R., ALLEN, L. H. & SINCLAIR, T. R. 1999. Soybean leaf growth and gas exchange response to drought under carbon dioxide enrichment. *Global Change Biology,* 5**,** 283-291.
SERRAJ, R., MCNALLY, K. L., SLAMET-LOEDIN, I., KOHLI, A., HAEFELE, S. M., ATLIN, G. & KUMAR, A. 2011. Drought resistance improvement in rice: an integrated genetic and resource management strategy. *Plant Production Science,* 14**,** 1-14.
SHARKEY, T. D., BERNACCHI, C. J., FARQUHAR, G. D. & SINGSAAS, E. L. 2007. Fitting photosynthetic carbon dioxide response curves for C3 leaves. *Plant, Cell & Environment,* 30**,** 1035-1040.
SHASHIDHAR, H., HENRY, A. & HARDY, B. 2012. *Methodologies for Root Drought Studies in Rice*, Int. Rice Res. Inst.
SHIMAZAKI, K.-I., DOI, M., ASSMANN, S. M. & KINOSHITA, T. 2007. Light regulation of stomatal movement. *Annu. Rev. Plant Biol.,* 58**,** 219-247.
SHINOZAKI, K. & YAMAGUCHI-SHINOZAKI, K. 2007. Gene networks involved in drought stress response and tolerance. *Journal of Experimental Botany,* 58**,** 221-227.
SHIONO, K., OGAWA, S., YAMAZAKI, S., ISODA, H., FUJIMURA, T., NAKAZONO, M. & COLMER, T. D. 2011. Contrasting dynamics of radial O2-loss barrier induction and aerenchyma formation in rice roots of two lengths. *Annals of Botany,* 107**,** 89-99.
SINGH, N., DANG, T. T., VERGARA, G. V., PANDEY, D. M., SANCHEZ, D., NEERAJA, C., SEPTININGSIH, E. M., MENDIORO, M., TECSON-MENDOZA, E. M. & ISMAIL, A. M. 2010. Molecular marker survey and expression analyses of the rice submergence-tolerance gene SUB1A. *Theoretical and Applied Genetics,* 121**,** 1441-1453.
SIRICHANDRA, C., WASILEWSKA, A., VLAD, F., VALON, C. & LEUNG, J. 2009. The guard cell as a single-cell model towards understanding drought tolerance and abscisic acid action. *Journal of Experimental Botany***,** ern340.
SMITH, S. & DE SMET, I. 2012. Root system architecture: insights from Arabidopsis and cereal crops. *Philosophical Transactions of the Royal Society B: Biological Sciences,* 367**,** 1441-1452.
SOMADO, E. A., GUEI, R. G. & KEYA, S. O. 2008. *NERICA: The new rice for Africa: A compendium*, Africa Rice Center (WARDA).
SUGANO, S. S., SHIMADA, T., IMAI, Y., OKAWA, K., TAMAI, A., MORI, M. & HARA-NISHIMURA, I. 2010. Stomagen positively regulates stomatal density in Arabidopsis. *Nature,* 463**,** 241-244.
SURALTA, R. R. & YAMAUCHI, A. 2008. Root growth, aerenchyma development, and oxygen transport in rice genotypes subjected to drought and waterlogging. *Environmental and Experimental Botany,* 64**,** 75-82.
SWARUP, R., KRAMER, E. M., PERRY, P., KNOX, K., LEYSER, H. O., HASELOFF, J., BEEMSTER, G. T., BHALERAO, R. & BENNETT, M. J. 2005. Root gravitropism requires lateral root cap and epidermal cells for transport and response to a mobile auxin signal. *Nature cell biology,* 7**,** 1057-1065.
TAIZ, L. & ZEIGER, E. 2002. Plant physiology. *EE. UU. California: Sinauer*.
TAKAI, T., ADACHI, S., TAGUCHI-SHIOBARA, F., SANOH-ARAI, Y., IWASAWA, N., YOSHINAGA, S., HIROSE, S., TANIGUCHI, Y., YAMANOUCHI, U. & WU, J. 2013. A natural variant of NAL1, selected in high-yield rice breeding programs, pleiotropically increases photosynthesis rate. *Scientific reports,* 3**,** 2149.
TAKATA, N., YOKOTA, K., OHKI, S., MORI, M., TANIGUCHI, T. & KURITA, M. 2013. Evolutionary relationship and structural characterization of the EPF/EPFL gene family. *PloS one,* 8**,** e65183.
TALBOTT, L. D., RAHVEH, E. & ZEIGER, E. 2003. Relative humidity is a key factor in the acclimation of the stomatal response to CO2. *Journal of Experimental Botany,* 54**,** 2141-2147.
TASAKI, T., SRIRAM, S. M., PARK, K. S. & KWON, Y. T. 2012. The N-end rule pathway. *Annual review of biochemistry,* 81**,** 261.
TAYLARAN, R. D., ADACHI, S., OOKAWA, T., USUDA, H. & HIRASAWA, T. 2011. Hydraulic conductance as well as nitrogen accumulation plays a role in the higher rate of leaf photosynthesis of the most productive variety of rice in Japan. *Journal of Experimental Botany,* 62**,** 4067-4077.

TERAO, T. & YAMASHITA, A. 1983. Physiological differentiation of crop cultivars in photosynthetic activity. 2. Principal component analysis of photosynthetic rate and its related leaf characters of semi-dwarf rice cultivars. *Japan. J. Breed,* 33**,** 94-95.
TEZARA, W., MITCHELL, V. J., DRISCOLL, S. D. & LAWLOR, D. W. 1999. Water stress inhibits plant photosynthesis by decreasing coupling factor and ATP. *Nature,* 401**,** 914-917.
THOMSON, C., COLMER, T., WATKIN, E. & GREENWAY, H. 1992. Tolerance of wheat (Triticum aestivum cvs Gamenya and Kite) and triticale (Triticosecale cv. Muir) to waterlogging. *New Phytologist,* 120**,** 335-344.
TOKI, S. 1997. Rapid and efficient Agrobacterium-mediated transformation in rice. *Plant Molecular Biology Reporter,* 15**,** 16-21.
TOKI, S., HARA, N., ONO, K., ONODERA, H., TAGIRI, A., OKA, S. & TANAKA, H. 2006. Early infection of scutellum tissue with Agrobacterium allows high-speed transformation of rice. *The Plant Journal,* 47**,** 969-976.
TOURNIER, B., SANCHEZ-BALLESTA, M. T., JONES, B., PESQUET, E., REGAD, F., LATCHÉ, A., PECH, J.-C. & BOUZAYEN, M. 2003. New members of the tomato ERF family show specific expression pattern and diverse DNA-binding capacity to the GCC box element. *FEBS letters,* 550**,** 149-154.
TRICKER, P. J., TREWIN, H., KULL, O., CLARKSON, G. J., EENSALU, E., TALLIS, M. J., COLELLA, A., DONCASTER, C. P., SABATTI, M. & TAYLOR, G. 2005. Stomatal conductance and not stomatal density determines the long-term reduction in leaf transpiration of poplar in elevated CO2. *Oecologia,* 143**,** 652-660.
TSUDA, M., YAMAGUCHI, H., TAKAMI, S. & IKEDA, K. 1994. Effects of panicle water potential on water stress susceptibility in rice [Oryza sativa]. *Japanese Journal of Crop Science (Japan)*.
UGA, Y., OKUNO, K. & YANO, M. 2011. Dro1, a major QTL involved in deep rooting of rice under upland field conditions. *Journal of Experimental Botany,* 62**,** 2485-2494.
UGA, Y., SUGIMOTO, K., OGAWA, S., RANE, J., ISHITANI, M., HARA, N., KITOMI, Y., INUKAI, Y., ONO, K., KANNO, N., INOUE, H., TAKEHISA, H., MOTOYAMA, R., NAGAMURA, Y., WU, J., MATSUMOTO, T., TAKAI, T., OKUNO, K. & YANO, M. 2013. Control of root system architecture by DEEPER ROOTING 1 increases rice yield under drought conditions. *Nat Genet,* 45**,** 1097-1102.
VALLIYODAN, B. & NGUYEN, H. T. 2006. Understanding regulatory networks and engineering for enhanced drought tolerance in plants. *Current Opinion in Plant Biology,* 9**,** 189-195.
VANDERBURGH, J., VISSCHER, H., DILCHER, D. L. & KURSCHNER, W. M. 1993. PALEOATMOSPHERIC SIGNATURES IN NEOGENE FOSSIL LEAVES. *Science,* 260**,** 1788-1790.
VARSHAVSKY, A. 1996. The N-end rule: functions, mysteries, uses. *Proceedings of the National Academy of Sciences,* 93**,** 12142-12149.
VARSHAVSKY, A. 2011. The N-end rule pathway and regulation by proteolysis. *Protein Science,* 20**,** 1298-1345.
VATÉN, A. & BERGMANN, D. C. 2012. Mechanisms of stomatal development: an evolutionary view. *EvoDevo,* 3**,** 11.
VERGARA, B., LOPEZ, F. & CHAUHAN, J. 1988. Morphology and physiology of ratoon rice. *INTERNATIONAL RICE RESEARCH INSTITUTE (Los Baños, Filipinas). Rice ratooning. Los Baños***,** 31-40.
WADE, L., FUKAI, S., SAMSON, B., ALI, A. & MAZID, M. 1999. Rainfed lowland rice: physical environment and cultivar requirements. *Field Crops Research,* 64**,** 3-12.
WAGIRAN, A., ISMAIL, I., CHE MOHD ZAIN, C. R. & ABDULLAH, R. 2010. 'Agrobacterium tumefaciens'-Mediated Transformation of the Isopentenyltransferase Gene in Japonica Rice Suspension Cell Culture.
WANI, S. H., SOFI, P. A., GOSAL, S. S. & SINGH, N. B. 2010. In vitro screening of rice (Oryza sativa L) callus for drought tolerance. *Commun Biometry Crop Sci,* 5**,** 108-115.
WASSMANN, R., JAGADISH, S., SUMFLETH, K., PATHAK, H., HOWELL, G., ISMAIL, A., SERRAJ, R., REDONA, E., SINGH, R. & HEUER, S. 2009. Regional vulnerability of

climate change impacts on Asian rice production and scope for adaptation. *Advances in Agronomy,* 102**,** 91-133.
WEBSTER, R. J., DRIEVER, S. M., KROMDIJK, J., MCGRATH, J., LEAKEY, A. D., SIEBKE, K., DEMETRIADES-SHAH, T., BONNAGE, S., PELOE, T. & LAWSON, T. 2016. High C3 photosynthetic capacity and high intrinsic water use efficiency underlies the high productivity of the bioenergy grass Arundo donax. *Scientific reports,* 6**,** 20694.
WIENGWEERA, A., GREENWAY, H. & THOMSON, C. J. 1997. The use of agar nutrient solution to simulate lack of convection in waterlogged soils. *Annals of Botany,* 80**,** 115-123.
WILSON, Z. A., SONG, J., TAYLOR, B. & YANG, C. 2011. The final split: the regulation of anther dehiscence. *Journal of experimental botany,* 62**,** 1633-1649.
WOODWARD, F. I. & KELLY, C. K. 1995. The influence of CO2 concentration on stomatal density. *New Phytologist,* 131**,** 311-327.
WU, W. & CHENG, S. 2014. Root genetic research, an opportunity and challenge to rice improvement. *Field Crops Research,* 165**,** 111-124.
XIAO, X., XU, X. & YANG, F. 2008. Adaptive Responses to Progressive Drought Stress in Two Populus cathayana Populations□□.
XU, K., XU, X., FUKAO, T., CANLAS, P., MAGHIRANG-RODRIGUEZ, R., HEUER, S., ISMAIL, A. M., BAILEY-SERRES, J., RONALD, P. C. & MACKILL, D. J. 2006. Sub1A is an ethylene-response-factor-like gene that confers submergence tolerance to rice. *nature,* 442**,** 705.
XU, Z. & ZHOU, G. 2008. Responses of leaf stomatal density to water status and its relationship with photosynthesis in a grass. *Journal of experimental botany,* 59**,** 3317-3325.
YAMAUCHI, T., SHIMAMURA, S., NAKAZONO, M. & MOCHIZUKI, T. 2013a. Aerenchyma formation in crop species: a review. *Field Crops Research,* 152**,** 8-16.
YAMAUCHI, T., WATANABE, K., FUKAZAWA, A., MORI, H., ABE, F., KAWAGUCHI, K., OYANAGI, A. & NAKAZONO, M. 2013b. Ethylene and reactive oxygen species are involved in root aerenchyma formation and adaptation of wheat seedlings to oxygen-deficient conditions. *Journal of experimental botany,* 65**,** 261-273.
YANG, L., ZHENG, B., MAO, C., QI, X., LIU, F. & WU, P. 2004. Analysis of transcripts that are differentially expressed in three sectors of the rice root system under water deficit. *Molecular Genetics and Genomics,* 272**,** 433-442.
YANG, P.-M., HUANG, Q.-C., QIN, G.-Y., ZHAO, S.-P. & ZHOU, J.-G. 2014. Different drought-stress responses in photosynthesis and reactive oxygen metabolism between autotetraploid and diploid rice. *Photosynthetica,* 52**,** 193-202.
YANG, X., LI, Y., REN, B., DING, L., GAO, C., SHEN, Q. & GUO, S. 2012. Drought-induced root aerenchyma formation restricts water uptake in rice seedlings supplied with nitrate. *Plant and Cell Physiology,* 53**,** 495-504.
YOSHIDA, S. & HASEGAWA, S. 1982. The rice root system: its development and function. *Drought resistance in crops with emphasis on rice,* 10.
YU, H., MURCHIE, E. H., GONZÁLEZ-CARRANZA, Z. H., PYKE, K. A. & ROBERTS, J. A. 2015. Decreased photosynthesis in the erect panicle 3 (ep3) mutant of rice is associated with reduced stomatal conductance and attenuated guard cell development. *Journal of experimental botany,* 66**,** 1543-1552.
YUKIYOSHI, K. & KARAHARA, I. 2014. Role of ethylene signalling in the formation of constitutive aerenchyma in primary roots of rice. *AoB Plants,* 6**,** plu043.
ZHANG, G. & LI, C. 2015. *Exploration, Identification and Utilization of Barley Germplasm*, Academic Press.
ZHANG, H., HAN, W., DE SMET, I., TALBOYS, P., LOYA, R., HASSAN, A., RONG, H., JÜRGENS, G., PAUL KNOX, J. & WANG, M. H. 2010a. ABA promotes quiescence of the quiescent centre and suppresses stem cell differentiation in the Arabidopsis primary root meristem. *The Plant Journal,* 64**,** 764-774.
ZHANG, J., JIA, W., YANG, J. & ISMAIL, A. M. 2006. Role of ABA in integrating plant responses to drought and salt stresses. *Field Crops Research,* 97**,** 111-119.

ZHANG, Z., LI, F., LI, D., ZHANG, H. & HUANG, R. 2010b. Expression of ethylene response factor JERF1 in rice improves tolerance to drought. *Planta,* 232**,** 765-774.

ZHENG, X., CHEN, B., LU, G. & HAN, B. 2009. Overexpression of a NAC transcription factor enhances rice drought and salt tolerance. *Biochemical and biophysical research communications,* 379**,** 985-989.

ZHOU, W., LI, Y., ZHAO, B.-C., GE, R.-C., SHEN, Y.-Z., WANG, G. & HUANG, Z.-J. 2009. Overexpression of< i> TaSTRG</i> gene improves salt and drought tolerance in rice. *Journal of plant physiology,* 166**,** 1660-1671.

ZHUANG, J., ANYIA, A., VIDMAR, J., XIONG, A.-S. & ZHANG, J. 2011. Discovery and expression assessment of the AP2-like genes in Hordeum vulgare. *Acta physiologiae plantarum,* 33**,** 1639-1649.

APPENDIX

TABLE OF ANOVA (GENOTYPE × ENVIRONMENT INTERACTION)

Comparison among Genotypes and Drought Treatment

Upland: CO_2 Assimilation rate (*A*): For figure 3.2 A

ANOVA table	SS	DF	MS	F (DFn, DFd)	P value
Interaction	367.3	9	40.81	F (9, 54) = 1.617	P=0.1339
Treatment	830.8	1	830.8	F (1, 54) = 32.91	P<0.0001
Genotype	1049	9	116.6	F (9, 54) = 4.619	P=0.0002
Residual	1363	54	25.24		

Lowland: CO_2 Assimilation rate (*A*): For figure 3.3 A

ANOVA table	SS	DF	MS	F (DFn, DFd)	P value
Interaction	72.5	4	18.12	F (4, 29) = 2.072	P=0.1103
Row Factor	94.43	1	94.43	F (1, 29) = 10.8	P=0.0027
Column Factor	217	4	54.25	F (4, 29) = 6.202	P=0.0010
Residual	253.7	29	8.747		

Upland: Stomatal conductance (*gs*): For figure 3.2 B

ANOVA table	SS	DF	MS	F (DFn, DFd)	P value
Interaction	0.2867	8	0.03584	F (8, 52) = 3.151	P=0.0055
Row Factor	0.3406	1	0.3406	F (1, 52) = 29.95	P<0.0001
Column Factor	0.2423	8	0.03028	F (8, 52) = 2.663	P=0.0157
Residual	0.5914	52	0.01137		

Lowland: Stomatal conductance (*gs*): For figure 3.3 B

ANOVA table	SS	DF	MS	F (DFn, DFd)	P value
Interaction	0.01612	4	0.00403	F (4, 29) = 5.294	P=0.0025
Row Factor	0.01688	1	0.01688	F (1, 29) = 22.18	P<0.0001
Column Factor	0.01195	4	0.002988	F (4, 29) = 3.926	P=0.0115
Residual	0.02207	29	0.000761		

Upland: Transpiration (*E*): For figure 3.2 C

ANOVA table	SS	DF	MS	F (DFn, DFd)	P value
Interaction	146.2	8	18.27	F (8, 52) = 3.21	P=0.0049
Row Factor	216	1	216	F (1, 52) = 37.96	P<0.0001
Column Factor	132.5	8	16.57	F (8, 52) = 2.911	P=0.0092
Residual	295.9	52	5.691		

Lowland: Transpiration (*E*): For figure 3.3 C

ANOVA table	SS	DF	MS	F (DFn, DFd)	P value
Interaction	15.97	4	3.993	F (4, 29) = 4.908	P=0.0038
Row Factor	19.55	1	19.55	F (1, 29) = 24.02	P<0.0001
Column Factor	8.555	4	2.139	F (4, 29) = 2.629	P=0.0547
Residual	23.59	29	0.8136		

Upland: Intrinsic WUE (*iWUE*): For figure 3.2 D

ANOVA table	SS	DF	MS	F (DFn, DFd)	P value
Interaction	14.9	8	1.863	F (8, 51) = 3.2	P=0.0051
Row Factor	4.846	1	4.846	F (1, 51) = 8.326	P=0.0057
Column Factor	17.42	8	2.178	F (8, 51) = 3.742	P=0.0016
Residual	29.68	51	0.582		

Lowland: Intrinsic WUE (*iWUE*): For figure 3.3 D

ANOVA table	SS	DF	MS	F (DFn, DFd)	P value
Interaction	3.403	4	0.8506	F (4, 28) = 3.091	P=0.0316
Row Factor	2.279	1	2.279	F (1, 28) = 8.283	P=0.0076
Column Factor	13.07	4	3.267	F (4, 28) = 11.87	P<0.0001
Residual	7.705	28	0.2752		

Canopy Temperature (*^{o}C)*: For figure 3.5

ANOVA table	SS	DF	MS	F (DFn, DFd)	P value
Interaction	75.22	13	5.786	F (13, 84) = 2.266	P=0.0131
Row Factor	103.3	1	103.3	F (1, 84) = 40.46	P<0.0001
Column Factor	952.6	13	73.28	F (13, 84) = 28.7	P<0.0001
Residual	214.5	84	2.553		

Upland: Maximum rate velocity of carboxylation by Rubisco (V_{cmax}): For figure 3.9 A

ANOVA table	SS	DF	MS	F (DFn, DFd)	P value
Interaction	1756	4	439	F (4, 19) = 0.6222	P=0.6523
Row Factor	3068	1	3068	F (1, 19) = 4.347	P=0.0508
Column Factor	5023	4	1256	F (4, 19) = 1.779	P=0.1747
Residual	13407	19	705.7		

Lowland: Maximum rate velocity of carboxylation by Rubisco (V_{cmax}): For figure 3.9 B

ANOVA table	SS	DF	MS	F (DFn, DFd)	P value
Interaction	540.7	2	270.3	F (2, 12) = 0.7598	P=0.4890
Row Factor	582.1	1	582.1	F (1, 12) = 1.636	P=0.2251
Column Factor	1773	2	886.4	F (2, 12) = 2.491	P=0.1245
Residual	4270	12	355.8		

Upland: Maximum rate of electron transport (J_{max}): For figure 3.9 C

ANOVA table	SS	DF	MS	F (DFn, DFd)	P value
Interaction	6235	4	1559	F (4, 19) = 1.268	P=0.3170
Row Factor	12528	1	12528	F (1, 19) = 10.19	P=0.0048
Column Factor	14882	4	3720	F (4, 19) = 3.027	P=0.0434
Residual	23351	19	1229		

Lowland: Maximum rate of electron transport (J_{max}): For figure 3.9 D

ANOVA table	SS	DF	MS	F (DFn, DFd)	P value
Interaction	1850	2	925.1	F (2, 12) = 0.7568	P=0.4903
Row Factor	764	1	764	F (1, 12) = 0.6251	P=0.4445
Column Factor	8106	2	4053	F (2, 12) = 3.316	P=0.0714
Residual	14668	12	1222		

Upland: Stomatal Limitation (L_s): For figure 3.10 B

ANOVA table	SS	DF	MS	F (DFn, DFd)	P value
Interaction	296.3	4	74.08	F (4, 19) = 0.2928	P=0.8790
Row Factor	830.8	1	830.8	F (1, 19) = 3.284	P=0.0858
Column Factor	1384	4	346	F (4, 19) = 1.368	P=0.2822
Residual	4806	19	253		

Lowland: Stomatal Limitation (L_s): For figure 3.10 C

ANOVA table	SS	DF	MS	F (DFn, DFd)	P value
Interaction	196.8	2	98.38	F (2, 12) = 0.218	P=0.8073
Row Factor	25.17	1	25.17	F (1, 12) = 0.05578	P=0.8173
Column Factor	2562	2	1281	F (2, 12) = 2.838	P=0.0979
Residual	5416	12	451.3		

Root Depth: For figure 3.13 A

ANOVA table	SS	DF	MS	F (DFn, DFd)	P value
Interaction	2419	10	241.9	F (10, 44) = 1.441	P=0.1947
Row Factor	4492	1	4492	F (1, 44) = 26.76	P<0.0001
Column Factor	7433	10	743.3	F (10, 44) = 4.428	P=0.0003
Residual	7387	44	167.9		

Root Length: For figure 3.13 B

ANOVA table	SS	DF	MS	F (DFn, DFd)	P value
Interaction	1.72E+09	10	1.72E+08	F (10, 48) = 1.627	P=0.1276
Row Factor	1.03E+09	1	1.03E+09	F (1, 48) = 9.793	P=0.0030
Column Factor	5.05E+09	10	5.05E+08	F (10, 48) = 4.777	P<0.0001
Residual	5.07E+09	48	1.06E+08		

Average Root Diameter

ANOVA table	SS	DF	MS	F (DFn, DFd)	P value
Interaction	0.02582	10	0.002582	F (10, 48) = 0.9079	P=0.5335
Row Factor	0.0133	1	0.0133	F (1, 48) = 4.676	P=0.0356
Column Factor	0.08648	10	0.008648	F (10, 48) = 3.041	P=0.0046
Residual	0.1365	48	0.002844		

Root Length at 0<0.5

ANOVA table	SS	DF	MS	F (DFn, DFd)	P value
Interaction	1.26E+09	10	1.26E+08	F (10, 48) = 1.749	P=0.0969
Row Factor	6.32E+08	1	6.32E+08	F (1, 48) = 8.744	P=0.0048
Column Factor	3.44E+09	10	3.44E+08	F (10, 48) = 4.765	P<0.0001
Residual	3.47E+09	48	72276400		

Root Length at 0<2.5

ANOVA table	SS	DF	MS	F (DFn, DFd)	P value
Interaction	3254	10	325.4	F (10, 48) = 0.883	P=0.5552
Row Factor	4952	1	4952	F (1, 48) = 13.44	P=0.0006
Column Factor	28986	10	2899	F (10, 48) = 7.866	P<0.0001
Residual	17687	48	368.5		

Hi Vs Lo Relative Humidity: CO_2 Assimilation rate (*A*): For figure 3.17 A

ANOVA table	SS	DF	MS	F (DFn, DFd)	P value
Interaction	40.68	5	8.137	F (5, 59) = 0.6333	P=0.6751
Row Factor	127.4	1	127.4	F (1, 59) = 9.919	P=0.0026
Column Factor	132.5	5	26.51	F (5, 59) = 2.063	P=0.0829
Residual	758	59	12.85		

Hi Vs Lo Relative Humidity: Stomatal conductance (*gs*): For figure 3.17 B

ANOVA table	SS	DF	MS	F (DFn, DFd)	P value
Interaction	0.1231	5	0.02461	F (5, 59) = 1.191	P=0.3245
Row Factor	0.4203	1	0.4203	F (1, 59) = 20.35	P<0.0001
Column Factor	0.4655	5	0.0931	F (5, 59) = 4.507	P=0.0015
Residual	1.219	59	0.02066		

Hi Vs Lo Relative Humidity: Transpiration (*E*): For figure 3.17 C

ANOVA table	SS	DF	MS	F (DFn, DFd)	P value
Interaction	17.51	5	3.502	F (5, 59) = 0.5782	P=0.7165
Row Factor	95.27	1	95.27	F (1, 59) = 15.73	P=0.0002
Column Factor	62.24	5	12.45	F (5, 59) = 2.055	P=0.0839
Residual	357.4	59	6.057		

Hi Vs Lo Relative Humidity: Vapour Pressure Deficit (VPD): For figure 3.17 D

ANOVA table	SS	DF	MS	F (DFn, DFd)	P value
Interaction	1.272	5	0.2544	F (5, 59) = 0.8731	P=0.5047
Row Factor	31.11	1	31.11	F (1, 59) = 106.8	P<0.0001
Column Factor	2.471	5	0.4942	F (5, 59) = 1.696	P=0.1497
Residual	17.19	59	0.2914		

High Relative Humidity: CO_2 Assimilation rate (*A*): For figure 3.18 A

ANOVA table	SS	DF	MS	F (DFn, DFd)	P value
Interaction	46.07	5	9.215	F (5, 22) = 0.6165	P=0.6885
Row Factor	447.1	1	447.1	F (1, 22) = 29.91	P<0.0001
Column Factor	53.98	5	10.8	F (5, 22) = 0.7223	P=0.6138
Residual	328.9	22	14.95		

High Relative Humidity: Stomatal conductance (*gs*): For figure 3.18 B

ANOVA table	SS	DF	MS	F (DFn, DFd)	P value
Interaction	0.09232	5	0.01846	F (5, 22) = 1.107	P=0.3853
Row Factor	0.5681	1	0.5681	F (1, 22) = 34.05	P<0.0001
Column Factor	0.0328	5	0.00656	F (5, 22) = 0.3931	P=0.8482
Residual	0.3671	22	0.01669		

High Relative Humidity: Transpiration (*E*): For figure 3.18 C

ANOVA table	SS	DF	MS	F (DFn, DFd)	P value
Interaction	25.38	5	5.075	F (5, 22) = 1.443	P=0.2485
Row Factor	176.6	1	176.6	F (1, 22) = 50.22	P<0.0001
Column Factor	5.244	5	1.049	F (5, 22) = 0.2982	P=0.9087
Residual	77.39	22	3.518		

High Relative Humidity: Vapour Pressure Deficit (VPD): For figure 3.18 D

ANOVA table	SS	DF	MS	F (DFn, DFd)	P value
Interaction	0.02973	5	0.005946	F (5, 22) = 0.7794	P=0.5752
Row Factor	0.03178	1	0.03178	F (1, 22) = 4.165	P=0.0534
Column Factor	0.07062	5	0.01412	F (5, 22) = 1.851	P=0.1443
Residual	0.1679	22	0.00763		

Low Relative Humidity: CO_2 Assimilation rate (*A*): For figure 3.19 A

ANOVA table	SS	DF	MS	F (DFn, DFd)	P value
Interaction	65.36	5	13.07	F (5, 24) = 0.7316	P=0.6068
Row Factor	324.8	1	324.8	F (1, 24) = 18.18	P=0.0003
Column Factor	232.6	5	46.51	F (5, 24) = 2.603	P=0.0512
Residual	428.8	24	17.87		

Low Relative Humidity: Stomatal conductance (*gs*): For figure 3.19 B

ANOVA table	SS	DF	MS	F (DFn, DFd)	P value
Interaction	0.1213	5	0.02426	F (5, 24) = 1.942	P=0.1244
Row Factor	0.5323	1	0.5323	F (1, 24) = 42.62	P<0.0001
Column Factor	0.1049	5	0.02098	F (5, 24) = 1.68	P=0.1779
Residual	0.2997	24	0.01249		

Low Relative Humidity: Transpiration (*E*): For figure 3.19 C

ANOVA table	SS	DF	MS	F (DFn, DFd)	P value
Interaction	51.2	5	10.24	F (5, 24) = 2.024	P=0.1113
Row Factor	270.5	1	270.5	F (1, 24) = 53.47	P<0.0001
Column Factor	49.9	5	9.98	F (5, 24) = 1.973	P=0.1193
Residual	121.4	24	5.059		

Low Relative Humidity: Vapour Pressure Deficit (VPD): For figure 3.19 D

ANOVA table	SS	DF	MS	F (DFn, DFd)	P value
Interaction	0.2703	5	0.05405	F (5, 24) = 1.095	P=0.3888
Row Factor	1.68	1	1.68	F (1, 24) = 34.02	P<0.0001
Column Factor	0.5248	5	0.105	F (5, 24) = 2.126	P=0.0970
Residual	1.185	24	0.04937		